CROSSLINKED POLYTRIAZOLES TOWARD CHEMICALLY STABLE SEPARATION MEMBRANES

A Dissertation
Presented to
The Academic Faculty

by

Breanne L. Hamlett

In Partial Fulfillment
of the Requirements for the Degree
Doctor of Philosophy in the
School of Chemistry and Biochemistry

Georgia Institute of Technology
December 2019

CROSSLINKED POLYTRIAZOLES TOWARD CHEMICALLY STABLE SEPARATION MEMBRANES

Approved by:

Dr. M.G. Finn, Advisor
School of Chemistry and Biochemistry
Georgia Institute of Technology

Dr. Ryan Lively, Co-advisor
School of Chemical and Biomolecular Engineering
Georgia Institute of Technology

Dr. Stefan France
School of Chemistry and Biochemistry
Georgia Institute of Technology

Dr. David Collard
School of Chemistry and Biochemistry
Georgia Institute of Technology

Dr. John Reynolds
School of Chemistry and Biochemistry
School of Materials Science and Engineering
Georgia Institute of Technology

Dr. J. Carson Meredith
School of Chemical and Biomolecular Engineering
Georgia Institute of Technology

Date Approved: October 28, 2019

ACKNOWLEDGEMENTS

"Your Ph.D. is what you make it." This was the first piece of advice I received when coming to GaTech in 2014 and it has held true through my entire graduate school experience. The journey to a Ph.D. is one of unique challenges and it has taken unyielding dedication to make to the end. However, it is also full of exceptional experiences that have helped shaped the person I am today. This journey would not have been possible without the endless support of others and for that I am truly grateful.

First and foremost, I would like to thank my family. My mother, Debbie Hamlett, has been dedicated to my educational and overall success since childhood. From staying up all night to help me with science fair projects in middle school to trying your best to understand my thesis work, you have always been there to give an outsider's perspective on my scientific challenges. I also want to thank you for babysitting your fur grandbabies when I spent long days in lab, even if you do feed them too many treats. Most of all, I would like to thank you for your unwavering love and advice during stressful times. My father, Lee Hamlett, has always emphasized the importance of education and has pushed me towards excellence in everything I do. The fact that you only make pressure transmitters and not pressure gauges will not ever stop me from asking if I can purchase a pressure gauge from your company. I think they are the same thing.

To my loving husband, Gino Ellis, you have been my rock throughout this journey. Your constant reminders to stop checking my email, put my computer away, and just shut off from schoolwork will always be appreciated. You didn't quite know what you were signing up for by marrying a graduate student, but you have loved me through all of the

stressful days and have given me the support I needed to never give up and always try my best. To Chewy and Charlie, you are the best pups a girl could hope for and your unconditional love has gotten me through many hard nights. To Goo, Sassy Pants, Sir Pounce-A-Lot, Felix Thunder Paws, Admiral Bouncy Boots, and Xander, sometimes you just need a cat, or six to give some love to and everything stressful in life just fades away.

To my research advisor, Professor M.G. Finn, thank you for teaching me how to ask the right questions and giving me the opportunity to explore chemistry and material science without restraints. You allowed me to not only focus on satisfying our funding sources, but to investigate my own scientific interests. To my co-advisor, Professor Ryan Lively, while the title of co-advisor is recent, you have been with me through the entirety of my Ph.D. journey and your "engineer's perspective" always helped me see the real-world applications to my small-scale chemistry. To my committee members: Dr. France, Dr. Collard, Dr. Reynolds, and Dr. Meredith, thank you for your time and the effort you put into my scientific development. You always challenged me to push past my comfort zone.

To my collaborators in the Lively lab: Dr. Yun-Ho, Dr. Melinda Jue, Ronita Mathias, and Matt Rivera, thank for you all the work you have done to help my polymers powders be transformed into functioning separation devices. An extra thank you for translating long mathematical equations into something I could marginally understand.

To Women in Chemistry (WiC), you have helped mold me into a confident and professional scientist, as well as, a well-round person. Thank you to Dr. Allison Aioub, Dr. Johanna Smeekens, and Dr. Hailey Bureau who helped me see that the chemistry

department was not a cut-throat competition, but that everyone can succeed. You were a strong support system for me at the start of my graduate school experience. To Kirstie Thompson, Asheley Chapman, and Dr. Sandy Pittelli, you have helped developed WiC into a thriving community where women can feel safe while learning to navigate graduate school and beyond. Thank you for always having an open ear and shoulder to lean on (although not actually involving physical contact).

To past Finn lab members: Dr. Cody Higginson, Dr. Craig McKay, Dr. Allison Aioub, and Dr. Zhishuai Geng, I couldn't have done this without mentorship from every single one of you. Cody, your love science always pushed me to ask why and understand every aspect of my work. Craig, your ability to jump headfirst into something new always reminded me that I could do anything if I worked hard enough. Allison and Zhishuai, you always made lab an enjoyable place to work and showed me how to be a "real" scientist, always leading by example. To current Lab members: Robert Hincapie, Asheley Chapman, Jeff Noble, Kirstie Thompson, Lu De Pascalis, Lu Pigliautile, Sonia Bhattacharya, Ruyi Yang, Jessica Lloyd, Dr. Liangjun Zhao, Dr. Nick Bruno, Dr. Soumen Das, Dr. Minghao Xu, and Dr. Saona Seth, graduate school would not have been nearly as much fun without you. Kirstie and Nick, Team Jim was like a family to me and I will really miss those expensive Exxon dinners with the weird food.

Lastly, to the group of people that have made the exclusive "friends" list: Dr. Sandy Pittelli, Dr. Evelyn Ligon, Dr. Allison Aioub, Dr. and Osiris Martinez Guzman, and Kirstie Thompson, I am really happy to call you my friends.

TABLE OF CONTENTS

LIST OF TABLES

LIST OF FIGURES

LIST OF SYMBOLS AND ABBREVIATIONS

^{1}H NMR	Proton Nuclear Magnetic Resonance
BET	Brunauer-Emmett-Teller
°C	Degrees Celsius
Cl^-	Chlorine Ion
CuAAC	Copper(I)-Catalyzed Azide-Alkyne Cycloaddition
Cu(0)	Copper metal, copper in the 0 oxidation state
Cu(I)	Copper in the +1 oxidation state
Cu(II)	Copper in the +2 oxidation state
Cu(II)O	Copper (II) oxide
DMF	Dimethylformamide
ESI	Electrospray ionization
GPC	Gel Permeation Chromatography
HCl	Hydrochloric acid
K_2CO_3	Potassium Carbonate
M	Molarity
mL	Milliliter
M_w	Weight Average Molecular Weight
NaClO	Sodium Hypochlorite
n.d.	Not determined
NaOH	Sodium Hydroxide
OSN	Organic Solvent Nanofiltration
OSRO	Organic Solvent Reverse Osmosis

PES	Polyethersulfone
PIM	Polymer of Intrinsic Microporosity
RI	Refractive index
SEM	Scanning electron microscope
S_NAr	Nucleophilic Aromatic Substitution
T_d	Degradation Temperature
T_g	Glass-transition Temperature
TLC	Thin-layer chromatography
TFPN	2,3,5,6-tetrafluoroterephthalonitrile
TTSBI	5,5′,6,6′-tetrahydroxy-3,3,3′,3′-tetramethylspirobisindane
UV	Ultraviolet

SUMMARY

The research reported in this thesis studies the use of polytriazoles as a selective, separation layer for use in membrane-based hydrocarbon separations and water desalination. Numerous polytriazoles were developed to compete with chemically unstable commercial polyamide membranes. The Copper-catalyzed Azide Alkyne Cycloaddition (CuAAC) reaction was used to create highly stable and chemical resistant triazole linkages throughout the polymer membrane. Additionally, triazoles were used to crosslink polymers of intrinsic microporosity (PIMs), to add to PIMs already exceptional gas separation properties. Furthermore, interfacial polymerization was used to create ultra-thin membranes of polytriazole-linked polymers. Lastly, CuO hollow fiber support membranes were used to add mechanical stability to the polytriazole membranes and additionally catalyze the CuAAC reaction, creating a polytriazole surface coating on CuO hollow fibers.

CHAPTER 1. INTRODUCTION

1.1 Industrial Separation Methods

A sizable portion of the world's overall energy expenditure is consumed by large-scale industrial separation processes. Thermal-based separations, such as distillation, drying, and evaporation, account for 10-15% of the world's total energy usage.[2] Although distillation is a mature, well-established technique in industry, the replacement of high-energy distillations with low-energy, pressure-driven membrane-based separations would reduce this energy consumption by 90%.[3] However, before industrial separations can completely transition from thermal techniques to pressure driven processes, membranes must decrease in cost and have competitive versatility and selectivities when compared to distillations.

1.1.1 Distillation

Distillations are thermally driven processes that separate fully miscible components based on their boiling points, or volatility. As heat is added to the system, constituents with lower boiling points and higher volatility will convert to the vapor phase, leaving the less volatile components as liquids.[4] With the ability to separate gases, organic compounds, and purify water, distillation is the most widely used industrial separations process. This robust and well-understood technique has several advantages over current membrane technology; including a low capital investment, the ability to achieve a high purity separation independent of flow rates, and the reusability of structural components.[2] However, alternative separation methods are being explored due to the exceptionally high energy

consumption of distillations and their inability to separate: low molecular weight compounds, heat-sensitive materials, components in low concentration, azeotropes, components with similar boiling points, or based on classes of components.[4]

1.1.2 Membranes

Membranes are semi-permeable, porous materials with the ability to separate molecules based on size or chemical affinity.[5] Their intrinsic performance properties result from both the chemical composition, which is synthetically incorporated, and the material morphology, which can be synthetically incorporated or arise based on casting techniques.[2] The main advantage of membrane is they do not require a phase change to achieve highly selective separations.[6] Hence, the energy requirement to perform a membrane-based separation is drastically lower than that of a distillation process. Additionally, molecules that are unable to be separated via distillation are easily separable using membranes. Furthermore, membranes are flexible in design which leads to a myriad of possibilities in potential separation applications.

Membranes may be composed of inorganic materials leading to high stability, organic polymers with solution processability, or a composite material in which each layer is optimized separately to achieve the desired performance.[7-8] In addition to the membrane's chemical composition, membrane fabrication into flat sheets or a cylindrical design also affect membrane transport properties and operational costs.[9] However, membranes are still underdeveloped as compared to distillation techniques and the materials are too expensive to completely replace distillations on the industrial scale.[3]

1.2 Separations Seeking Improvement

1.2.1 Hydrocarbon Separations

Crude oil is produced naturally from the decaying of ancient plants and animals and is the source of hydrocarbons that are used in many commercial products. Hydrocarbons are of great interest due to their ability to go through a combustion reaction and produce a large amount of energy. Hydrocarbon can take on many forms and the majority of crude oil contain: (1) alkanes, also known as paraffins, (2) aromatics (3) cycloalkanes, and (4) alkenes and is most commonly purified by fractional distillation based on boiling points of each component (Figure 1-1).[10]

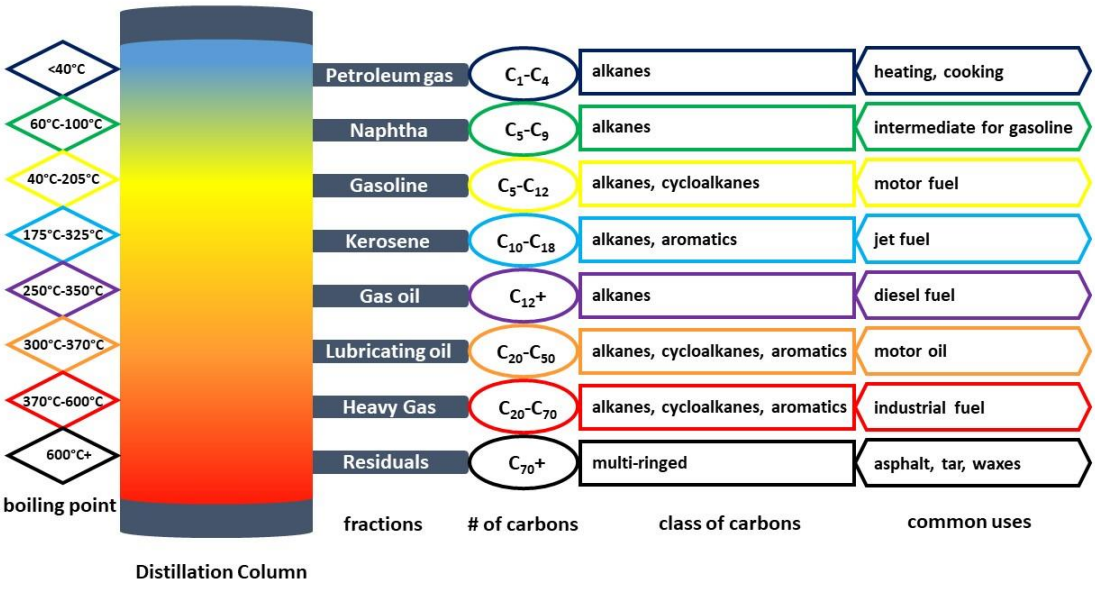

Figure 1-1: Fractional distillation of crude oil into eight major hydrocarbon fractions based on boiling point.

While distillation works to separate hydrocarbons into broad categories based on boiling point, additional processing is needed to further separate and purify molecules with similar boiling points. Additionally, the energy required to process hydrocarbons via

distillations is exceptionally large and reducing this energy consumption is a major research focus in both academia and industry.

Applying membrane technology to hydrocarbon separations is greatly lacking due to the instability of traditional polymer membranes to organic solvents.[11] Additionally, the ability of membranes to separate molecules of similar size has not been fully explored. Organic solvent nanofiltration (OSN) can differentiate molecules with larger than one order of magnitude in size difference; while organic solvent reverse osmosis (OSRO) has the ability to achieve an even finer distinction in size variations.[12-13] However, both processes are in their infancy and a true structure-property relationship has not been fully developed.

1.2.2 Water Desalination

As the population continuously rises, there is an increase in demand for clean and consumable water, fueling a push towards alternative water sources.[14] For ocean water and brackish water to be considered potable, the water must first be subjected to a desalination process. While thermally-driven distillations were the industry standard for many years, it is an energy intensive process and in recent years membrane-based separations have supplanted it as the most widely used method of desalination. Membranes are capable of separating water from salts and biomaterials with the same efficiency as evaporation-based methods, with a large decrease in operational energy cost.[15]

Typically, membranes are made of polymer materials and tend to clog or foul during the desalination process.[16-18] (Figure 1-2) Fouling results in higher pressure along the membrane system and a decrease in flow through the membrane, translating into higher energy consumption for the system. Regular cleanings with acids, bases, and oxidants are necessary to maintain a high level of membrane performance.[19-21] However, aromatic polyamides, commonly used as water desalination membranes, are sensitive to the chlorine treatment used as an antibacterial agent.[22-23] Since chlorine usage is routine in water pretreatment and defouling, polyamides are not an ideal material. A chemically and oxidatively stable membrane is preferred for water desalination.

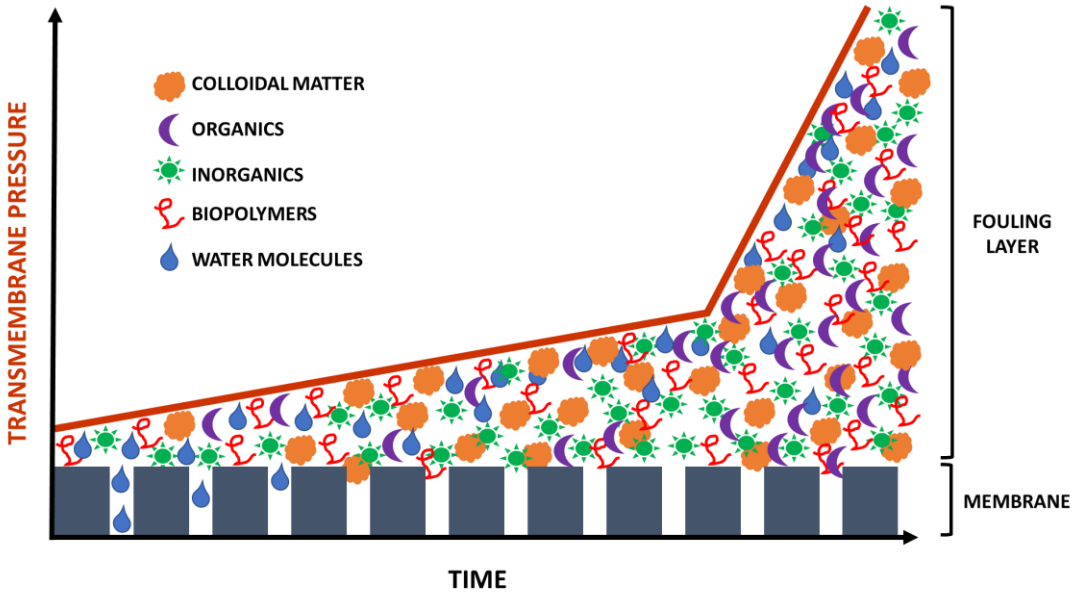

Figure 1-2: An increase in membrane fouling layer over time results in an increase in transmembrane pressure and in turn an increase in operational energy cost. Adapted from Schmitt [1].

1.3 Chemical Composition of Membranes

The commercial worth of a membrane is determined by the parameters of selectivity, the extent to which molecules are separated and permeability, the rate at which molecules pass through the membrane.[24] The ideal polymer membrane has both a high selectivity and permeability. However, there is usually a trade-off between permeability and selectivity. Key design features that lead to ideal membrane parameters are a small pore size and small pore size distributions, and a thin separation layer, or active layer. The former can be accessed and manipulated synthetically, and a reduction in pore size and pore size distributions can lead to higher selectivities.[25]

1.3.1 Polymer of Intrinsic Microporosity (PIM)

First reported in 2004 by McKeown and coworkers, PIMs are defined as a polymer whose unsystematic, highly contorted, and rigid structure hinders rotational movement in the polymer backbone. As a result, the polymer cannot efficiently pack in the solid state, creating an interconnected, microporous (pore size < 2 nm) material with a large, accessible surface area.[26] The rigidity and lack of rotational freedom originates from the completely fused-ringed backbone, or ladder linkage structure of the polymers. Spirocenters or other non-planar units, such as triptycene, provide the sites of contortion. PIMs are prepared via a step-growth polymerization using a bis-catechol aromatic monomer and fluorinated aromatic monomers. PIM-1, the archetypal PIM polymer, can reach M_w of 100-200kDa via relative GPC, demonstrating the efficiency of the double S_NAr polymerization reaction. (Figure 1-3)

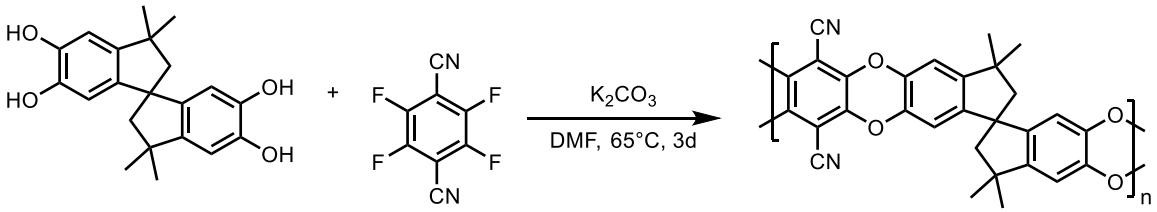

Figure 1-3: Synthesis of PIM-1

A key difference between PIMs and other highly rigid polymers is their solution processability, which is a highly attractive trait when developing casting methods and fabrication techniques for PIM membranes. Generally, PIMs show good chemical stability in the presence of acids, bases, and oxidants, and show excellent thermal stability with temperatures up to 450°C. Additionally, they have shown no chemical or surface area degradation after storage at ambient conditions for several years. PIMs central feature is their high levels of microporosity. BET analyses different PIMs reveal surface areas in the range of 500–1730 $m^2\ g^{-1}$. This high surface area has led to promising results for gas separation membranes prepared with PIMs. However, PIM-drastically swells in the presence of organic solvents, limiting their use as hydrocarbon separation membranes.[27] In addition, water desalination using PIM-1 has not been thoroughly explored due to the high hydrophobicity of the polymer, resulting in higher pressures and energy needs to run a PIM-based water purification system.[28-29]

1.3.2 Stable Triazole Linkers Formed by the CuAAC Reaction

Click chemistry is defined as a set of fast, high-yielding reactions that are simple to perform, easy to purify, stereospecific, and give high product yields.[30-31] The copper(I)-catalyzed azide-alkyne cycloaddition (CuAAC) reaction of azides with terminal alkyne is a principal example of a click reaction (Figure 1-4). The CuAAC reaction is regiospecific, producing a 1,4-disubstituted 1,2,3-triazole as the exclusive product.[32-33] CuAAC also leads as a foremost linkage forming reaction in organic synthesis, material science, medicine and industry due to the ease of installing azides and alkynes into starting materials, the ability of the reaction and starting materials to tolerate a variety of reaction conditions, and the chemical stability of the product due to the electron poor and oxidatively stable nature of triazoles.[34-35]

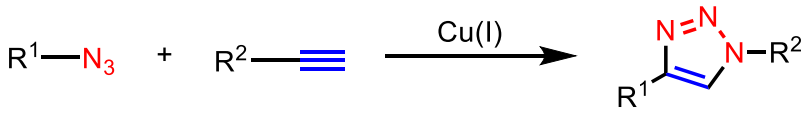

Figure 1-4: Copper(I)-Catalyzed Azide-Alkyne Cycloaddition (CuAAC) reaction between an azide and a terminal alkyne in the presence of Cu(I) to form a 1,4-disubstituted 1,2,3-triazole.

While CuAAC been studied to synthesize and functionalize separation membranes [36-37], to date, the CuAAC reaction in combination with PIMs has not been explored to create or functionalize separation membranes for use in hydrocarbon separation or water desalination. This reaction is particularly attractive in material science because azides and alkynes can be introduced easily, monomer design can be readily tuned to influence bulk properties.

1.4 Membrane Fabrication Techniques

While the chemical composition is important to for determining selectivity and permeability of a membrane, casting methods and fabrication techniques also influence the effectiveness of the membrane.

Thin-film composites are made by combining a thin microporous layer that is highly selective with a macroporous support layer that adds mechanical strength (Figure 1-5). A sub-micrometer selective layer is ideal to achieve a high flux and permeability through the membrane, and in turn a low operational cost. Flux is the amount of material that is able to cross the membrane per membrane area per time. Permeance is the amount of material that is able to cross the membrane per membrane area per time per pressure. Permeability is the same as permeance, but additionally includes the thickness of the membrane. While the macroporous support layer is less important in terms of selectivity, it must have high permeability and be mechanically, thermally, and chemical robust, as well as cost efficient.

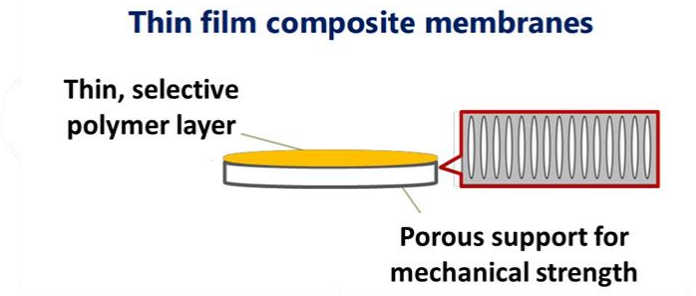

Figure 1-5: Thin-film composite. The thin, selective polymer layer (shown in yellow) makes a continuous coating on the macroporous support layer.

1.4.1 Liquid-Liquid Interfacial Polymerization

Interfacial polymerization is a common technique to make thin crosslinked polymer membranes.[38] In interfacial polymerization, each monomer is dissolved in one of two immiscible solvent. Upon contact between the two solutions, a crosslinked polymer film is formed at the interface (Figure 1-6). Once the initial layer of polymer is formed, the unreacted monomers are separated by the crosslinked polymer membrane and the polymerization reaction stops. This principle is extended to the case of thin, composite membranes where a macroporous support is used.[38]

Water desalination composite membranes made of a crosslinked aromatic polyamide active layer and a polysulfone support layer commonly used this fabrication technique. For polyamide composites, the polysulfone support is saturated in the aqueous amine solution and placed in an organic solution containing the acyl halide. The thin film polymer then forms at the surface of the solid support. The thin film of polyamide provides the separation properties of a full membrane made of polyamide, however, by decreasing the membrane thickness, the permeability of the system is increased.

While CuAAC has not been explored to make thin, flat sheet membranes using interfacial polymerization, PIM-like membranes have been synthesized with this method.[39] While these thin films showed good initial separation abilities for both gas and organic solvents, repeatability in membrane fabrication was an issue.

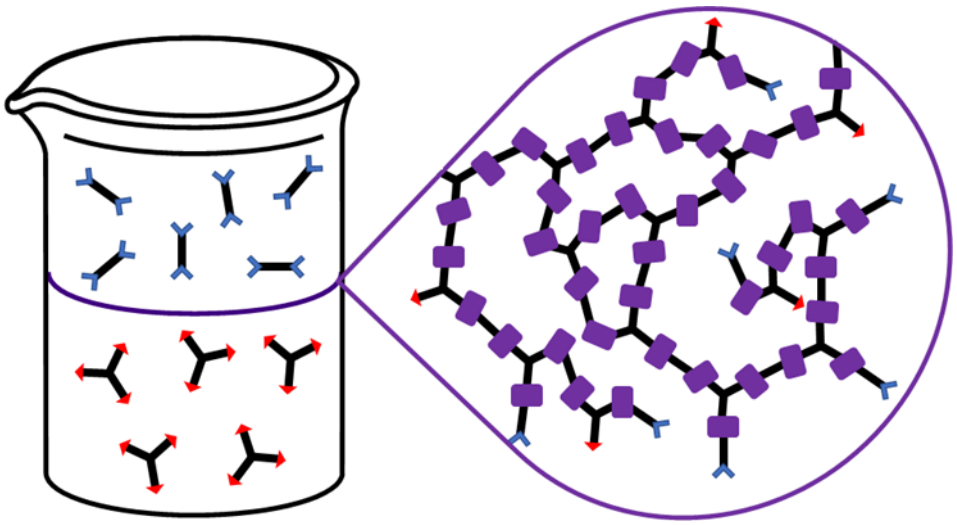

Figure 1-6: Interfacial polymerization of two multi-functional monomers (red and blue) in two immiscible solvents. A crosslinked polymer is formed at the interface (purple).

1.4.2 Solid-Liquid Surface Polymerization

Similar to liquid-liquid interfacial polymerization, reactions of a liquid at a solid surface are also self-limiting and will create thin polymer layers. However, in surface polymerization, both monomer units are solubilized in a solvent, while a reaction catalyst is displayed on a solid substrate. The solid support is then dip coated into the monomer solution, where a reaction will occur at the solid-liquid interface. Once a thin polymer layer is formed at the surface of the solid, the monomers and catalyst no longer have an interface to react at and polymerization stops.

While this process has not been explored for use in membranes, it has been thoroughly studied using the CuAAC reaction for materials applications. Copper metal (Cu(0)) or Copper (II) Oxide can be used as the Cu(I) source in these applications. A small

amount of Cu(I) present at the surface of the Cu(0) from oxidation in air and also present in Cu(II)O from trace amounts of Cu(I) contamination.[40] Solid copper tubing has been used in flow reactor systems to catalyze the CuAAC reaction of small molecular azides and alkynes as they move through the copper tubing.[41] Copper metal has also been used as CuAAC catalyst for adhesive applications.[42-43] Polytriazoles were able to adhere the Cu(0) together after a surface polymerization of a thin layer of multi-functional azides and alkynes in solution reacted at the solid copper interface. This method could be transitioned to membrane technology by coating a thin layer of azide and alkyne functionalized membrane building blocks onto a porous copper support layer.

CHAPTER 2. STABILITY OF 1,4-DISUBSTITUTED 1,2,3-TRIAZOLE FOR USE IN WATER DESALINATION MEMBRANES

(Currently, this work is being drafted into a manuscript that will be submitted for peer review.)

Polyamide thin-film composite membranes are commercially used for water desalination.[22] Overtime the membranes will foul or clog and chemical cleaning is needed to ensure high flux at low operational pressure.[17] Acids, bases, and oxidants are typically used to clean the fouling layer off the membrane, however amide bonds will cleave in the presence of oxidants resulting in lower selectivity.[22-23] Replacing amide linkages with chemical stable linkage will increase the lifetime of water desalination membranes and allow for unrestricted chemical cleaning of membrane fouling.

1,2,3-triazoles are important heterocyclic compounds as they have numerous uses in industry.[35, 44] Both 1,4- and 1,5- disubstituted 1,2,3-triazoles can easily synthetically accessed via metal-catalyzed 1,3-dipolar cycloaddition or the thermal Huisgen cycloaddition.[30, 34, 45] Selectively, the 1,4-disubstituted 1,2,3-triazole can be afforded as the sole product of the copper(I)-catalyzed azide-alkyne cycloaddition (CuAAC) reaction.[32-33] Due to: (1) the ease of synthesis of the starting azides and alkynes, (2) the ability of the reaction to tolerate a variety of reaction conditions, and (3) the high thermodynamic driving force that pushes the reaction quickly and irreversibly to a single reaction product with high yield and specificity, 1,4-disubstituted 1,2,3-triazoles have become a premier linker

in organic synthesis, material science, medicine, and industry. [31, 35] 1,4-disubstituted 1,2,3-triazoles are presumed to be stable in the presence of acids, bases, and oxidants,[46] which is expected due to the electron poor and oxidatively stable nature of the triazole. However, to date no experimental analysis has been conducted to validate the stability of the triazole.

In this study, various 1,4-disubstituted 1,2,3-triazoles were synthesized and the stability of each was studied in the presence of acids, bases, and oxidants that are relevant to their use in water desalination membranes.[20-21] The degradation of each triazole was studied via ^{1}H NMR and the triazole degradation was compared to that of an aromatic amide, similar to the polyamides used in current water desalination membranes.[22-23] The stability of PIM-1 in membrane cleaning conditions was also explored. Since PIM-1 has shown promise in gas and organic separation properties,[47-48] the polymer's stability in water treatment conditions is an important initial step towards its potential use in water desalination. PIM-1 stability was determined via ^{1}H NMR and changes in retention time indicating a change in M_w via GPC an analysis.

2.1 Triazole Design

A series of triazoles containing benzyl, ether, aryl, and alkyl substituents (Figure 2-1) were synthesized and treated with oxidants, acids, and bases. A representative amide was also synthesized for comparison. Additionally, PIM-1 was included to probe its stability for potential use in water desalination membranes.

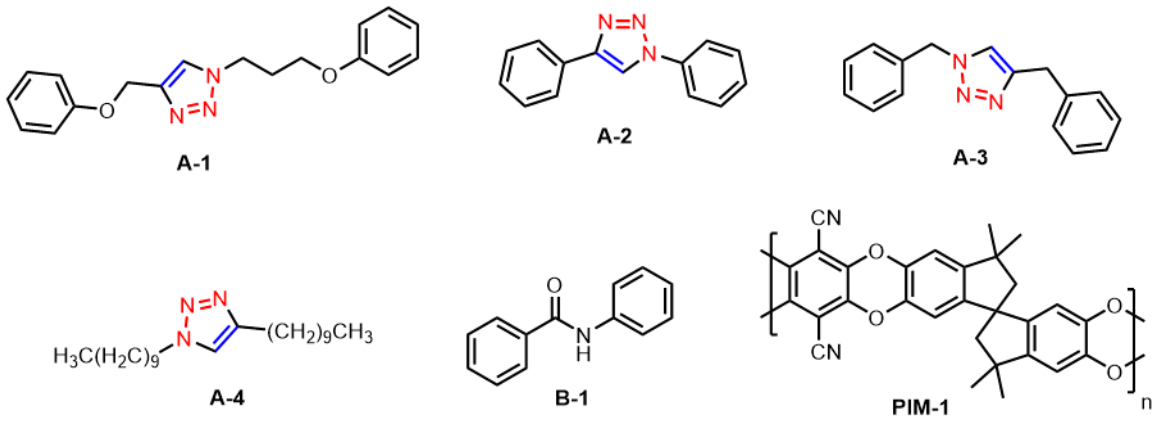

Figure 2-1: Triazoles with various pendant groups, amide, and PIM-1 studied for chemical stability.

Molecule A-1 contains an ether-linked triazole, which may be susceptible to hydrolysis in the presence of very strong acids, however, is included in this series of tests because this linkage a practical approach to attach azides and alkynes to multi-functional backbones. Additionally, the ether linkages of PIM-1 could be susceptible to hydrolysis, resulting in a degradation of the polymer. A-2 is hypothesized to be the most stable triazole, as breaking aromaticity would be unfavorable. Additionally, benzylic and pseudo-benzylic positions in molecules A-3 and A-4 could also be susceptible to oxidation. The phenylbenzamide, B-1, provided a direct comparison between a triazole and amide linkage.

While functionality is the ultimate test of a membrane's stability, these small molecule representations will simulate the degradation of the polymer membrane linkages and will allude to the inevitable membrane failure as more polymer linkages are broken. By using small molecules, the degradation can be easily tracked by chemical analysis instead of membrane functionality.

2.2 Cleaning Conditions

Due to the various contaminants desalination plants receive in their water feeds, the fouling layer can contain numerous combinations of proteins, polysaccharides, fatty acids, microbes, and inorganic precipitations. The complex fouling layer requires multiple cleaning treatments to fully remove the layer from the membrane including chemical treatments with acids, bases, and oxidants. Acids and bases are commonly used between 0.01-0.001M to clean aromatic polyamide membranes.[21] Additionally, polyamides are not usually cleaned with bleach, due to their instability to oxidants, leading to a less efficient cleaning process. However, membranes composed of other materials are often cleaned with NaClO with an active Cl^- concentration of 500-5000ppm.[49] For the chemical stability of the triazole linkages, concentrated HCl (12M) was used as the acidic cleaning agent, NaOH (1M) was used the basic cleaning agent, and NaClO (50,000ppm) was used as an oxidative agent. While these concentrations are far above the recommended and commonly used membrane cleaning concentrations, which would stimulate an accelerated degradation process. The ability of the triazole linkage to withstand these conditions while the amide linkage degrades, demonstrates the extremely high chemical stability of the triazole.

Temperatures of a desalination membrane setups are usually elevated above room temperature due to the kinetic energy created by the fast movement of the water.[21, 49] temperatures of 23°C (room temperature) and 60°C were evaluated in this study.

While industrial membrane cleaning usually last less than 1 hour, cleaning times from 1 hour and 1 week were studied.[21] This was chosen to evaluate the degradation of linkages over many separate chemical cleanings.

2.3 Experimental Setup

A known amount of each target molecule (A-1, A-2, A-3, A-4, B-1, or PIM-1) was added to a vial followed by 1mL of cleaning solution. The reaction was stirred via a Teflon™ stir bar at the corresponding temperature and time interval. Once the time interval had elapsed, the acidic solutions were neutralized to pH=7 with 1M NaOH. The neutralization was necessary due to the protonation of the triazole in strong acid, and the increased water solubility of the resulting protonated triazole product.[50] The bleach and basic solutions were not neutralized, since the molecules remained solids. The resulting solids were then filtered and washed repeatedly with water. They were then dried in a vacuum oven to remove any remaining water. Additionally, the water washes were combined, and water was removed. The washes were also analyzed due to the increased water solubility of potential degradation products, especially of the amide-linked molecule.

2.4 Analysis of Target Molecules

The filtered solids and the dried water washes were analyzed by ^{1}H NMR. Any spectra that deviated from the standard spectra resulted in a "degraded" result (Figure 2-2). Additionally, the presence of molecule peaks in the water washes resulted in a "degraded" result, due to the initial hydrophobicity of the non-altered (or non-degraded) starting compounds. GPC was also conducted on the PIM-1 samples. Changes in M_w of more than 20% of the standard were considered "degraded" (Figure 2-3). While the GPC curves of PIM-1 was not completely gaussian, the small M_w shoulder of the GPC trace was also included for M_w calculations purposed. "Stable" samples showed ^{1}H NMR spectra and GPC data identical to the standard.

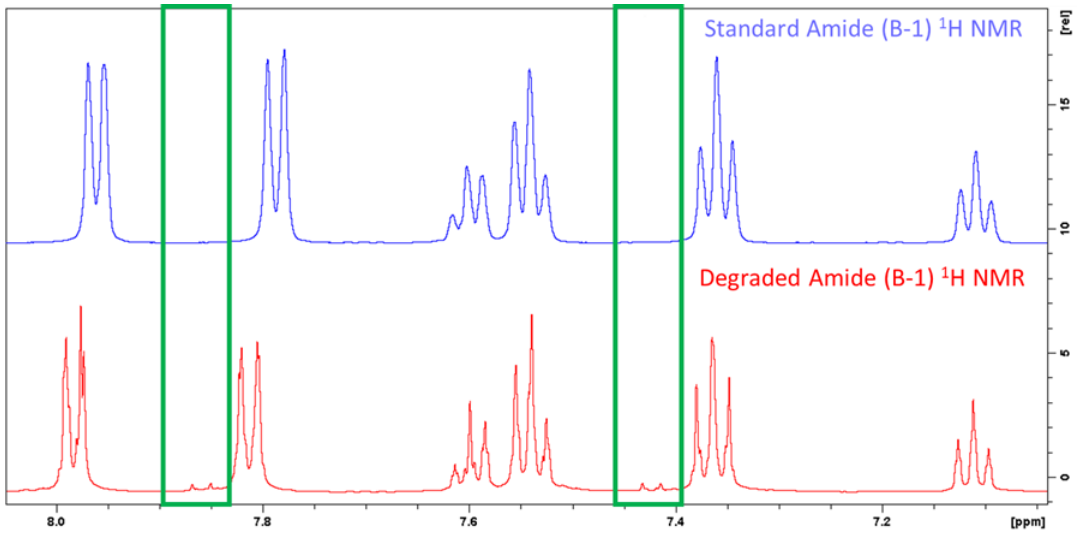

Figure 2-2: Zoomed in aromatic region of the ^{1}H NMR of B-1 amide molecule. The blue spectrum shows the standard of B-1. The red spectrum shows the degradation of the B-1 molecule indicated in the green boxes.

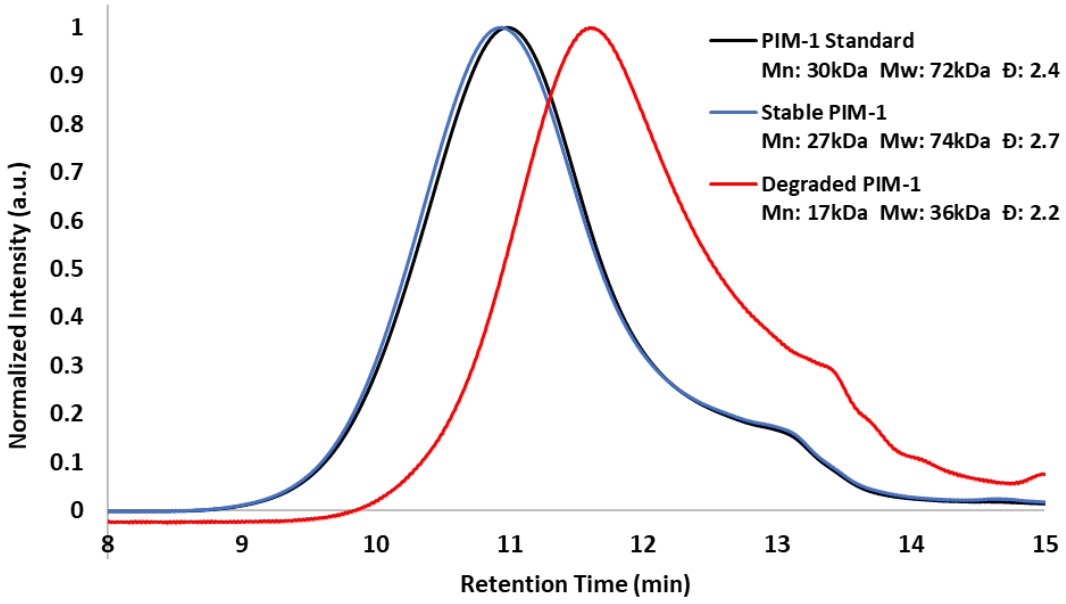

Figure 2-3: Normalized GPC analysis of PIM-1 from 8-15 minutes retention time. A standard PIM-1 samples is shown in black; a stable PIM-1 sample is shown in blue; and a degraded PIM-1 samples is shown in red with a retention time that is at a higher retention time compared to the other two samples.

2.5 Results and Discussion

2.5.1 Stability in Neutral Solutions

The stability of various triazoles, PIM-1, and N-phenylbenzamide in neutral H_2O at elevated temperatures (60°C) are summarized in Table 2-1. This was also run as the negative control for all cleaning conditions.

Table 2-1: H_2O Stability of Triazoles, PIM-1, and Amide. Stable compounds are shown in green and degraded compounds are shown in red.

	Temp (°C)	Time						
			A-1	A-2	A-3	A-4	PIM-1	B-1
H_2O	60	1 hour	stable	stable	stable	stable	stable	stable
H_2O	60	1 day	stable	stable	stable	stable	stable	stable
H_2O	60	1 week	stable	stable	stable	stable	stable	stable

2.5.2 Stability in Acidic Solutions

The stability of various triazoles, PIM-1, and N-phenylbenzamide to HCl are summarized in Table 2-2. In concentrated (12M) HCl at 60 °C all traizoles and PIM-1 are stable with no degradation is found in the solid samples or washes. While the solid aromatic amide (B-1) was non-degraded, the water washes showed degraded amide peaks present. B-1 showed degradation in the water washes in as low as 0.0012M HCl solutions. While the degraded product was not analyzed further to determine the identity, amides often undergo a hydrolytic cleavage in the presence of strong acids.

Table 2-2: Acid Stability of Triazoles, PIM-1, and Amide in HCl. Stable compounds are shown in green and degraded compounds are shown in red. "n.d." were not determined, however are presumed stable since the harsher conditions were stable.

[C]	Temp (°C)	Time						
			A-1	A-2	A-3	A-4	PIM-1	B-1
12M	60	1 hour	stable	stable	stable	stable	stable	degraded
		1 day	stable	stable	stable	stable	stable	degraded
		1 week	stable	stable	stable	stable	stable	degraded
	23	1 hour	n.d.	n.d.	n.d.	n.d.	n.d.	degraded
		1 day	n.d.	n.d.	n.d.	n.d.	n.d.	degraded
		1 week	n.d.	n.d.	n.d.	n.d.	n.d.	degraded
0.0012M	60	1 hour	n.d.	n.d.	n.d.	n.d.	n.d.	degraded
		1 day	n.d.	n.d.	n.d.	n.d.	n.d.	degraded
		1 week	n.d.	n.d.	n.d.	n.d.	n.d.	degraded
	23	1 hour	n.d.	n.d.	n.d.	n.d.	n.d.	degraded
		1 day	n.d.	n.d.	n.d.	n.d.	n.d.	degraded
		1 week	n.d.	n.d.	n.d.	n.d.	n.d.	degraded

2.5.3 Stability in Basic Solution

The stability of triazoles A-1 – A-4, PIM-1, and N-phenylbenzamide to NaOH are summarized in Table 2-3. No samples showed degradation in the solids or washes in 40% NaOH at 60 °C for up to 1 week.

Table 2-3: Basic Stability of Triazoles, PIM-1, and Amide in NaOH. Stable compounds are shown in green and degraded compounds are shown in red.

[C]	Temp (°C)	Time						
			A-1	A-2	A-3	A-4	PIM-1	B-1
1M	60	1 hour	stable	stable	stable	stable	stable	stable
		1 day	stable	stable	stable	stable	stable	stable
		1 week	stable	stable	stable	stable	stable	stable

2.5.4 Stability in Oxidative Conditions

The stability of various triazoles, PIM-1, and N-phneylbenzamide to NaClO are summarized in Table 2-4. Triazoles A-1, A-2, and A-4 show no degradation in the solid or

water washes up to one week in 50,000ppm NaClO solution at 60 °C. Triazole A-3 does show degradation in one hour in 5% NaClO at 60 °C, one day at 1% NaClO at 60 °C, and one week at 1% NaClO at room temperature. This was not presented as degradation of the solid, but as A-3 peaks in the water washes. While the degraded product was not analyzed, the stability of a radical at the benzyl position makes the double benzyl triazole likely to undergo oxidation. This oxidation could lead to increased water solubility of A-3. Additionally, N-phneylbenzamide (B-1) showed degradation of the solid in one hour in 5% NaClO at 60 °C. While the oxidative instability of amides is documented in the literature, the exact mechanism is not known. It is hypothesized that N-Cl compounds are formed, subsequently chlorinating the aromatic rings via an Orton rearrangement and rendering the amide more susceptible to hydrolysis. [22]

Table 2-4: Oxidative Stability of Triazoles, PIM-1, and Amide in NaClO solution. Stable compounds are shown in green and degraded compounds are shown in red. "n.d." were not determined, however are presumed stable since the harsher

[C]	Temp (°C)	Time						
			A-1	A-2	A-3	A-4	PIM-1	B-1
50,000ppm	60	1 hour	stable	stable	degraded	stable	stable	degraded
		1 day	stable	stable	degraded	stable	stable	degraded
		1 week	stable	stable	degraded	stable	stable	stable
	23	1 hour	n.d.	n.d.	stable	n.d.	n.d.	stable
		1 day	n.d.	n.d.	degraded	n.d.	n.d.	stable
		1 week	n.d.	n.d.	degraded	n.d.	n.d.	stable
10,000ppm	60	1 hour	n.d.	n.d.	stable	n.d.	n.d.	stable
		1 day	n.d.	n.d.	degraded	n.d.	n.d.	stable
		1 week	n.d.	n.d.	degraded	n.d.	n.d.	stable
	23	1 hour	n.d.	n.d.	stable	n.d.	n.d.	n.d.
		1 day	n.d.	n.d.	stable	n.d.	n.d.	n.d.
		1 week	n.d.	n.d.	degraded	n.d.	n.d.	n.d.
1000ppm	60	1 hour	n.d.	n.d.	stable	n.d.	n.d.	n.d.
		1 day	n.d.	n.d.	stable	n.d.	n.d.	n.d.
		1 week	n.d.	n.d.	stable	n.d.	n.d.	n.d.

2.6 Conclusion

In this study, it was shown that ether-linked triazoles, aryl triazoles, and alkyl triazoles are stable under cleaning conditions that are common in water desalination membrane defouling protocols. PIM-1 is also stable under these conditions, and its use in water desalination applications can be further studied. Benzyl triazoles show degradation in strongly oxidizing conditions due to the stability of radicals on the benzyl position. Their use should be limited and monitored for use in water desalination membranes. Compared to amides, triazoles, with the except of benzyl triazole, were more stable in both oxidative and acidic conditions and performed equally in basic conditions. In conclusion, triazole are a stable alternative linkage to amide for defouling cleaning conditions in water desalination membranes.

2.7 Methods and Characterization

2.7.1 Materials

Reagents and solvents were purchased from commercial sources and used as received, unless otherwise stated. Chromatography was performed on an Isolera One: Accelerated Chromatographic Isolation unit from Biotage with a UV and ELSD detector and a KP-Sil column. Analytical TLC was performed on glass-backed plates and visualized by exposure to UV light.

2.7.2 Synthetic Methods

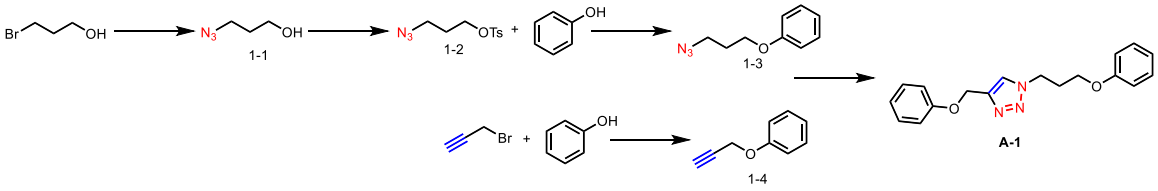

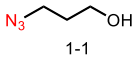

3-azidopropan-1-ol (1-1)[51] 3-Bromo-1-propanol (10.0 g, 72.0 mmol, 1 equiv.) was dissolved in deionized water (75 mL) and sodium azide (9.35 g, 144 mmol, 2 equiv.) was added in one portion. The reaction was heated at 50 °C for 24 hours. After cooling to room temperature, the mixture was extracted with CH_2Cl_2 (3×200 mL). The combined organic fractions were dried over sodium sulfate, filtered, and concentrated via rotary evaporation. The resulting pale-yellow liquid was purified by fractional distillation under vacuum (bp 62 °C at 3–4 mbar[3]) to yield 9.0 g (62%) of 3- azidopropan-1-ol as a colorless oil. **^{1}H NMR** (500 MHz, Chloroform-*d*) δ 3.74 (t, *J* = 6.0 Hz, 2H), 3.44 (t, *J* = 6.6 Hz, 2H), 1.82 (p, *J* = 6.2 Hz, 2H).

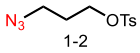

3-azidopropyl 4-methylbenzenesulfonate (1-2)[52] Compound 1-1 (10.0 g, 99 mmol, 1 equiv.) was dissolved in DCM at 0 °C. TsCl (20.8 g, 109 mmol, 1.1 equiv.) and Et_3N (20.8 mL, 149 mmol, 1.5 equiv.) were added slowly and the reaction was allowed to heat to room temperature. Reaction was stirred at room temperature for 16 hours. The mixture was extracted with CH_2Cl_2 (3×500 mL). The combined organic fractions were dried over sodium sulfate, filtered, and concentrated via rotary evaporation. The crude product was purified on a silica column (5:1 Hex:EA) to afford 15.1g (60%) of 3-azidopropyl 4-methylbenzenesulfonate as a colorless liquid. **^{1}H NMR** (400 MHz,

Chloroform-*d*) δ 7.87-7.75 (m, 2H), 7.46 – 7.34 (m, 2H), 4.13 (t, *J* = 5.9 Hz, 2H), 3.40 (t, *J* = 6.5 Hz, 2H), 2.48 (s, 3H), 1.91 (p, *J* = 6.2 Hz, 2H).

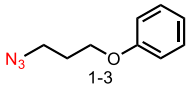

1-3

3-azidopropoxy)benzene (1-3)[53] Phenol (1 g, 10.6 mmol, 1 equiv.) was dissolved in MeCN(35mL). Compound 1-2 (5.4 g, 21.2 mmol, 2 equiv.) and KOH (2.4 g, 42.4 mmol, 4 equiv.) was added in one portion. The reaction was allowed to stir at reflux for 16 hours. The crude reaction cooled to room temperature and poured into H_2O (100mL). The mixture was extracted with DCM (3x100 mL) and washed with H_2O (2x100 mL). The combined organic fractions were dried over sodium sulfate, filtered, and concentrated via rotary evaporation. The crude product was purified on a silica column (9:1 Hex:EA) to afford 1.7g (90%) of 3-azidopropoxy)benzene as a pale-yellow oil. **^{1}H NMR** (500 MHz, Chloroform-d) δ 7.30 (ddd, J = 8.6, 7.4, 1.2 Hz, 2H), 6.96 (ddq, J = 8.6, 7.4, 1.3 Hz, 1H), 6.91 (dq, J = 8.8, 1.3 Hz, 2H), 4.06 (t, J = 5.9 Hz, 2H), 3.53 (t, J = 6.7 Hz, 2H), 2.06 (p, J = 6.3 Hz, 2H).

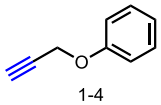

1-4

(prop-2-yn-1-yloxy)benzene (1-4)[54] Phenol (5 g, 53 mmol, 1 equiv.) was dissolved in acetone (200mL). Propargyl bromide (9.5 mL, 63.6 mmol, 1.2 equiv.) was added dropwise, then K_2CO_3 (29.3 g, 212 mmol, 4 equiv.) was added slowly and the reaction as allowed to stir for 16 hours at 60°C. The reaction was allowed to cool to room temperature and was filtered through a plug of celite. The solvent was removed under

reduced pressure. The reaction afforded 6.16g (88%) of (prop-2-yn-1-yloxy)benzene as a colorless oil. **^{1}H NMR** (500 MHz, Chloroform-*d*) δ 7.34 – 7.28 (m, 2H), 7.00 (dd, *J* = 10.5, 7.8 Hz, 3H), 4.70 (d, *J* = 2.3 Hz, 2H), 2.52 (t, *J* = 2.3 Hz, 1H).

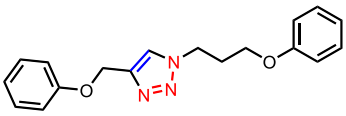

A-1

4-(phenoxymethyl)-1-(3-phenoxypropyl)-1H-1,2,3-triazole (A-1)[55] Compounds 1-3 (1.5 g, 11.4 mmol, 1 equiv.) and 1-4 (2.9 g, 16.5 mmol, 1.45 equiv.) were dissolved in DCM (12mL). $(PPh_3)_2CuOAc$ (0.37 g, 0.6 mmol, 0.05 equiv.) was added and the reaction was allowed to stir at room temperature for 16 hours. The solvent was removed, and the crude material was purified by flash chromatography (5:1 Hex:EA) to afford 3.3g (95%) of 4-(phenoxymethyl)-1-(3-phenoxypropyl)-1H-1,2,3-triazole as a white solid. **^{1}H NMR** (500 MHz, Chloroform-*d*) δ 7.28 (ddd, *J* = 8.8, 7.4, 1.7 Hz, 4H), 7.00 – 6.94 (m, 4H), 6.89 – 6.84 (m, 2H), 5.23 (s, 2H), 4.61 (t, *J* = 6.9 Hz, 2H), 3.97 (t, *J* = 5.7 Hz, 2H), 2.46 – 2.37 (m, 2H).

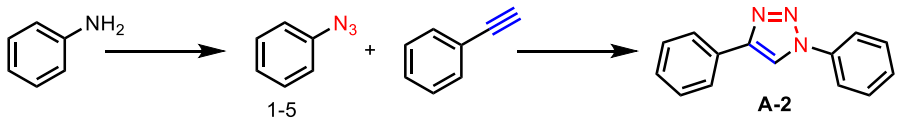

1-5 A-2

1-5

azidobenzene (1-5)[56] Aniline (2 mL, 21.9 mmol, 1 equiv.) was added to ethyl acetate (40 mL) and H_2O (5 mL) and cooled to 0 °C. 12 mL of HCl was added and allowed

to stir at 0 °C for 10 minutes. $NaNO_2$ (2.55 g, 37 mmol, 1.7 equiv.) was dissolved in H_2O (8 mL) and added over 3 minutes. The reaction was allowed to stir for 30 minutes. NaN_3 (2.4 g, 37 mmol, 1.7 equiv.) was dissolved in H_2O (8 mL) and added over 5 minutes. The reaction was allowed to stir for 30 minutes. The crude reaction mixture was poured into H_2O (50 mL) and extracted with ethyl acetate (2x50 mL) and washed with H_2O. The combined organic fractions were dried over sodium sulfate, filtered, and concentrated via rotary evaporation to afford 1.8g (68%) of azidobenzene as a pale-yellow oil. **^{1}H NMR** (500 MHz, Chloroform-*d*) δ 7.42 – 7.35 (m, 2H), 7.17 (td, *J* = 7.5, 1.1 Hz, 1H), 7.09 – 7.03 (m, 2H).

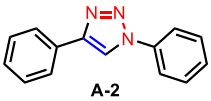

A-2

1,4-diphenyl-1H-1,2,3-triazole (A-2)[57] Compound 1-5 (1.5 g, 12.6 mmol, 1.1 equiv.) was dissolved in DCM (13 mL). Ethynylbenzene (1.7 g, 11.5 mmol, 1 equiv.) and $(PPh_3)_2CuOAc$ (0.74g, 1.2 mmol, 0.1 eq.) was added ice and the reaction was allowed to warm to room temperature and stir at room temperature for 16 hours. The crude mixture was poured into H_2O (40 mL) and extracted with ethyl acetate (3x30 mL). The organic layer was washed with brine (2x30 mL) and the combined organic fractions were dried over sodium sulfate, filtered, and concentrated via rotary evaporation to afford 2.0 g (80%) of 1,4-diphenyl-1H-1,2,3-triazole as an off-white solid. **^{1}H NMR** (500 MHz, Chloroform-*d*) δ 8.28 (s, 1H), 7.94 (d, *J* = 7.7 Hz, 2H), 7.82 (d, *J* = 7.9 Hz, 2H), 7.73 – 7.34 (m, 8H).

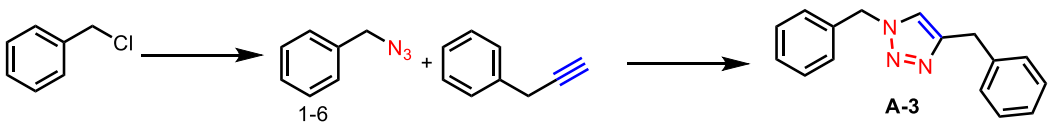

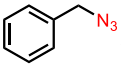

benzyl azide (1-6)[58] NaN_3 (2.8 g, 43.4 mmol, 1.1 equiv.) was added to stirring solution of benzyl chloride (4.6 mL,39.5 mmol, 1 equiv.) in DMSO (115mL). The reaction was heated at 95°C for 24 hours. The reaction was quenched with H_2O (50 mL), extracted with diethyl ether (3x30 mL), washed with H_2O (2x30 mL) and brine (1x30 mL). The combined organic fractions were dried over sodium sulfate, filtered, and concentrated via rotary evaporation to afford 1.7 g (32%) (azidomethyl)benzene as a pale-yellow liquid. **^{1}H NMR** (500 MHz, Chloroform-*d*) δ 7.42 – 7.31 (m, 5H), 4.35 (s, 2H).

1,4-dibenzyl-1H-1,2,3-triazole (A-3)[59] Compound 1-6 (1.7 g, 12.8 mmol, 1.1 equiv.) was dissolved in DCM (12 mL) and prop-2-yn-1-ylbenzene (1.45 mL, 11.7 mmol, 1 equiv.) was added dropwise. $(PPh_3)_2CuOAc$ (0.75 g, 1.2 mmol, 0.1 equiv.) was added and the reaction was allowed to stir at room temperature for 16 hours. The crude mixture was poured into H_2O (40 mL) and extracted with ethyl acetate (3x30 mL). The organic layer was washed with brine (2x30 ml) and the combined organic fractions were dried over sodium sulfate, filtered, and concentrated via rotary evaporation to afford 2.9 g (>99%) of 1,4-diphenyl-1H-1,2,3-triazole as an off- white solid. **^{1}H NMR** (500 MHz, Chloroform-d)7 δ 7.34 (m, 2H), 7.28 (m, 2H), 7.24 (m, 5H), 7.09 (m, 1H), 5.46 (s, 2H), 4.07 (s, 2H). (500 MHz, Chloroform-d) δ 7.39 – 7.18 (m, 22H), 5.49 (s, 4H).

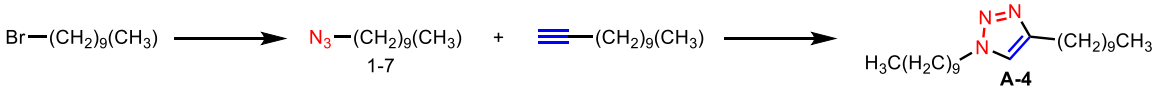

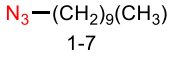

1-azidodecane (1-7)[60] 1-bromodecane (4.8 mL, 22.6 mmol, 1 equiv.) was dissolved in DMSO (100mL). NaN_3 (2.2 g, 33.9 mmol, 1.5 equiv.) was added and the reaction was allowed to stir at 95°C for 16 hours. The product was extracted with diethyl ether (1x100 mL) was the organic layer was washed with water (2x50 mL) and brine (1x50 mL). The combined organic fractions were dried over sodium sulfate, filtered, and concentrated via rotary evaporation to afford 3.4 g (83%) of 1-azidodecane as a pale-yellow liquid. **^{1}H NMR** (500 MHz, Chloroform-d) δ 3.25 (t, J = 7.0 Hz, 2H), 1.60 (p, J = 7.0 Hz, 2H), 1.39 – 1.22 (m, 14H), 0.91 – 0.86 (m, 3H).

1,4-didecyl-1H-1,2,3-triazole (A-4) Compound 1-7 (3.4 g, 18.7 mmol, 1.1 equiv.) was dissolved in DCM (17 mL). Dodec-1-yne (3.6 mL, 17.0 mmol, 1 equiv.) and $(PPh_3)_2CuOAc$ (1.1g, 1.7 mmol, 0.1 eq.) were added on ice and the reaction was allowed to warm to room temperature and stir at room temperature for 16 hours. The crude mixture was poured into H_2O (40 mL) and extracted with ethyl acetate (3x30 mL). The organic layer was washed with brine (2x30 ml) and the combined organic fractions were dried over sodium sulfate, filtered, and concentrated via rotary evaporation to afford 5.5g (85%) of 1,4-diphenyl-1H-1,2,3-triazole as an off-white solid. **^{1}H NMR** (500 MHz,

Chloroform-*d*) δ 4.45 (s, 4H), 2.76 (s, 4H), 2.10 – 1.66 (m, 4H), 1.57 – 1.00 (m, 24H), 0.88 (m, 6H).

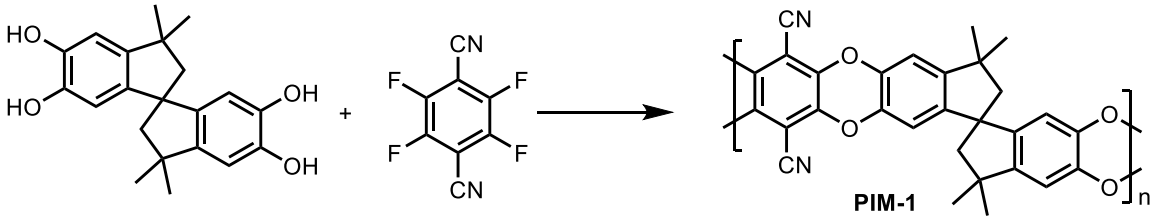

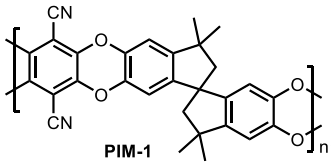

PIM-1[61] Tetrafluoroterephthalonitrile was purified via sublimation before use. 5,5',6,6'-tetrahydroxy-3,3,3',3'-tetramethyl1,1'-spirobisindane was purified via reprecipitation from acetone into DCM before use. To a three-neck round-bottom flask was added tetrafluoroterephthalonitrile (6.02 g, 30.1 mmol, 1 equiv.), 5,5',6,6'-tetrahydroxy-3,3,3',3'-tetramethyl1,1'-spirobisindane (10.25 g, 30.1 mmol, 1 equiv.) and anhydrous DMF (200 mL) under argon. The mixture was stirred at 65 °C until the complete dissolution of both monomers. Potassium carbonate (10.25 g, 75.3mmol, 2.5 equiv.) was then added and the reaction mixture was stirred for 72 hours. After cooling to room temperature, the reaction mixture was poured into H_2O (300 mL) and the precipitate was collected by vacuum filtration. The crude PIM-1 was then dissolved in chloroform (400 mL) and precipitated from MeOH (600 mL). The product was dried in an oven at 110 °C overnight to give 11 g (75%) PIM-1 as a bright yellow solid. **^{1}H NMR** (500 MHz, Chloroform-*d*) δ 6.89 – 6.73 (m, 2H), 6.42 (s, 2H), 2.33 (d, *J* = 16.3 Hz, 2H), 2.25 – 2.03 (m, 2H), 1.34 (d, *J* = 29.5 Hz, 12H).

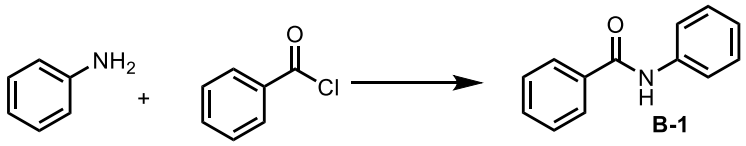

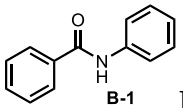

N-phenylbenzamide (B-1)[62] Benzoyl chloride (13.1 mL, 112.8 mmol, 1.05 equiv.) was added dropwise to a mixture of aniline (9.8 mL, 107.4 mmol, 1 equiv.), Et_3N (15.7 mL, 112.8 mmol, 1.05 equiv.), and DCM (215mL) at 0 °C. and the reaction was allowed to warm to room temperature and stir for 16 hours. H_2O was added (100 mL) and the reaction was extracted with DCM (2x100 mL). The organic layer was washed with 1M HCl (1x200 mL) and sodium bicarbonate (1x200 mL). The combined organic fractions were dried over sodium sulfate, filtered, and concentrated via rotary evaporation. The crude product was washed with hexane and filtered to afford 20.56 g (97%) of N-phenylbenzamide as a white solid.**^{1}H** (500 MHz, DMSO-d_6) δ 10.25 (s, 1H), 8.00 – 7.91 (m, 2H), 7.79 (d, J = 8.0 Hz, 2H), 7.60 (td, J = 7.4, 1.5 Hz, 1H), 7.57 – 7.50 (m, 2H), 7.36 (t, J = 7.7 Hz, 2H), 7.11 (td, J = 7.4, 1.2 Hz, 1H).

2.7.3 Characterization

2.7.3.1 General Analytical Information

NMR spectra were obtained on Brüker DRX-500 and a Brüker AV3-400 instrument in deuterated solvents and referenced to the signals of residual protium in the NMR solvent. Spectra were processed in TopSpin 4.0.7. GPCs were performed on a Tosoh EcoSEC HLC-8320GPC in chloroform with an RI detector.

2.7.3.2 Precursors

^{1}H NMR, $CDCl_3$, 500MHz, 294K

(1-1)

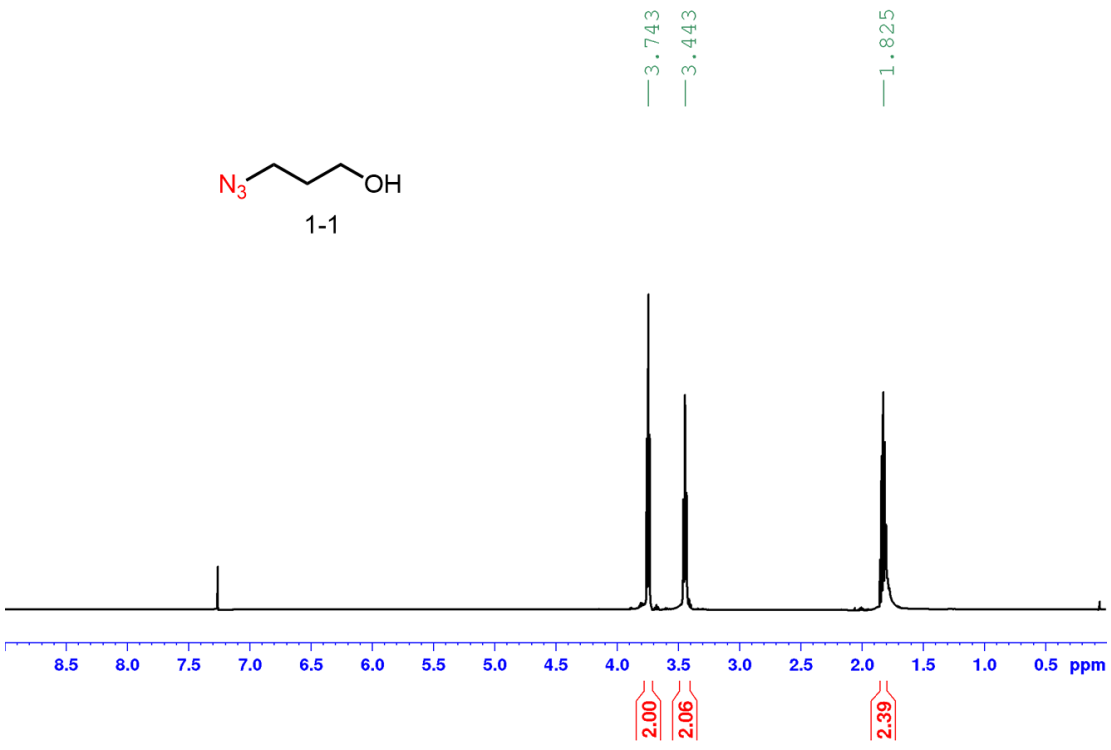

^{1}H NMR, $CDCl_3$, 400MHz, 294K

(1-2)

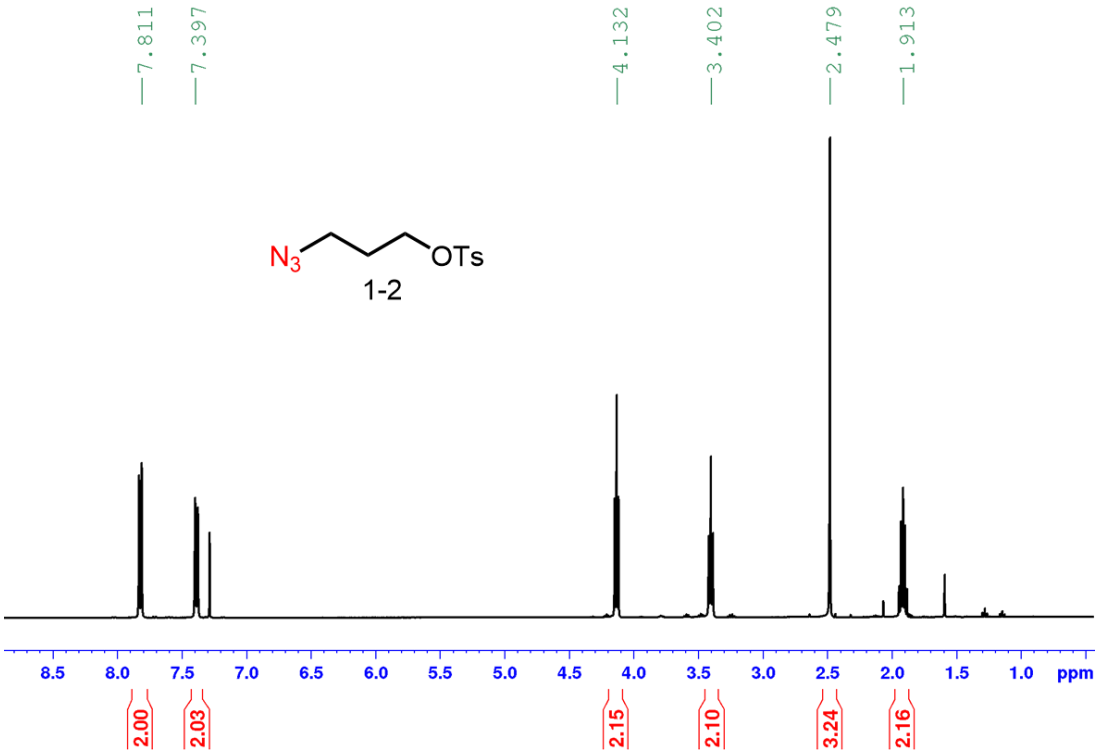

^{1}H NMR, $CDCl_3$, 500MHz, 294K

(1-3)

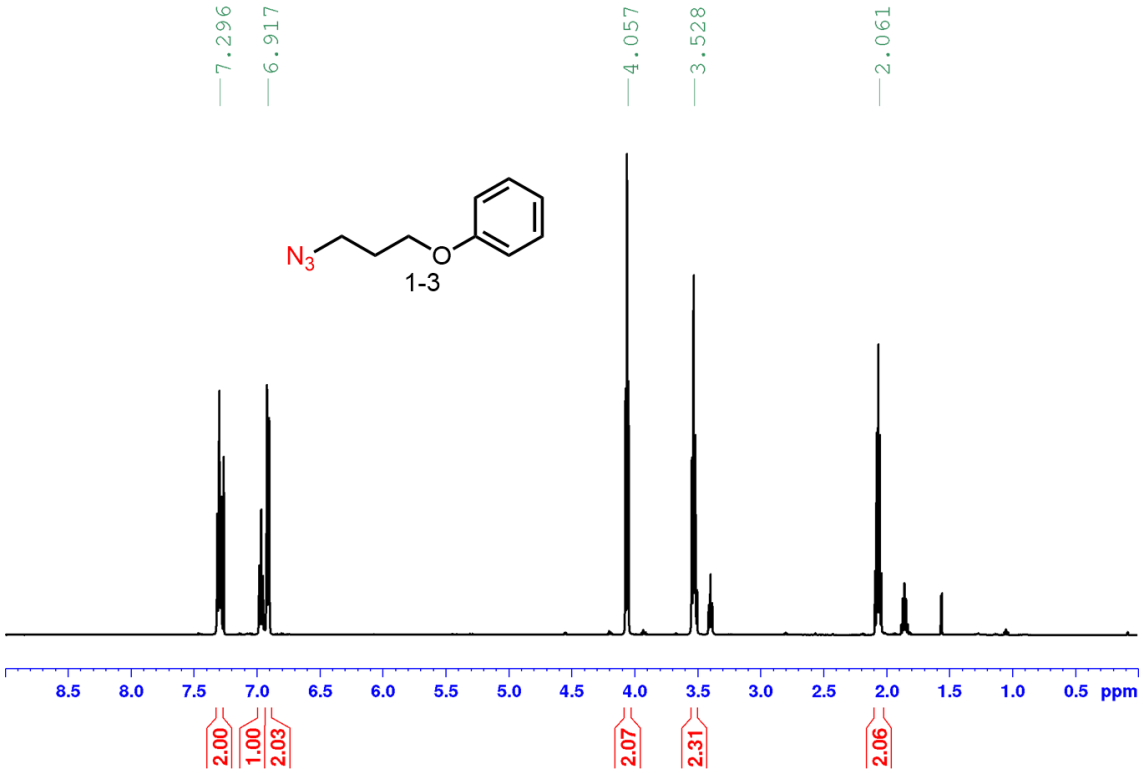

^{1}H NMR, $CDCl_3$, 500MHz, 294K

(1-4)

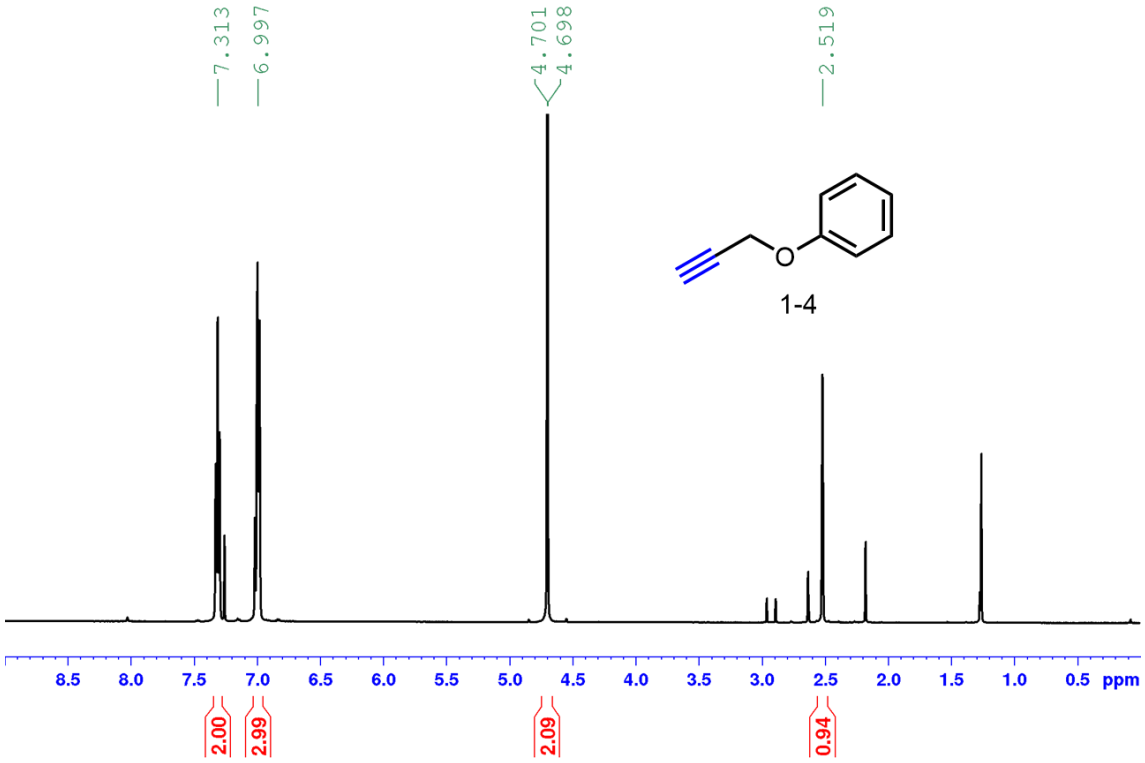

^{1}H NMR, $CDCl_3$, 500MHz, 294K

(1-5)

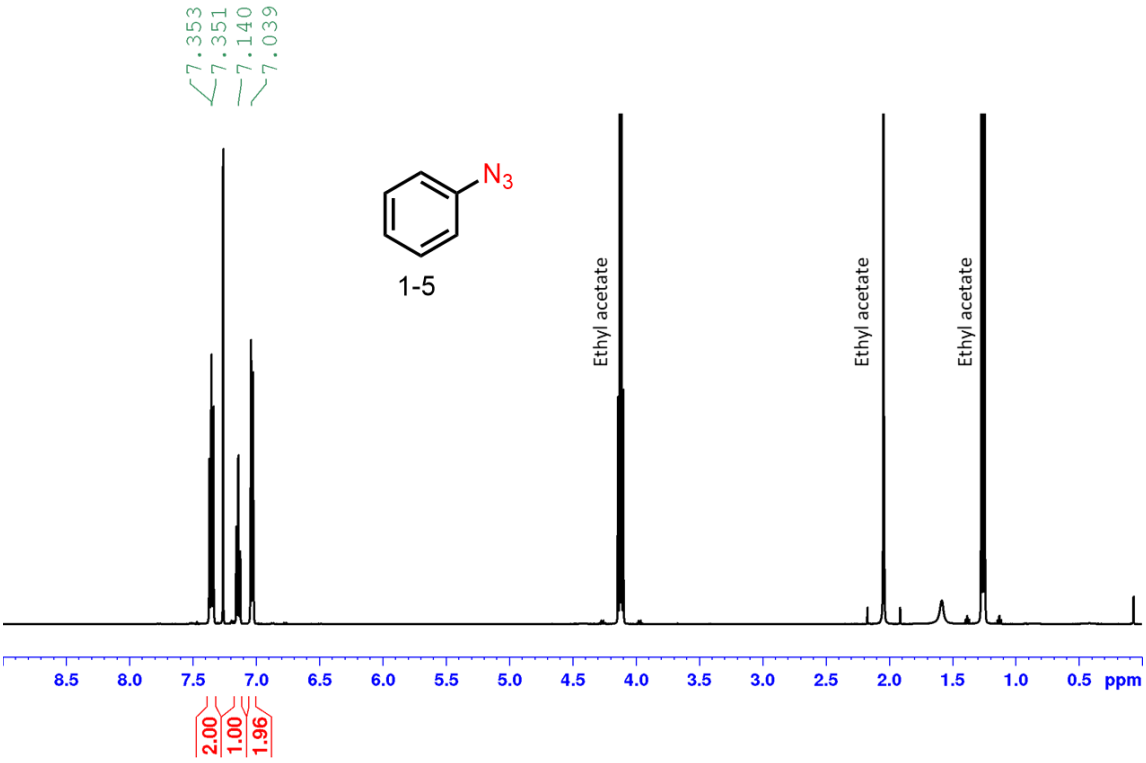

^{1}H NMR, $CDCl_3$, 500MHz, 294K

(1-6)

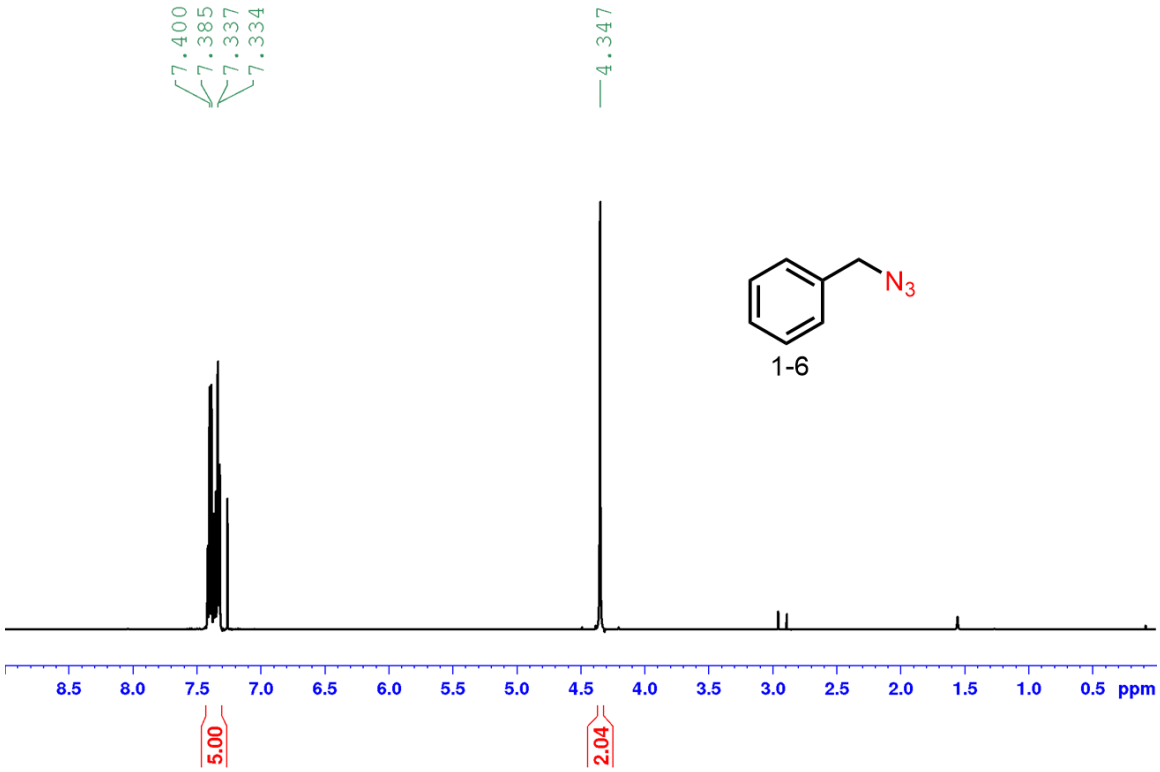

^{1}H NMR, $CDCl_3$, 500MHz, 294K

(1-7)

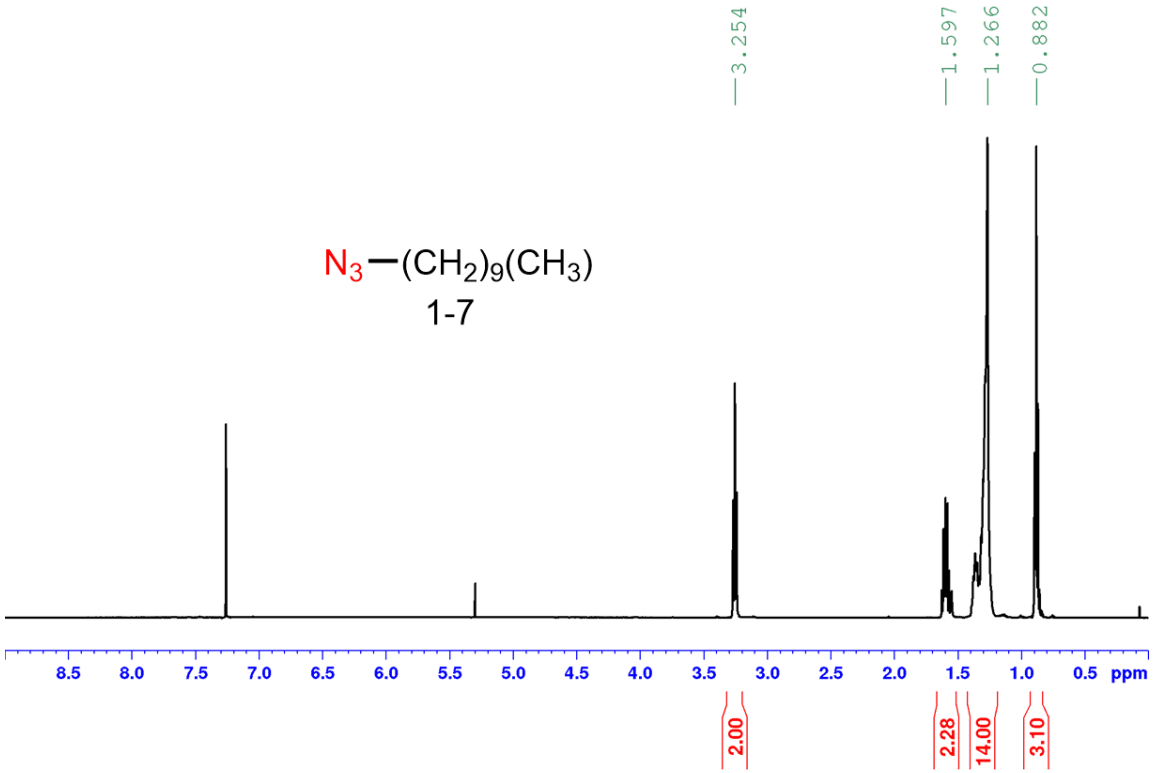

2.7.3.3 Ether Triazole

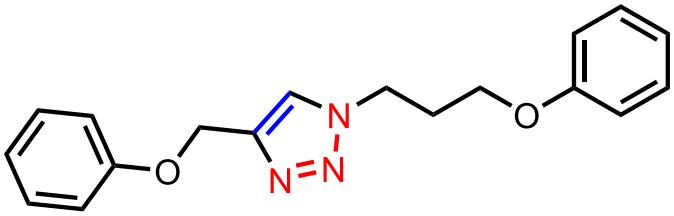

4-(phenoxymethyl)-1-(3-phenoxypropyl)-1H-1,2,3-triazole (A-1)

^{1}H NMR, $CDCl_3$, 500MHz, 294K

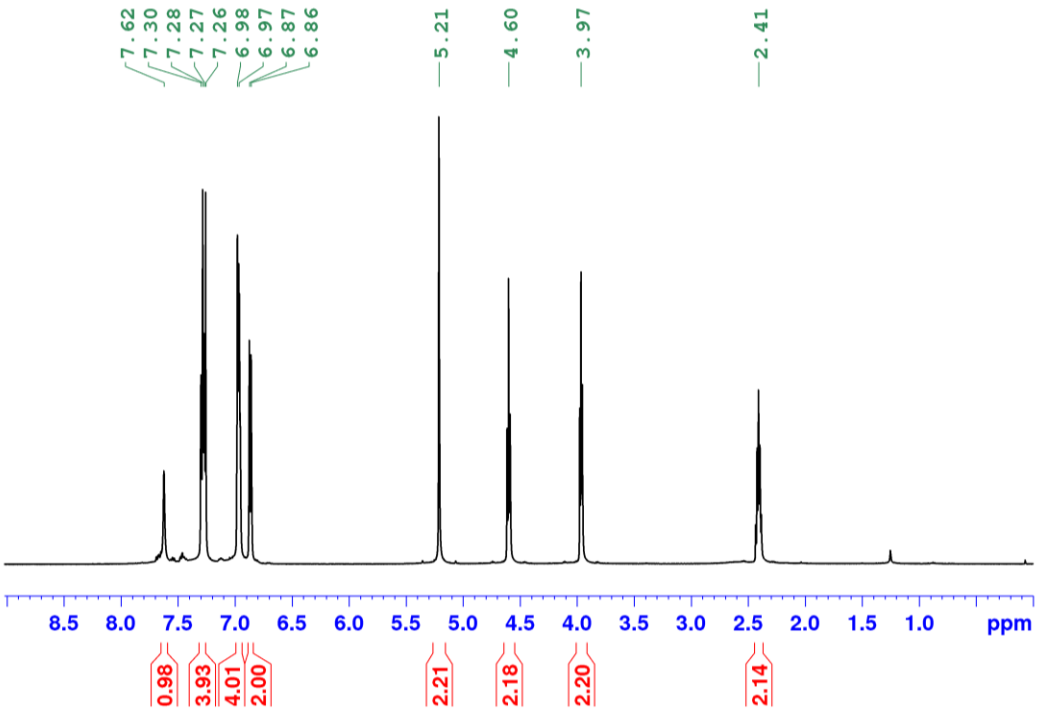

^{1}H NMR spectrum of ether triazole

Acidic Stability of Ether Triazole

Ether Precipitate After 12M HCl Reaction

^{1}H NMR, $CDCl_3$, 500MHz, 294K

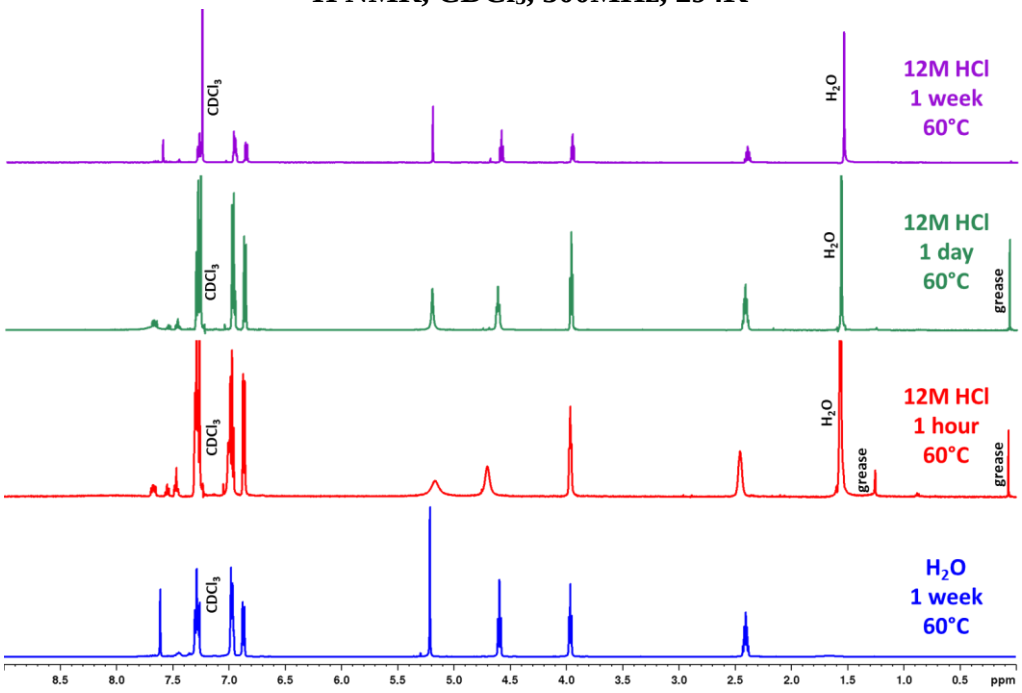

^{1}H NMR spectra of ether triazole after reacting in 12M HCl. A negative control was run in water for 1 week at 60°C (blue). Reactions were run in 12M HCl at 60°C for 1 hour (red), 1 day (green), and 1 week (purple).

Water Washes of Ether Precipitate After 12M HCl Reaction

^{1}H NMR, $CDCl_3$, 500MHz, 294K

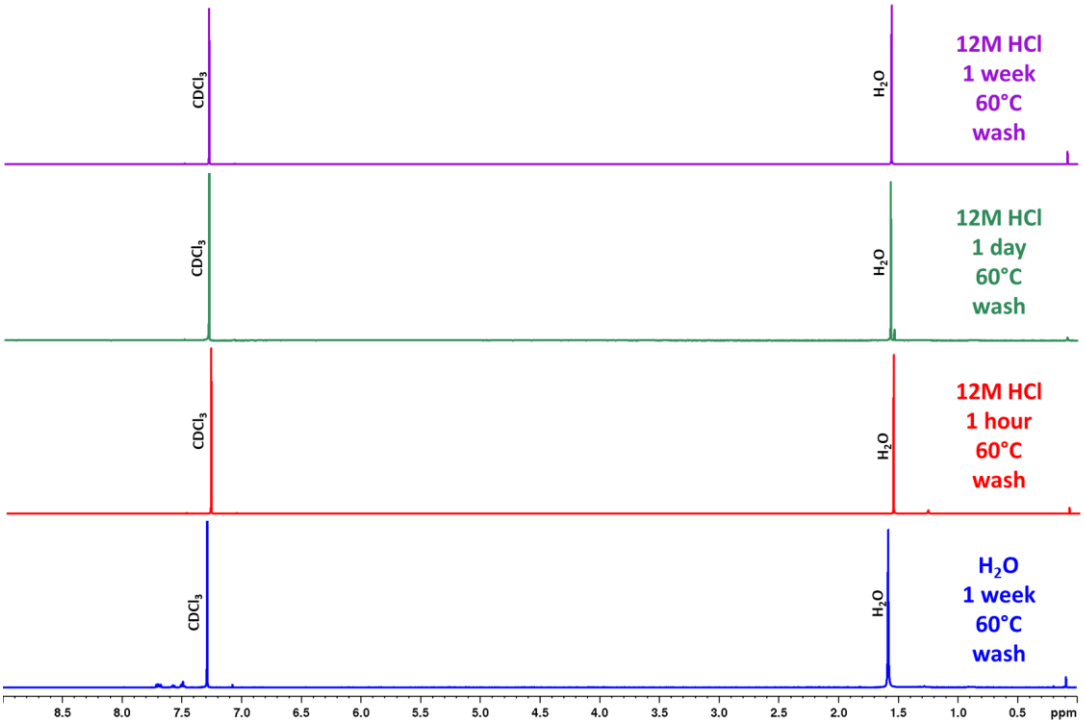

^{1}H NMR spectra of ether triazole wash after reacting in 12M HCl. A negative control was run in water for 1 week at 60°C (blue). Reactions were run in 12M HCl at 60°C for 1 hour (red), 1 day (green), and 1 week (purple).

Basic Stability of Ether Triazole

Ether Precipitate After 1M NaOH Reaction

^{1}H NMR, $CDCl_3$, 500MHz, 294K

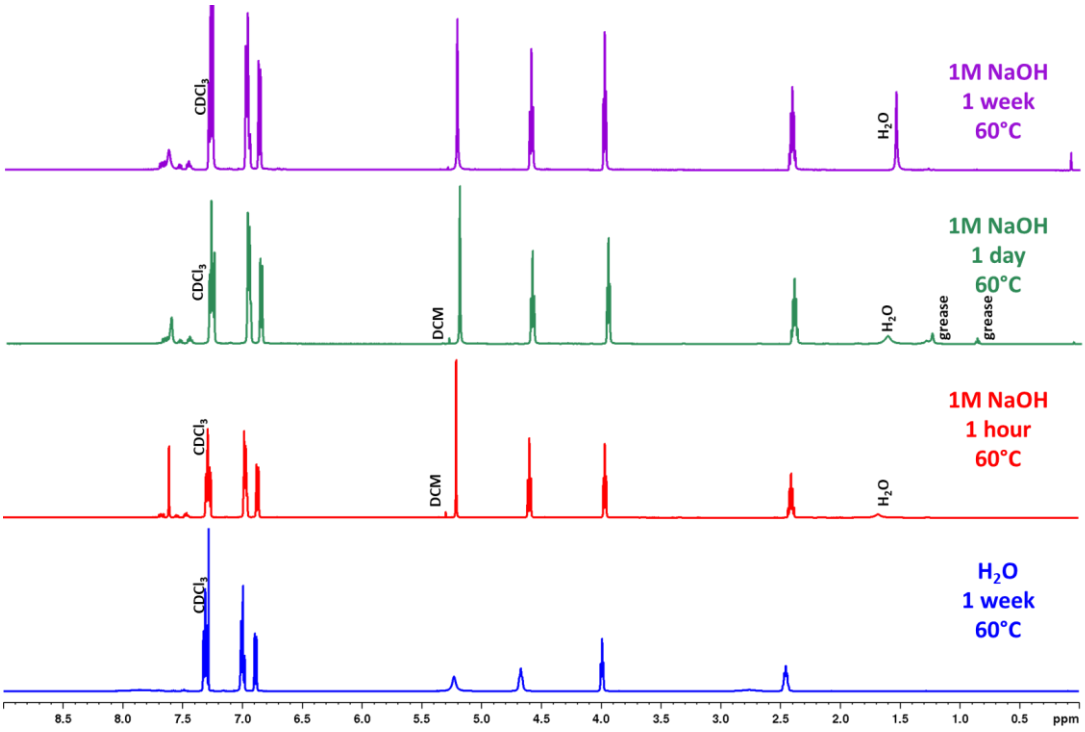

^{1}H NMR spectra of ether triazole after reacting in 1M NaOH. A negative control was run in water for 1 week at 60°C (blue). Reactions were run in 1M NaOH at 60°C for 1 hour (red), 1 day (green), and 1 week (purple).

Water Washes of Ether Precipitate After 1M NaOH Reaction

^{1}H NMR, $CDCl_3$, 500MHz, 294K

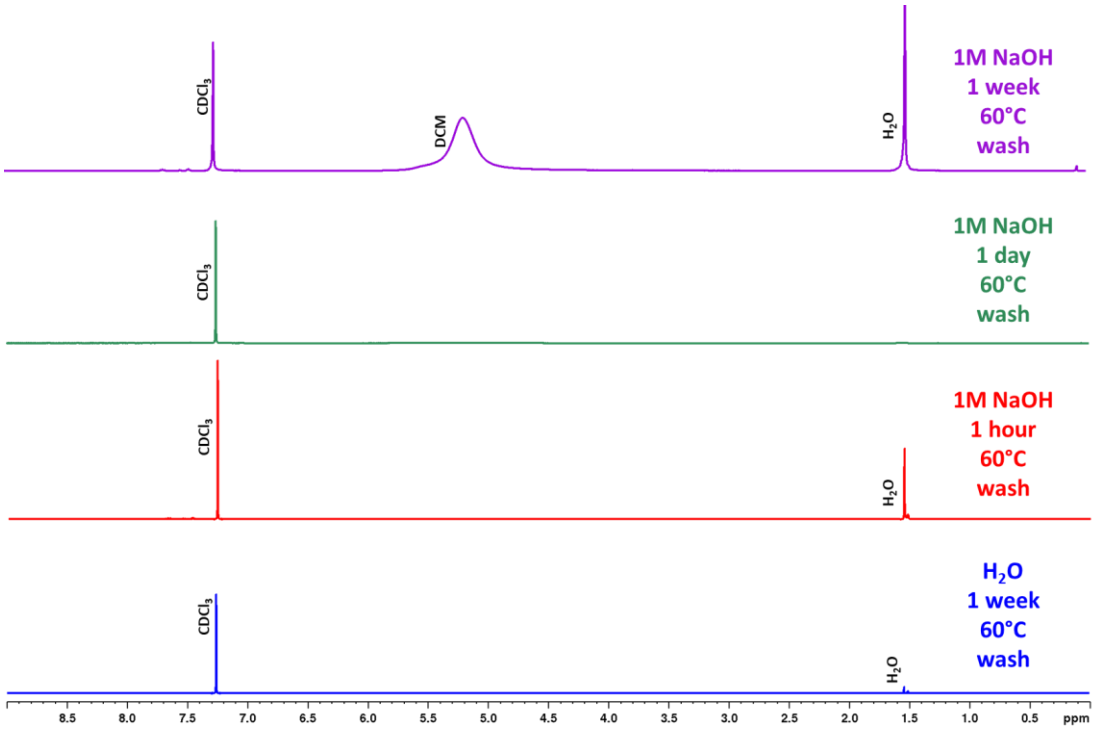

^{1}H NMR spectra of ether triazole wash after reacting in 1M NaOH. A negative control was run in water for 1 week at 60°C (blue). Reactions were run in 1M NaOH at 60°C for 1 hour (red), 1 day (green), and 1 week (purple).

Oxidative Stability of Ether Triazole

Ether Precipitate After 50,000ppm NaClO Reaction

^{1}H NMR, $CDCl_3$, 500MHz, 294K

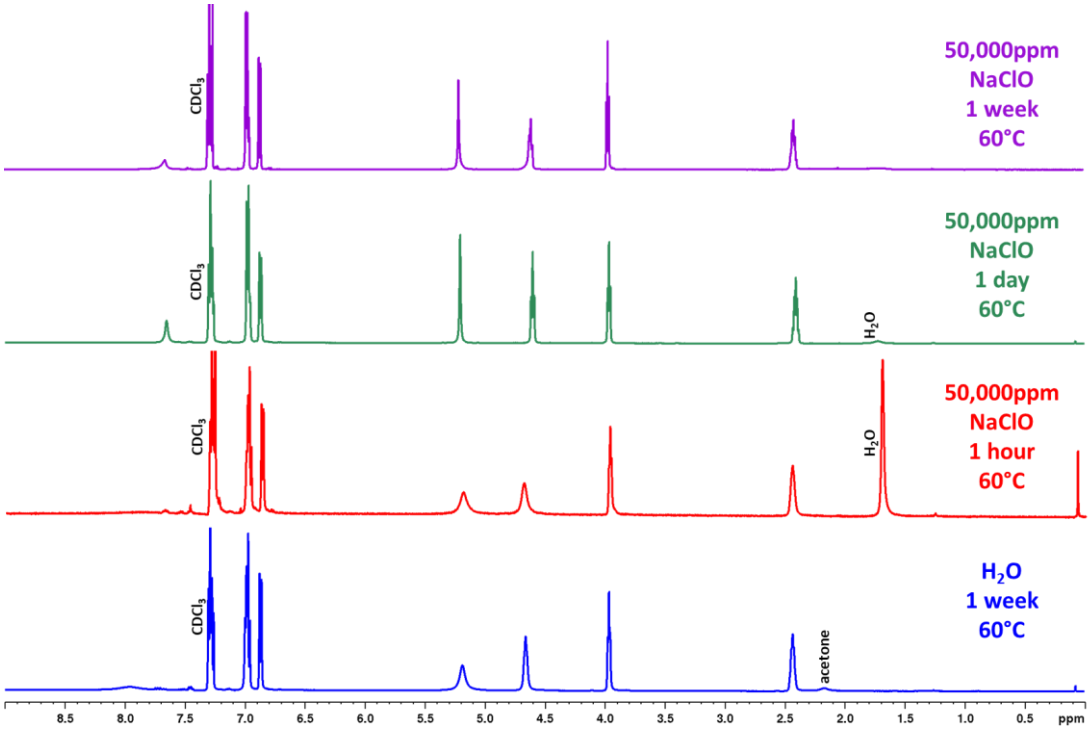

^{1}H NMR spectra of ether triazole after reacting in 50,000ppm NaClO. A negative control was run in water for 1 week at 60°C (blue). Reactions were run in 50,000ppm NaClO at 60°C for 1 hour (red), 1 day (green), and 1 week (purple).

Water Washes of Ether Precipitate After 50,000ppm NaClO Reaction

^{1}H NMR, $CDCl_3$, 500MHz, 294K

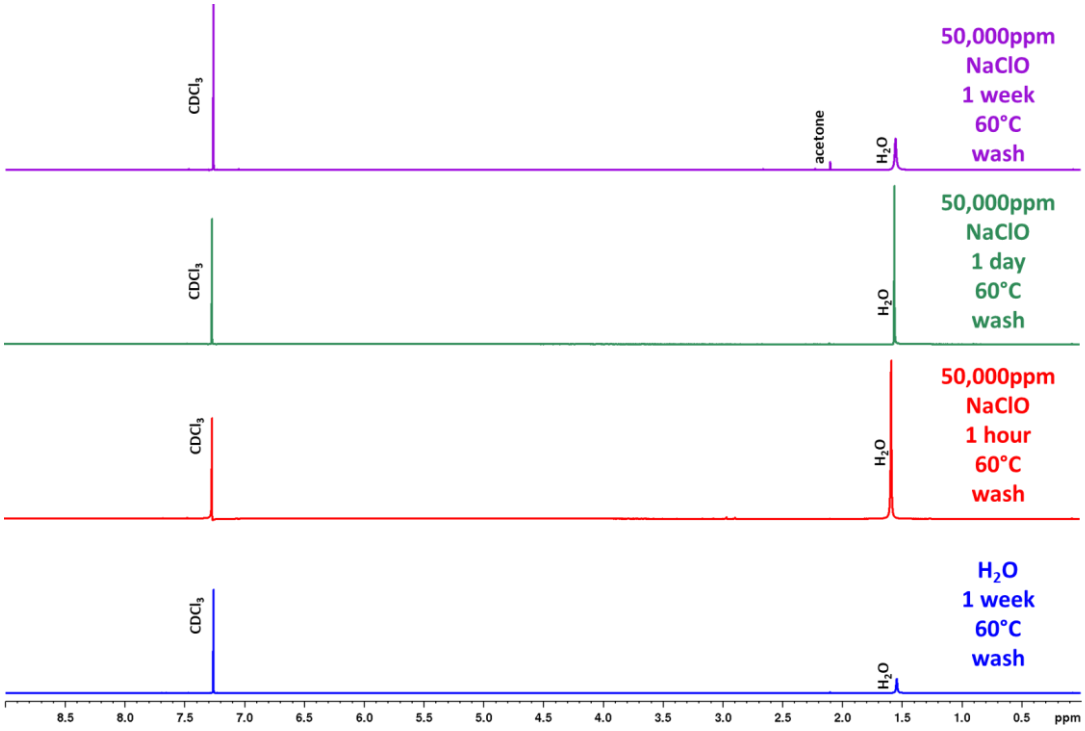

^{1}H NMR spectra of ether triazole wash after reacting in 50,000ppm NaClO. A negative control was run in water for 1 week at 60°C (blue). Reactions were run in 50,000ppm NaClO at 60°C for 1 hour (red), 1 day (green), and 1 week (purple).

2.7.3.4 Aryl Triazole

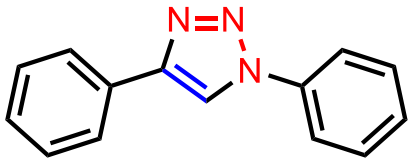

1,4-diphenyl-1H-1,2,3-triazole (A-2)

^{1}H NMR, $CDCl_3$, 500MHz, 294K

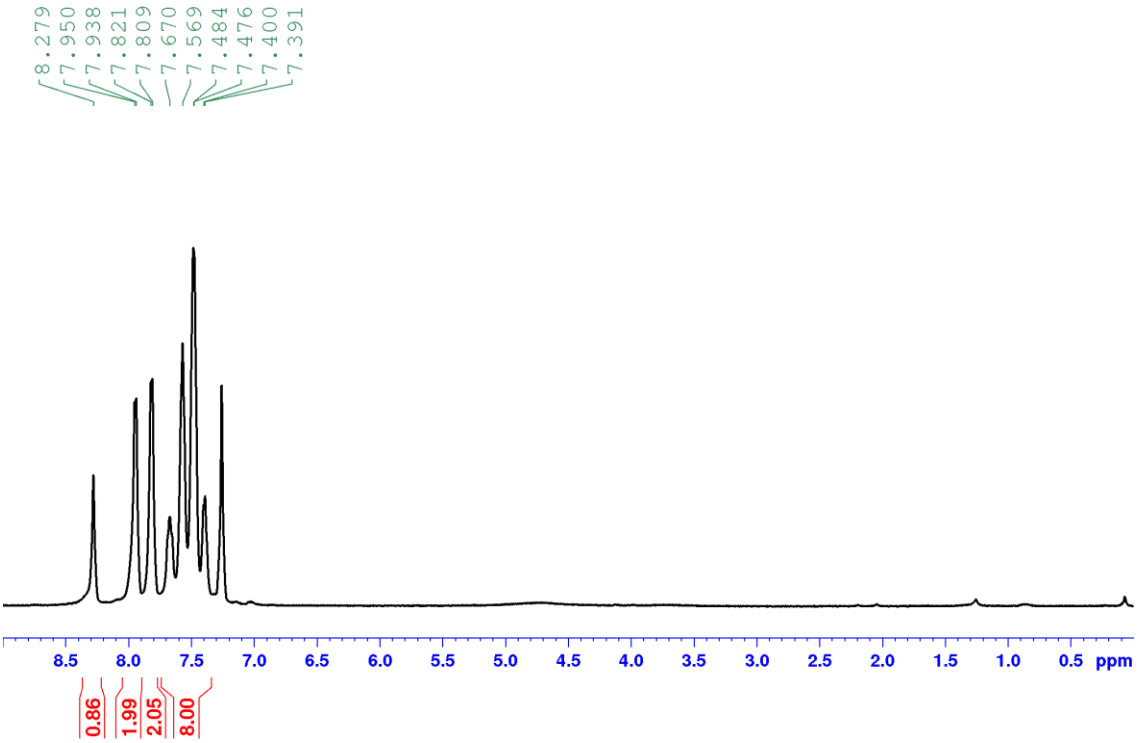

^{1}H NMR spectrum of aryl triazole

Acidic Stability of Aryl Triazole

Aryl Triazole Precipitate After 12M HCl Reaction

^{1}H NMR, $CDCl_3$, 500MHz, 294K

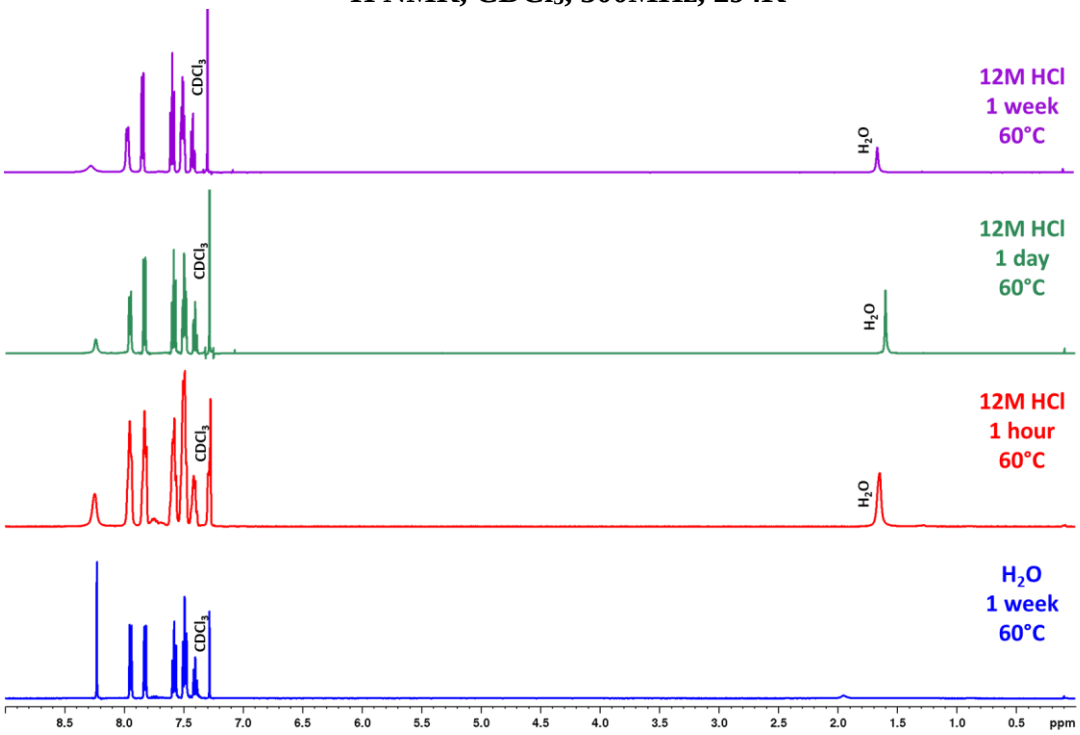

^{1}H NMR spectra of aryl triazole after reacting in 12M HCl. A negative control was run in water for 1 week at 60°C (blue). Reactions were run in 12M HCl at 60°C for 1 hour (red), 1 day (green), and 1 week (purple).

Water Washes of Aryl Triazole Precipitate After 12M HCl Reaction

^{1}H NMR, $CDCl_3$, 500MHz, 294K

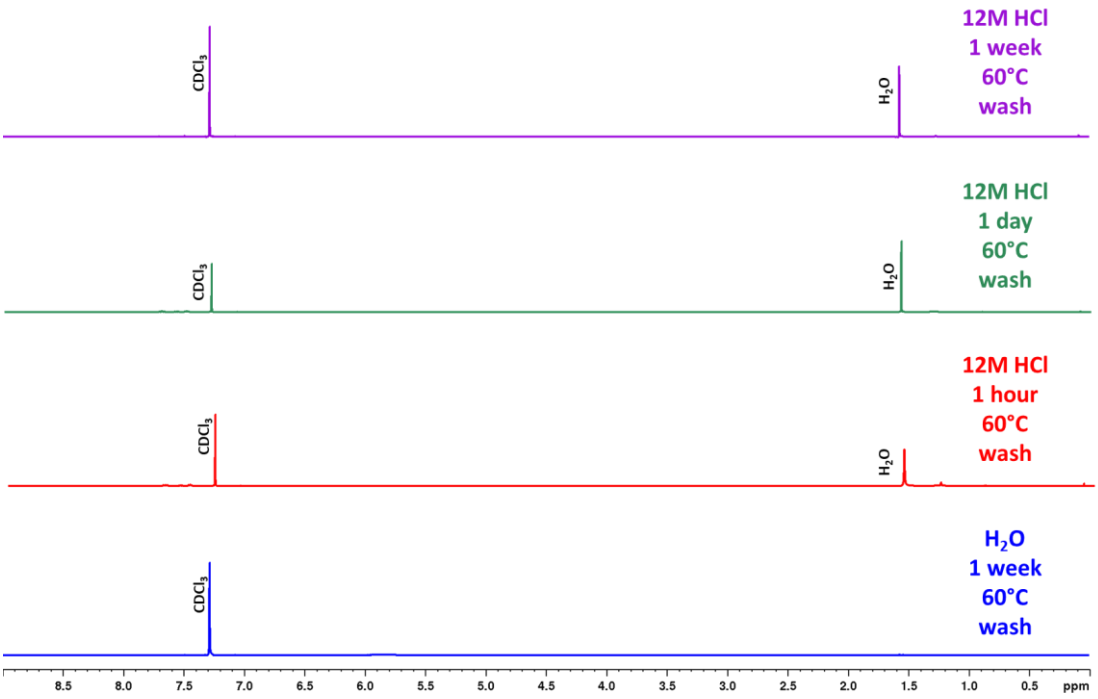

^{1}H NMR spectra of aryl triazole wash after reacting in 12M HCl. A negative control was run in water for 1 week at 60°C (blue). Reactions were run in 12M HCl at 60°C for 1 hour (red), 1 day (green), and 1 week (purple).

Basic Stability of Aryl Triazole

Aryl Triazole After 1M NaOH Reaction

^{1}H NMR, $CDCl_3$, 500MHz, 294K

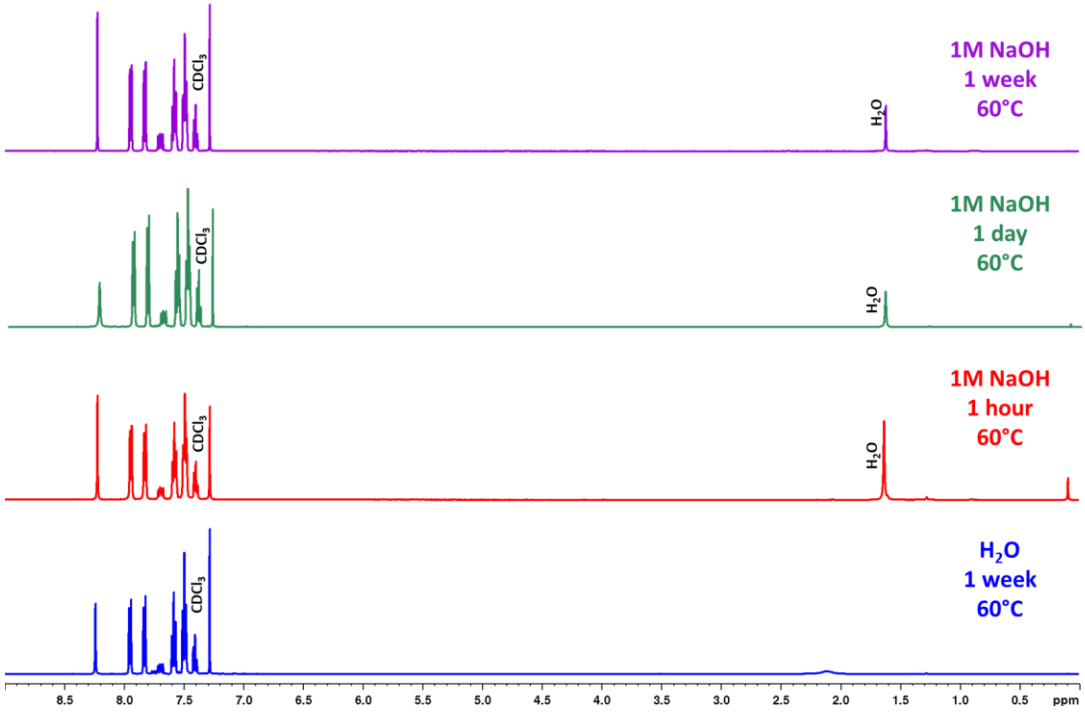

^{1}H NMR spectra of aryl triazole after reacting in 1M NaOH. A negative control was run in water for 1 week at 60°C (blue). Reactions were run in 1M NaOH at 60°C for 1 hour (red), 1 day (green), and 1 week (purple).

Water Washes of Aryl Triazole Precipitate After 1M NaOH Reaction

^{1}H NMR, $CDCl_3$, 500MHz, 294K

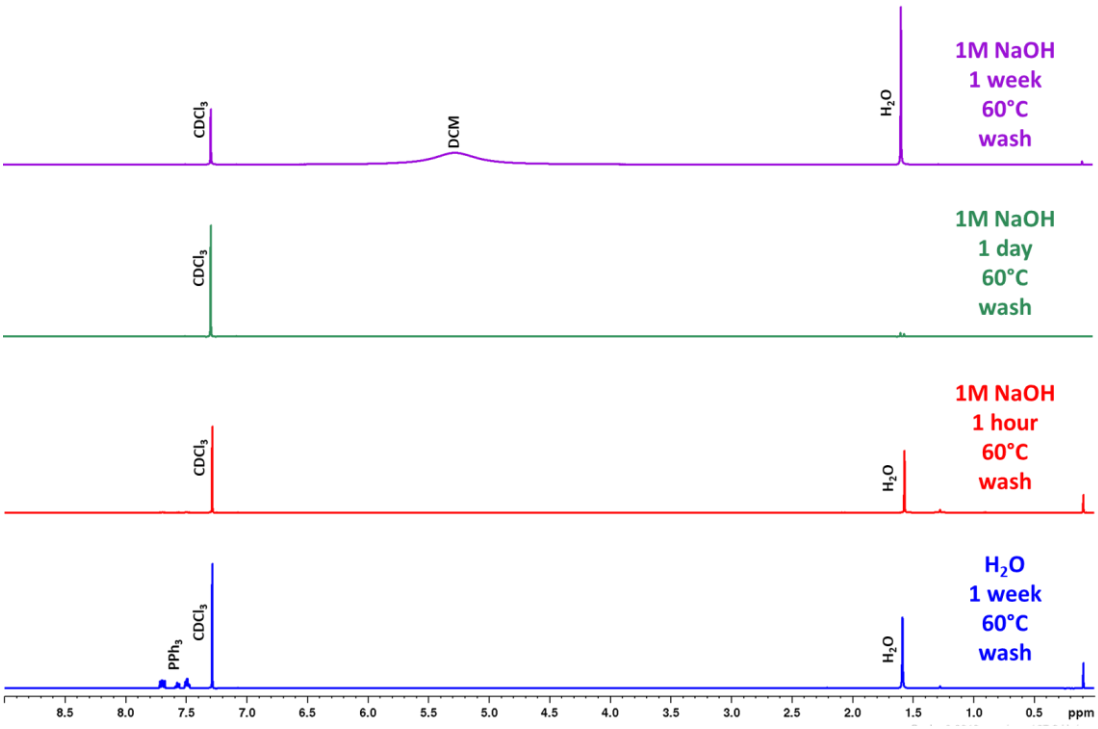

^{1}H NMR spectra of aryl triazole wash after reacting in 1M NaOH. A negative control was run in water for 1 week at 60°C (blue). Reactions were run in 1M NaOH at 60°C for 1 hour (red), 1 day (green), and 1 week (purple).

Oxidative Stability of Aryl Triazole

Aryl Triazole Precipitate After 50,000ppm NaClO Reaction

^{1}H NMR, $CDCl_3$, 500MHz, 294K

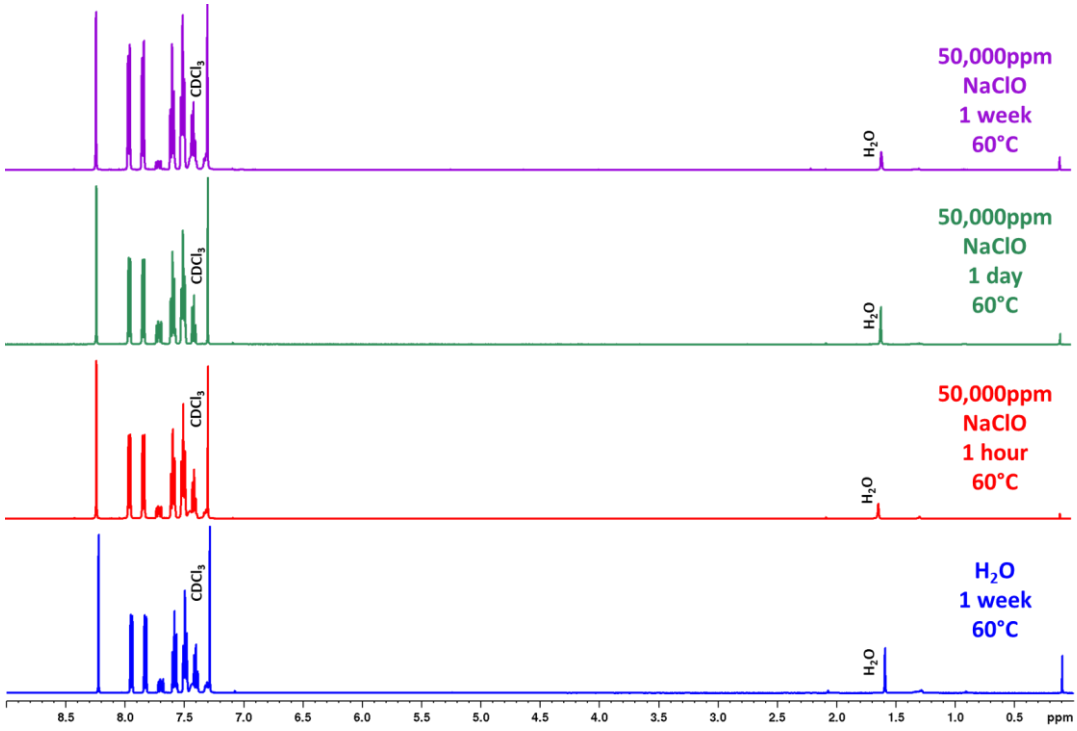

^{1}H NMR spectra of aryl triazole after reacting in 50,000ppm NaClO. A negative control was run in water for 1 week at 60°C (blue). Reactions were run in 50,000ppm NaClO at 60°C for 1 hour (red), 1 day (green), and 1 week (purple).

Water Washes of Aryl Triazole Precipitate After 50,000ppm NaClO Reaction

^{1}H NMR, $CDCl_3$, 500MHz, 294K

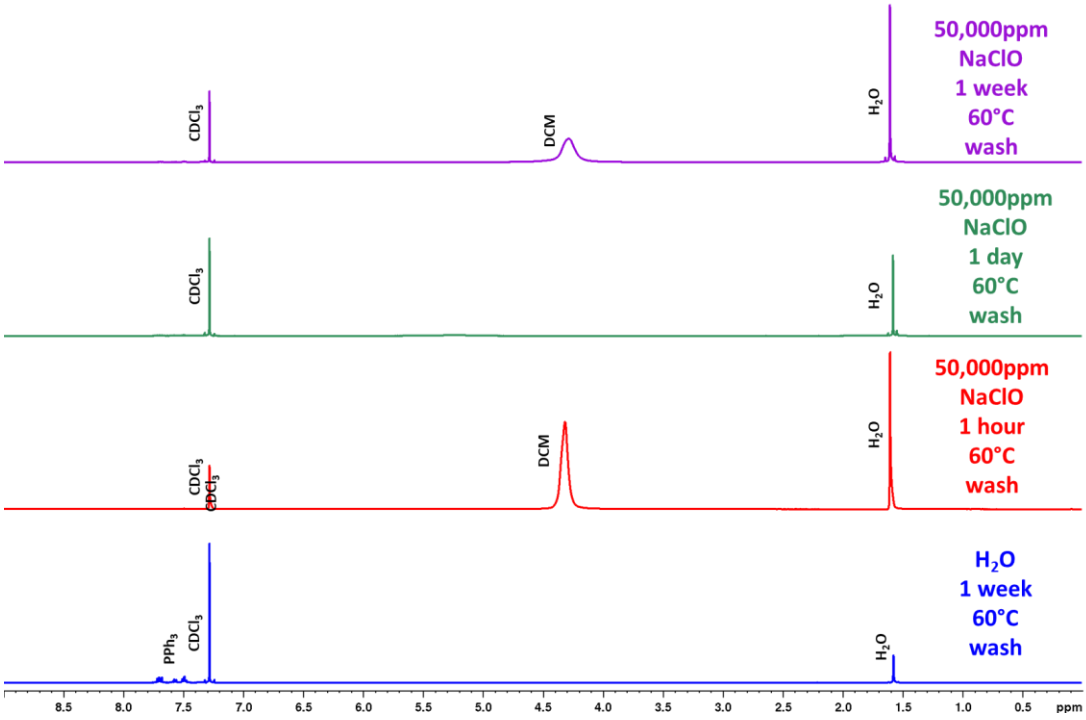

^{1}H NMR spectra of aryl triazole wash after reacting in 50,000ppm NaClO. A negative control was run in water for 1 week at 60°C (blue). Reactions were in 50,000ppm NaClO at 60°C for 1 hour (red), 1 day (green), and 1 week (purple).

2.7.3.5 Benzyl Triazole

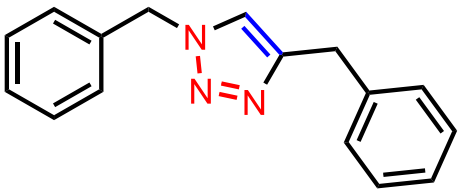

1,4-dibenzyl-1H-1,2,3-triazole (A-3)

^{1}H NMR, $CDCl_3$, 500MHz, 294K

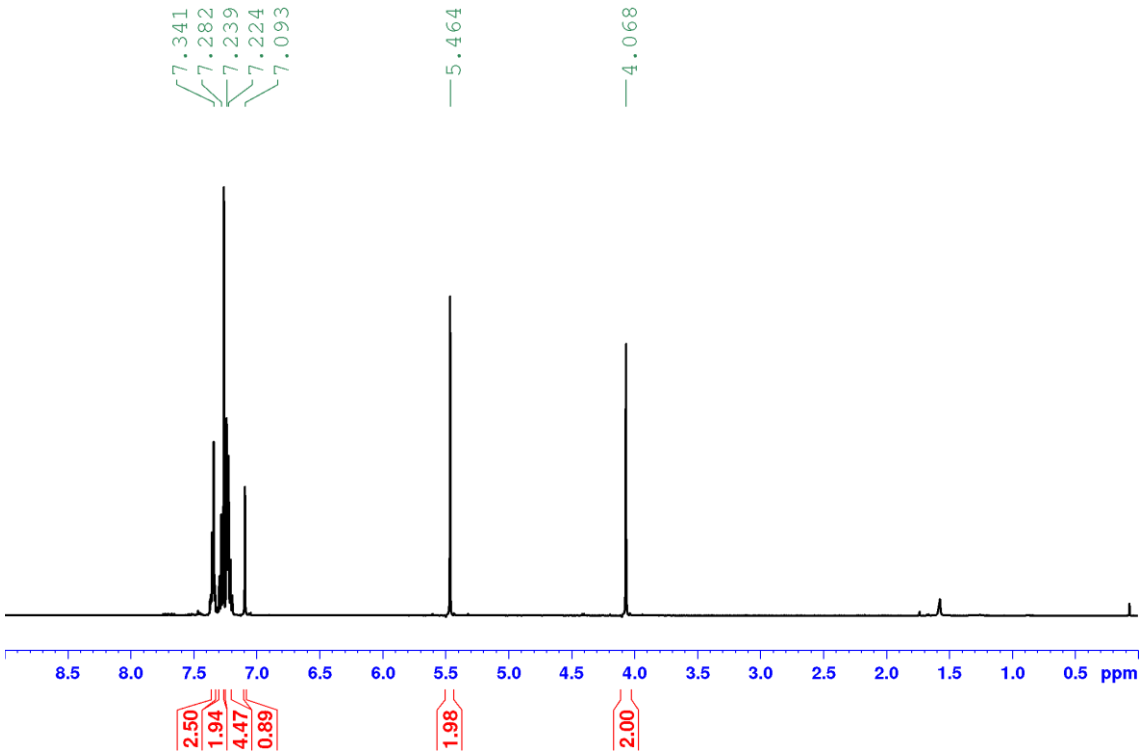

^{1}H NMR spectrum of benzyl triazole

Acidic Stability of Benzyl Triazole

Benzyl Triazole Precipitate After 12M HCl Reaction

^{1}H NMR, $CDCl_3$, 500MHz, 294K

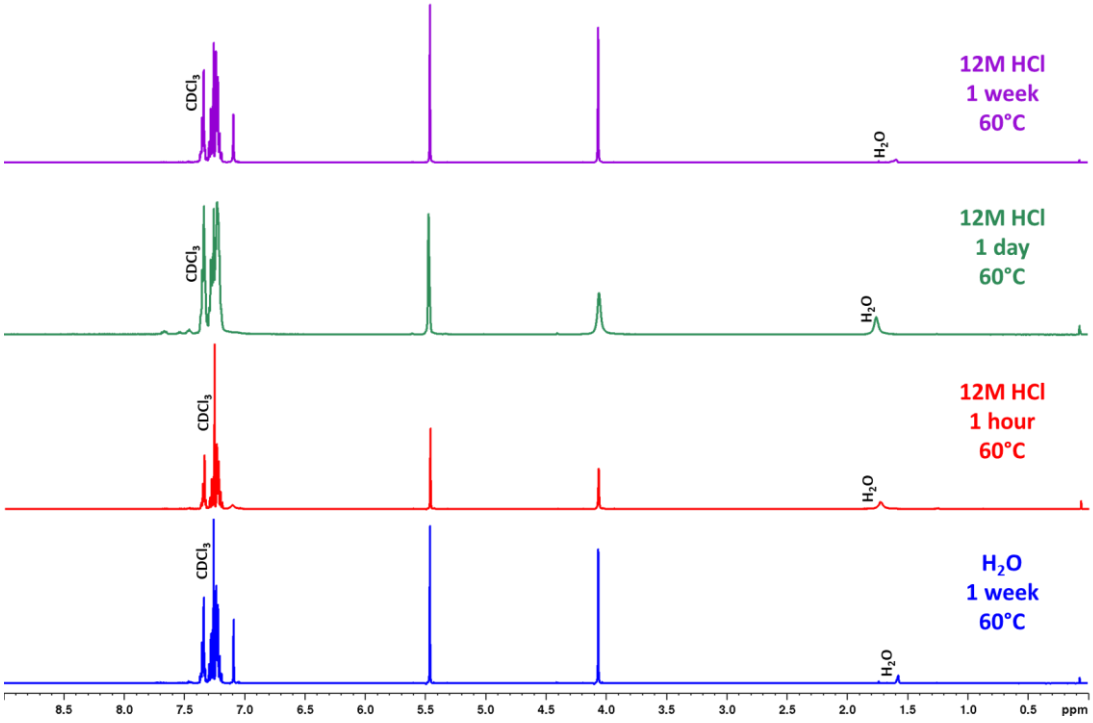

^{1}H NMR spectra of benzyl triazole after reacting in 12M HCl. A negative control was run in water for 1 week at 60°C (blue). Reactions were run in 12M HCl at 60°C for 1 hour (red), 1 day (green), and 1 week (purple).

Water Washes of Benzyl Triazole Precipitate After 12M HCl Reaction

^{1}H NMR, $CDCl_3$, 500MHz, 294K

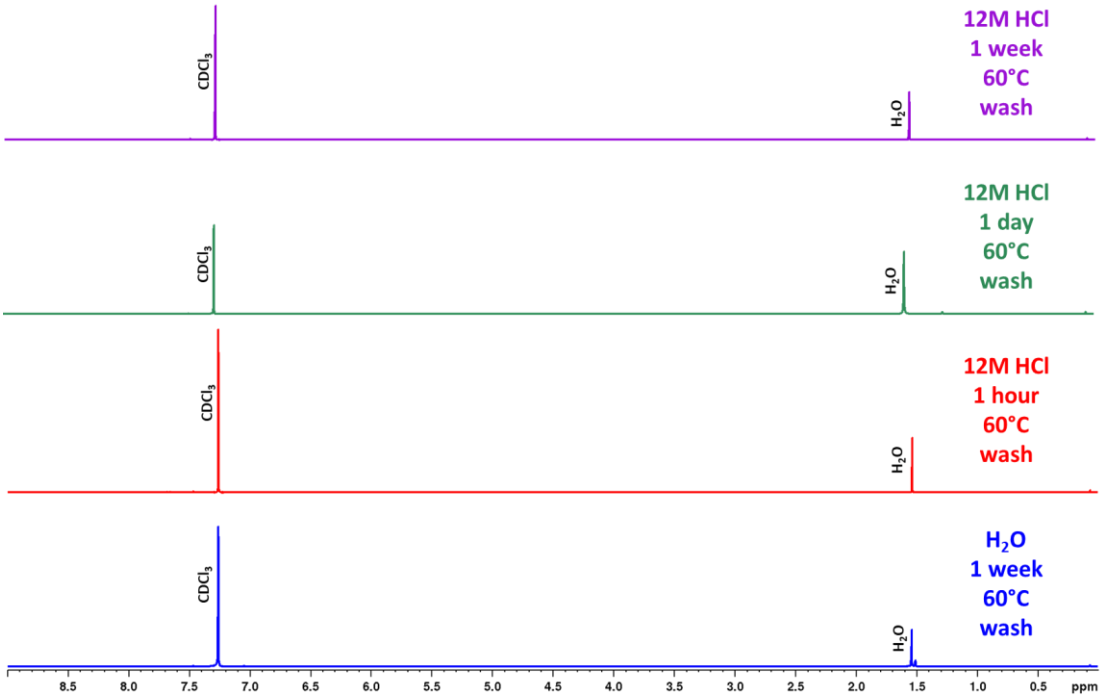

^{1}H NMR spectra of benzyl triazole wash after reacting in 12M HCl. A negative control was run in water for 1 week at 60°C (blue). Reactions were run in 12M HCl at 60°C for 1 hour (red), 1 day (green), and 1 week (purple).

Basic Stability of Benzyl Triazole

Benzyl Triazole After 1M NaOH Reaction

^{1}H NMR, $CDCl_3$, 500MHz, 294K

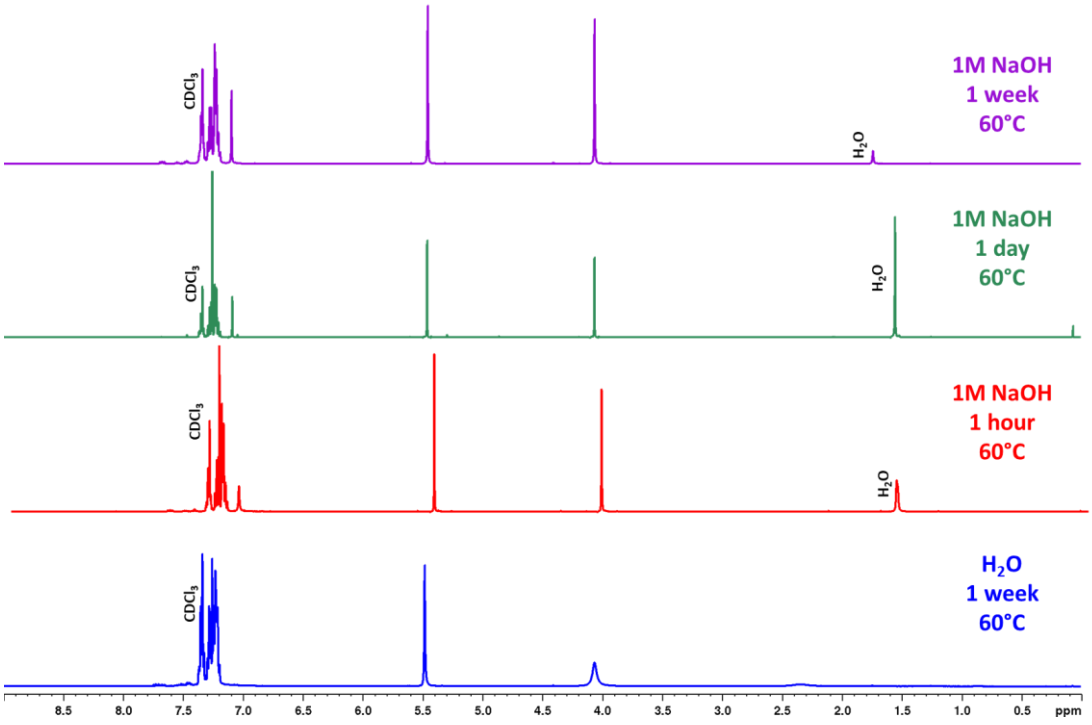

^{1}H NMR spectra of benzyl triazole after reacting in 1M NaOH. A negative control was run in water for 1 week at 60°C (blue). Reactions were run in 1M NaOH at 60°C for 1 hour (red), 1 day (green), and 1 week (purple).

Water Washes of Benzyl Triazole Precipitate After 1M NaOH Reaction

^{1}H NMR, $CDCl_3$, 500MHz, 294K

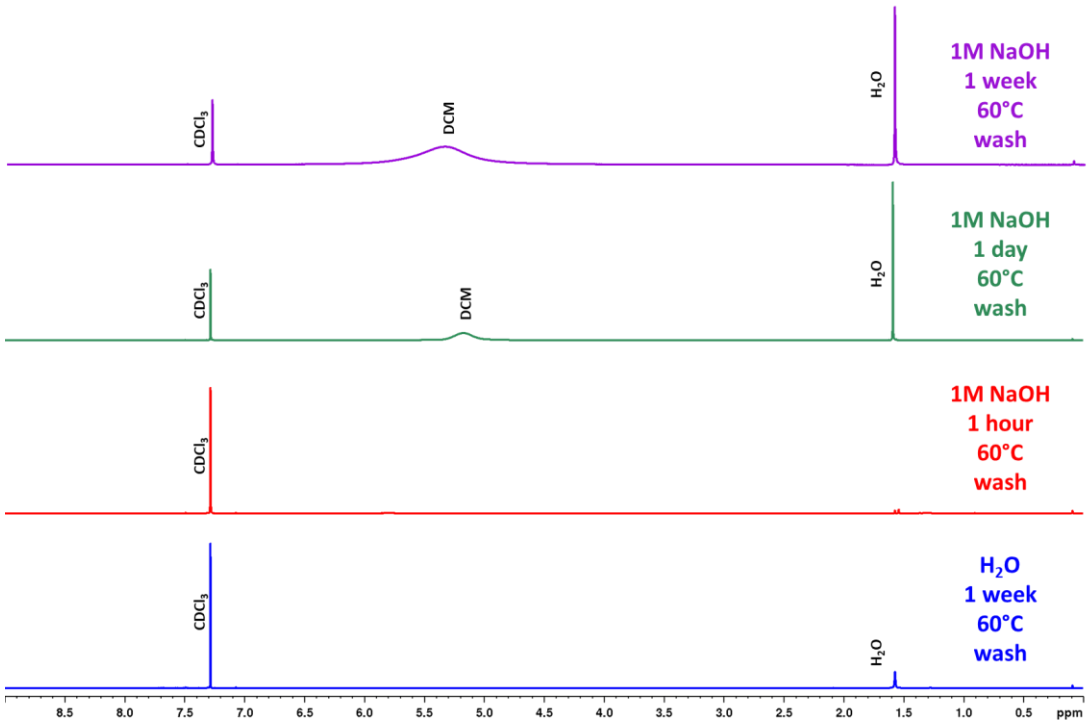

^{1}H NMR spectra of benzyl triazole wash after reacting in 1M NaOH. A negative control was run in water for 1 week at 60°C (blue). Reactions were run in 1M NaOH at 60°C for 1 hour (red), 1 day (green), and 1 week (purple).

Oxidative Stability of Benzyl Triazole

Benzyl Triazole Precipitate After 50,000ppm NaClO Reaction

^{1}H NMR, $CDCl_3$, 500MHz, 294K

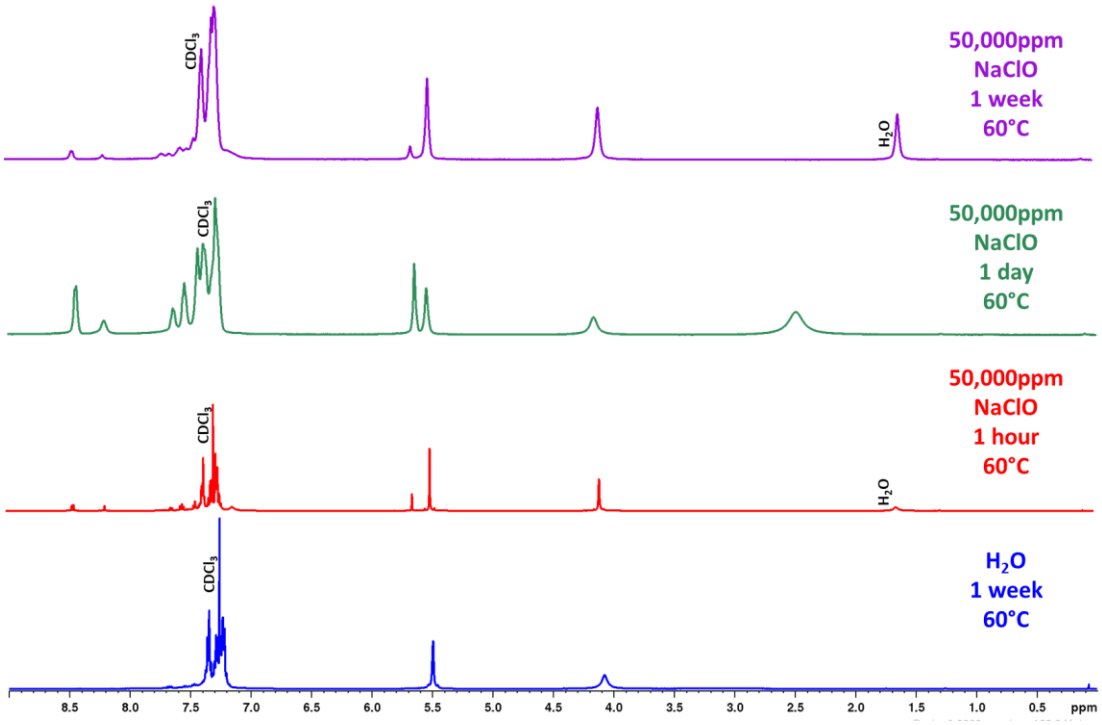

^{1}H NMR spectra of benzyl triazole after reacting in 50,000ppm NaClO. A negative control was run in water for 1 week at 60°C (blue). Reactions were run in 5% NaClO at 60°C for 1 hour (red), 1 day (green), and 1 week (purple).

Benzyl Triazole Precipitate After 50,000ppm NaClO Reaction-Room Temperature

^{1}H NMR, $CDCl_3$, 500MHz, 294K

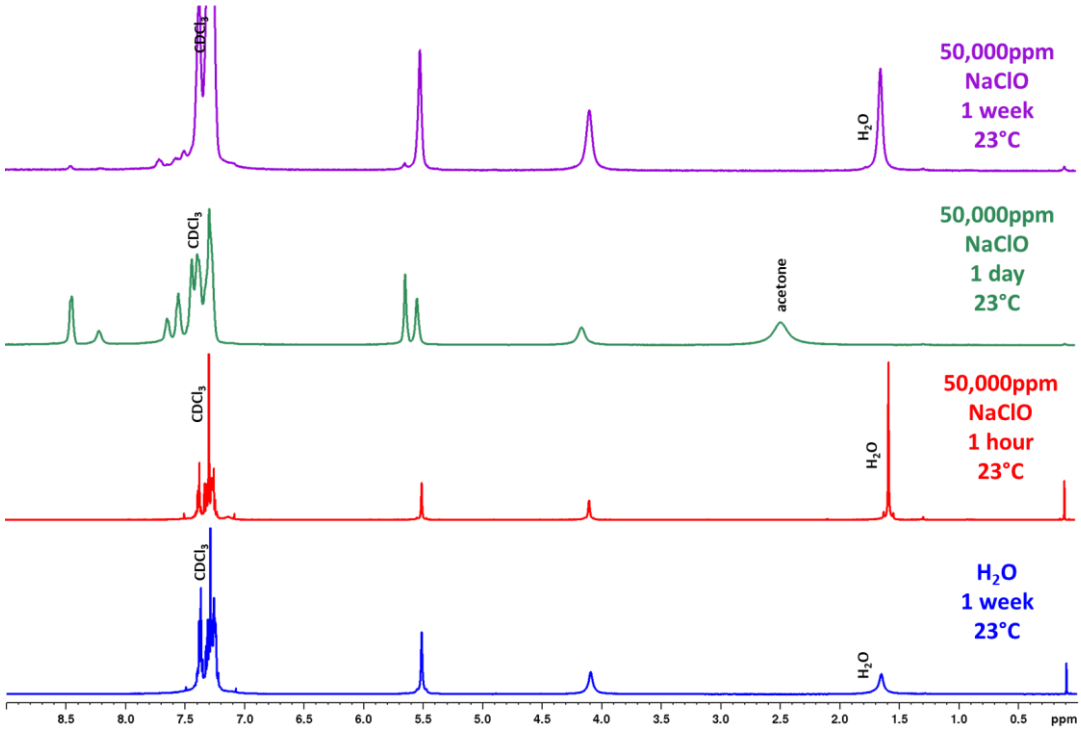

^{1}H NMR spectra of benzyl triazole after reacting in 50,000ppm NaClO. A negative control was run in water for 1 week at 23°C (blue). Reactions were run in 50,000ppm NaClO at 23°C for 1 hour (red), 1 day (green), and 1 week (purple).

Benzyl Triazole Precipitate After 10,000ppm NaClO Reaction

^{1}H NMR, $CDCl_3$, 500MHz, 294K

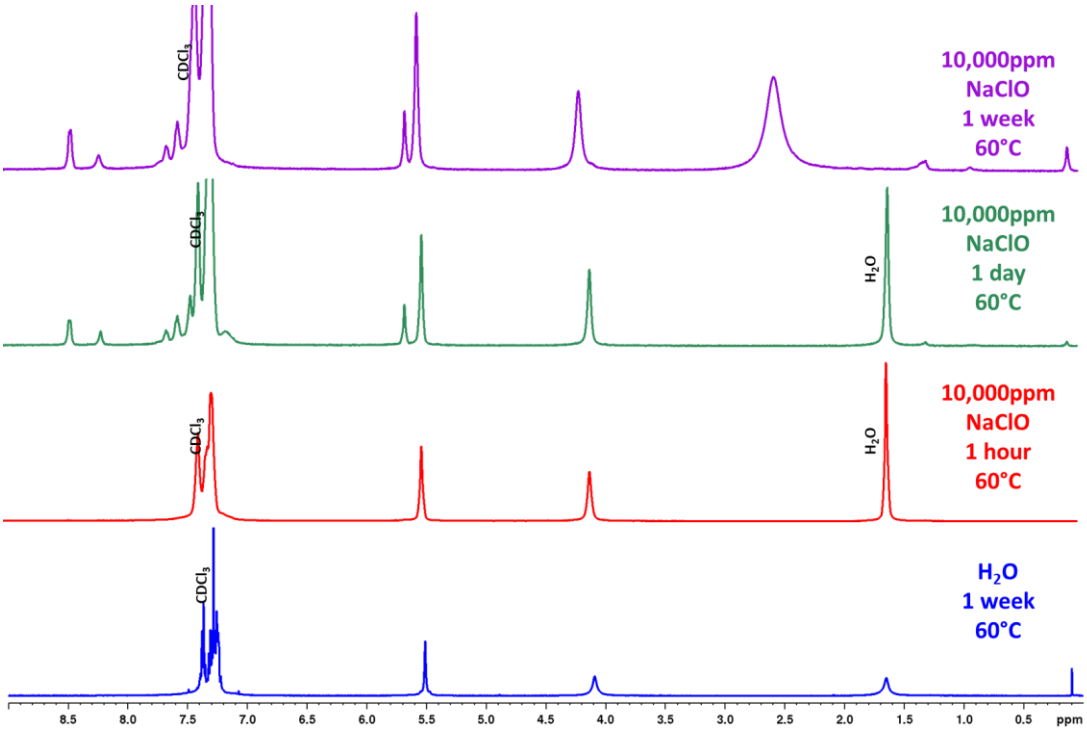

^{1}H NMR spectra of benzyl triazole after reacting in 10,000ppm NaClO. A negative control was run in water for 1 week at 60°C (blue). Reactions were run in 10,000ppm NaClO at 60°C for 1 hour (red), 1 day (green), and 1 week (purple).

Benzyl Triazole Precipitate After 10,000ppm NaClO Reaction-Room Temperature

^{1}H NMR, $CDCl_3$, 500MHz, 294K

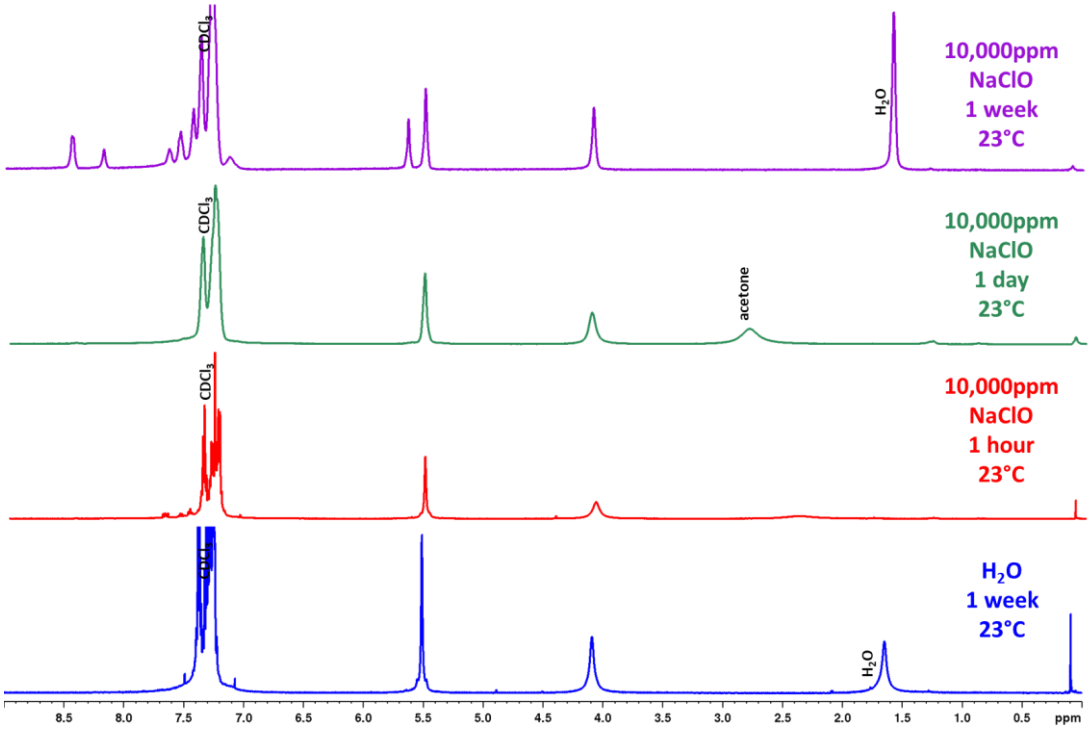

^{1}H NMR spectra of benzyl triazole after reacting in 10,000ppm NaClO. A negative control was run in water for 1 week at 23°C (blue). Reactions were run in 10,000ppm NaClO at 23°C for 1 hour (red), 1 day (green), and 1 week (purple).

Benzyl Triazole Precipitate After 1,000ppm NaClO Reaction

^{1}H NMR, $CDCl_3$, 500MHz, 294K

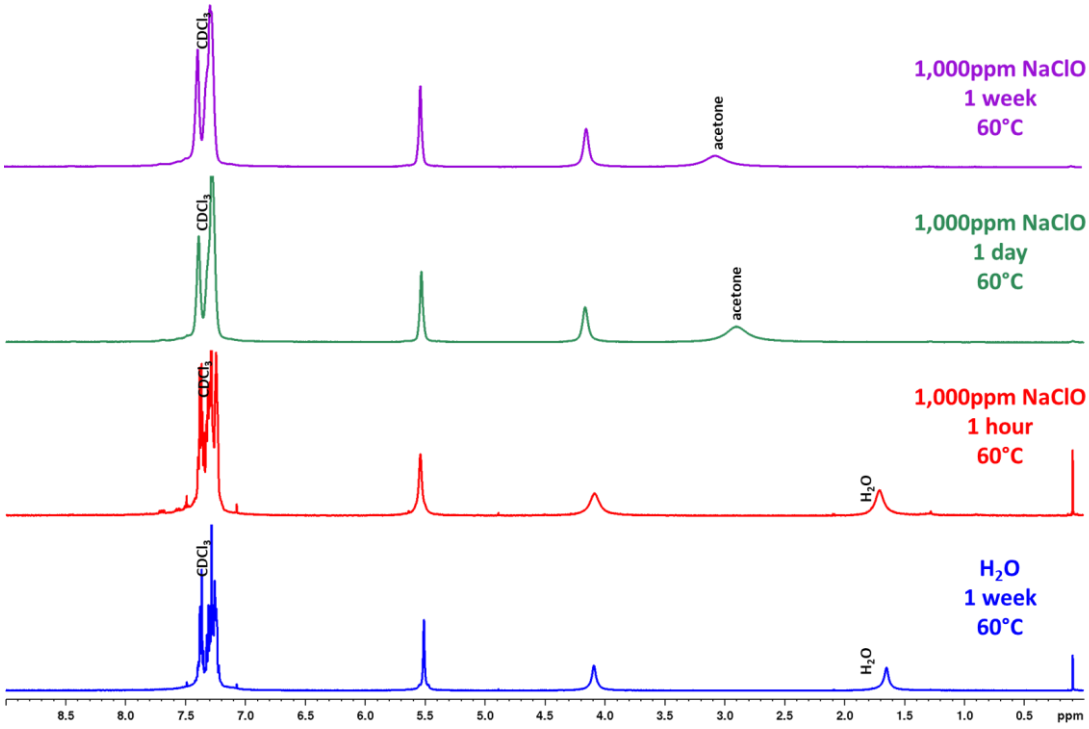

^{1}H NMR spectra of benzyl triazole after reacting in 1,000ppm NaClO. A negative control was run in water for 1 week at 60°C (blue). Reactions were run in 1,000ppm NaClO at 60°C for 1 hour (red), 1 day (green), and 1 week (purple).

Water Washes of Benzyl Triazole Precipitate After 50,000ppm NaClO Reaction

^{1}H NMR, $CDCl_3$, 500MHz, 294K

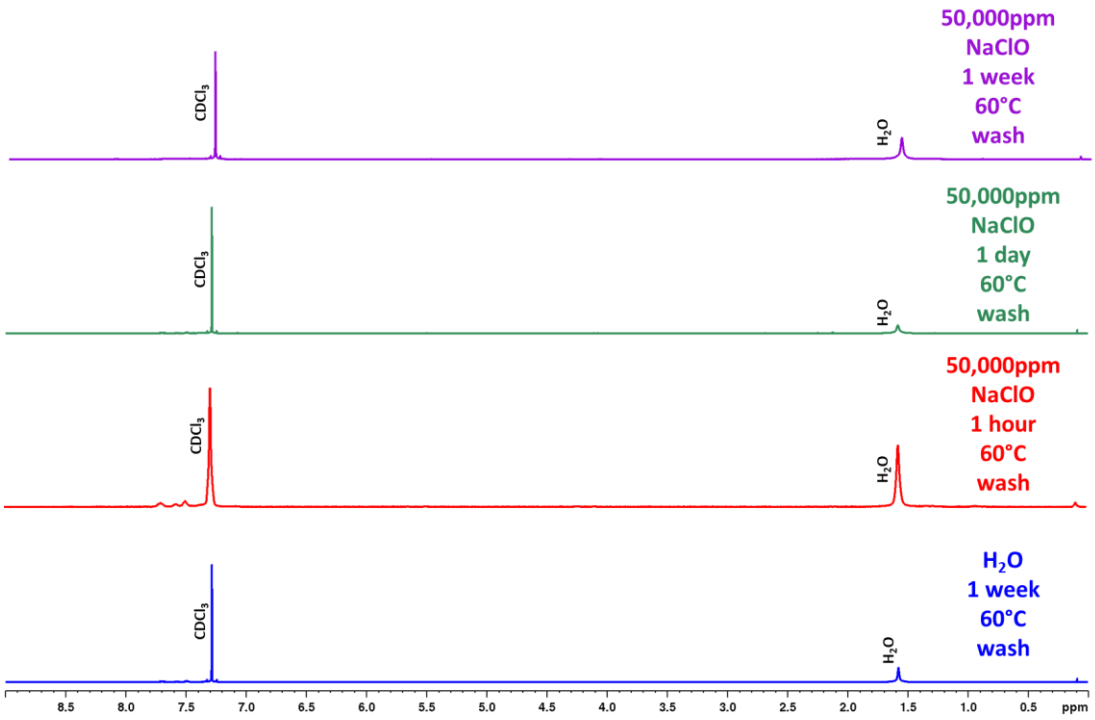

^{1}H NMR spectra of benzyl triazole wash after reacting in 50,000ppm NaClO. A negative control was run in water for 1 week at 60°C (blue). Reactions were run in 50,000ppm NaClO at 60°C for 1 hour (red), 1 day (green), and 1 week (purple).

2.7.3.6 Alkyl Triazole

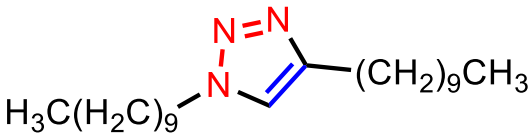

1,4-didecyl-1H-1,2,3-triazole (A-4)

^{1}H NMR, $CDCl_3$, 500MHz, 294K

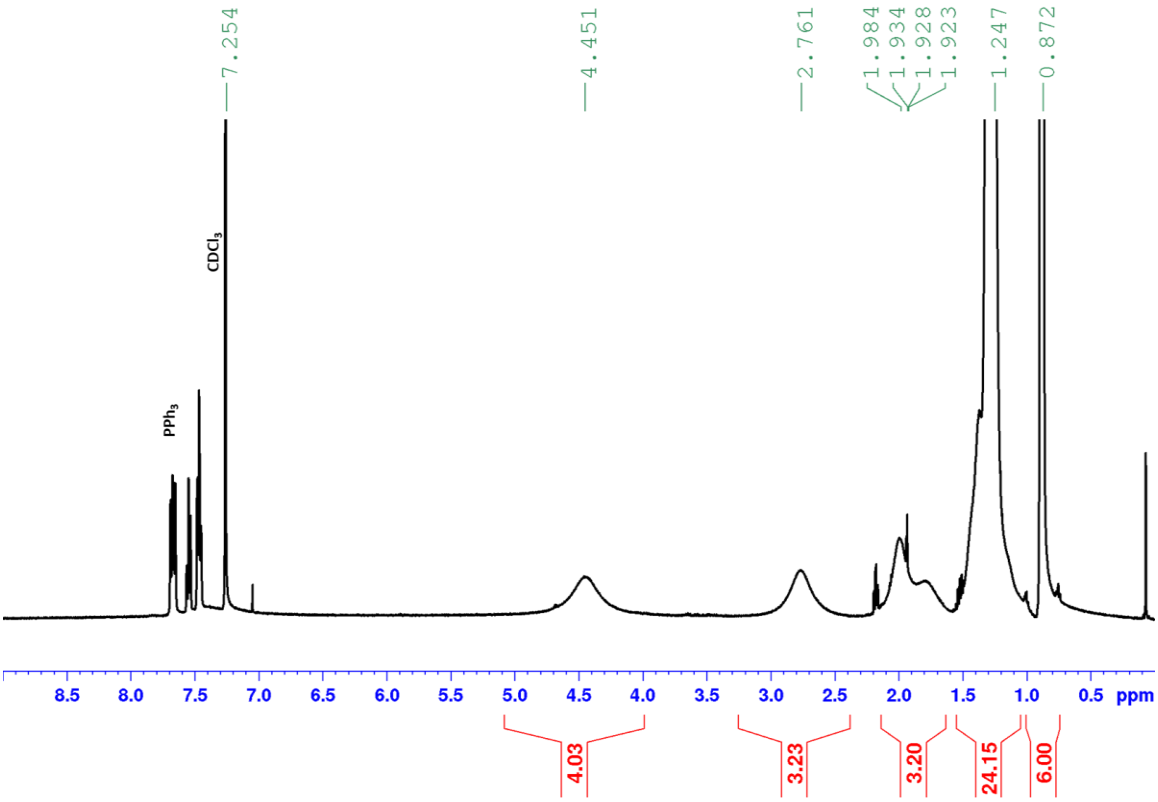

^{1}H NMR spectrum of alkyl triazole

Acidic Stability of Alkyl Triazole

Alkyl Triazole Precipitate After 12M HCl Reaction

^{1}H NMR, $CDCl_3$, 500MHz, 294K

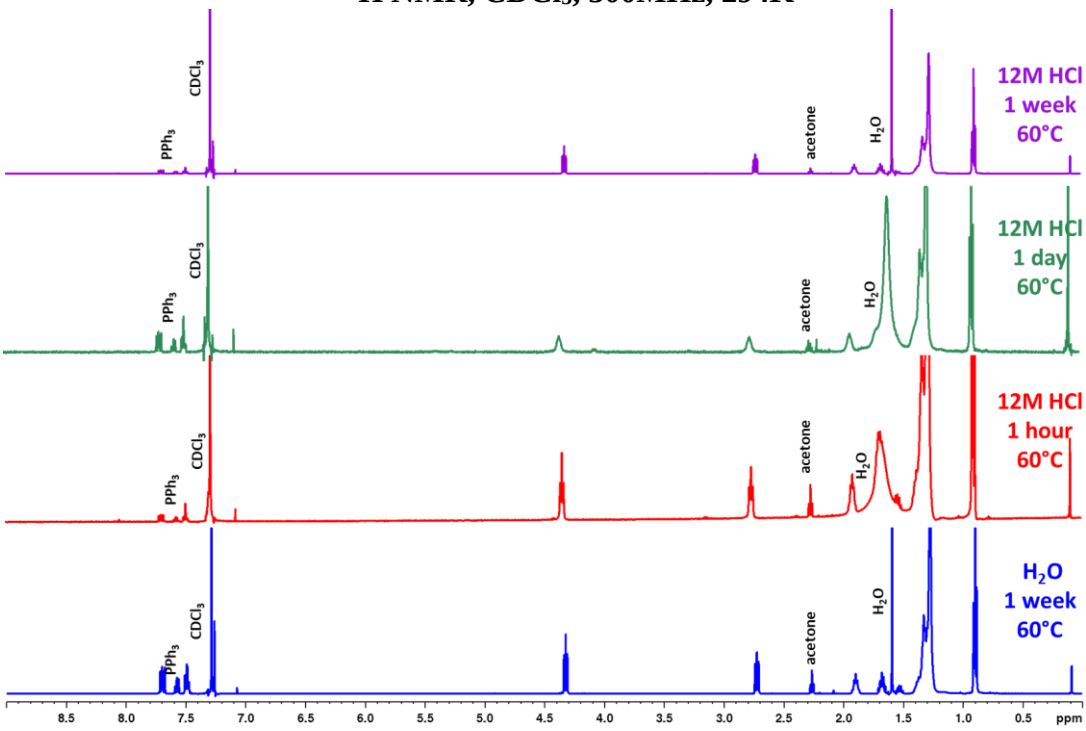

^{1}H NMR spectra of alkyl triazole after reacting in 12M HCl. A negative control was run in water for 1 week at 60°C (blue). Reactions were run in 12M HCl at 60°C for 1 hour (red), 1 day (green), and 1 week (purple).

Water Washes of Alkyl Triazole Precipitate After 12M HCl Reaction

^{1}H NMR, $CDCl_3$, 500MHz, 294K

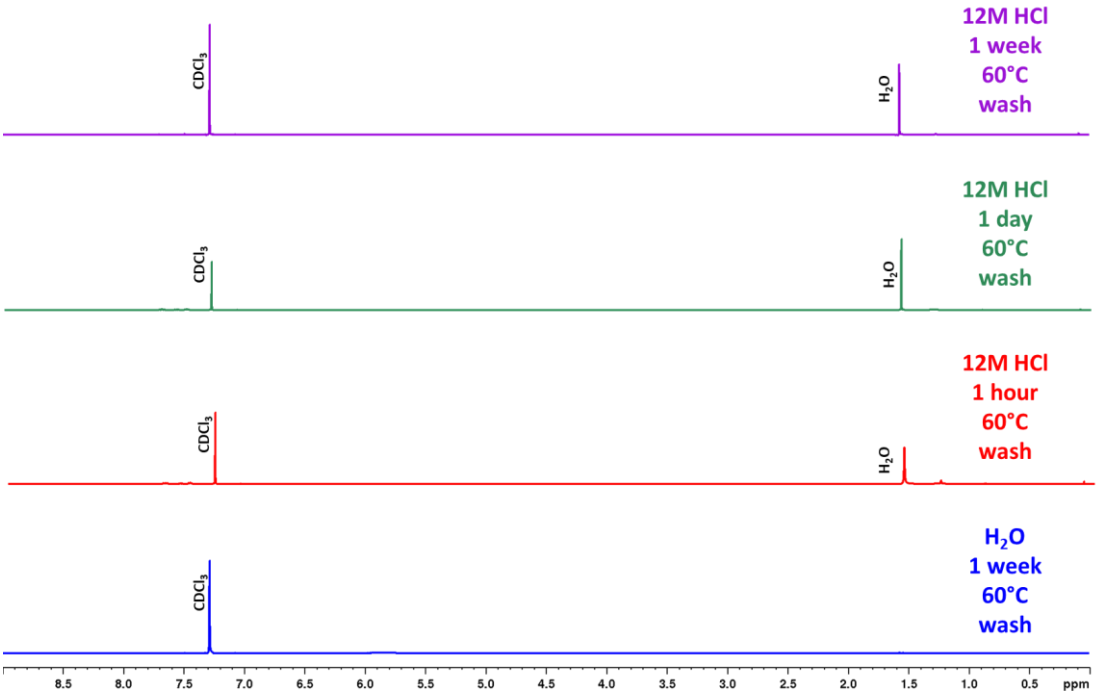

^{1}H NMR spectra of alkyl triazole wash after reacting in 12M HCl. A negative control was run in water for 1 week at 60°C (blue). Reactions were run in 12M HCl at 60°C for 1 hour (red), 1 day (green), and 1 week (purple).

Basic Stability of Alkyl Triazole

Alkyl Triazole Precipitate After 1M NaOH Reaction

^{1}H NMR, $CDCl_3$, 500MHz, 294K

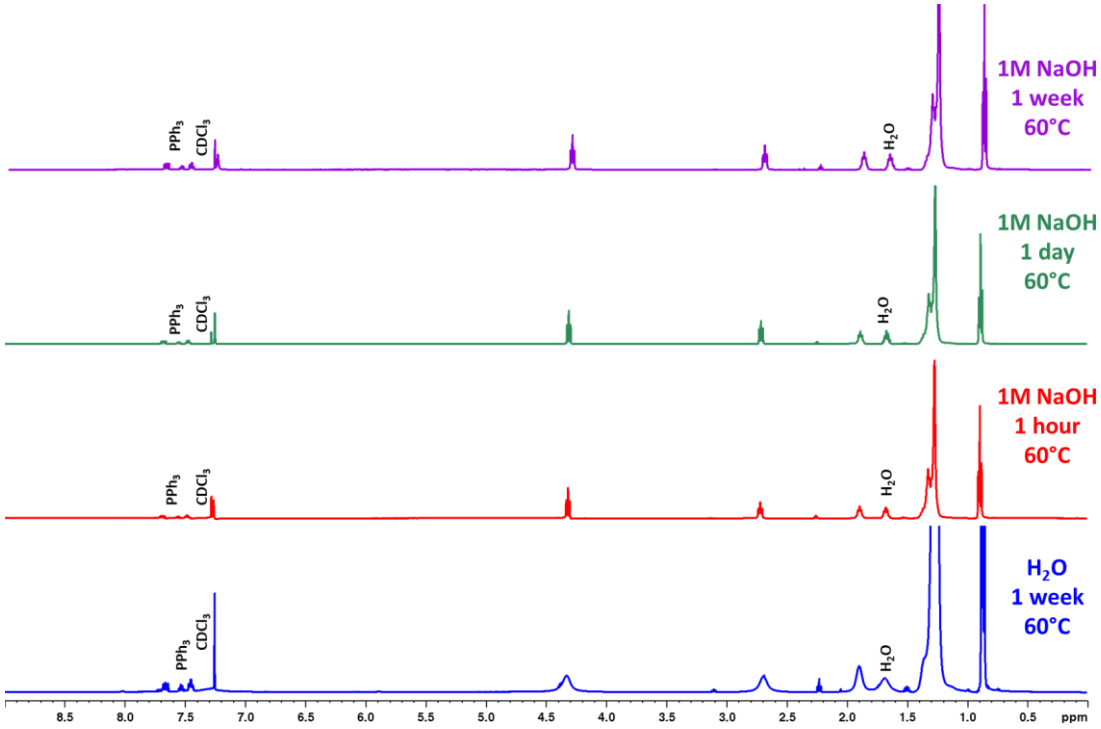

^{1}H NMR spectra of alkyl triazole after reacting in 1M NaOH. A negative control was run in water for 1 week at 60°C (blue). Reactions were run in 1M NaOH at 60°C for 1 hour (red), 1 day (green), and 1 week (purple).

Water Washes of Alkyl Triazole Precipitate After 1M NaOH Reaction

^{1}H NMR, $CDCl_3$, 500MHz, 294K

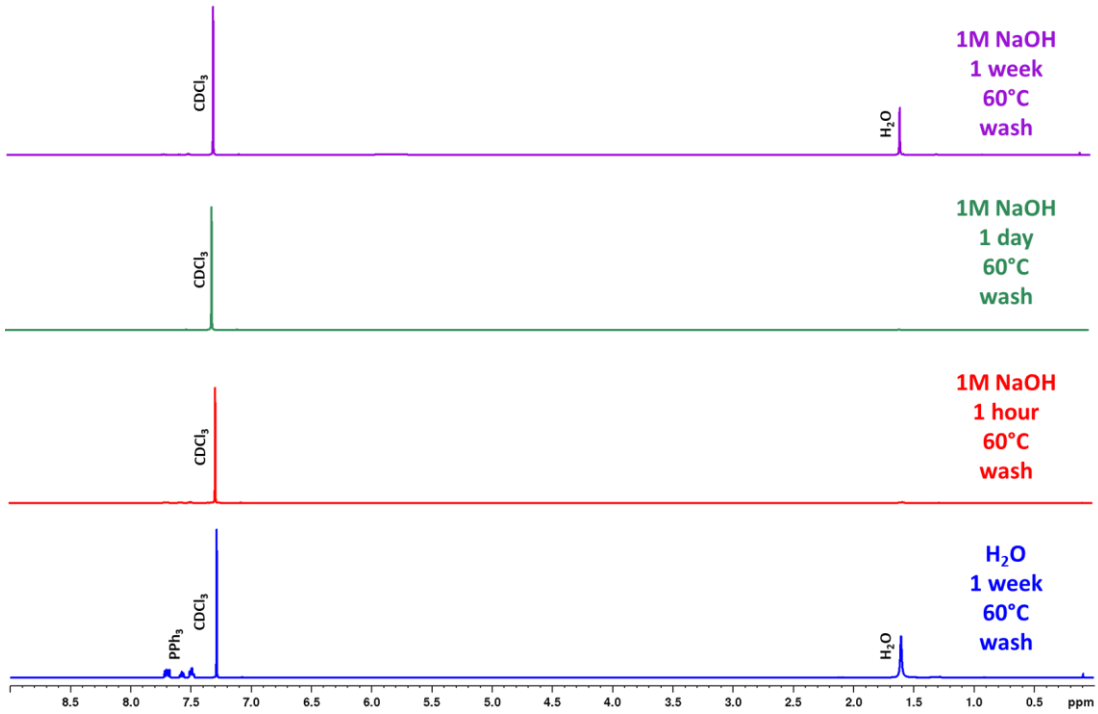

^{1}H NMR spectra of alkyl triazole wash after reacting in 1M NaOH. A negative control was run in water for 1 week at 60°C (blue). Reactions were run in 1M NaOH at 60°C for 1 hour (red), 1 day (green), and 1 week (purple).

Oxidative Stability of Alkyl Triazole

Alkyl Triazole Precipitate After 50,000ppm NaClO Reaction

^{1}H NMR, $CDCl_3$, 500MHz, 294K

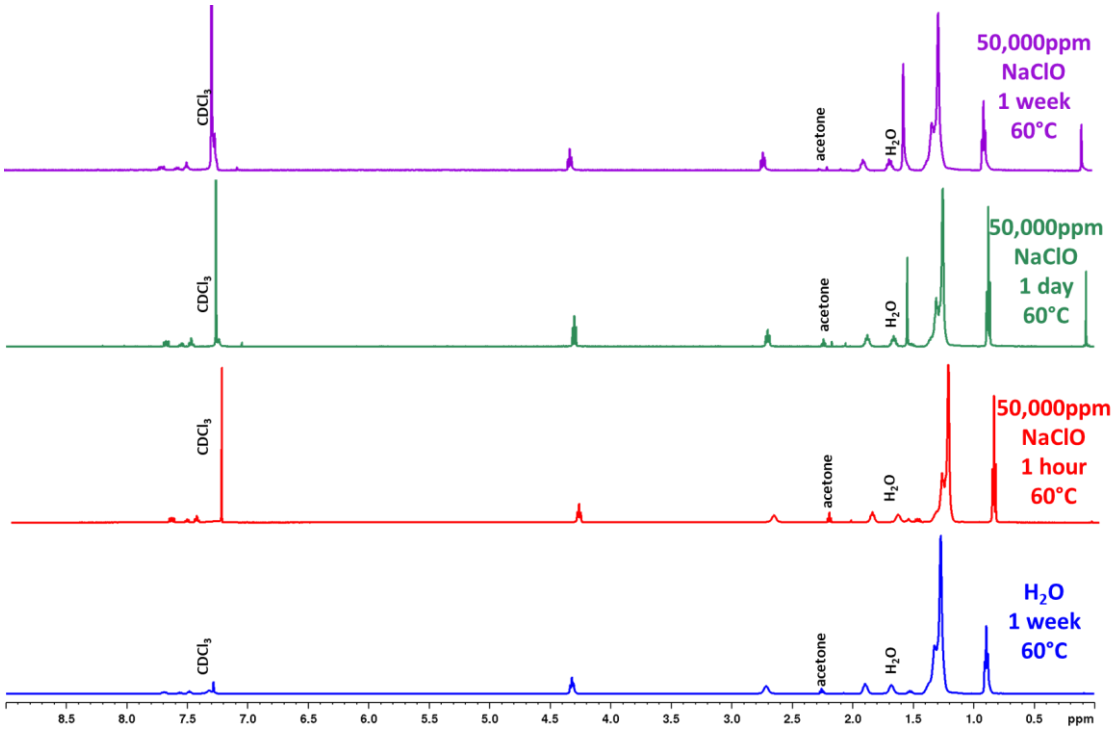

^{1}H NMR spectra of alkyl triazole after reacting in 50,000ppm NaClO. A negative control was run in water for 1 week at 60°C (blue). Reactions were run in 50,000ppm NaClO at 60°C for 1 hour (red), 1 day (green), and 1 week (purple).

Water Washes of Alkyl Triazole Precipitate After 50,000ppm NaClO Reaction

^{1}H NMR, $CDCl_3$, 500MHz, 294K

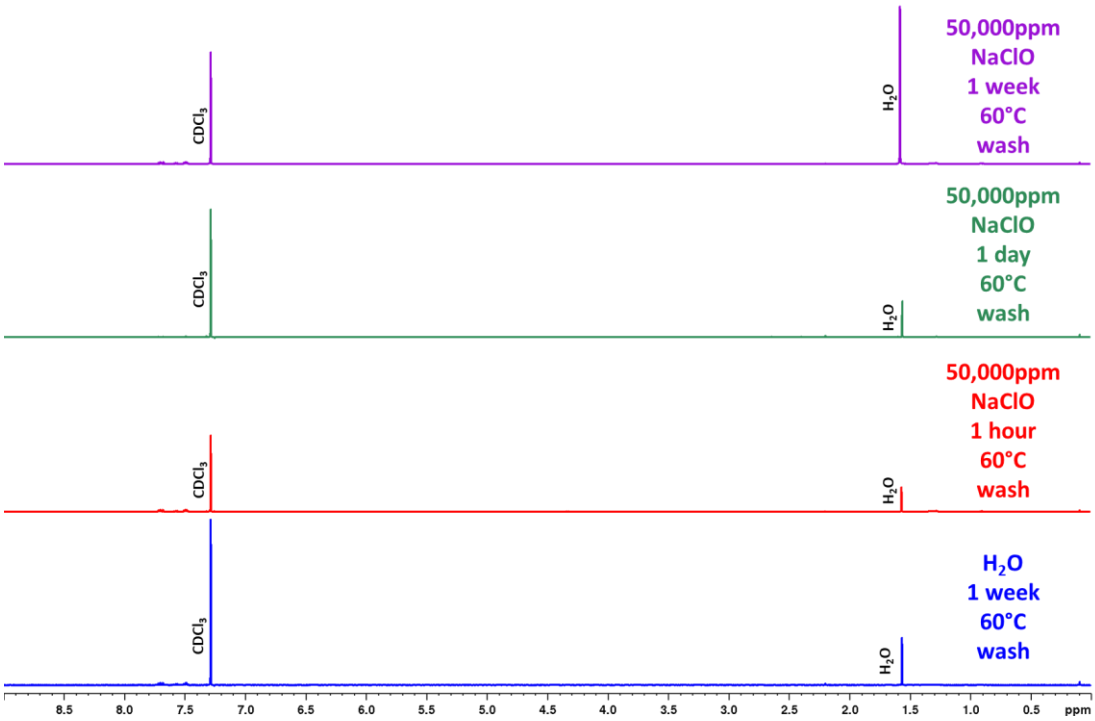

^{1}H NMR spectra of alkyl triazole wash after reacting in 50,000ppm NaClO. A negative control was run in water for 1 week at 60°C (blue). Reactions were run in 50,000ppm NaClO at 60°C for 1 hour (red), 1 day (green), and 1 week (purple).

2.7.3.7 PIM-1

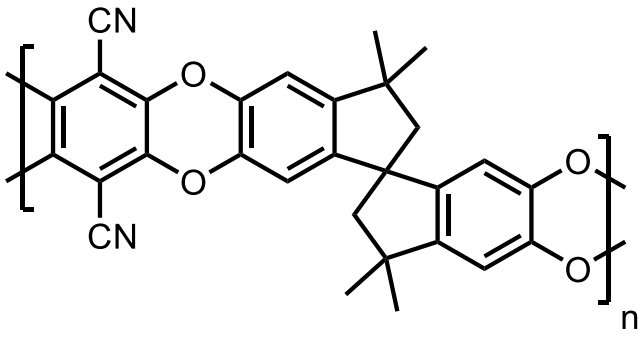

Polymer of Intrinsic Microporosity- 1

^{1}H NMR, $CDCl_3$, 500MHz, 294K

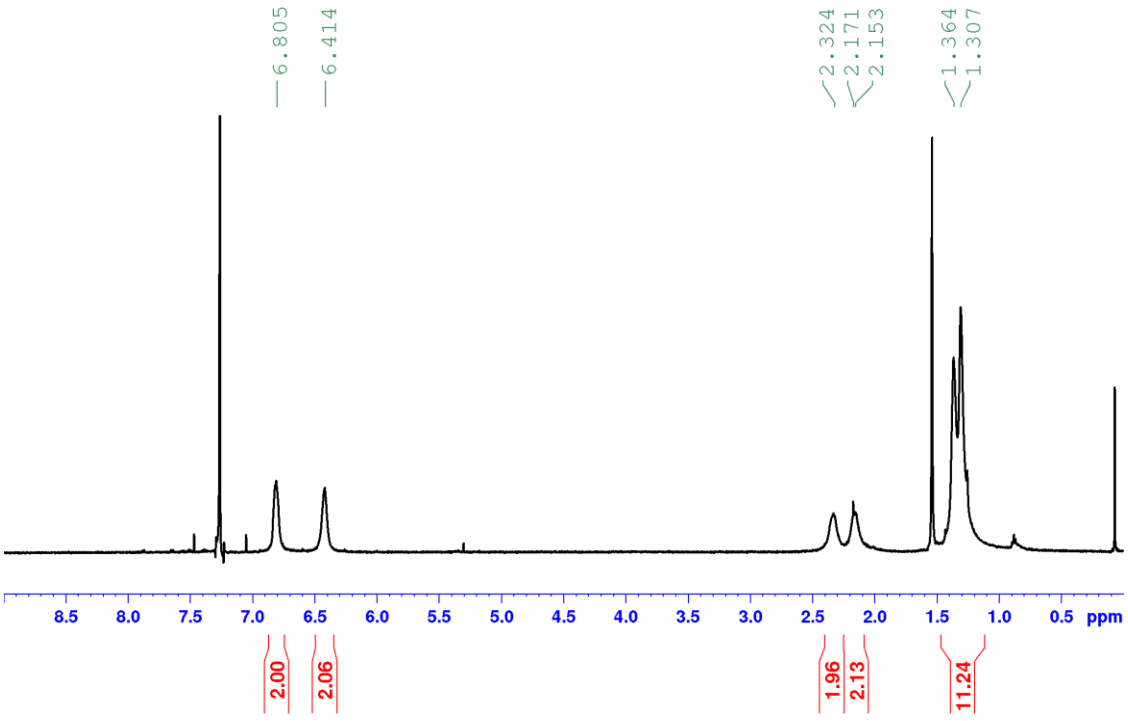

^{1}H NMR spectrum of PIM-1

Acidic Stability of PIM-1

PIM-1 Precipitate After 12M HCl Reaction

^{1}H NMR, $CDCl_3$, 500MHz, 294K

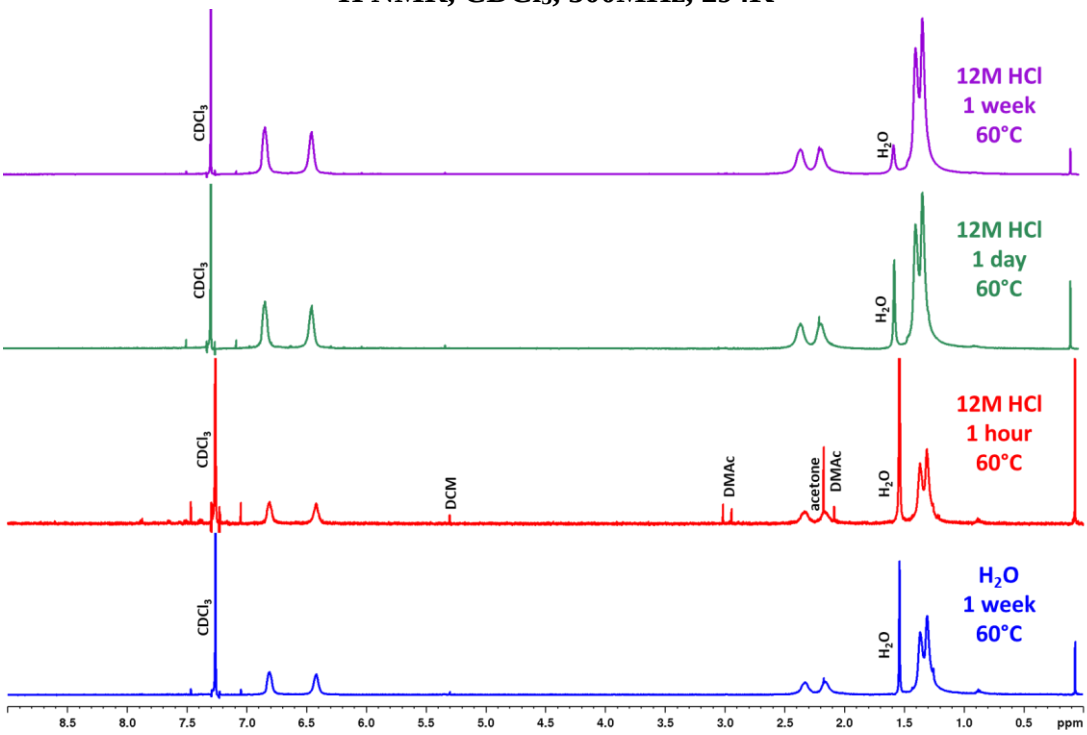

^{1}H NMR spectra of PIM-1 after reacting in 12M HCl. A negative control was run in water for 1 week at 60°C (blue). Reactions were run in 12M HCl at 60°C for 1 hour (red), 1 day (green), and 1 week (purple).

PIM-1 Precipitate After 12M HCl Reaction

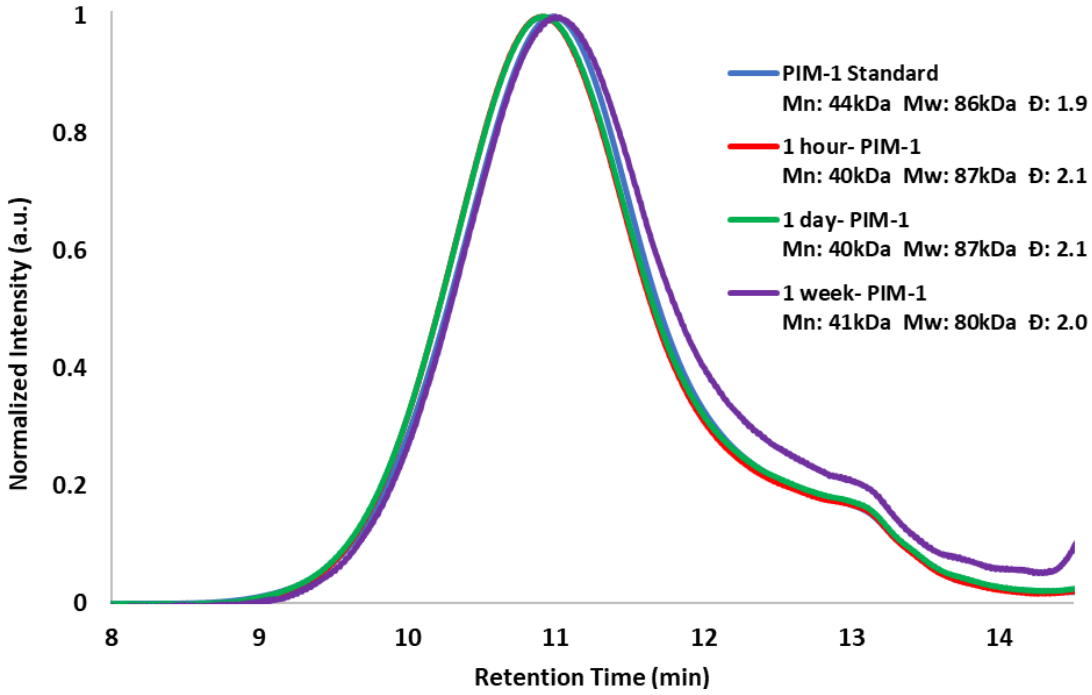

GPC data of PIM-1 after reacting in 12M HCl. A negative control was run in water for 1 week at 60°C (blue). Reactions were run in 12M HCl at 60°C for 1 hour (red), 1 day (green), and 1 week (purple).

Water Washes of PIM-1 Precipitate After 12M HCl Reaction

^{1}H NMR, $CDCl_3$, 500MHz, 294K

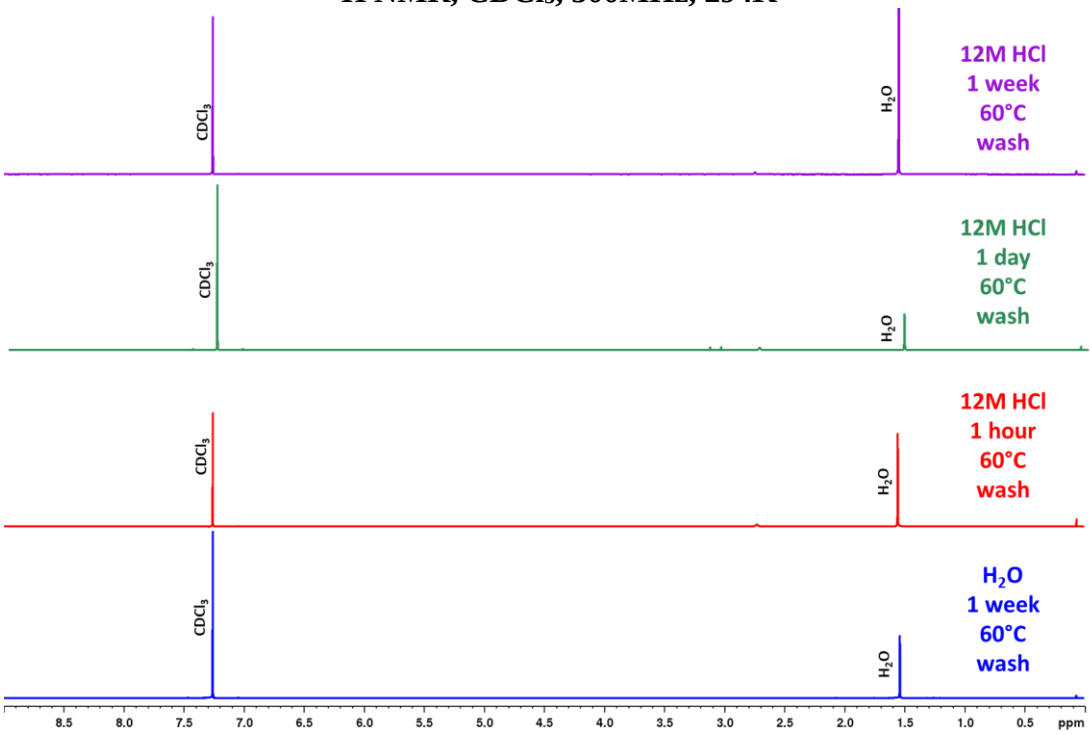

^{1}H NMR spectra of PIM-1 wash after reacting in 12M HCl. A negative control was run in water for 1 week at 60°C (blue). Reactions were run in 12M HCl at 60°C for 1 hour (red), 1 day (green), and 1 week (purple).

Basic Stability of PIM-1

PIM-1 Precipitate After 1M NaOH Reaction

^{1}H NMR, $CDCl_3$, 500MHz, 294K

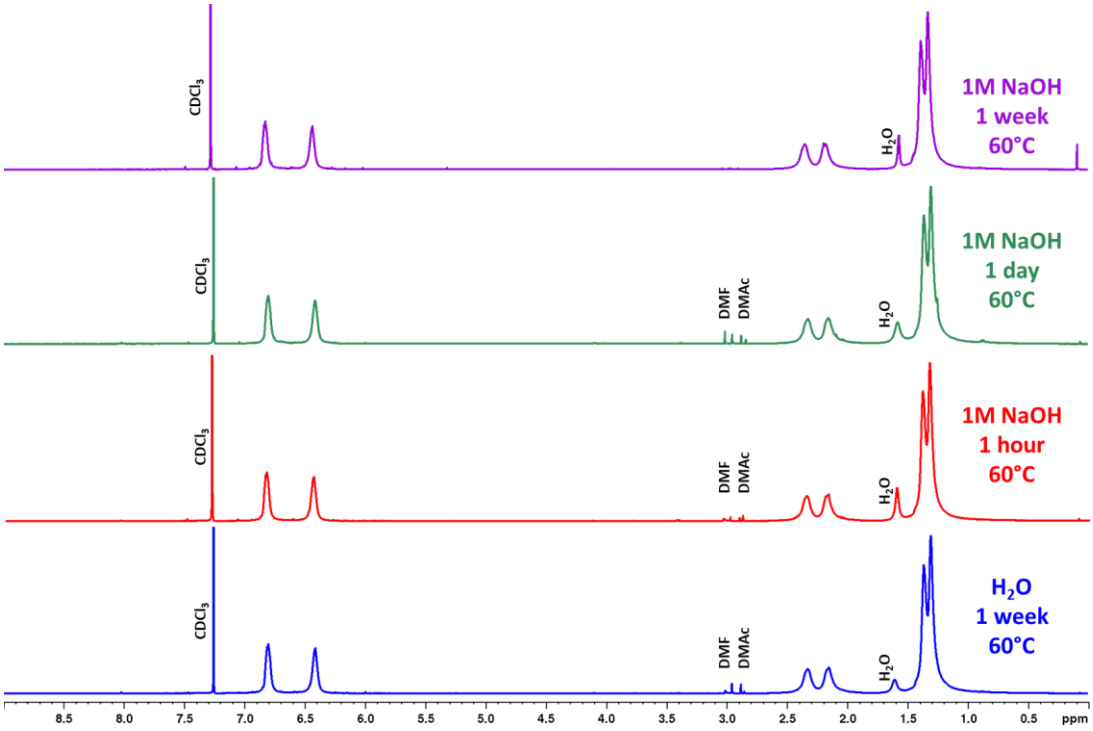

^{1}H NMR spectra of PIM-1 after reacting in 1M NaOH. A negative control was run in water for 1 week at 60°C (blue). Reactions were run in 1M NaOH at 60°C for 1 hour (red), 1 day (green), and 1 week (purple).

Water Washes of PIM-1 Precipitate After 1M NaOH Reaction

^{1}H NMR, $CDCl_3$, 500MHz, 294K

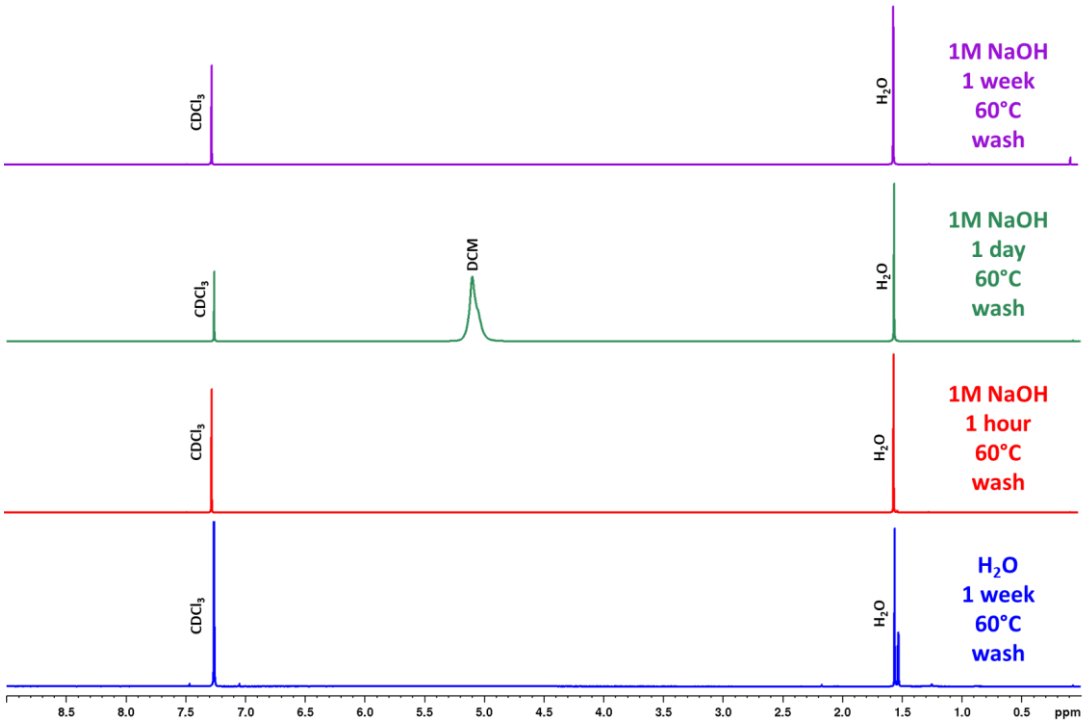

^{1}H NMR spectra of PIM-1 wash after reacting in 1M NaOH. A negative control was run in water for 1 week at 60°C (blue). Reactions were run in 1M NaOH at 60°C for 1 hour (red), 1 day (green), and 1 week (purple).

PIM-1 Precipitate After 1M NaOH Reaction

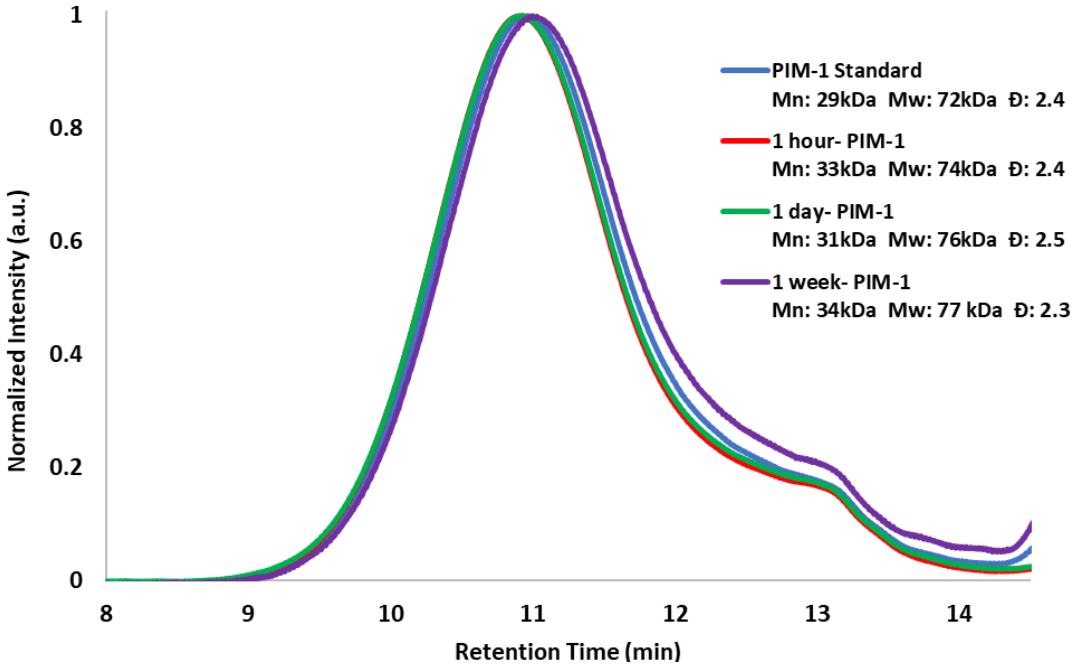

GPC data of PIM-1 after reacting in 1M NaOH. A negative control was run in water for 1 week at 60°C (blue). Reactions were run in 1M NaOH at 60°C for 1 hour (red), 1 day (green), and 1 week (purple).

Oxidative Stability of PIM-1

PIM-1 Precipitate After 50,000ppm NaClO Reaction

^{1}H NMR, $CDCl_3$, 500MHz, 294K

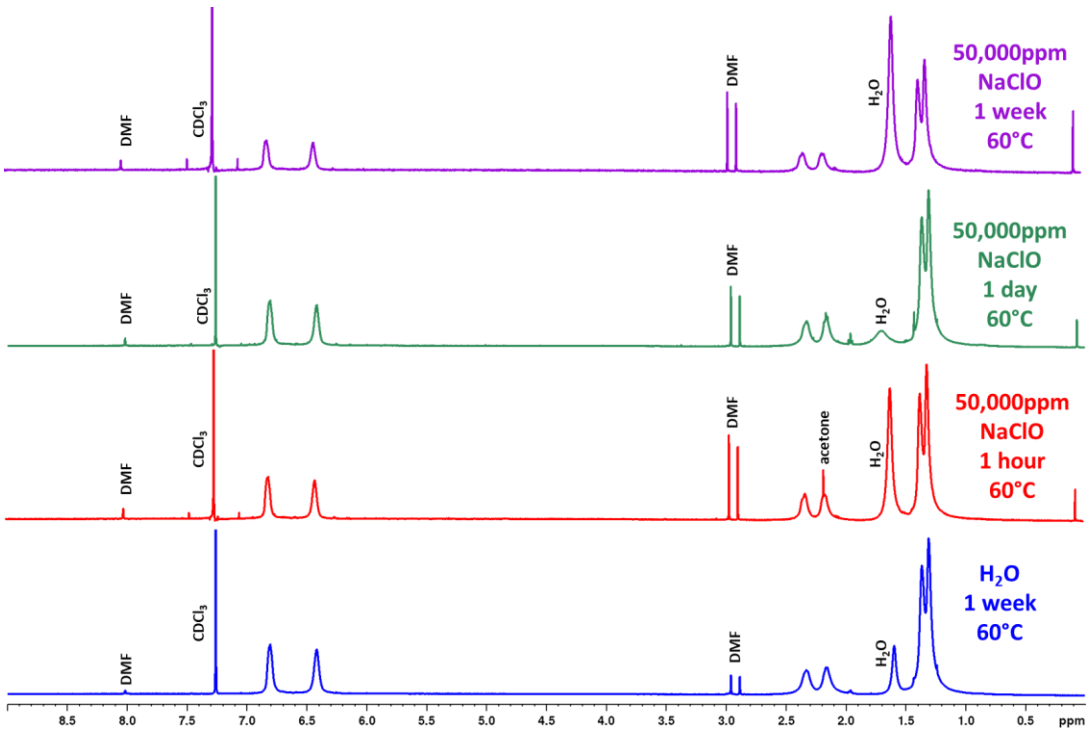

^{1}H NMR spectra of PIM-1 after reacting in 50,000ppm NaClO. A negative control was run in water for 1 week at 60°C (blue). Reactions were run in 50,000ppm NaClO at 60°C for 1 hour (red), 1 day (green), and 1 week (purple).

Water Washes of PIM-1 Precipitate After 50,000ppm NaClO Reaction

^{1}H NMR, $CDCl_3$, 500MHz, 294K

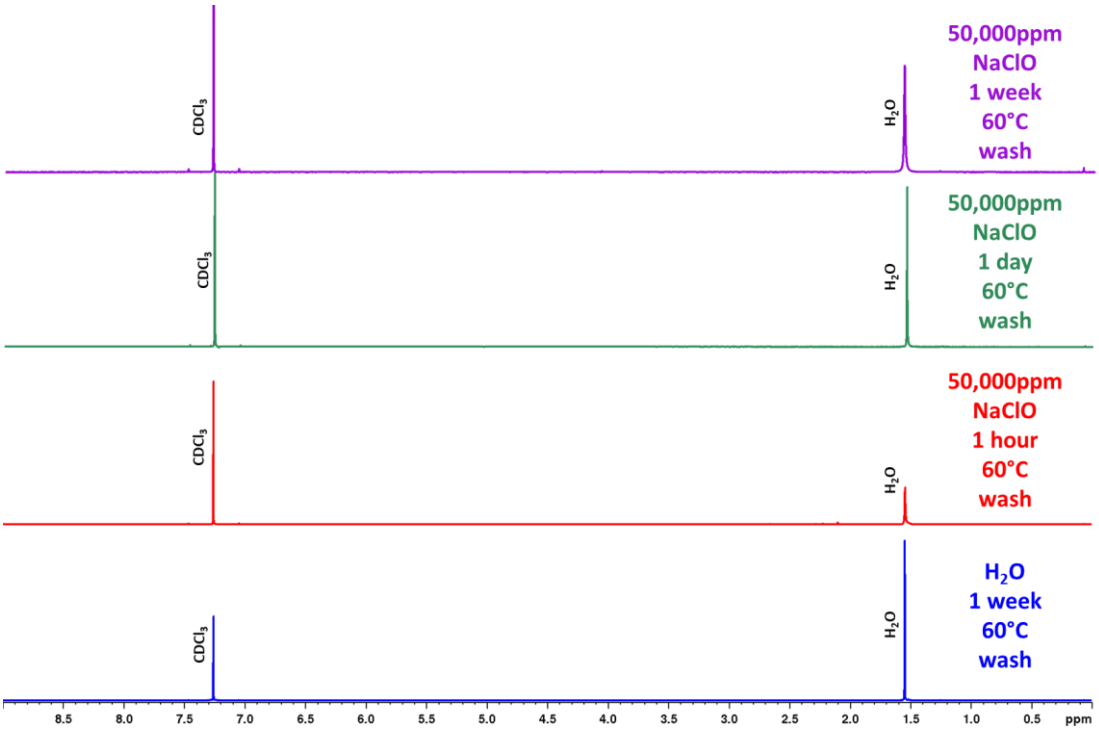

^{1}H NMR spectra of PIM-1 wash after reacting in 50,000ppm NaClO. A negative control was run in water for 1 week at 60°C (blue). Reactions were run in 50,000ppm NaClO at 60°C for 1 hour (red), 1 day (green), and 1 week (purple).

PIM-1 Precipitate After 50,000ppm NaClO Reaction

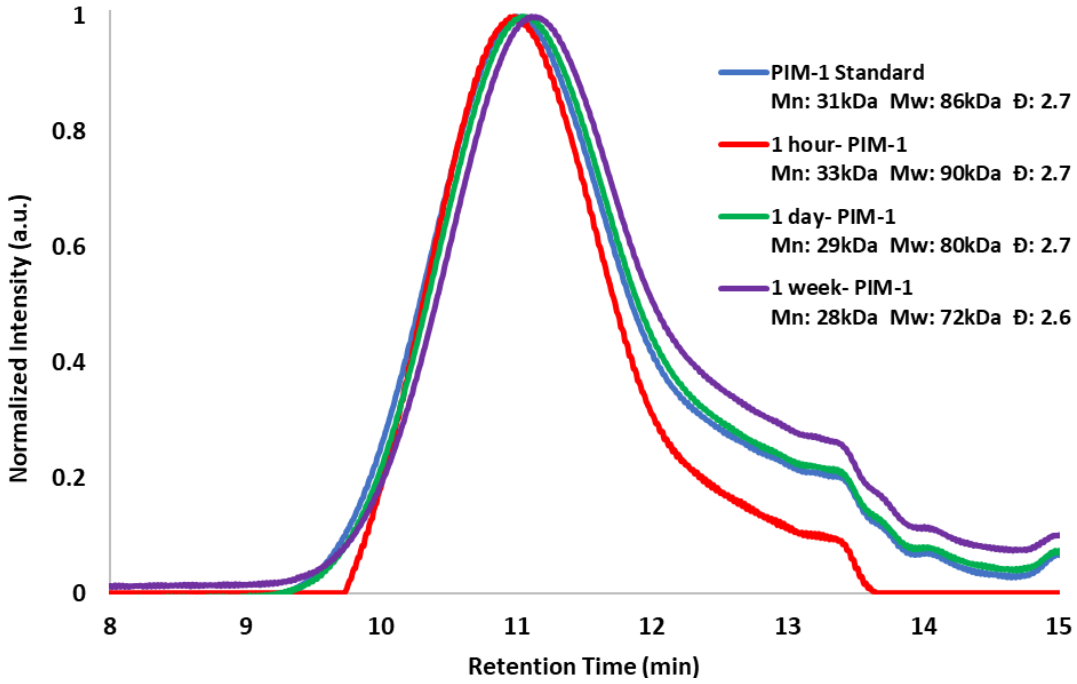

GPC data of PIM-1 after reacting in 50,000ppm NaClO. A negative control was run in water for 1 week at 60°C (blue). Reactions were run in 50,000ppm NaClO at 60°C for 1 hour (red), 1 day (green), and 1 week (purple).

2.7.3.8 N-phenylbenzamide

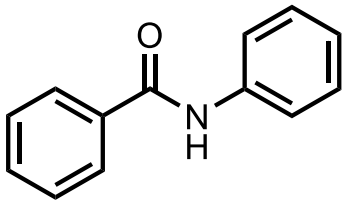

N-phenylbenzamide (B-1)

^{1}H NMR, DMSO-d$_6$, 500MHz, 294K

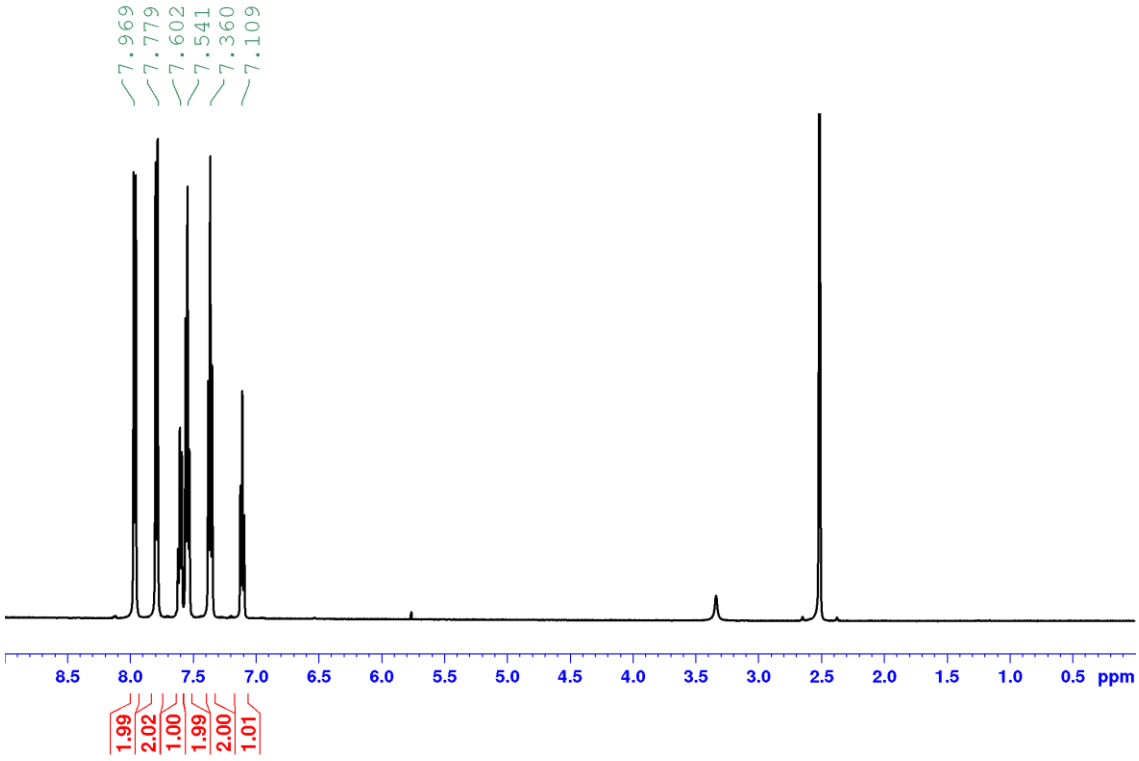

^{1}H NMR spectrum of N-phenylbenzamide

Acidic Stability of Amide

Amide Precipitate After 12M HCl Reaction

^{1}H NMR, DMSO-d_6, 500MHz, 294K

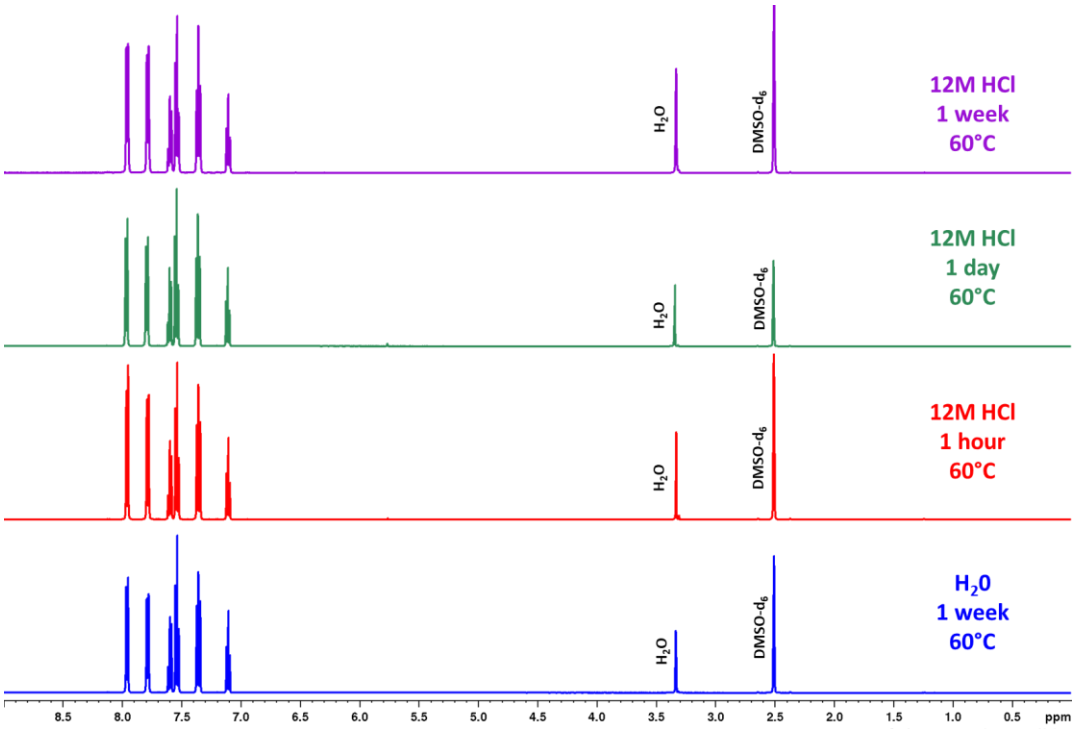

^{1}H NMR spectra of amide after reacting in 12M HCl. A negative control was run in water for 1 week at 60°C (blue). Reactions were run in 12M HCl at 60°C for 1 hour (red), 1 day (green), and 1 week (purple).

Water Washes of Amide Precipitate After 12M HCl Reaction

^{1}H NMR, $CDCl_3$, 500MHz, 294K

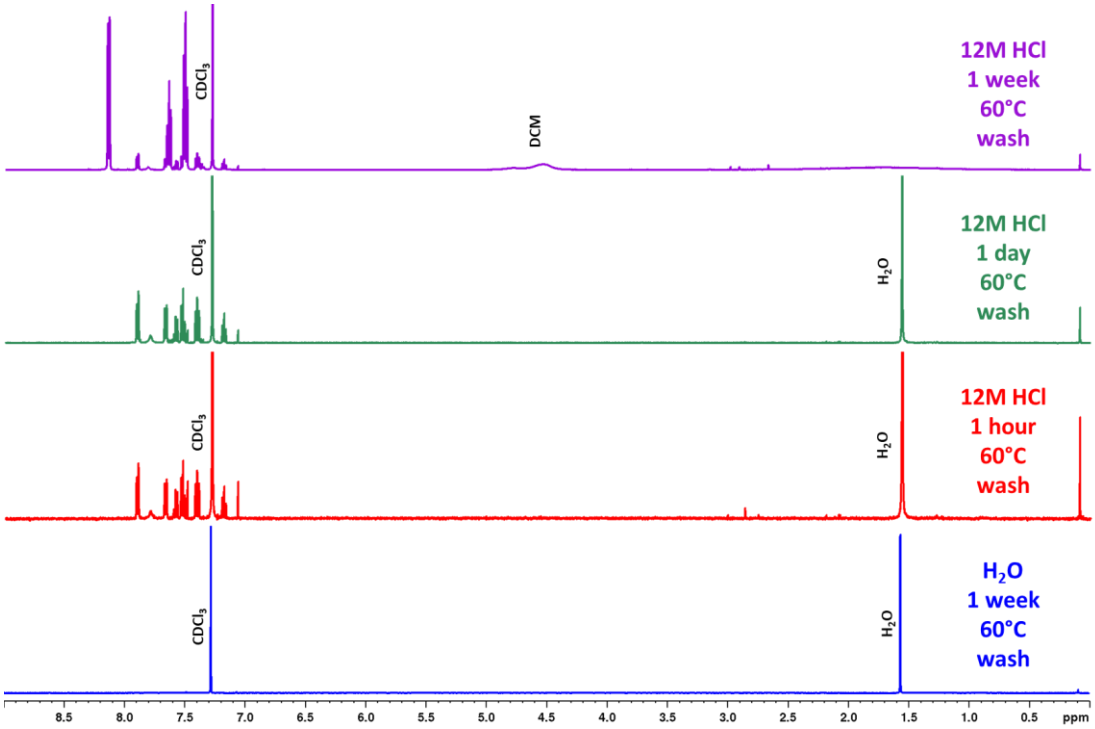

^{1}H NMR spectra of amide wash after reacting in 12M HCl. A negative control was run in water for 1 week at 60°C (blue). Reactions were run in 12M HCl at 60°C for 1 hour (red), 1 day (green), and 1 week (purple).

Water Washes of Amide Precipitate After 0.0012M HCl Reaction

^{1}H NMR, $CDCl_3$, 500MHz, 294K

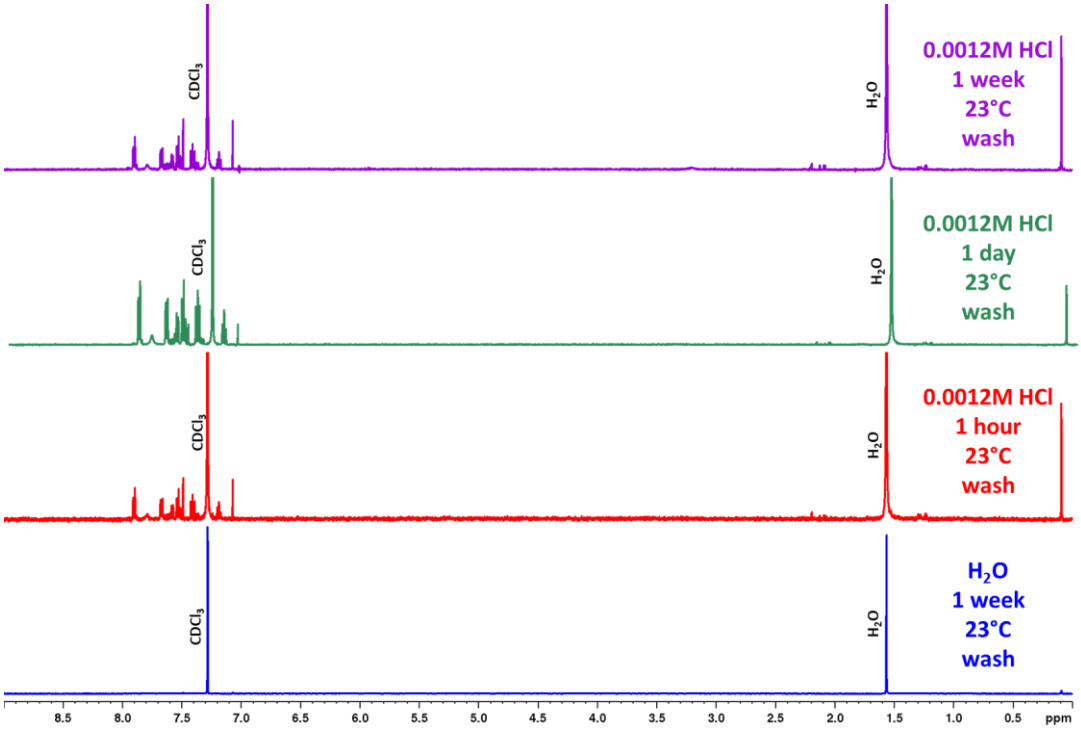

^{1}H NMR spectra of amide wash after reacting in 0.0012M HCl. A negative control was run in water for 1 week at 23°C (blue). Reactions were run in 0.0012M HCl at 23°C for 1 hour (red), 1 day (green), and 1 week (purple).

Basic Stability of Amide

Amide Precipitate After 1M NaOH Reaction

^{1}H NMR, DMSO-d_6, 500MHz, 294K

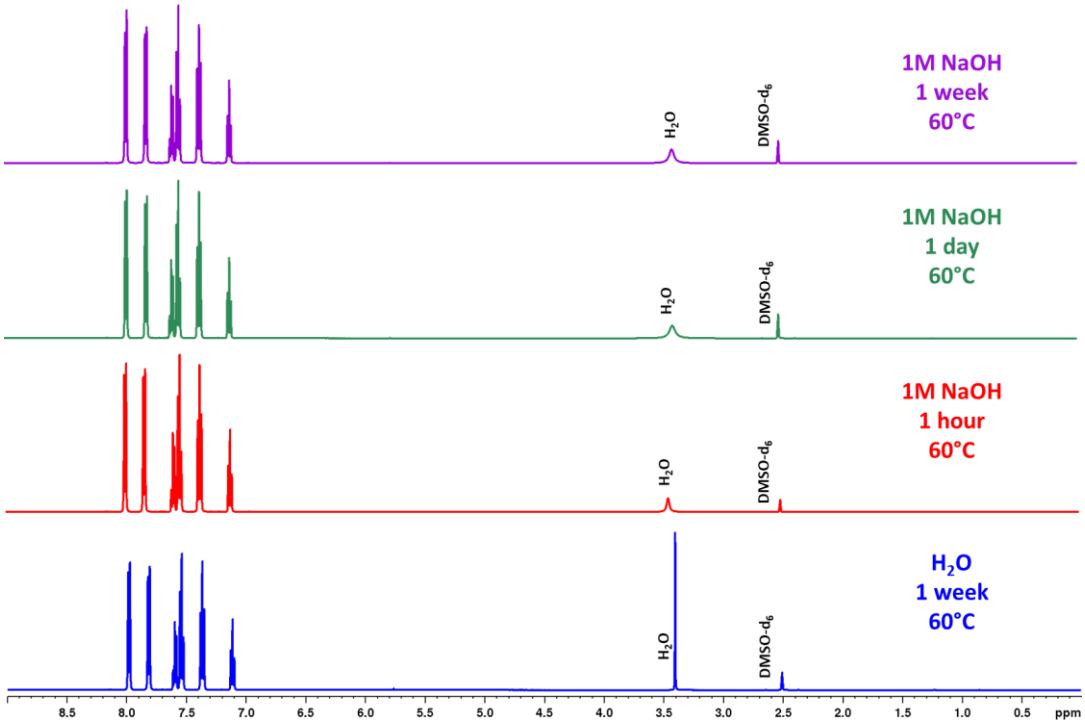

^{1}H NMR spectra of amide after reacting in 1M NaOH. A negative control was run in water for 1 week at 60°C (blue). Reactions were run in 1M NaOH at 60°C for 1 hour (red), 1 day (green), and 1 week (purple).

Water Washes of Amide Precipitate After 1M NaOH Reaction

^{1}H NMR, DMSO-d$_6$, 500MHz, 294K

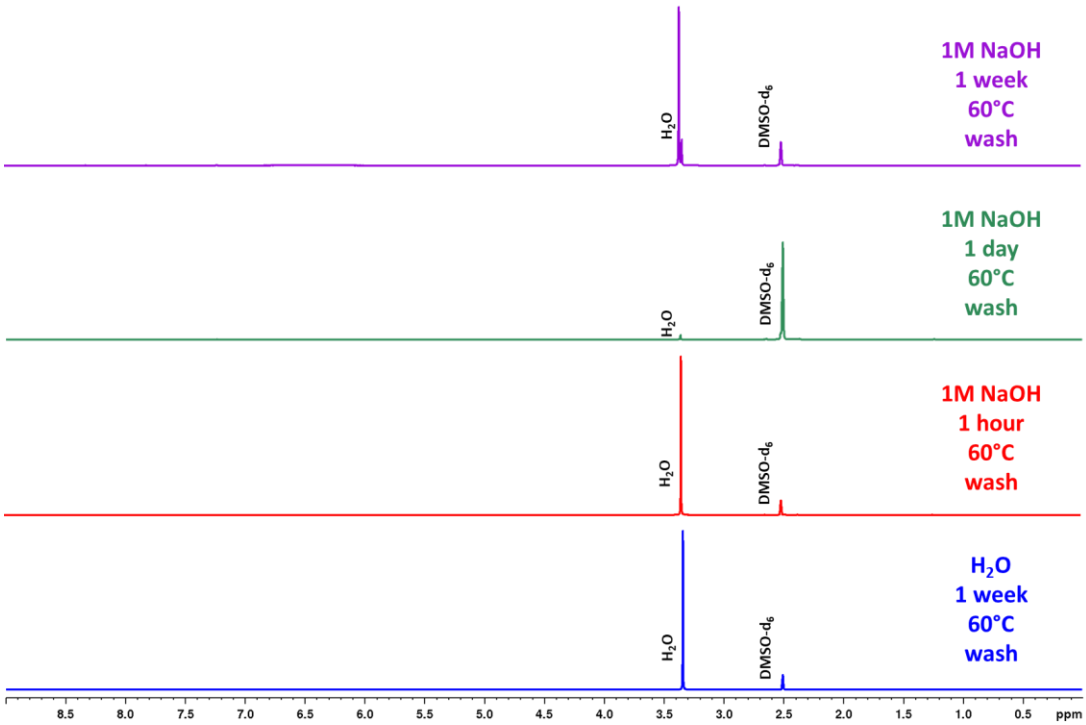

^{1}H NMR spectra of amide wash after reacting in 1M NaOH. A negative control was run in water for 1 week at 60°C (blue). Reactions were run in 1M NaOH at 60°C for 1 hour (red), 1 day (green), and 1 week (purple).

Oxidative Stability of Amide

Amide Precipitate After 50,000ppm NaClO Reaction

^{1}H NMR, DMSO-d_6, 500MHz, 294K

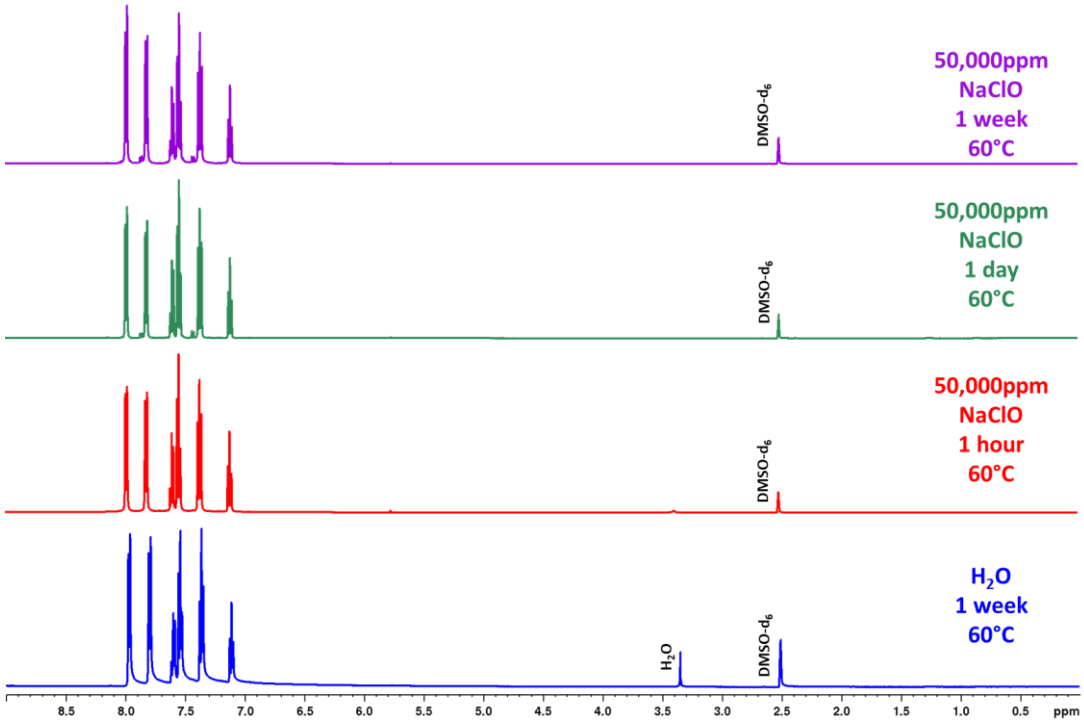

^{1}H NMR spectra of amide after reacting in 50,000ppm NaClO. A negative control was run in water for 1 week at 60°C (blue). Reactions were run in 50,000ppm NaClO at 60°C for 1 hour (red), 1 day (green), and 1 week (purple).

Amide Precipitate After 50,000ppm NaClO Reaction- Aromatic Region

^{1}H NMR, DMSO-d$_6$, 500MHz, 294K

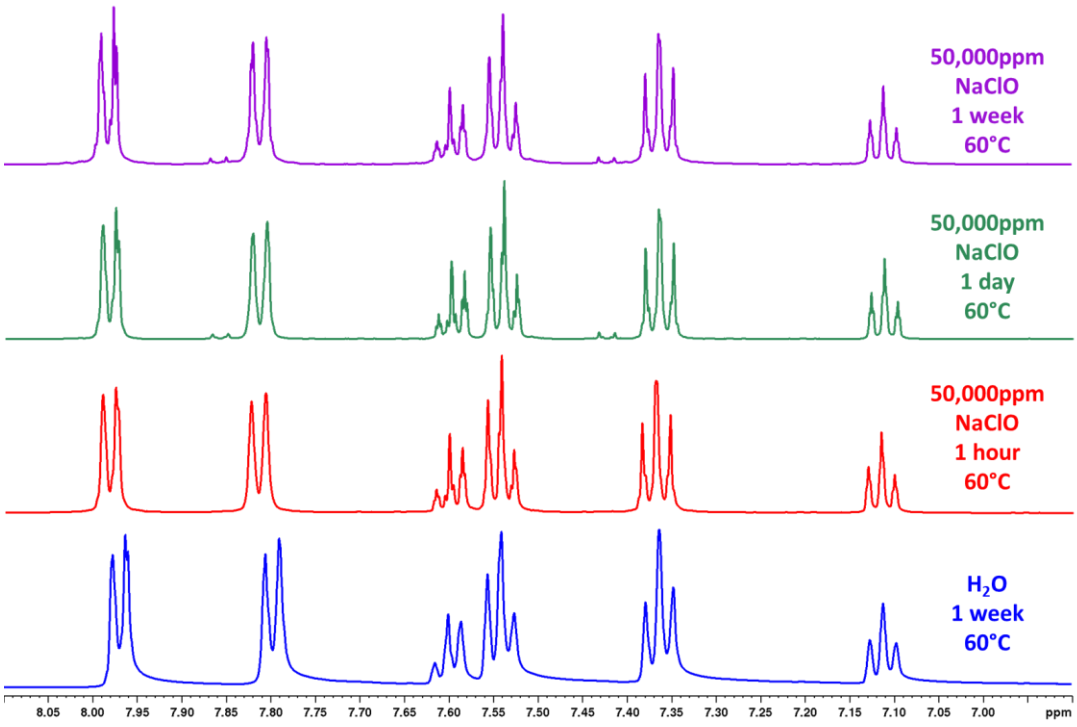

Zoomed in aromatic region: ^{1}H NMR spectra of amide after reacting in 50,000ppm NaClO. A negative control was run in water for 1 week at 60°C (blue). Reactions were run in 50,000ppm NaClO at 60°C for 1 hour (red), 1 day (green), and 1 week (purple).

Amide Precipitate After 50,000ppm NaClO Reaction- Aromatic Region-Room Temperature

^{1}H NMR, DMSO-d_6, 500MHz, 294K

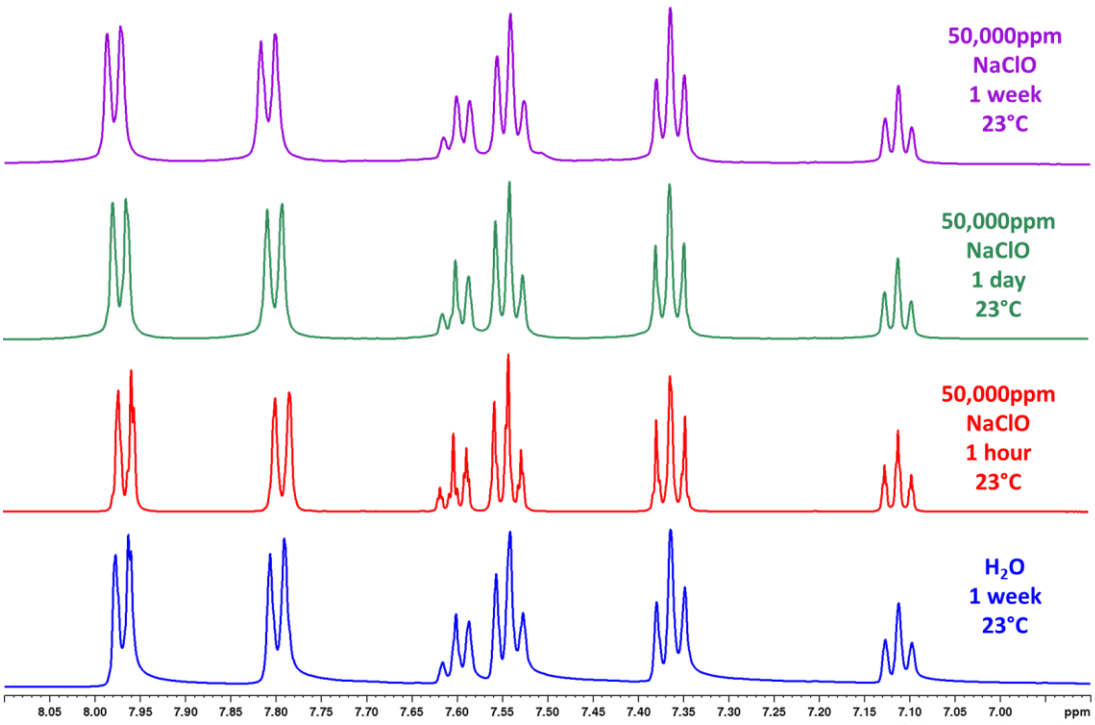

Zoomed in aromatic region: ^{1}H NMR spectra of amide after reacting in 50,000ppm NaClO. A negative control was run in water for 1 week at 23°C (blue). Reactions were run in 50,000ppm NaClO at 23°C for 1 hour (red), 1 day (green), and 1 week (purple).

Amide Precipitate After 10,000ppm NaClO Reaction- Aromatic Region

^{1}H NMR, DMSO-d_6, 500MHz, 294K

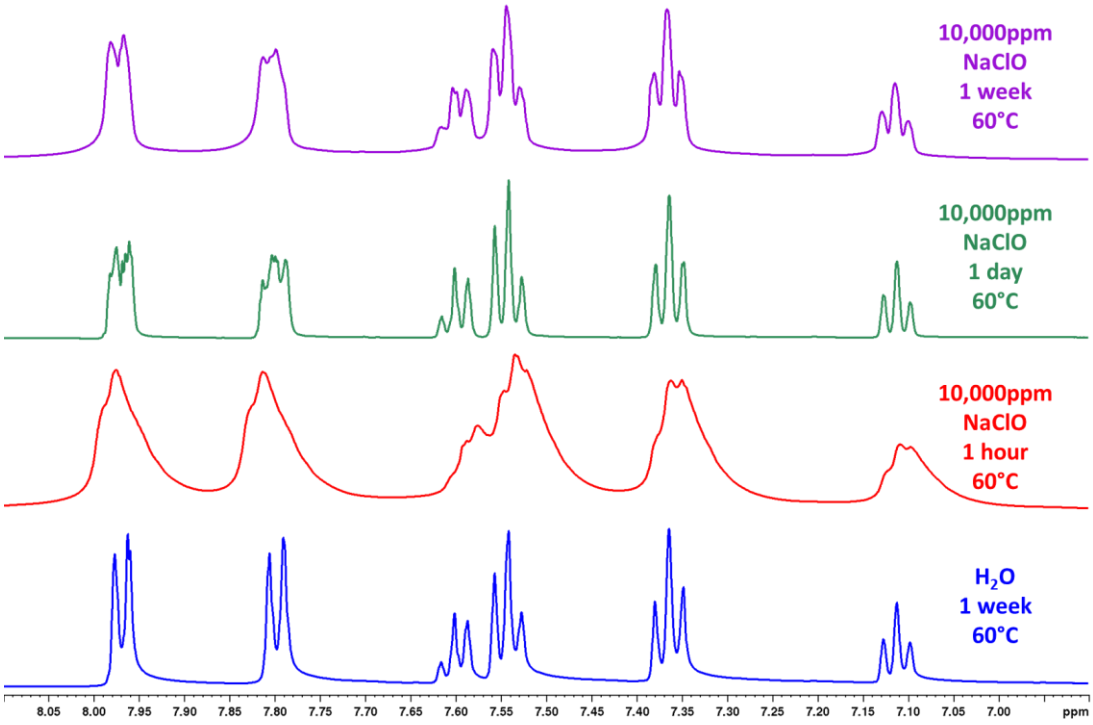

Zoomed in aromatic region: ^{1}H NMR spectra of amide after reacting in 10,000ppm NaClO. A negative control was run in water for 1 week at 60°C (blue). Reactions were run in 10,000ppm NaClO at 60°C for 1 hour (red), 1 day (green), and 1 week (purple).

Water Washes Amide Precipitate After 50,000ppm NaClO Reaction

^{1}H NMR, $CDCl_3$, 500MHz, 294K

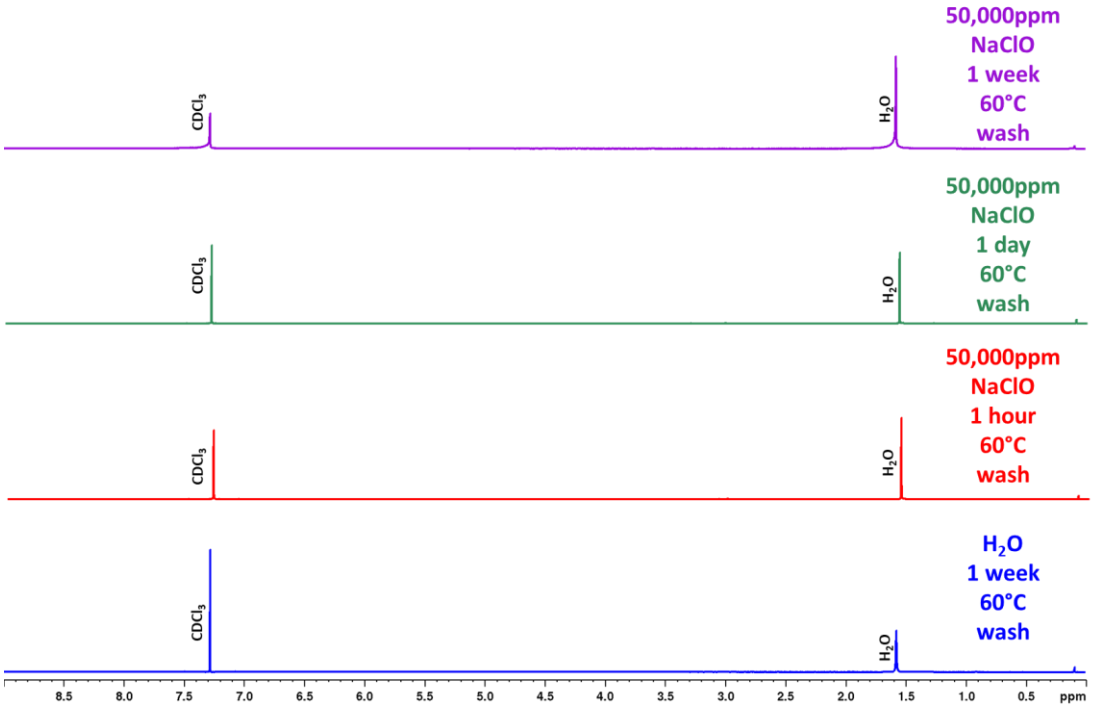

^{1}H NMR spectra of amide wash after reacting in 50,000ppm NaClO. A negative control was run in water for 1 week at 60°C (blue). Reactions were run in 50,000ppm NaClO at 60°C for 1 hour (red), 1 day (green), and 1 week (purple).

CHAPTER 3. INTERFACIAL POLYMERIZATION OF POLYTRIAZOLES AS FLAT SHEET MEMBRANES

(Adapted with permission from Bruno, Nicholas; Mathias, Ronita; Ma, Ya; Thompson, Kirstie; Hamlett, Breanne; Lively, Ryan; Zhou, Huaxing; Finn, M.G.; Bhandari, Dhavel; McKay, Craig; Jue, Melinda. Functionalized Membranes and Methods of Production Thereof. US Patent 16/295,918, September 12, 2019.)

The work presented in Chapter 3 could not have been possible without the collaboration from Dr. Ryan Lively's lab in the department of Chemical and Biomolecular Engineering at the Georgia Institute of Technology. TGAs were conducted by Matthew Rivera in Dr. Lively's lab. Additionally, instrumentation including DSC, GPC, and nitrogen physisorption were provided by Science and Technology of Advance Materials and Interfaces (STAMI) at the Georgia Institute of Technology.

Interfacial polymerization is commonly used to make thin, crosslinked polymer membranes for use in several separation applications, most notably to produce crosslinked polyamides for water desalination. Thin membranes are localized at the interface of two immiscible solvents as a crosslinking reaction of di-, tri- or multi-functionalized monomers occurs. Each solvent contains one monomer and as the membrane is formed, the crosslinked polymer separates the two monomer solutions, stopping the reaction, and resulting in nanometer thick films (Figure 3-1 a-b).[63]

While the CuAAC has not been explored to make flat-sheet membranes using a interfacial polymerization, it has been explored in an emulsion-type interfacial

polymerization to create nanocapsules.[64-65] As the two immiscible solvents are rapidly stirred, pockets of on solvent are created within the other. Crosslinked polymer is formed at the liquid-in-liquid interface of the two solvents, resulting in a spherical shaped nanocapsule. Since the CuAAC reaction is a three-component system (azide, alkyne, and copper catalyst), water soluble and organic soluble azides, alkynes, and copper sources can be used in many combinations to create membranes with different properties. (Figure 3-1c-h). This is not unique to CuAAC interfacial polymerization and other 3-component systems have been studied in the past. [66]

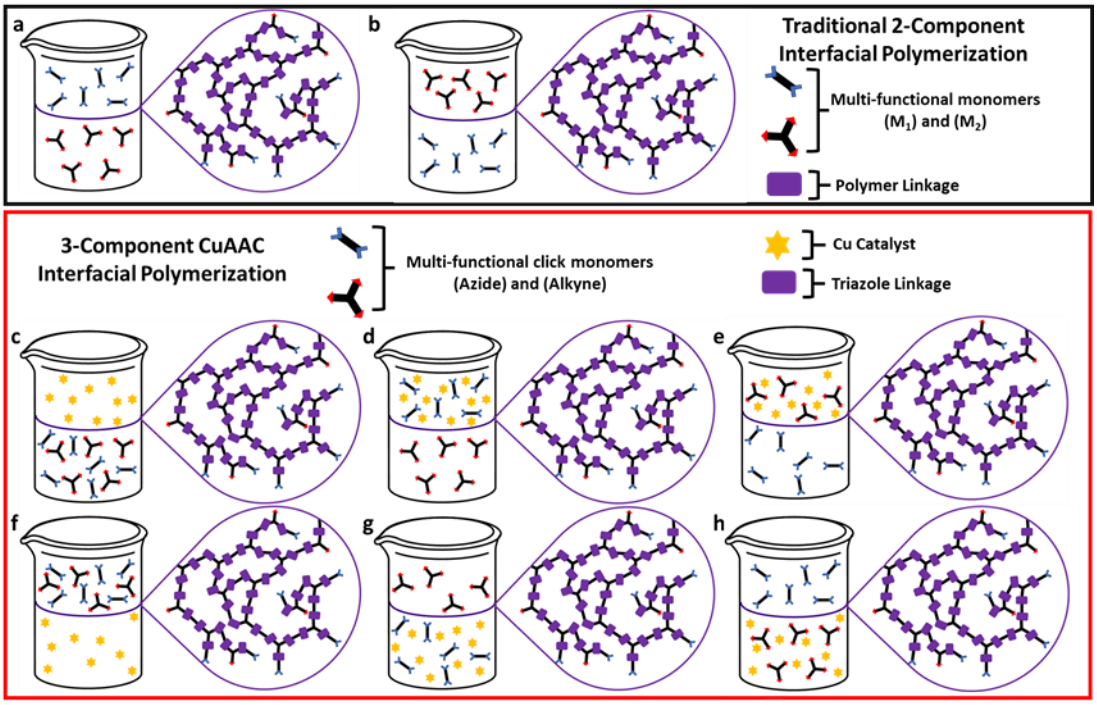

Figure 3-1: 2-Component Traditional Interfacial Polymerization versus 3-Component CuAAC Polymerization. Regardless of which layer the component are in, a crosslinked network is always formed at the interface.

In this study, multi-functional azides and alkynes were polymerized into flat sheet membranes using interfacial polymerization in the presence of Cu(I). The transfer of flat sheet membranes onto solid supports was attempted for functional testing in gas and liquid separations, however, the lack of mechanical strength of the resulting membranes

prevented functional testing from being performed. Nevertheless, film-forming properties were determined. After establishing which monomer combinations were film-forming, emulsion-type interfacial polymerizations were conducted to created crosslinked polytriazole powders. These powders were analysis for BET surface area, decomposition temperature (T_d), and glass transition temperature (T_g).

3.1 Azide and Alkyne Monomer and Polymer Design

Due to the relative ease of azides and alkynes synthesis, a large series of azide- and alkyne- functionalized monomers were synthesized for testing in interfacial polymerization (Figure 3-2). To help develop a structure-to-function relationship of monomers to membrane formation and function four variables were investigated: (1) organic-soluble versus water-soluble monomers, (2) rigid versus flexible monomers, (3) crosslinking of linear, contorted polymers, and (4) monomers with contorted backbones.

Small molecule monomers included: organic-soluble azides (1, 2) organic-soluble alkynes (A, B, C, D, E, F, G), and water-soluble alkynes (H). Changing each components solubility allowed for the use of both water-soluble ($CuSO_4$ + sodium ascorbate) and organic-soluble ($(PPh_3)_2CuOAc$) copper source. Both flexible (2, E, F, G, I, H) and rigid (1, A, B, C, D) monomers were synthesized to determine the effects of rigidity in the polymer backbone on both membrane formation and properties. Highly rigid, aromatic monomers tend to have good separations properties, but also tend to precipitate out of solution before membranes form due to π- π stacking.[67]

In addition to small molecules, azide-(3, 4) and alkyne-(J, K) functionalized PIMs were synthesized to test interfacial crosslinking on a linear polymer. While PIMs have

shown promising gas separation results due to their high surface areas,[47-48] their use as hydrocarbon separation membranes is limited due to a large degree of swelling in organic solvents.[27] However, it has been shown that, in general, crosslinking polymers will reduce swelling in various solvents. [68] Using interfacial polymerization to crosslink functionalized PIM would not only reduce swelling in organic solvent, but also form ultra-thin (<1 μm) PIM membranes.

Lastly, spirocenter monomers (C, D) were synthesized to form a PIM-like, contorted backbone in the crosslinked polymer membrane. The bent backbone could imitate the PIM properties: (1) retain solvent solubility despite the highly aromatic structure, favoring membrane formation as opposed to polymer powders and (2) create materials with high porosity.

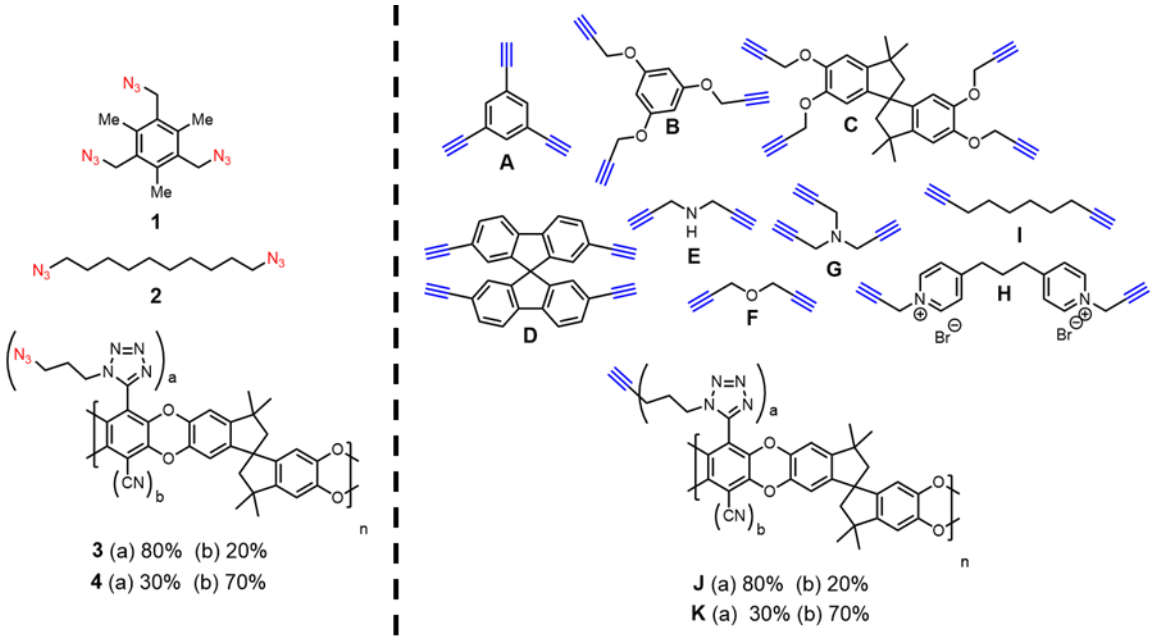

Figure 3-2: Multi-functional azide and alkyne monomers used in interfacial polymerization.

3.2 Results and Discussion

3.2.1 Film-Forming Properties

The film-forming properties of each monomer combination were evaluated after reacting for 16 hours at room temperature. After the reaction time, the aqueous (top layer when chloroform is used) was removed from the reaction and the tube was inverted to determine if a continuous membrane had formed (Figure 3-3). While the majority of small molecule azide and alkyne combinations with $CuSO_4$ gave continuous membranes (Table 3-1), reactions involving monomer F and G, did not result in any membrane formation but instead a powder at the interface. It is difficult to determine why membrane formation was not favored in polymers containing that monomers. All crosslinking reactions involving functionalized PIM polymers, with the exception of PIM with monomers F and G, resulted in a continuous membrane at the interface.

Multiple attempts to remove the intact membranes from the reaction vessel were unsuccessful. Once the membranes were unadhered from the walls of the vials, they curled into a ball and could not be flatten out without tearing or breaking the membrane. The membranes were not able to go through functional testing due to the low mechanical strength of the unsupported membranes and the inability to make intact membrane composites. However, once non-intact membranes were removed from the reaction mixture, they were subjected to washes with various solvents. The membranes did not dissolve in any solvents, indicating that crosslinking had occurred.

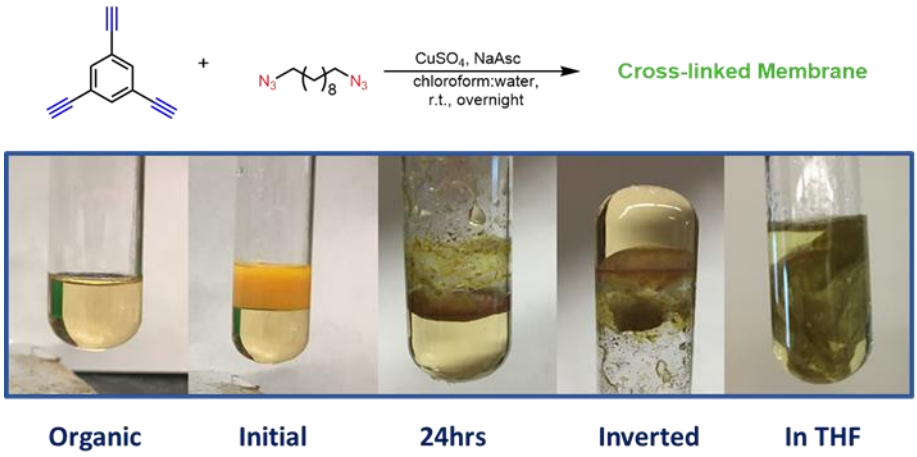

Figure 3-3: Example of interfacial polymerization where a flat sheet membrane was formed at the interface of the organic and aqueous layers. The membrane was noted as continuous if the membrane could be inverted without the organic layer flowing out of the tube.

In reactions where the water-soluble alkyne was in the same aqueous layer at the copper, a large amount of solid was produced in the aqueous layer. This could be caused by the alkynes participating in Glaser coupling due to the presence of copper.[69] While normally the CuAAC reaction would out compete Glaser coupling, the proximity of the alkyne and the copper away from the azide could result in this reaction.

Water-soluble alkynes also allowed for the use organic copper catalysts to be used for interfacial polymerization. (PPh_3)CuOAc was chosen for this study due to its fast reaction kinetics in solution-based CuAAC reactions.[46] For this set of interfacial polymerizations, the water-soluble monomer was restricted to the aqueous layer, while the complimentary azide monomer and Cu(I) source were confined to the organic layer. In all reactions where organic copper was used, only powder formed at the interface instead of a continuous membrane. This could be due to the fast reaction kinetics favoring a solid precipitate instead of membrane formation

In the CuAAC reaction, the copper catalyst first reacts with the alkyne to create an Cu-acetylide species.[70] We initially hypothesized that when the Cu is in the same layer as the alkyne monomer the CuAAC reaction would proceed at a faster rate from pre-forming the copper acetylide complex.

However, no reactions where organic Cu was used formed a continuous membrane at the interface, however, they did form powders. This could be due to the fast reaction kinetics favoring a solid precipitate instead of membrane formation.

Table 3-1: The film-forming behavior of each monomer combination with $CuSO_4$ and $(PPh_3)_2CuOAc$ as the Cu catalyst.

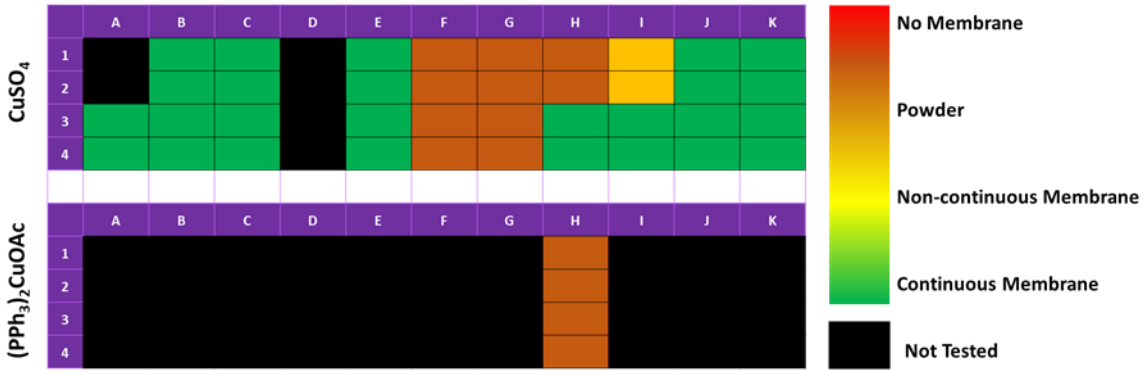

3.2.2 Macroporous Supports for Interfacial Polymerization of Thin Film Composites

Macroporous stainless-steel discs from Sterlitech were used as the support layer for polytriazole composites. While the Sterlitech stainless steel discs were not tested for chemical stability, stainless steel in general has "poor" acid stability, "good" base stability, and "excellent" oxidative stability.[71] Due to the low acid stability of stainless steel this would not be an ideal support for water desalination membrane but was used as an initial

support for this study. Similar to the production of polyamides on polysulfone supports, the stainless-steel supports were submerged in the aqueous solution for ~30 seconds and then immersed in the organic solution overnight. Once removed from the organic solutions, the composite membranes were dried in a vacuum oven (50°C) overnight and SEM imaging was completed. While membrane did form on the surface of the support, the polytriazole composite membranes made by this method always resulted in uneven or cracked membranes (Figure 3-4).This is likely due to: (1) the diameter of macropores of the stainless steel support being too large and polytriazoles forming into the bulk of the support instead of the surface or (2) the rigidity of the polytriazoles creating brittle membrane material once dried.

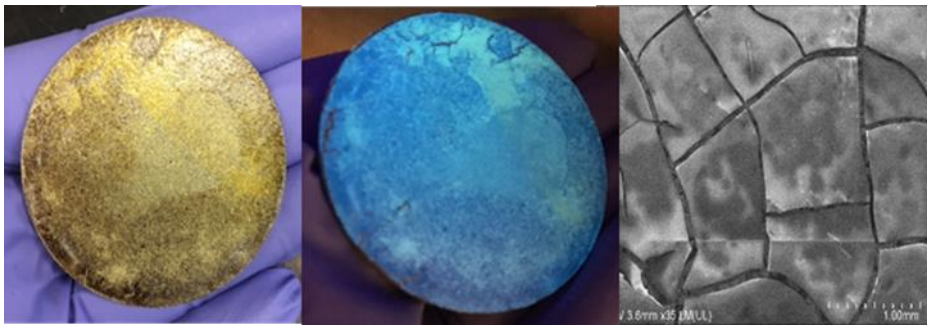

Figure 3-4: Interfacial polymerization of polytriazoles on stainless-steel microporous supports. This method created uneven and cracked polytriazole composites.

3.2.3 Testing of Crosslinked Membranes as a Powder

Due to the low mechanical strength of the thin polytriazole membranes, functional test for hydrocarbon separations and water desalination could not be performed. However, polymer properties could be tested on the crosslinked materials as powders. Emulsions-type interfacial polymerizations using the same combinations of azides and alkynes that

were used in the traditional interfacial polymerizations, were conducted to synthesize crosslinked polytriazole powders (Table 5). This data pairs well with that of Table 4. In traditional interfacial polymerization, if a continuous membrane, non-continuous membrane, or powder formed at the interface, then a powder was formed in the complimentary emulsion polymerization.

Table 3-2: The powder forming behavior of each monomer combination with $CuSO_4$ and $(PPh_3)_2CuOAc$ as the Cu catalyst. Green indicates that a cross-linked powder was formed. Red indicates that no solid was present after 24 hours. Black was not tested.

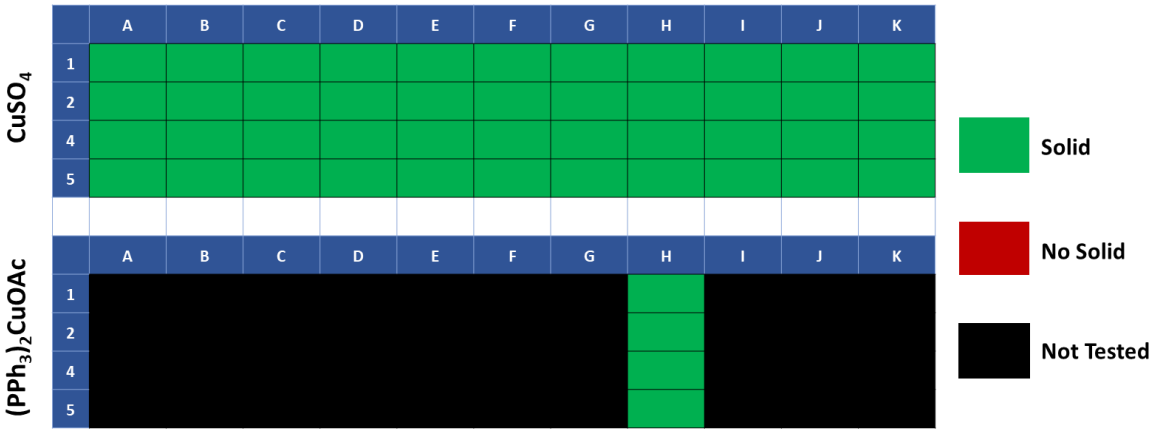

3.2.3.1 Brunauer, Emmett, and Teller (BET) Surface Area

Nitrogen physisorption at 77K is commonly used in the determination of the surface area and pore size distribution of porous materials. The amount of adsorbed nitrogen gas is related to the total surface area of the polymers. The surface area is determined by physical adsorption of a monolayer of nitrogen on the surface of the solid. Physical adsorption results from relatively weak van der Waals forces result in physical adsorption of the nitrogen to the surface of the powders.[72] Pores are classified based on size and can

exist as micropores (<2nm diameters), mesopores (2-50nm diameter), and macropores (>50nm diameter).[73]

Adsorbed amounts of nitrogen are volumetrically measured as a function of absolute pressure and saturated pressure and resulting isotherms are used to determine surface area and pore size distribution.[74] While BET surface area gives information about pores that exist in the polytriazole powders in the presence of nitrogen, this is not a direct correlation to the properties of the pores in organic solvents or water. Although the polymers are crosslinked, a small amount of swelling can occur in the presence of solvent, changing the surface area and pore size of the polymer. Additionally, solvents can move through a nonporous polymer matrix based on solubility and diffusivity of the solvent in the polymer. Lastly, pores smaller than the diameter of nitrogen (0.37nm) cannot be determine by this method.

It was hypothesized that the majority of polytriazoles would not show a large amount of surface area or micropores, due to the π-π stacking of the highly aromatic monomers and their ability to stack resulting in a reduction of free volume in the polymer. It was thought that adding contorted monomers to the polymer would reduce the amount of stacking and increase the surface area of the polytriazoles containing spirocenters. Lastly, it was thought that crosslinking functionalized PIM would show comparable surface area to non-functionalized PIM-1. However, earlier work showed that the functionalization of the PIM-1 polymers with tetrazoles, followed by alkylation with azides and alkynes greatly reduced the surface area of the polymers. This is likely due to the pendant functional group now occupying the once empty pore volume.[75] This led us to believe that crosslinking functionalized PIM would also show low to no surface area.

Physisorption experiments show almost all of the synthesized polytriazoles to be nonporous with low BET surface area (Table 3-3). Small molecule polytriazoles were non-porous via BET analysis, due to no aspect of the polymers providing free volume. Adding spirocenter-containing monomers to the reaction did not alleviate the stacking effects and polymers still exhibited very low surface areas. Additionally, crosslinked functionalized PIMs also showed low surface area, which was consistent with previous data showing that once pendant groups were added to the PIM polymers, surface area was greatly reduced.

Table 3-3: Summary of BET surface area (m^2/g) from nitrogen physisorption analysis of polytriazoles created with $CuSO_4$ and $(PPh_3)_2CuOAc$ catalyst. BET surface area has not been determined for the black cells.

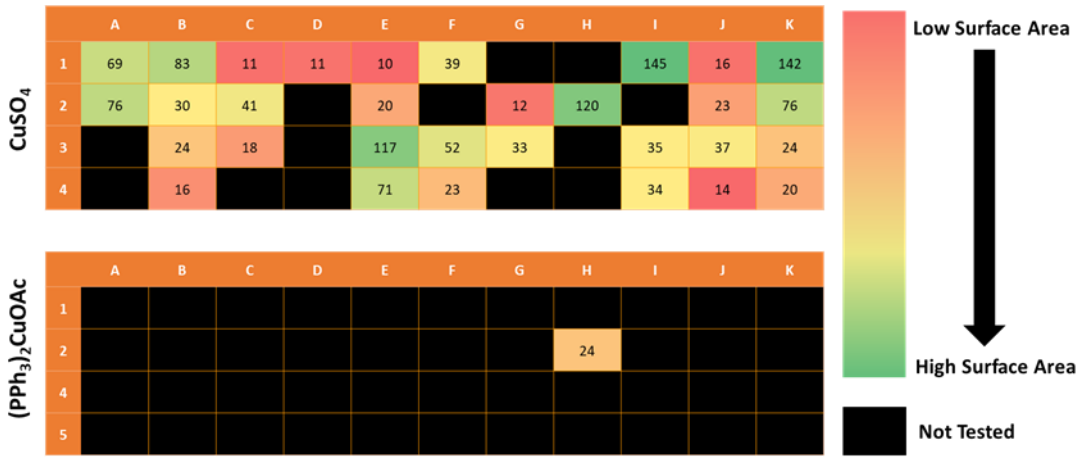

3.2.3.2 Decomposition Temperature (T_d)

Decomposition temperature, or T_d, is the temperature at which a compound chemical decomposes and is measured via a weight change in thermal gravimetric analysis (TGA). It is important to understand the decomposition temperature in polymers to ensure they are suitable for applications at elevated temperature. For membranes, separation processing temperature should be well below T_d to avoid degrading the polymer, changing pore sizes, or destroying the selective layer. The temperature at which each polytriazole polymer reaches 10% decomposition, T_{d10} is shown in Table 3-4. Since all polymer networks are connected by triazole linkages, the T_{d10} is in a similar range for the polytriazoles tested. However, rigid monomers, such as A and 1 showed higher T_d than flexible monomers, such as 2, E, and F.

Table 3-4: Summary T_{d10} reported in °C for polytriazoles as calculated from TGA analysis. White cells were not analyzed.

$CuSO_4$

	A	B	C	D	E	F	G	H	I	J	K
1	316		338	327	242						
2	296		275		252	232		208			
4											
5											

$(PPh_3)_2CuOAc$

Column1	A	B	C	D	E	F	G	H	I	J	K
1	316		338	327	242						
2	296		275		252	232					
4											
5											

3.2.3.3 Glass Transition Temperature (T_g)

Glass transition temperature, or T_g is the temperature at which amorphous polymers transition from a hard, rigid glassy state to a flexible, rubbery state. Above the T_g, polymer chains can move freely around each other and change confirmations. The T_g is accompanied by a change in the heat capacity of the polymer, which can be measures by differential scanning calorimetry (DSC).[76] For polymers to be used as separation membranes, they must be below their T_g at membrane operation temperatures to ensure consistency in pore size.

There are many factors that can affect a polymer's T_g including rigidity, intermolecular forces, pendant groups, and crosslinking. Highly rigid polymers have a reduced chain mobility and tend to have higher T_g than flexible polymers. Molecules with strong intermolecular forces, such as hydrogen bonding or dipole-dipole interactions, are locked into a confirmation by those intermolecular forces and have a higher T_g. Pendant groups on the polymer backbone also affect T_g. Bulky sidechains increase chain entanglement and lead to a higher T_g, while flexible sidechains have increases rotational freedom and lower T_g. Lastly, crosslinking a polymer locks a polymer into a confirmation, reducing rotational freedom, and increasing T_g.

However, all of the polytriazole networks did not shown a T_g before their T_{d10}. This can be a result the increase in T_g due to high levels of crosslinking in these polymers.

3.3 Conclusion

In this study, several multi-functional azides and alkynes were synthesized, including water and organic soluble, flexible and rigid, and pendant groups off of polymers. The film-forming properties of the CuAAC interfacial polymerization of these azides and alkynes were determined, and most combinations created thin membranes through this method. However, the synthesis of thin film composites using CuAAC interfacial polymerization was unsuccessful, due to the low mechanical strength of the polytriazole films. Emulsion polymerizations were used to create polytriazole powders that were composed of the same polytriazole structures. All polytriazole powders showed low to no surface area, similar T_d, and no T_g. For these materials to be used as separation membranes, a casting technique onto a macroporous support is needed to increase the strength of the membranes.

3.4 Methods and Characterization

3.4.1 General Interfacial Polymerization Method

Stock solutions of organic-soluble monomers were made in chloroform at 0.75M. Stock solutions of water-soluble monomers were made in H_2O at 0.045M. A stock solution of $CuSO_4$ was made at 0.045M and a stock solution of sodium ascorbate was made in H_2O at 0.9M. A stock solution of $(PPh_3)_2CuOAc$ was made in chloroform at 0.05M. For all polymerizations, 1mL of each component was added to a 20 mL test tube. **Flat Sheet Membranes:** Reaction mixtures were covered with parafilm and allowed to sit at room temperature for 16 hours. **Emulsion Powders:** Reaction mixtures were sealed in 4 mL vials and stirred vigorously at room temperature for 16 hours. After the completion of the

reaction resulting solids were filtered and washed with H_2O (3x). The solids were then purified via Soxhlet extraction (acetone, MeOH, DCM) to remove unreacted starting materials. The polymers were dried in the vacuum oven overnight at 150°C before BET surface area analysis.

3.4.2 Materials

Reagents and solvents were purchased from commercial sources and used as received, unless otherwise stated. Chromatography was performed on an Isolera One: Accelerated Chromatographic Isolation unit from Biotage with a UV and ELSD detector with KP-Sil columns. Analytical TLC was performed on glass-backed plates and visualized by exposure to UV light.

3.4.3 Synthetic Methods

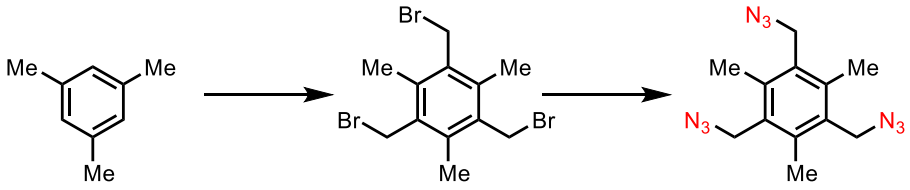

2-1 **1**

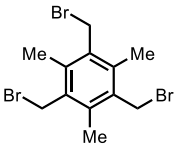

1,3,5-tris(bromomethyl)-2,4,6-trimethylbenzene[77] (2-1) Mesitylene (12g, 100mmol, 1 equiv.) and formaldehyde (10.3g, 340 mmol, 3.4 equiv.) were added to a round bottom flask with acetic acid (60 mL). 33% HBr in acetic acid (75mL) was added in one portion and the reaction mixture stirred at 95 °C for 12 hours. Once the reaction was complete, it was allowed to cool to room temperature and was poured onto ice. The solids were filtered, washed with H_2O (3x100mL), and dried under

vacuum to give 29.7 g (74 %) 1,3,5-tris(bromomethyl)-2,4,6-trimethylbenzene as a white solid.

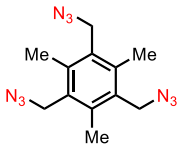

1,3,5-tris(azidomethyl)-2,4,6-trimethylbenzene (1)[78] Compound 2-1 (7.9 g, 19.5 mmol, 1 equiv.) was dissolved in DMF (20mL). NaN_3 (7.6 g, 117.2 mmol, 6 equiv.) was added and the reaction stirred at 60°C for 16 hours. The reaction was cooled to room temperature and poured into H_2O. The resulting solid was filtered and washed with H_2O (3x50 mL). It was then dried under vacuum to afford 5.4g (95%)) 1,3,5-tris(azidomethyl)-2,4,6-trimethylbenzene as a white solid. **^{1}H NMR** (500MHz, $CDCl_3$) δ 4.50 (6H), and 2.46 (9H).

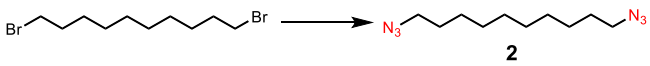

2

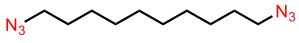

1,10-diazidodecane (2)[78] 1,10-dibromodecane (7.5 mL, 33.3 mmol, 1 equiv.) was added to DMF (50mL). NaN_3 (4.3 g, 66.7 mmol, 2 equiv.) was added and the reaction stirred at 60°C for 10 hours. The reaction was cooled to room temperature and poured into 300mL H_2O. The compound was extracted with DCM (3x100 mL), and the organic layer was washed with H_2O. The combined organic fractions were dried over sodium sulfate, filtered, and concentrated via rotary evaporation to afford 7.34g (98%) 1,10-diazodecane as a clear, pale yellow oil. **^{1}H NMR** (500 MHz, Chloroform-*d*) δ 3.25 (t, J = 7.0 Hz, 4H), 1.65 – 1.54 (m, 4H), 1.43 – 1.24 (m, 12H).

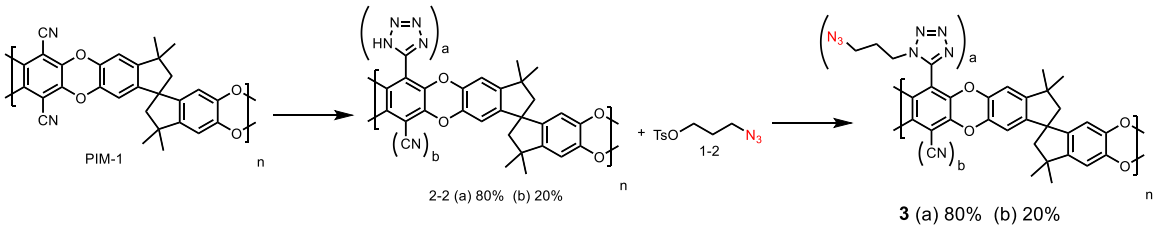

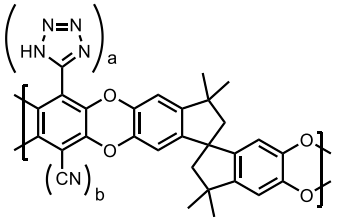

Tz-PIM-80 (Tetrazole-PIM-80% Functionalized) (2-2)[79]

PIM-1 (20 g, 43.4 mmol, 1 equiv.) was completely dissolved in DMF (400mL) at 130°C. NaN_3 (22.6 g, 347.4 mmol, 8 equiv.) and $ZnCl_2$ (47.4 g, 347.4 mmol, 8 equiv.) were added and the reaction was allowed to stir at 130 °C for 4 days. The reaction was cooled to room temperature and poured into H_2O (400mL) and filtered. The solid was resuspended in 1M HCl (300mL) and stirred at 65°C for 4 hours. The reaction was cooled to room temperature, poured into H_2O and filtered. The polymer was then washed with H_2O (3x100mL) and dried in the vacuum oven at 50°C for 16 hours. The Tz-PIM was sparingly soluble and was used directly in the next step without characterization.

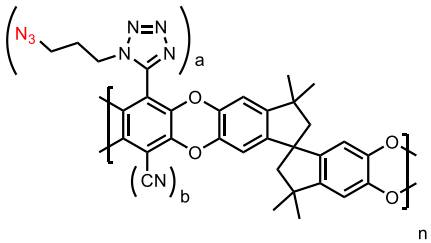

3 (a) 80% (b) 20%

(3) Tz-PIM-80-PAz (Tetrazole-PIM-80% Functionalized with Propylazide) Tz-PIM-80 (3g) was suspended in NMP (75mL). Compound 1-2 (14.4g) and K_2CO_3 (5.2 g) was added and the reaction was stirred under Ar at 85°C for 3 days. The reaction was allowed to cool to room temperature and was poured into H_2O (200mL). Solids were filtered over celite, and the solids on celite were dried in the vacuum oven at 50°C for 16 hours. The solids on celite were dissolved in $CHCl_3$ and the dissolved polymer was filtered. The $CHCl_3$ was removed until only a minimal amount of $CHCl_3$ remained. The polymer solution was precipitated into MeOH, filtered, and dried to afford 1.9g of Tz-PIM-80-PAz. **^{1}H NMR** 500 MHz, Chloroform-*d*) δ 6.93 – 5.89 (m, 4H), 5.03 – 4.23 (m, 3H), 3.62 – 3.10 (m, 4H), 2.61 – 1.82 (m, 6H), 1.24 (s, 12H).

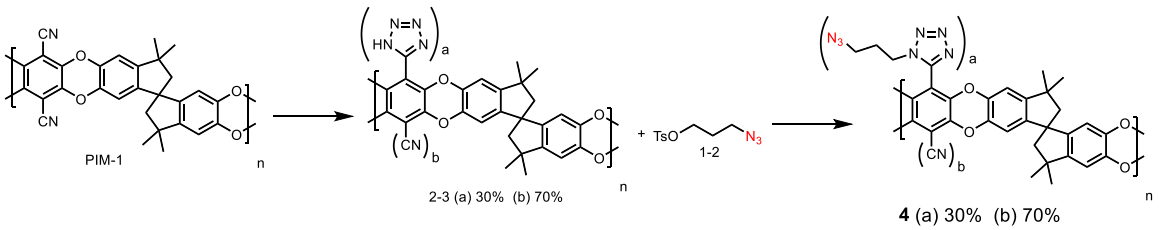

PIM-1 → 2-3 (a) 30% (b) 70% + TsO 1-2 → **4** (a) 30% (b) 70%

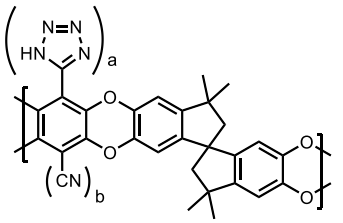

2-3 (a) 30% (b) 70%

Tz-PIM-30 (Tetrazole-PIM-30% Functionalized) (2-3) PIM-1 (10g, 21.7 mmol, 1 equiv.) was completely dissolved in DMF (200mL) at 130°C. NaN_3 (0.85 g, 13.2 mmol, 0.6 equiv.) and $(PPh_3)_2PdCl_2$ (0.46 g, 0.65 mmol, 0.03 equiv.) were added and the reaction was allowed to stir at 130°C for 16 hours. The reaction was cooled to room temperature and poured into H_2O (400mL) and filtered. The solid was resuspended in 1M HCl (300mL) and stirred at 65°C for 4 hours. The reaction was cooled to room temperature, poured into H_2O and filtered. The polymer was then washed with H_2O (3x100mL) and dried in the vacuum oven at 50°C for 16 hours. The Tz-PIM was sparingly soluble and was used directly in the next step without characterization.

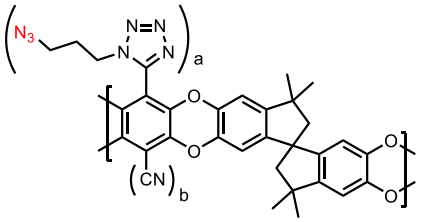

4 (a) 30% (b) 70%

Tz-PIM-30-PAz (Tetrazole-PIM-30% Functionalized with Propylazide) (4) Tz-PIM-30 (1.5 g) was suspended in NMP (75mL). Compound 1-2 (7.2 g) and K_2CO_3 (5.2 g) was added and the reaction was stirred under Ar at 85°C for 3 days. The reaction was allowed to cool to room temperature and was poured into H_2O (200mL). Solids were filtered over celite, and the solids on celite were dried in the vacuum oven at 50°C for 16 hours. The solids on celite were dissolved in $CHCl_3$ and the dissolved polymer was filtered and $CHCl_3$ was removed until only a minimal amount of $CHCl_3$ remained. The polymer solution was precipitated into MeOH, filtered, and dried

to afford Tz-PIM-30-Paz. **^{1}H NMR** (500 MHz, Chloroform-*d*) δ 6.48 (dd, *J* = 197.6, 143.5 Hz, 4H), 5.17 – 4.35 (m, 1.22H), 3.76 – 3.06 (m, 6H), 2.61 – 2.00 (m, 4H), 1.72 – 0.64 (m, 12H).

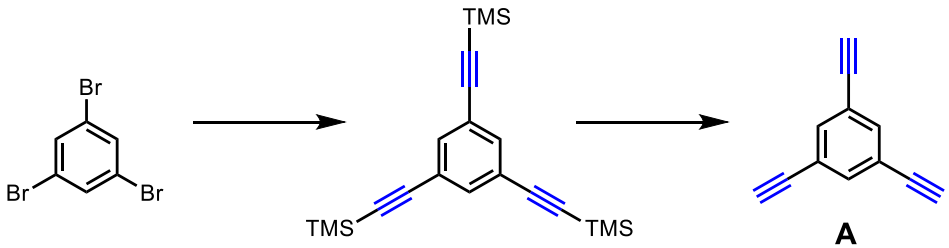

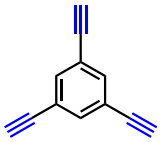

1,3,5-triethynylbenzene (A)[80] 1,3,5-tribromobenzene (5 g, 15.9 mmol, 1 equiv.), $(PPh_3)_2PdCl_2$ (0.33 g, 0.48 mmol, 0.03 equiv.), and CuI (0.09 g, 0.48 mmol, 0.03 equiv.) were added to a round-bottom flask. The flask was then evacuated and backfilled with nitrogen (this process was performed a total of three times). Dry, degassed Et_3N (90mL) was added and trimethylsilylacetylene (8.8 mL, 63.5 mmol, 4 equiv.) were then added slowly by syringe. The reaction mixture stirred under nitrogen at 65 °C for 16 hours. The reaction mixture was then cooled to room temperature and solvent was removed under reduced pressure. The crude product was dissolved in hexane and filtered through a silica plug and solvent was removed. 1:1 DCM:MeOH (200 mL) and K_2CO_3 (excess, 10 g) were added and the reaction was allowed to stir for 16 hours at room temperature. Solvent was removed and the crude product was

dissolved in DCM (200 mL) and H_2O (200 mL), extracted with DCM (2x200 mL), washed with H_2O (200 mL). The combined organic fractions were dried over sodium sulfate, filtered, and concentrated via rotary evaporation to afford 0.9 g (50%) 1,3,5-triethynylbenzen as an off-white powder. **^{1}H NMR** (500 MHz, Chloroform-*d*) δ 7.57 (s, 3H), 3.10 (s, 3H).

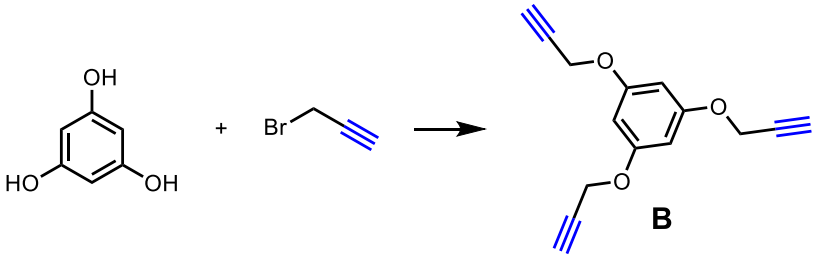

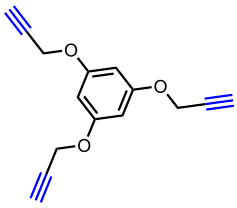

1,3,5-tris(prop-2-yn-1-yloxy)benzene (B)[81] Phloroglucinol (10 g, 79.3 mmol, 1 equiv.) was added to 1:8 MeOH:DMF (250mL). K_2CO_3 (67 g, 476 mmol, 6 equiv.) was added and the reaction was stirred at 50°C for 1 hour. Propargyl bromide (56.6 g, 476 mmol, 6 equiv.) was added dropwise and the reaction stirred at 65°C for 16 hours. The reaction mixture was cooled to room temperature and poured into H_2O (300 mL), extracted with ethyl acetate (3x300 mL), and washed with brine (1x300 mL). The combined organic fractions were dried over sodium sulfate, filtered, and concentrated via rotary evaporation. The crude material was purified by column chromatography, eluting with 1:5 EA:Hex to afford 3.5g (19%) of 1,3,5-tris(prop-2-

yn-1-yloxy)benzene as a white solid. **^{1}H NMR** (500 MHz, Chloroform-*d*) δ 6.26 (s, 3H), 4.64 (d, *J* = 2.4 Hz, 6H), 2.53 (t, *J* = 2.4 Hz, 3H).

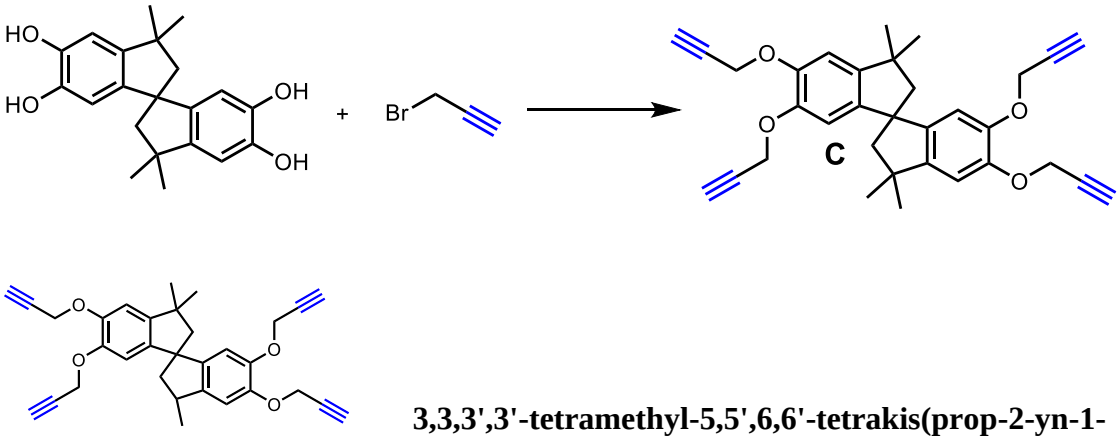

3,3,3',3'-tetramethyl-5,5',6,6'-tetrakis(prop-2-yn-1-yloxy)-2,2',3,3'-tetrahydro-1,1'-spirobi[indene] (C) Tetrahydroxyspirobisindane (5 g, 14.7 mmol, 1 equiv.) and K_2CO_3 (12.2g , 88.1 mmol, 6 equiv.) were stirred in acetone (37mL) for 5 minutes. Propargyl bromide (13.1 mL, 88.1 mmol, 6 equiv.) was added dropwise and the reaction stirred at reflux for 16 hours. The reaction was cool to room temperature and filtered over celite, washed with DCM, and concentrated via rotary evaporation. This resulted in 6.3 g (87%) of 3,3,3',3'-tetramethyl-5,5',6,6'-tetrakis(prop-2-yn-1-yloxy)-2,2',3,3'-tetrahydro-1,1'-spirobi[indene] as a white powder. **^{1}H NMR** (400 MHz, Chloroform-*d*) δ 6.88 (s, 2H), 6.47 (s, 2H), 4.79 (dd, *J* = 2.4, 1.1 Hz, 2H), 4.63 (dd, *J* = 7.6, 2.4 Hz, 2H), 2.56 (t, *J* = 2.4 Hz, 2H), 2.42 (t, *J* = 2.4 Hz, 2H), 2.35 (d, *J* = 13.0 Hz, 2H), 2.22 (d, *J* = 13.1 Hz, 2H), 1.37 (d, *J* = 17.2 Hz, 12H). **^{13}C NMR** (100MHz, Chloroform-*d*) 147.23, 146.94, 145.45, 143.17, 110.94, 108.45, 78.74,

78.55, 75.49, 75.39, 59.24, 57.04, 43.13, 31.31, 30.17. **HRMS** (ESI-TOF) calculated for $C_{33}H_{32}O_4$ ($M+H^+$) 493.23, found 493.28 *m/z*.

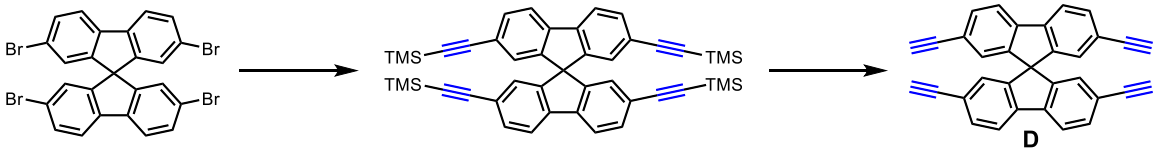

2,2',7,7'-tetraethynyl-9,9'-spirobi[fluorene] (D)[82] 2,2',7,7'-tetrabromo-9,9'-spirobi[fluorene] (0.9 g, 1.42 mmol, 1 equiv.), $(PPh_3)_2PdCl_2$ (0.078 g, 0.108 mmol, 0.075 equiv.), PPh_3 (0.072 g, 0.28 mmol, 0.2 equiv.), and CuI (0.022 g, 0.116 mmol, 0.08 equiv.) were added to a flask. The flask was then evacuated and backfilled with nitrogen (this process was performed a total of three times). Dry, degassed diisopropaylamine (48mL) was added to the flask. Trimethylsilylacetylene (1.5 mL, 10.6 mmol, 7.4 equiv.) was added slowly and the reaction stirred at 90 °C for 22 hours. The reaction mixture was cooled to room temperature and solvent was removed via rotary evaporation. The crude material was purified by column chromatography, eluting with hexanes. The resulting solid was dissolved in 1:1 MeOH:DCM (44mL) and K_2CO_3 (excess, 1.2 g) were added and the reaction was stirred at room temperature for 16 hours. The

reaction was poured into 100 mL H_2O, extracted with DCM (3x100 mL), and washed with brine (1x100 mL). The combined organic fractions were dried over sodium sulfate, filtered, and concentrate via rotary evaporation to afford 0.23 g (44%) of 2,2',7,7'-tetraethynyl-9,9'-spirobi[fluorene] as an off-white solid. **^{1}H NMR** (500 MHz, Chloroform-*d*) δ 7.78 (d, J = 7.9 Hz, 5H), 7.53 (dd, J = 7.9, 1.4 Hz, 5H), 6.83 (d, J = 1.4 Hz, 4H), 3.01 (s, 4H).

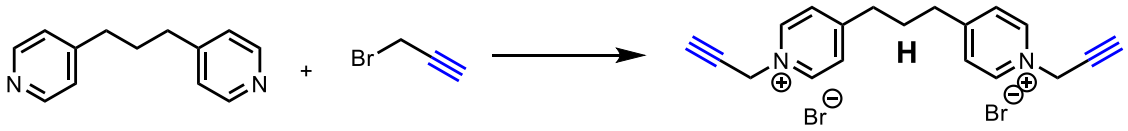

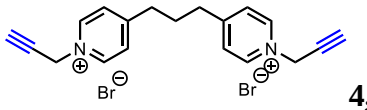

4,4'-(propane-1,3-diyl)bis(1-(prop-2-yn-1-yl)pyridin-1-ium) (H) 1,3-di(pyridin-4-yl)propane (10 g, 50.5 mmol, 1 equiv.) was dissolved in MeCN (200mL). Propargyl bromide (22 mL, 202 mmol, 4 equiv.) was added dropwise and the reaction stirred at room temperature for 16 hours. The reaction mixture was poured into diethyl ether and the solid was filtered and dried under vacuum to afford 7.1g (54%) 4,4'-(propane-1,3-diyl)bis(1-(prop-2-yn-1-yl)pyridin-1-ium) as a brown powder. **^{1}H NMR** (400 MHz, Deuterium Oxide) δ 9.11 – 8.72 (m, 4H), 8.34 – 7.71 (m, 4H), 5.48 (d, *J* = 2.6 Hz, 4H), 3.29 (t, *J* = 2.6 Hz, 2H), 3.18 – 2.89 (m, 4H), 2.38 – 2.14 (m, 2H). **^{13}C NMR** (100MHz, $CDCl_3$) 163.51, 143.23, 128.02, 79.93, 73.80, 49.69, 34.33, 28.39.

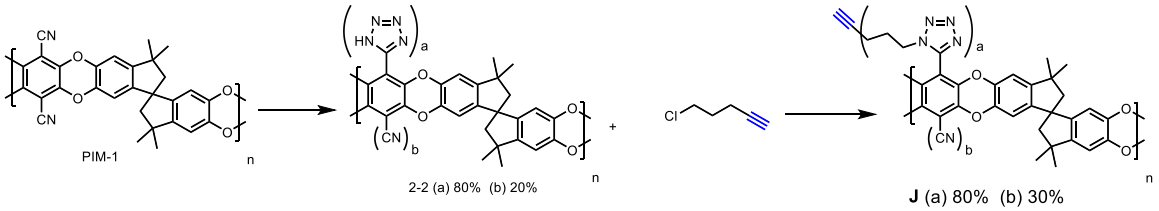

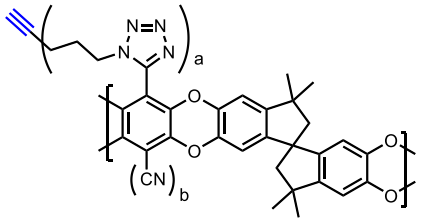

[n]Tz-PIM-80-PA (Tetrazole-PIM-80% Functionalized with Propylalkyne) (J) Tz-PIM-80 (3 g) was suspended in NMP (75 mL). 5-chloropent-1-yne (6 mL) and K_2CO_3 (5.2 g) was added and the reaction was stirred under Ar at 85°C for 3 days. The reaction was allowed to cool to room temperature and was poured into H_2O (200 mL). The solids were filtered over celite, and the solids on celite were dried in the vacuum oven at 50°C for 16 hours. The solids on celite were dissolved in $CHCl_3$ and the dissolved polymer was filtered and $CHCl_3$ was removed until only a minimal amount of $CHCl_3$ remained. The polymer solution was precipitated into MeOH, filtered, and dried to afford 1.9 g of Tz-PIM-80-PA. **^{1}H NMR** (500 MHz, Chloroform-*d*) δ 6.43 (dd, *J* = 190.4, 141.2 Hz, 4H), 5.09 – 4.15 (m, 3H), 2.63 – 1.72 (m, 10H), 1.22 (d, *J* = 18.4 Hz, 12H).

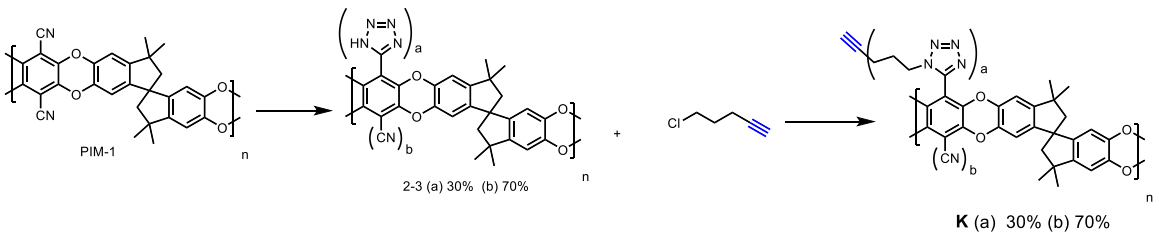

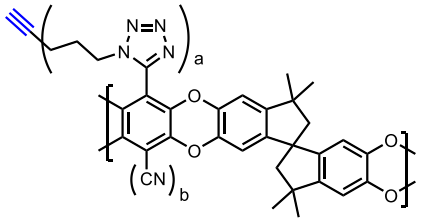

Tz-PIM-30-Pa (Tetrazole-PIM-30% Functionalized with Propylalkyne) (K) Tz-PIM-30 (1.5 g) was suspended in NMP (75 mL). 5-chloropent-1-yne (6 mL) and K_2CO_3 (5.2 g) was added and the reaction was stirred under Ar at 85°C for 3 days. The reaction was allowed to cool to room temperature and was poured into H_2O (200mL). Solids were filtered over celite, and the solids on celite were dried in the vacuum oven at 50°C for 16 hours. The solids on celite were dissolved in $CHCl_3$ and the dissolved polymer was filtered and $CHCl_3$ was removed until only a minimal amount of $CHCl_3$ remained. The polymer solution was precipitated into MeOH, filtered, and dried to afford Tz-PIM-30-Paz. **^{1}H NMR** (500 MHz, Chloroform-*d*) δ 6.45 (dd, *J* = 195.8, 137.2 Hz, 4H), 5.13 – 4.17 (m, 1.46H), 2.60 – 1.71 (m, 6H), 1.32 (d, *J* = 36.1 Hz, 12H).

3.4.4 Monomer Characterizations

3.4.4.1 General Analytical Information

NMR spectra were obtained on Brüker DRX-500 instrument in deuterated solvents and referenced to the signals of residual protium in the NMR solvent. Spectra were processed in TopSpin 4.0.7. Nitrogen physisorption was conducted on a Micromeritics 3 Flex Physisorption instrument. Porosity of the materials was assessed via nitrogen physisorption at 77 K and surface areas were calculated from the data using the Brunauer–Emmett–Teller (BET) method. Scanning Differential Calorimetry (DSC) was taken on a TA Instruments Q200 DSC in a nitrogen atmosphere with a heating/cooling rate of 10 ºC/min Thermogravimetric analysis (TGA) was probed on a TA Instruments Q500 TGA. The samples were heated to the desired temperature at 5 ºC/min under a flow of N_2 and held for 9 hours. High-resolution imaging of the composite morphology was achieved using a Hitachi SU8230. Cold Field Emission Scanning Electron Microscope (CFE-SEM). The dry samples were attached to aluminium stubs using copper tape. The samples were then coated with a 20 nm layer of gold/palladium using a Hummer 6 Gold/Palladium Sputterer. Imaging was taken at a working distance of 8 mm and a working voltage of 3 kV using a mix of upper and lower secondary electron detectors.

^{1}H NMR, $CDCl_3$, 500MHz, 294K

Compound 1

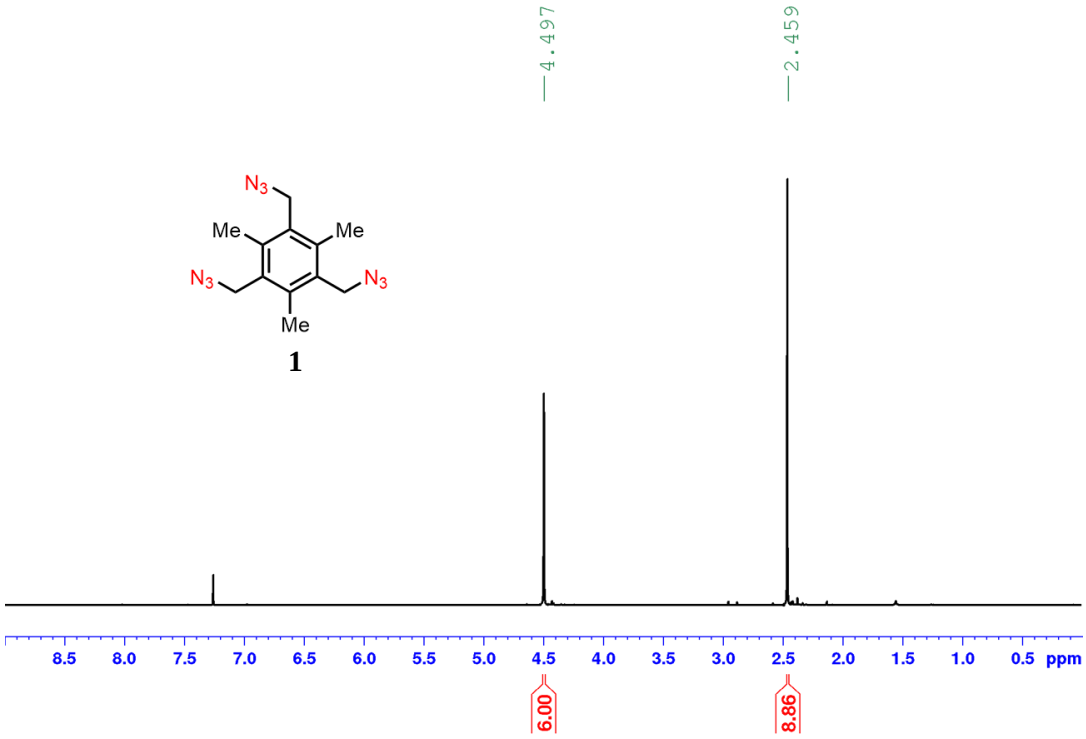

1

^{1}H NMR, $CDCl_3$, 500MHz, 294K

Compound 2

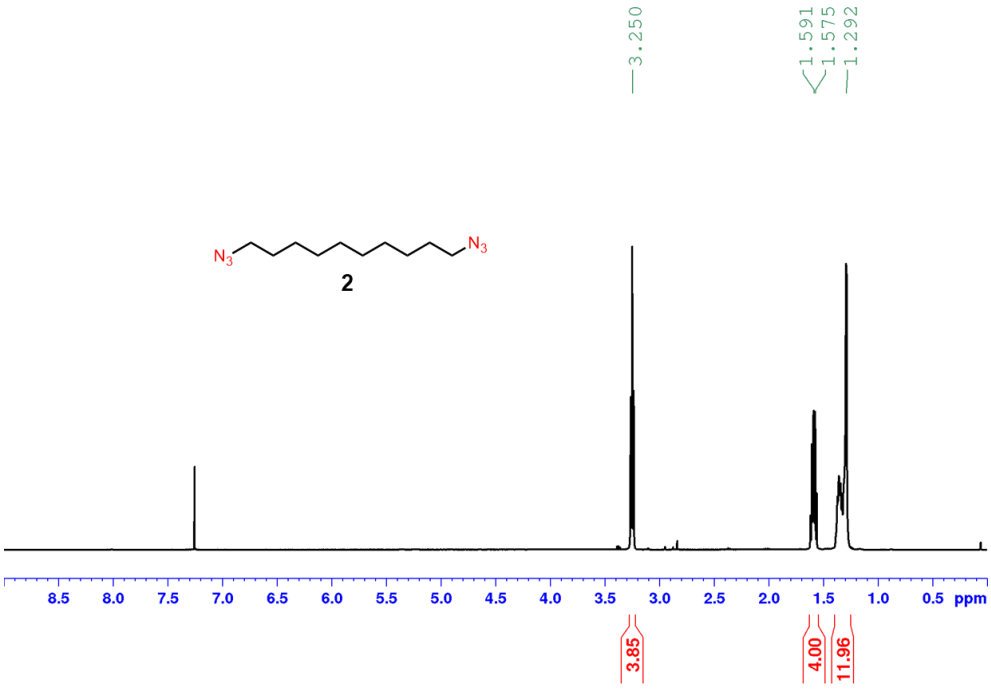

^{1}H NMR, $CDCl_3$, 500MHz, 294K

Compound 3

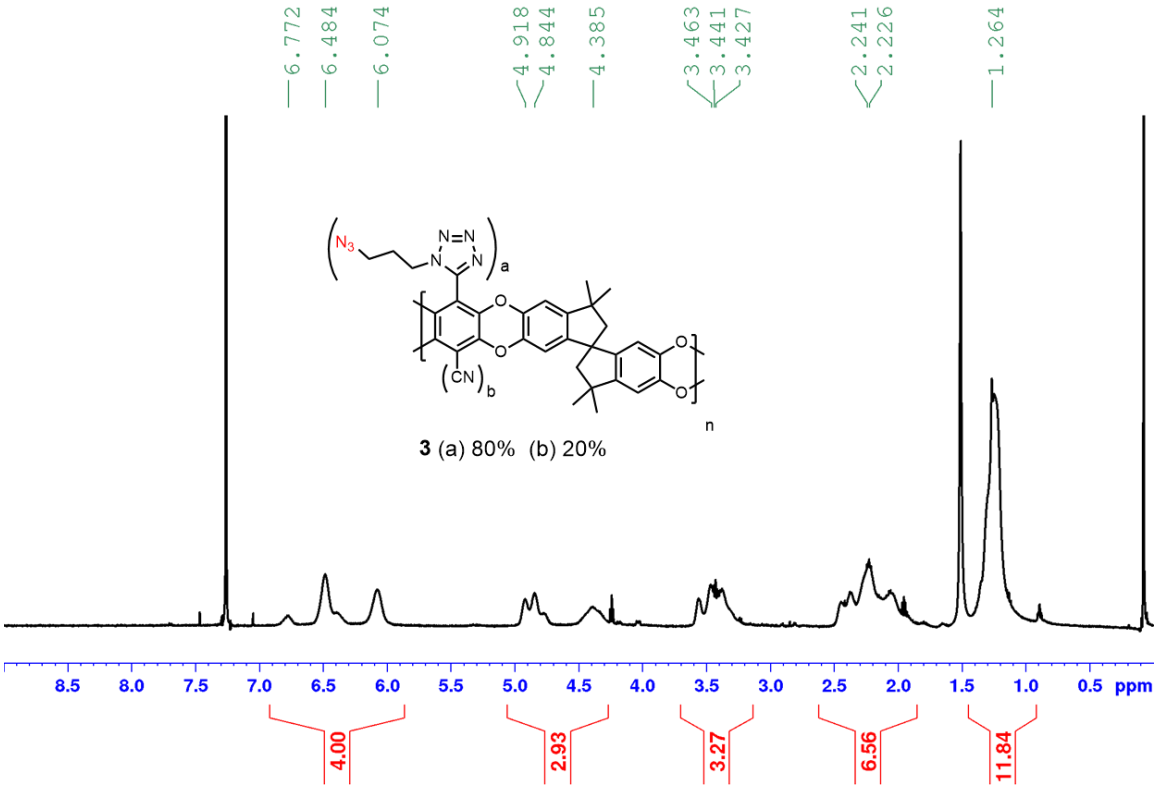

^{1}H NMR, $CDCl_3$, 500MHz, 294K

Compound 4

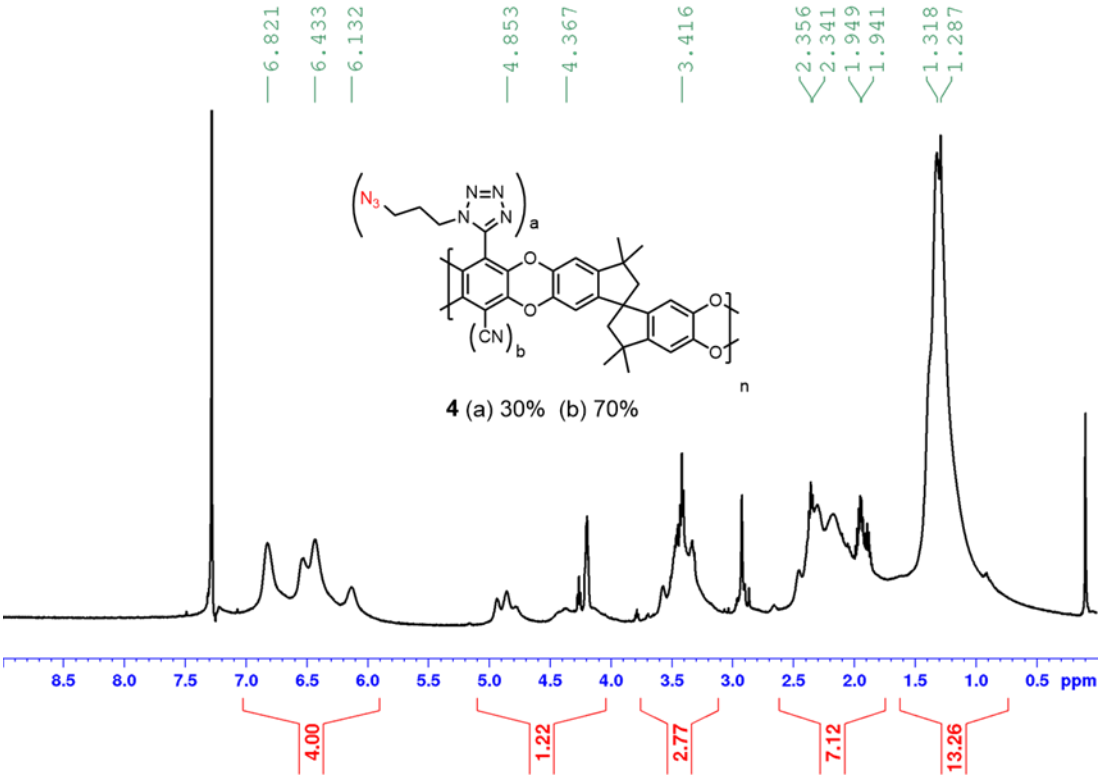

^{1}H NMR, $CDCl_3$, 500MHz, 294K

Compound A

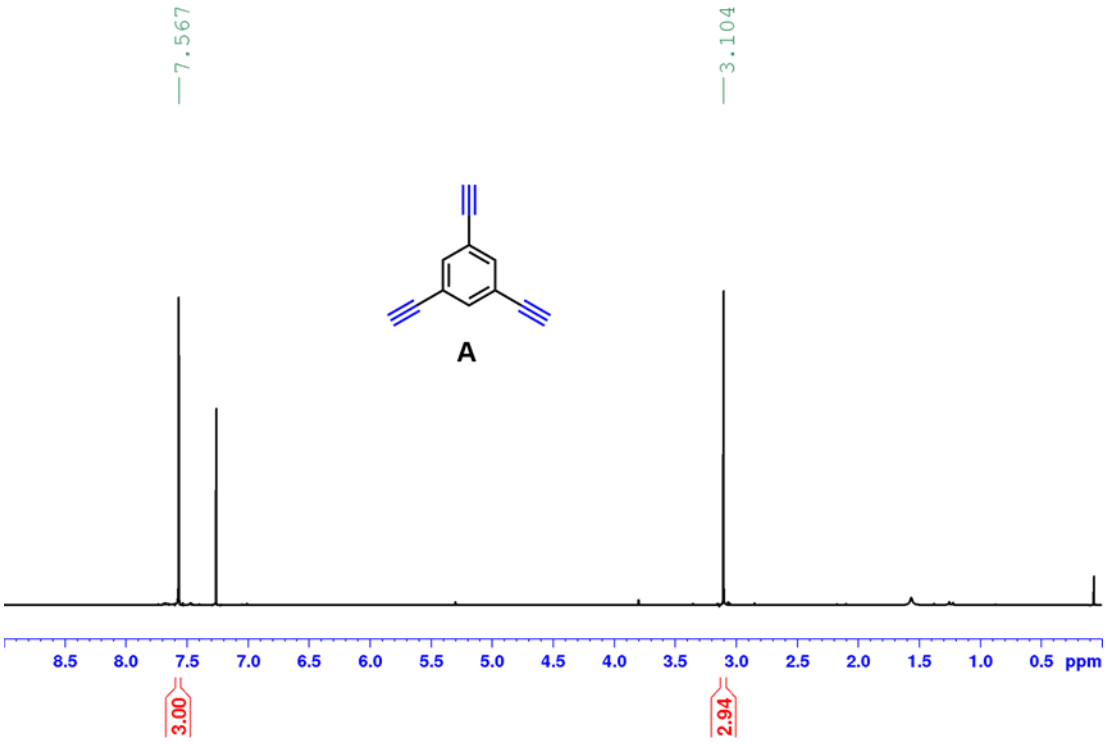

^{1}H NMR, $CDCl_3$, 500MHz, 294K

Compound B

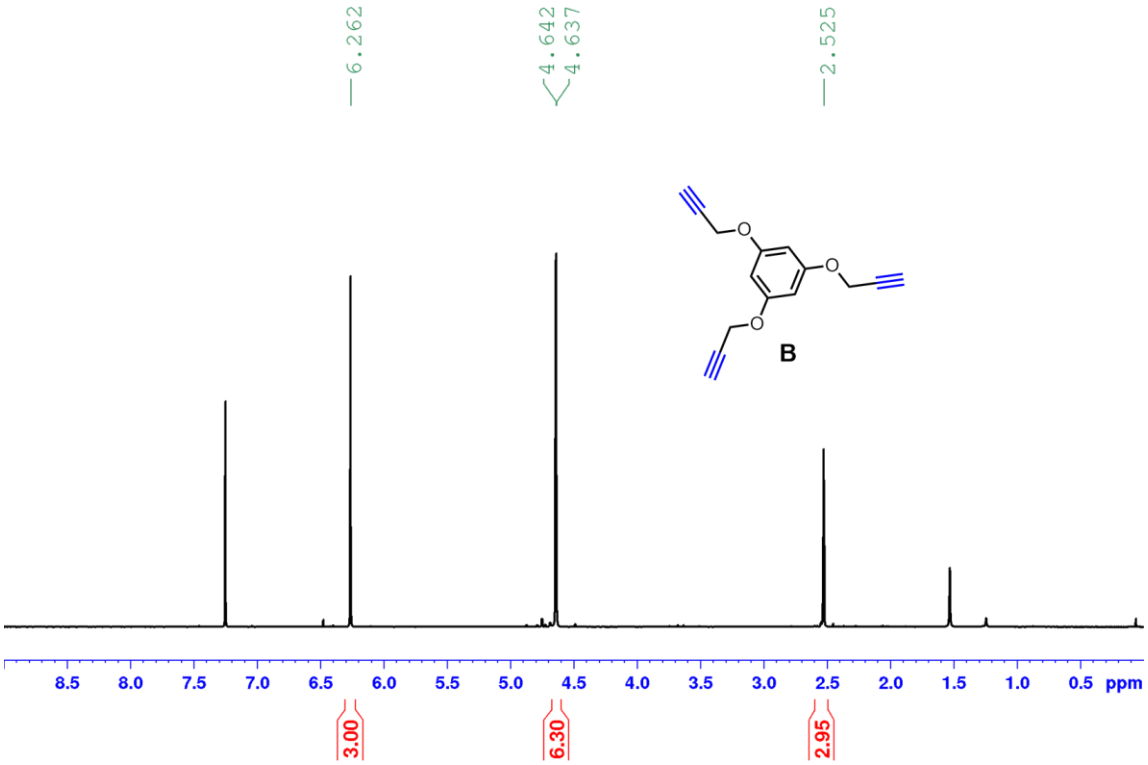

^{1}H NMR, $CDCl_3$, 400MHz, 294K

Compound C

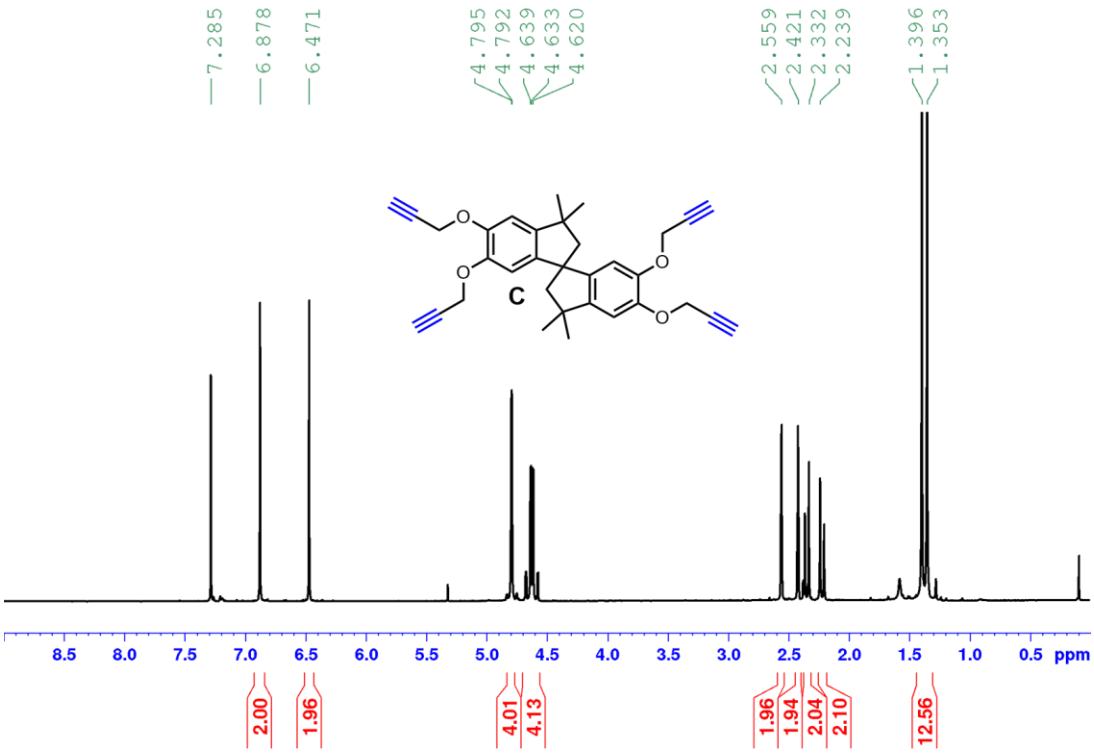

^{13}C NMR, $CDCl_3$, 100MHz, 294K

Compound C

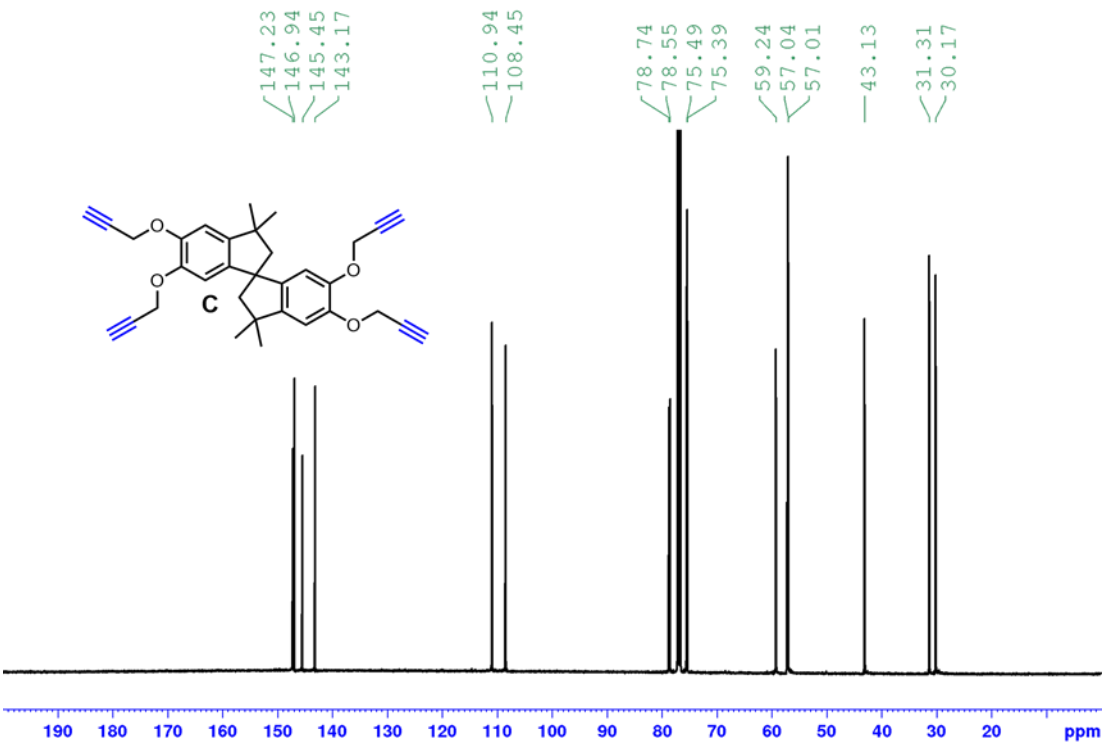

^{1}H NMR, $CDCl_3$, 500MHz, 294K

Compound D

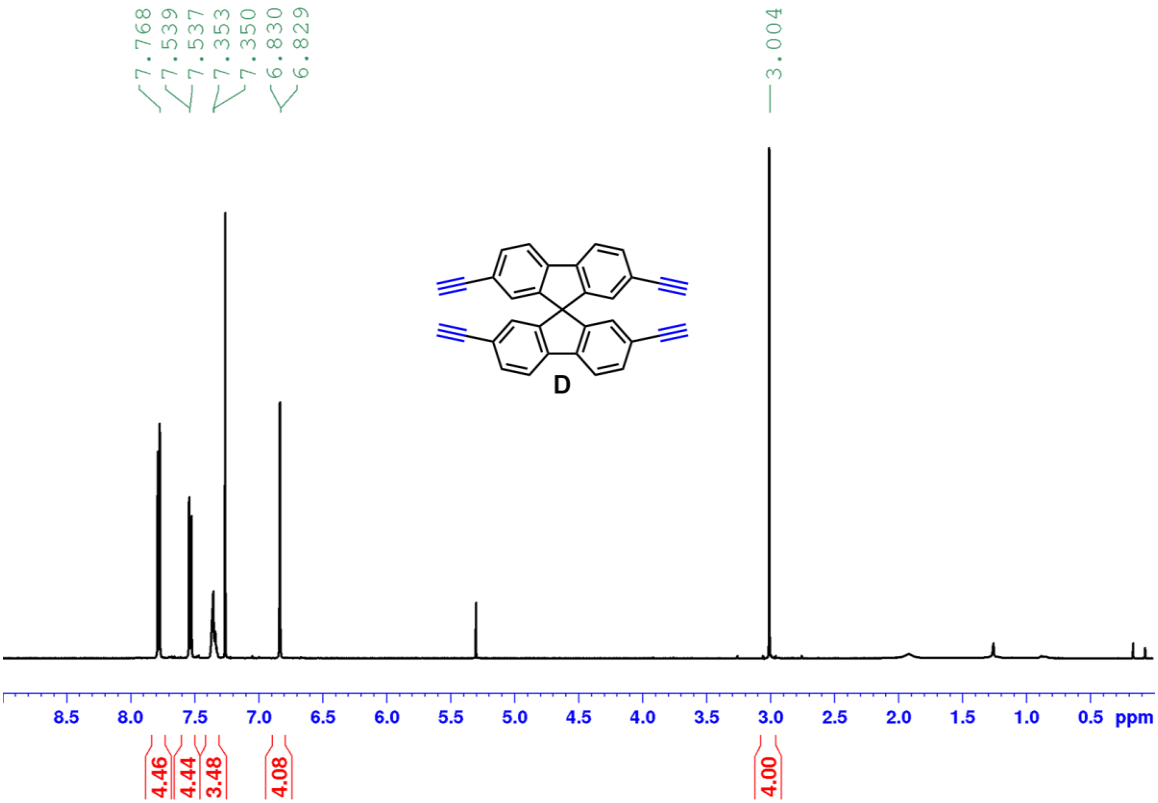

^{1}H NMR, D_2O, 400MHz, 294K

Compound H

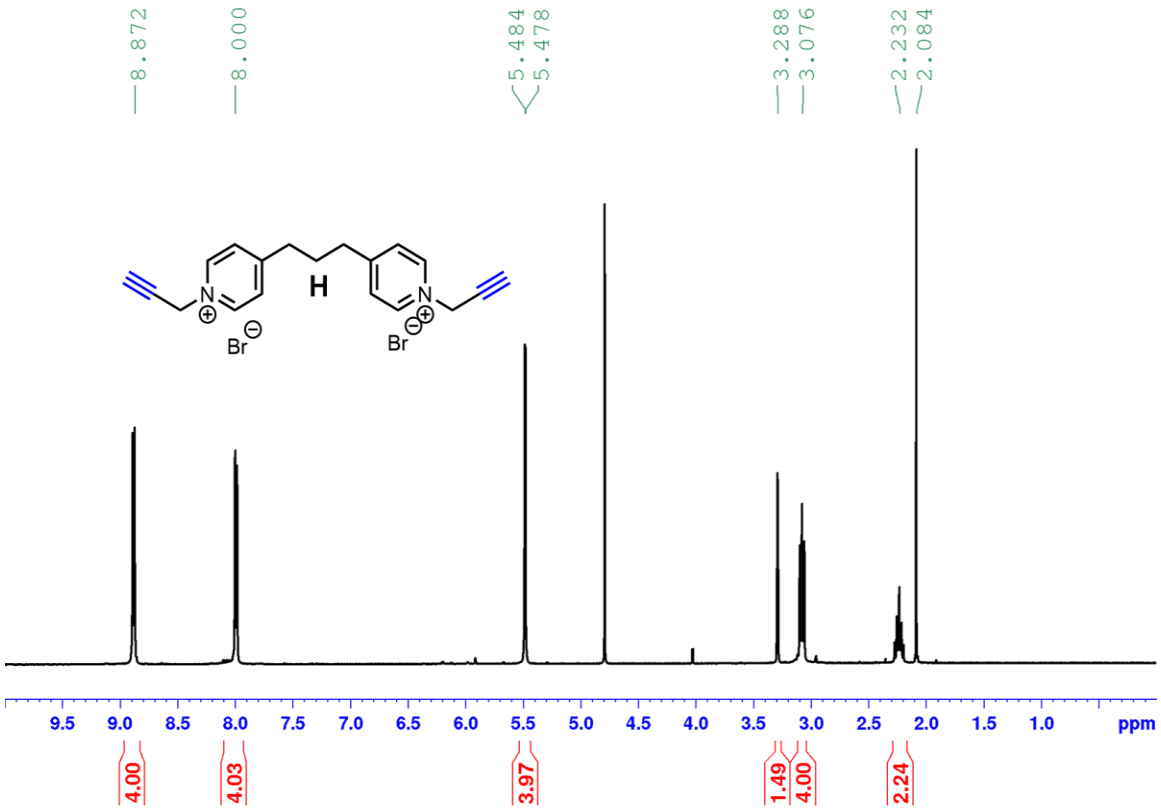

^{13}C NMR, D_2O, 100MHz, 294K

Compound H

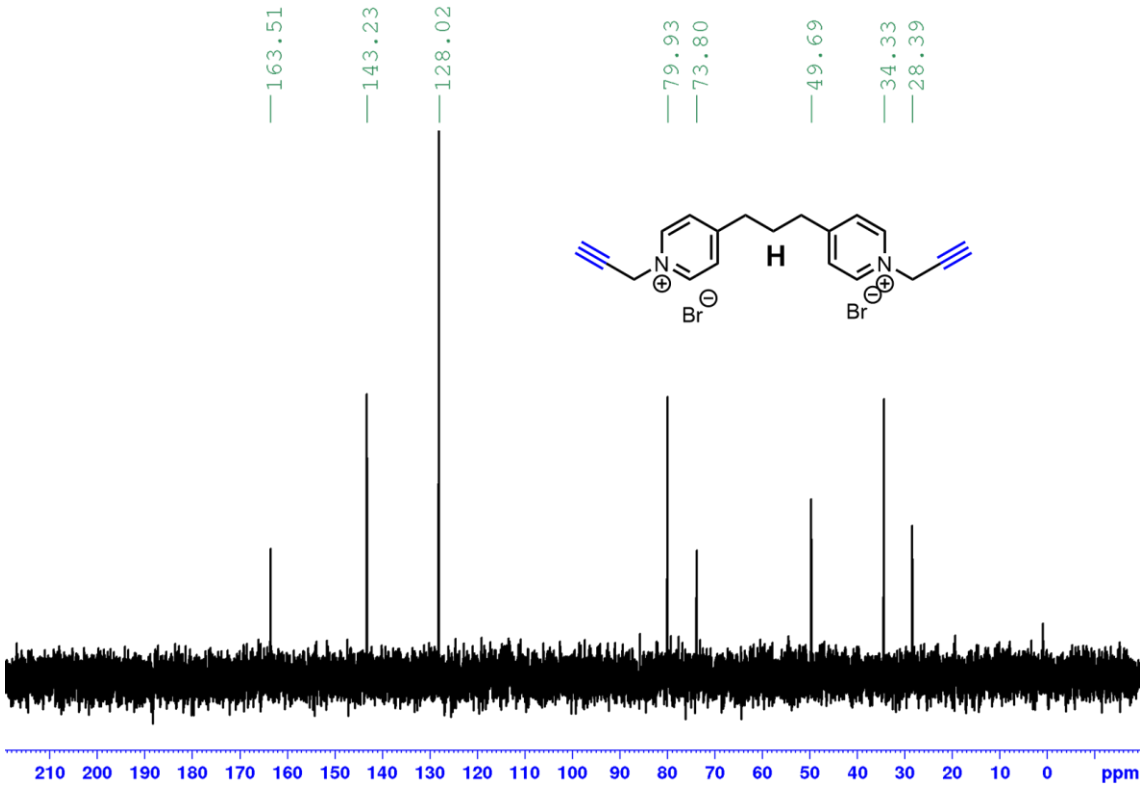

^{1}H NMR, $CDCl_3$, 500MHz, 294K

Compound J

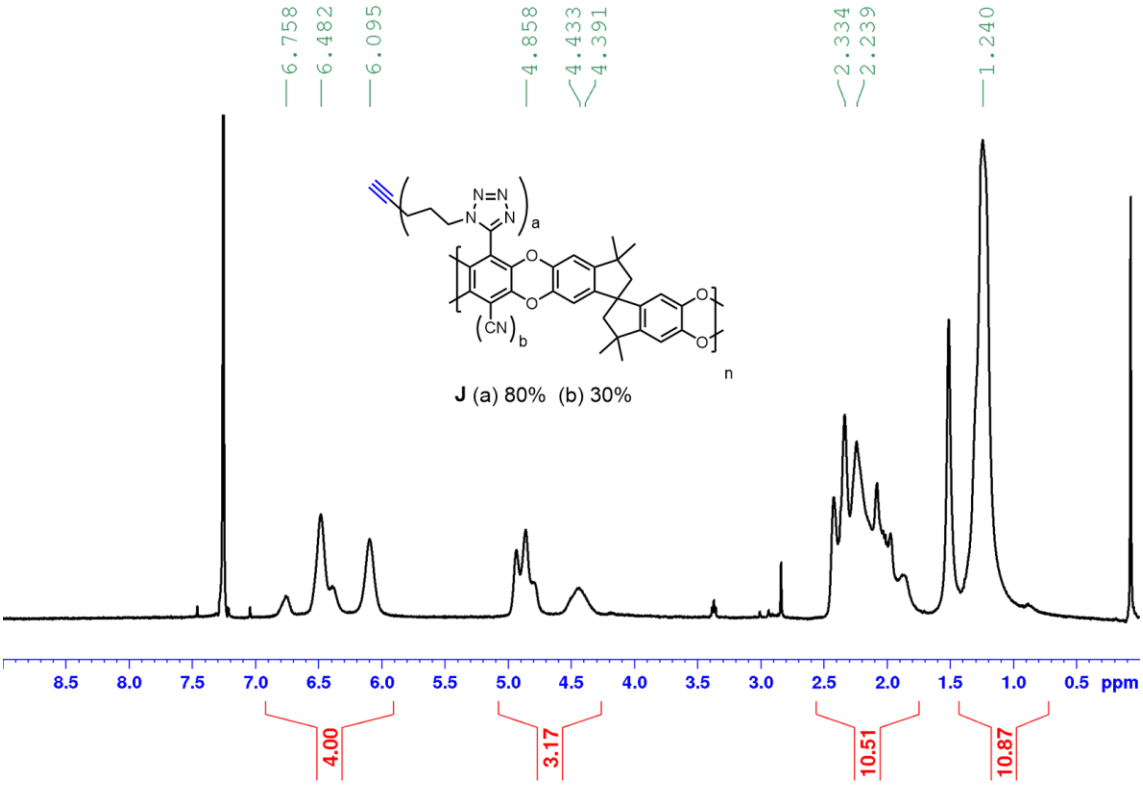

^{1}H NMR, $CDCl_3$, 500MHz, 294K

Compound K

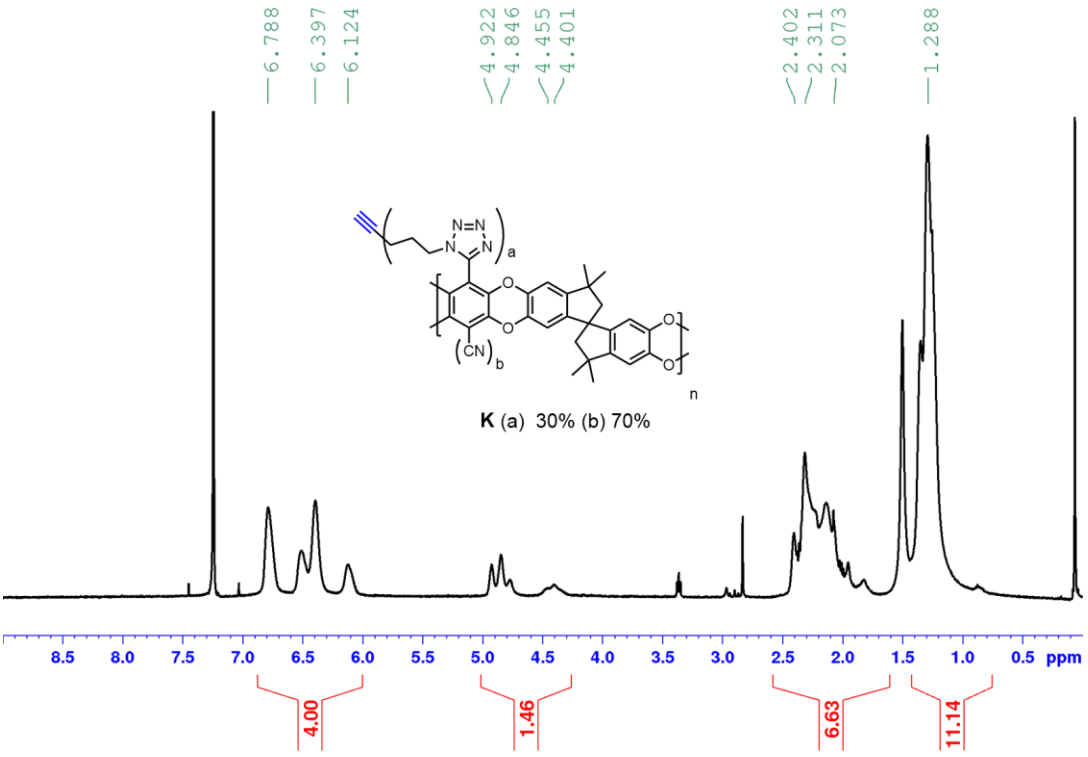

3.4.5 Visualization of Film Forming Properties

Aqueous $CuSO_4$ Interfacial Polymerizations

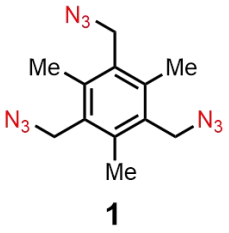

1

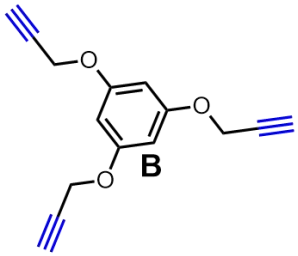

B

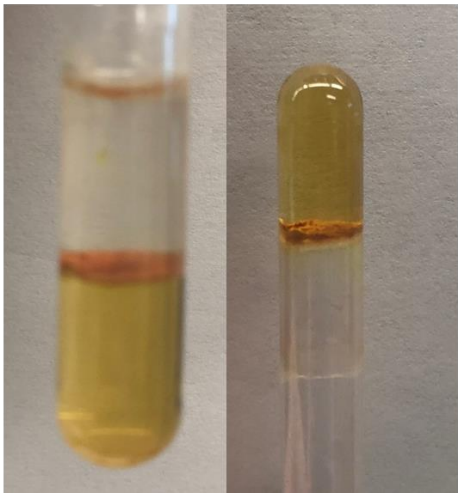

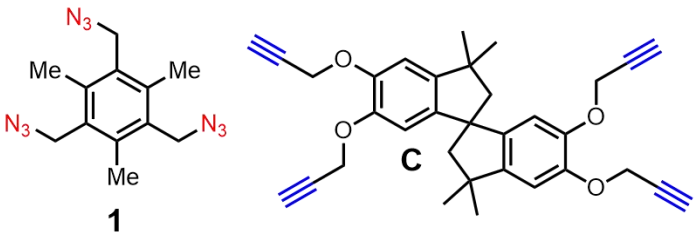
N3
Me
Me
N3
N3
Me
1
O
O
O
O
C

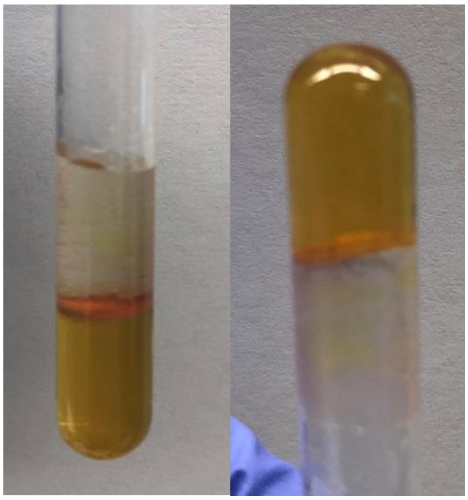

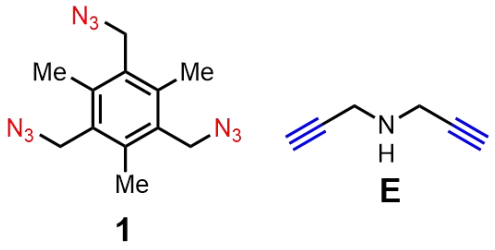
N3
Me
Me
N3
N3
Me
1
N
H
E

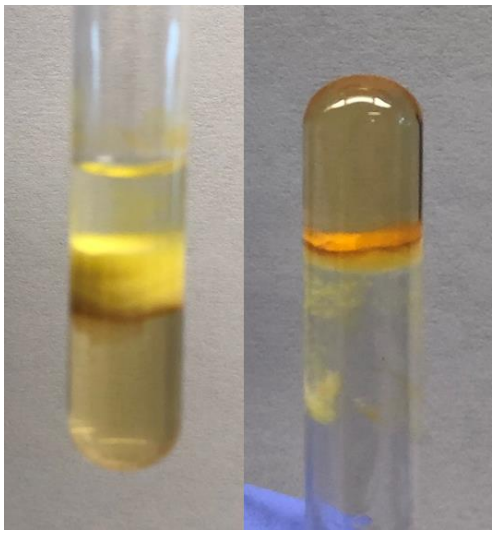

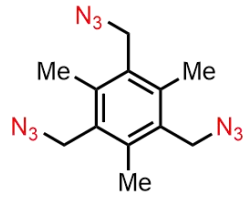

1

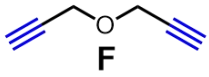

F

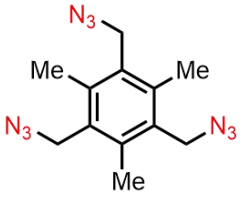

1

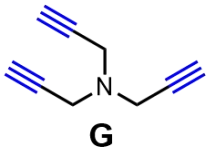

G

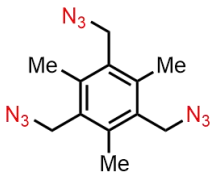
N3
Me
Me
N3
N3
Me

1

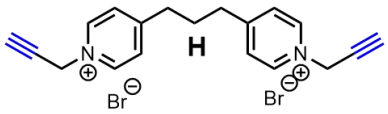
H
N
Br
N
Br

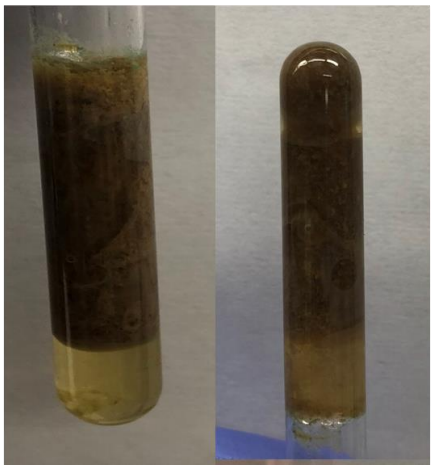

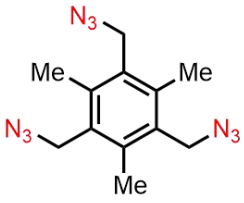
N3
Me
Me
N3
N3
Me

1

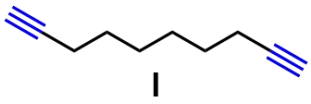

I

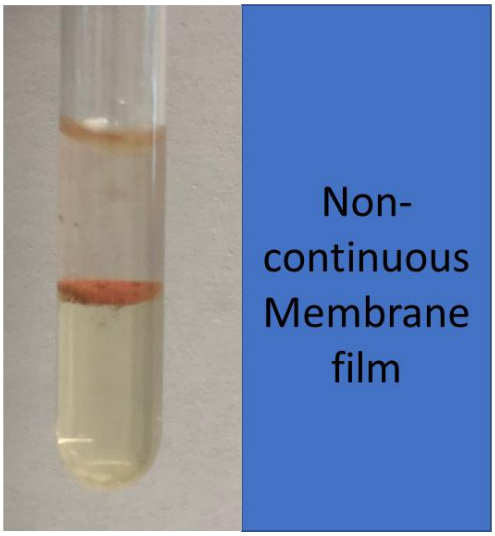
Non-
continuous
Membrane
film

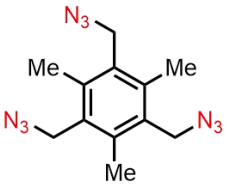

1

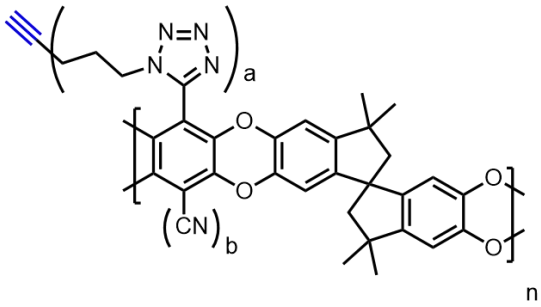

J (a) 80% (b) 20%

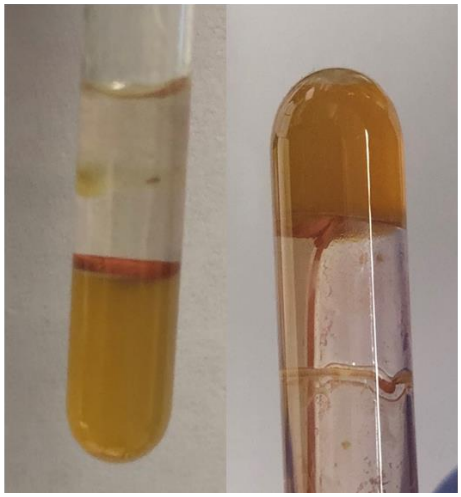

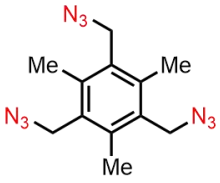

1

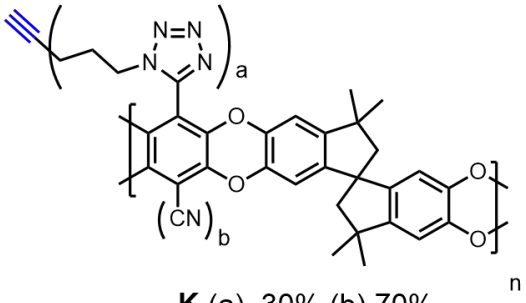

K (a) 30% (b) 70%

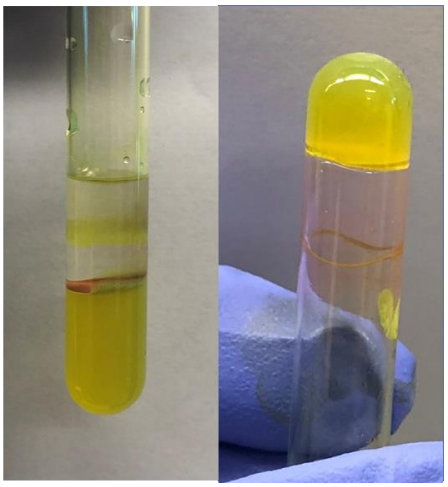

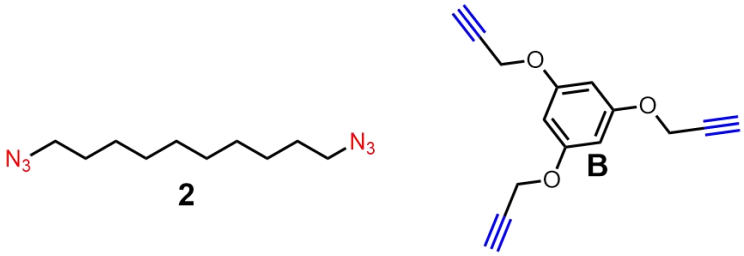
N3
N3
2
O
O
O
B

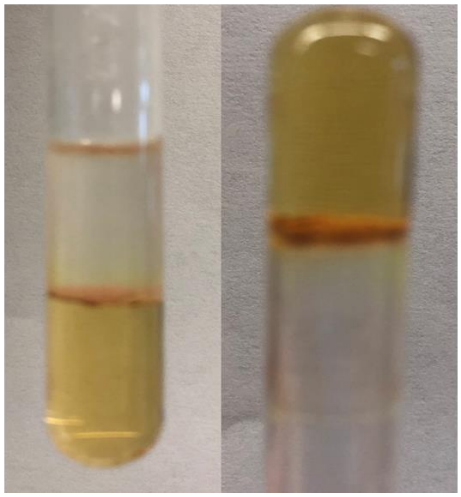

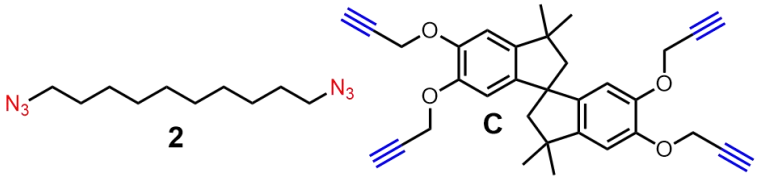
N3
N3
2
O
O
O
O
C

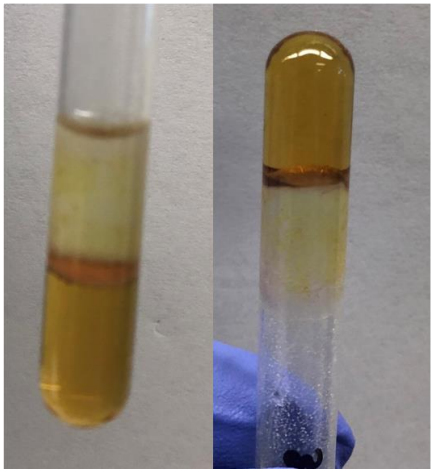

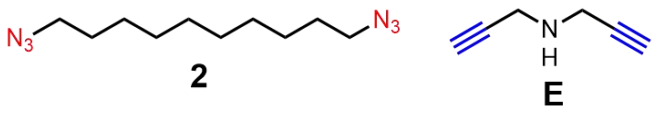
N3
N3
2
N
H
E

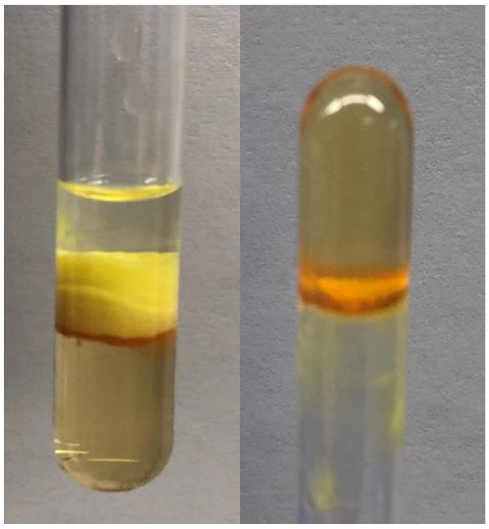

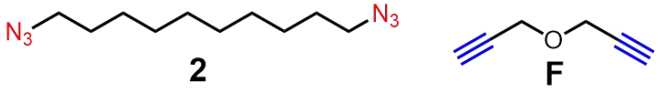
N3
N3
2
O
F

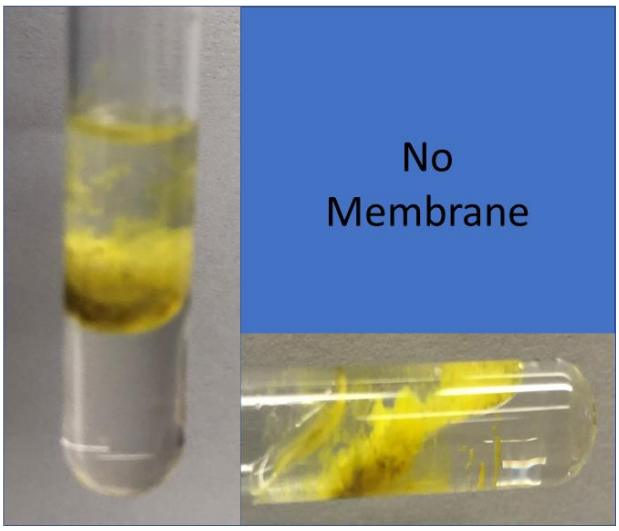
No
Membrane

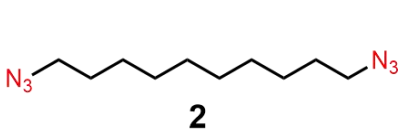

2

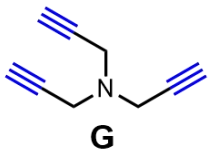

G

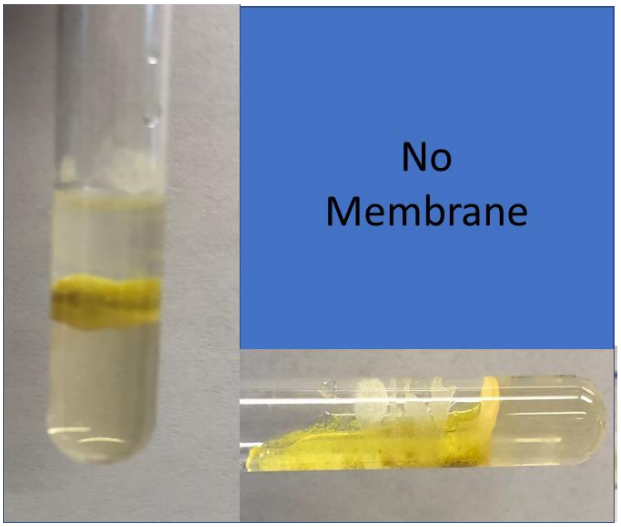

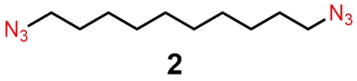

2

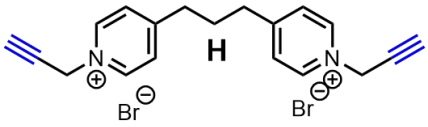

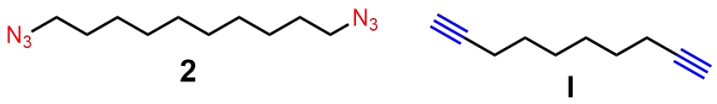

2 **I**

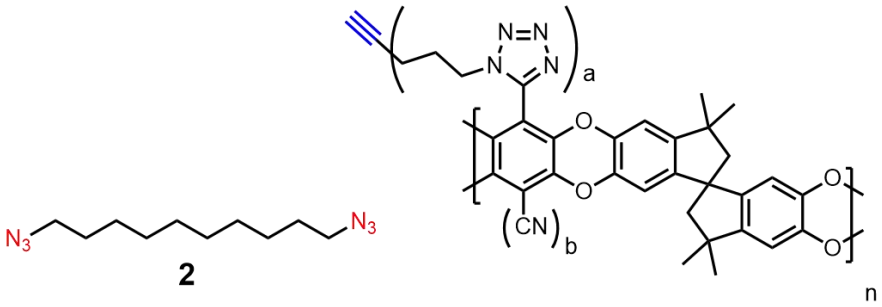

2

J (a) 80% (b) 20%

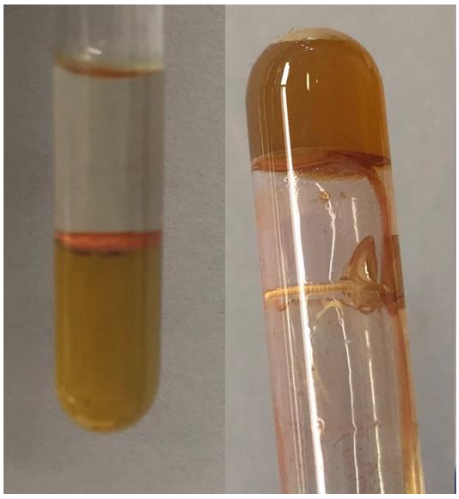

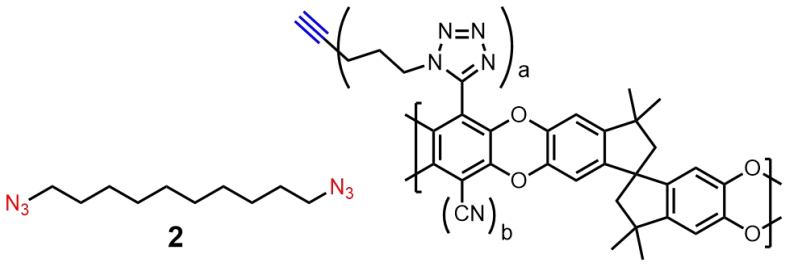

2

K (a) 30% (b) 70%

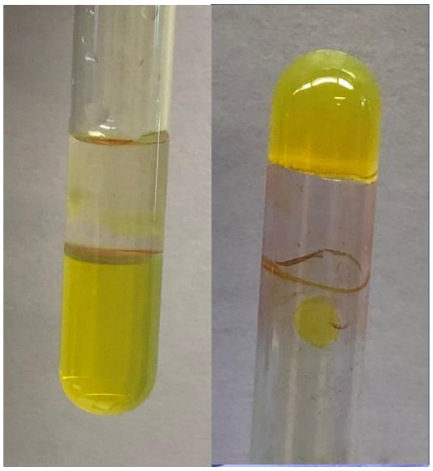

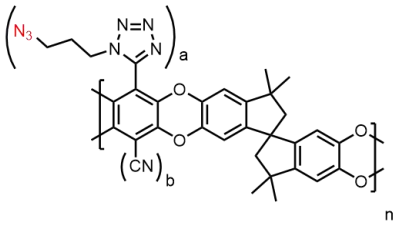

3 (a) 80% (b) 20%

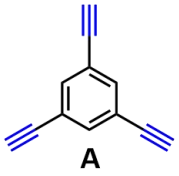

A

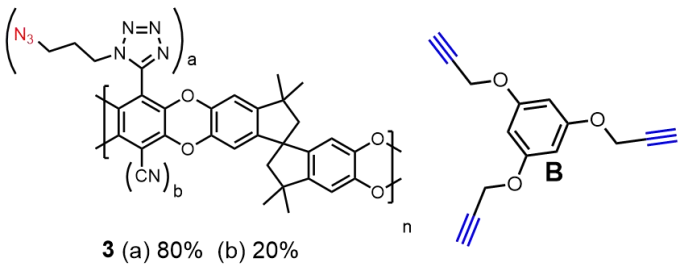

3 (a) 80% (b) 20%

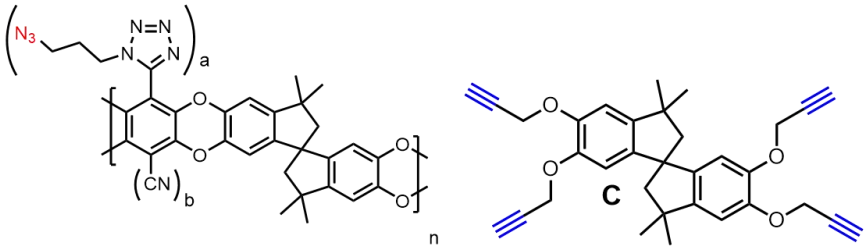

3 (a) 80% (b) 20%

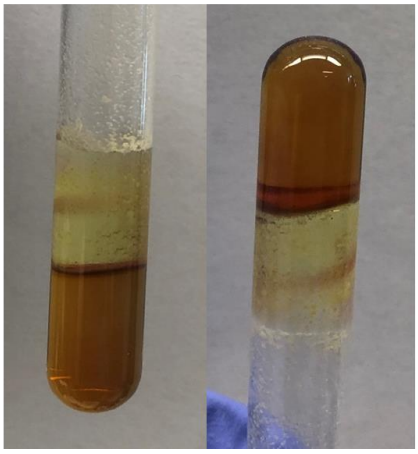

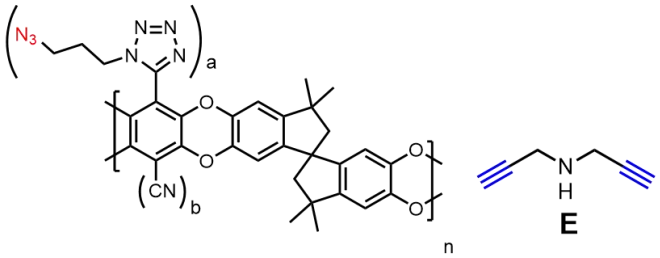

3 (a) 80% (b) 20%

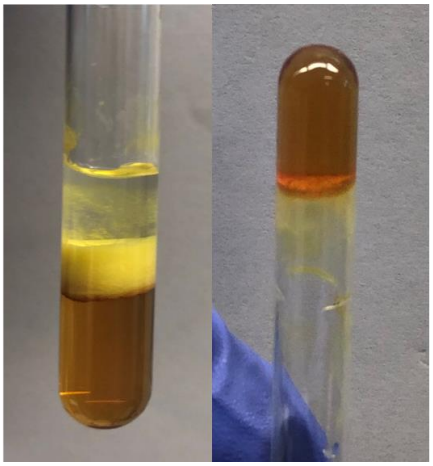

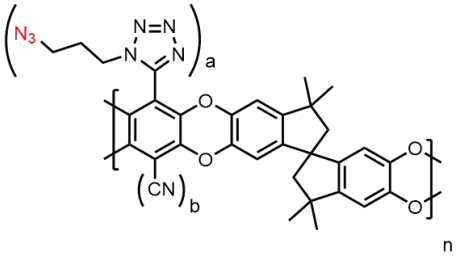

3 (a) 80% (b) 20%

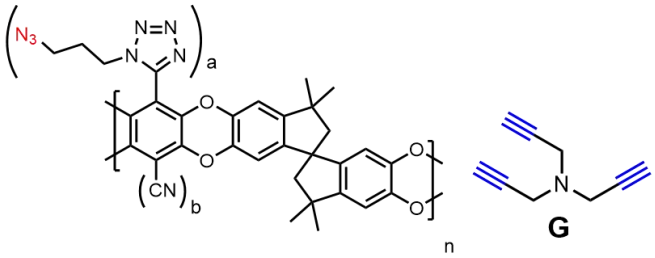

G

3 (a) 80% (b) 20%

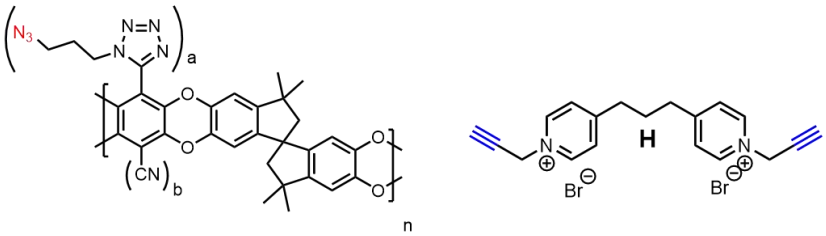

H

3 (a) 80% (b) 20%

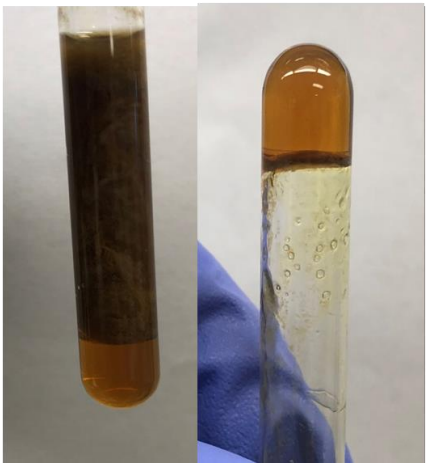

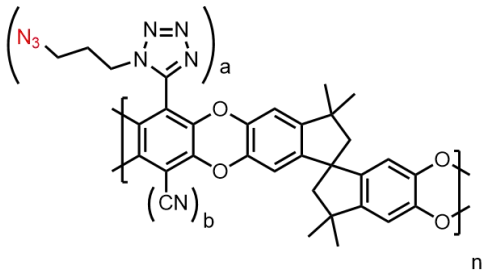

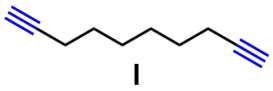

3 (a) 80% (b) 20%

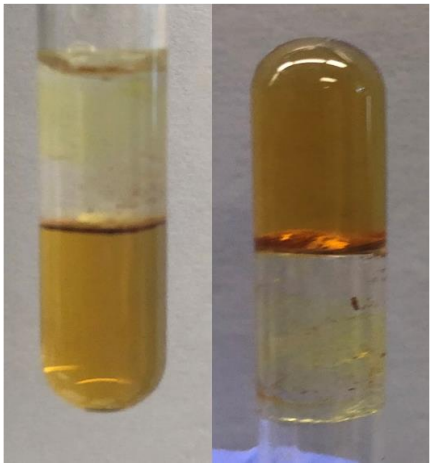

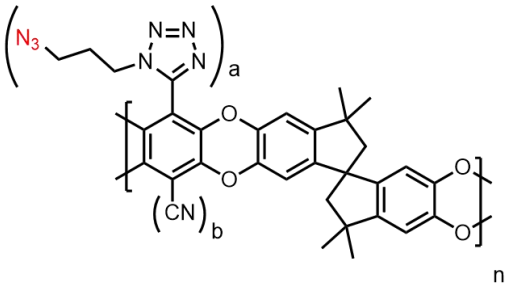

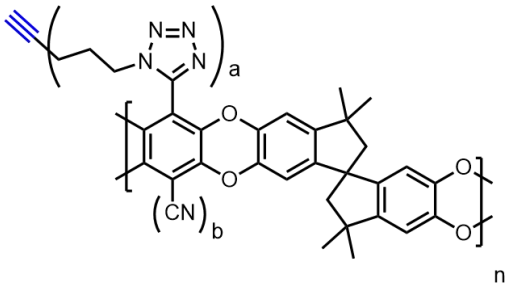

3 (a) 80% (b) 20%

J (a) 80% (b) 20%

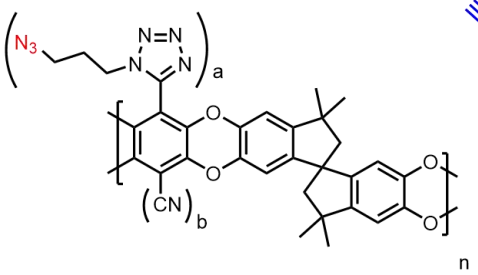

3 (a) 80% (b) 20%

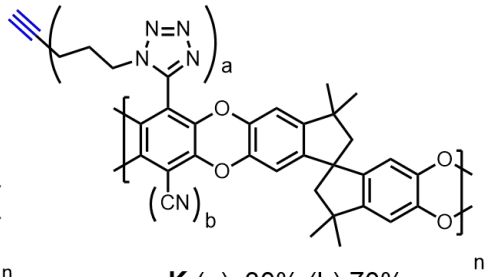

K (a) 30% (b) 70%

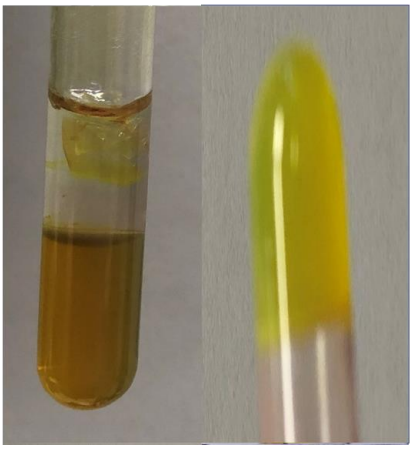

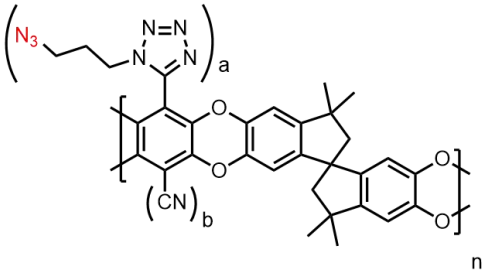

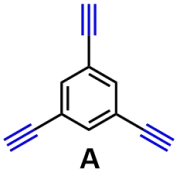

A

4 (a) 30% (b) 70%

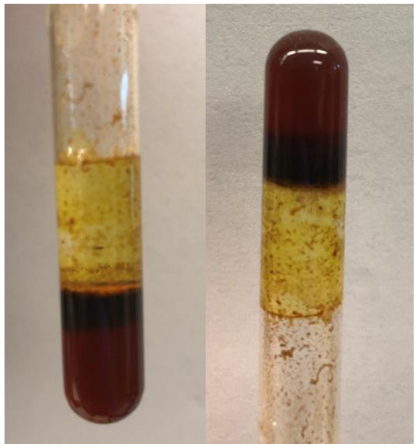

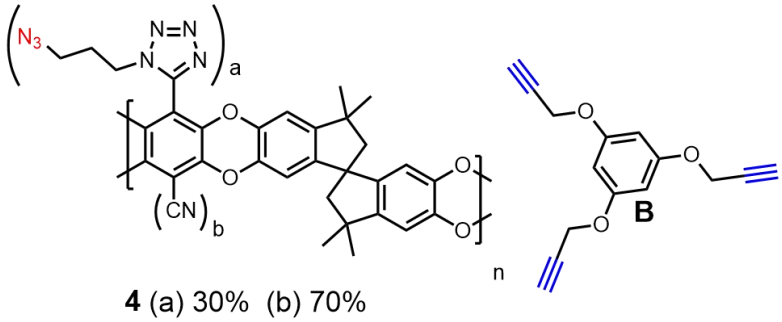

4 (a) 30% (b) 70%

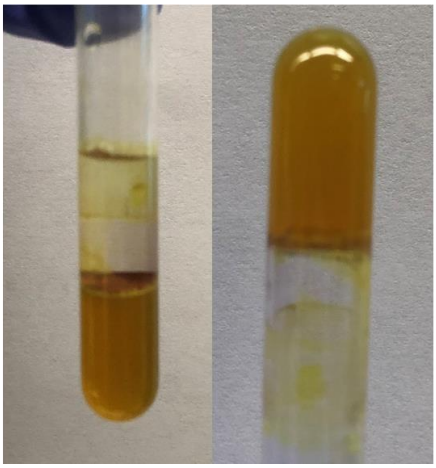

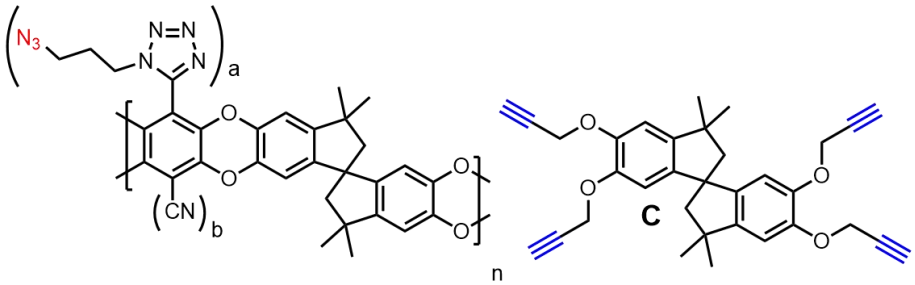

4 (a) 30% (b) 70%

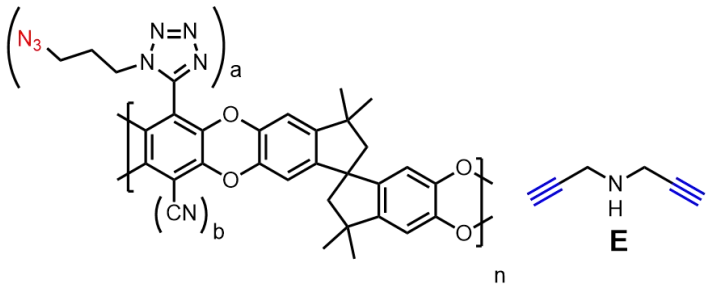

4 (a) 30% (b) 70%

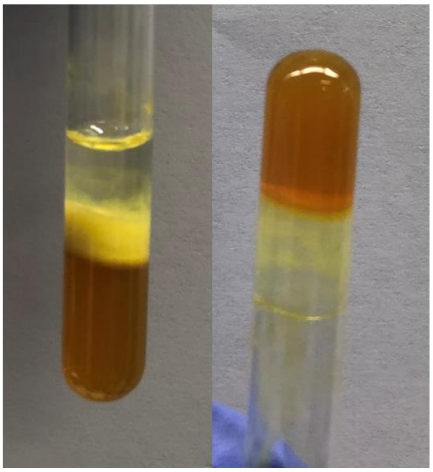

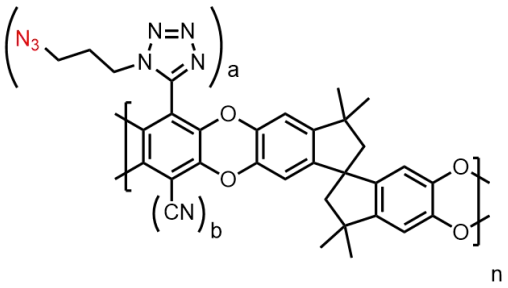

4 (a) 30% (b) 70%

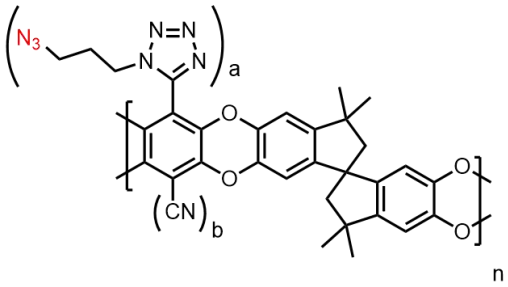

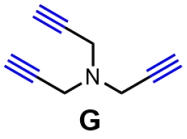

4 (a) 30% (b) 70%

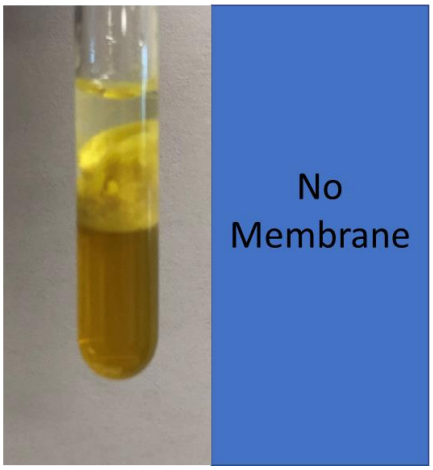

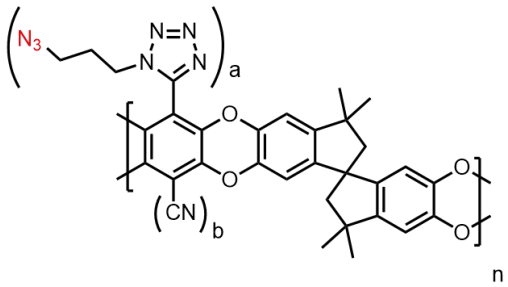

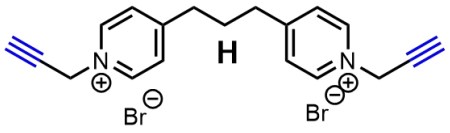

4 (a) 30% (b) 70%

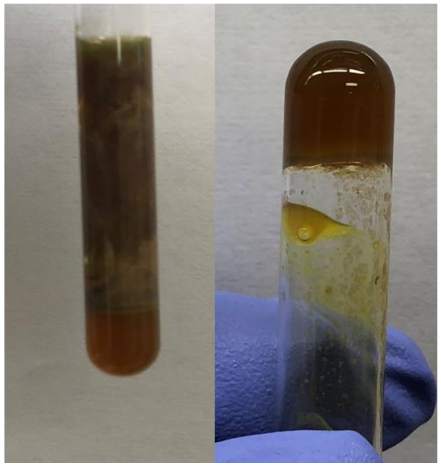

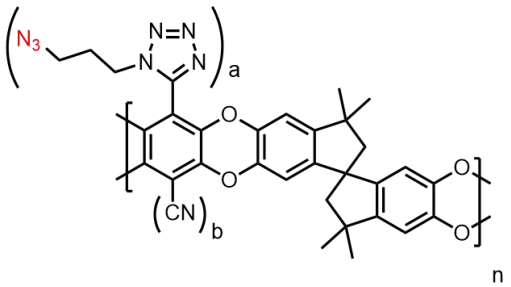

4 (a) 30% (b) 70%

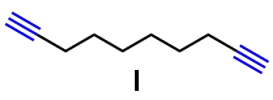

I

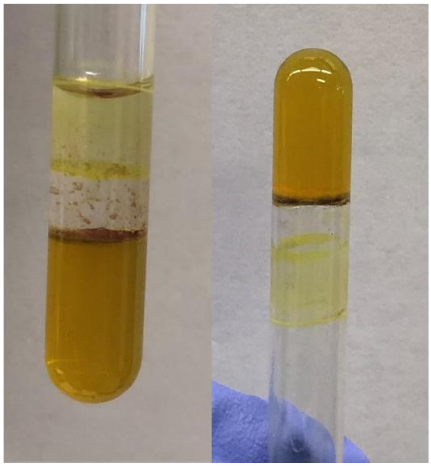

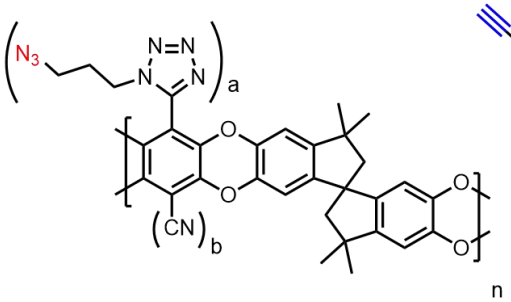

4 (a) 30% (b) 70%

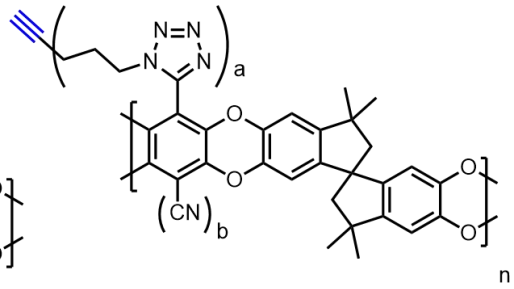

J (a) 80% (b) 20%

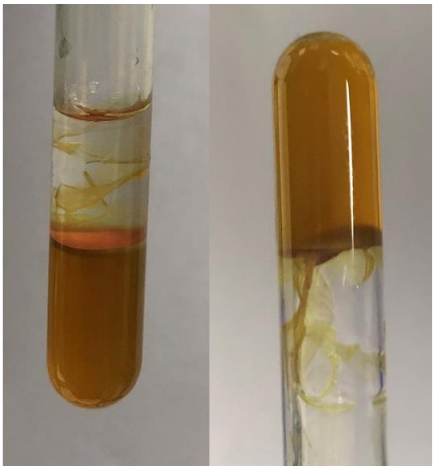

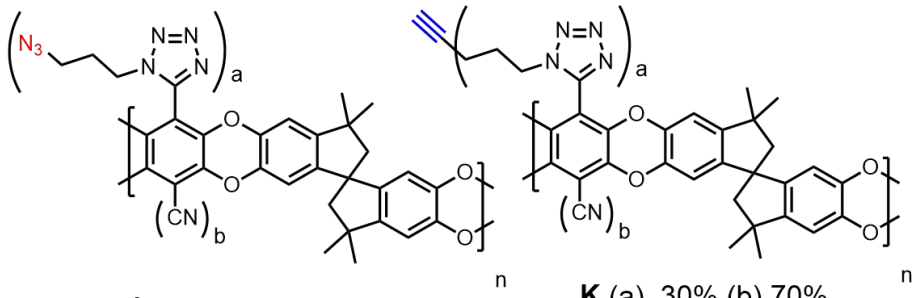

4 (a) 30% (b) 70%

K (a) 30% (b) 70%

Organic $(PPh_3)_2CuOAc$ Interfacial Polymerizations

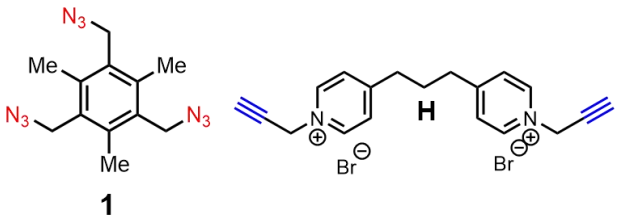

1

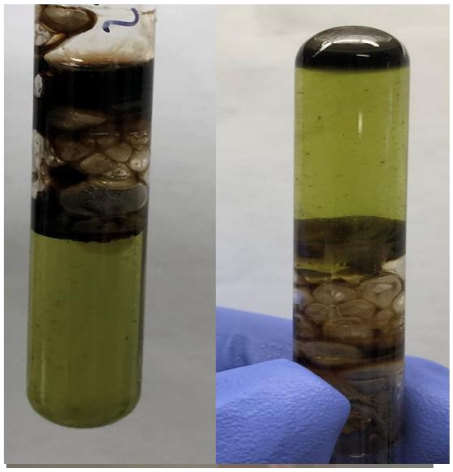

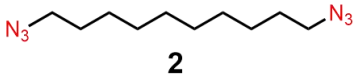

2

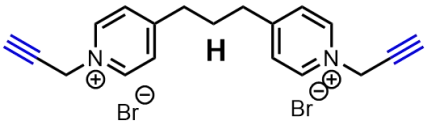

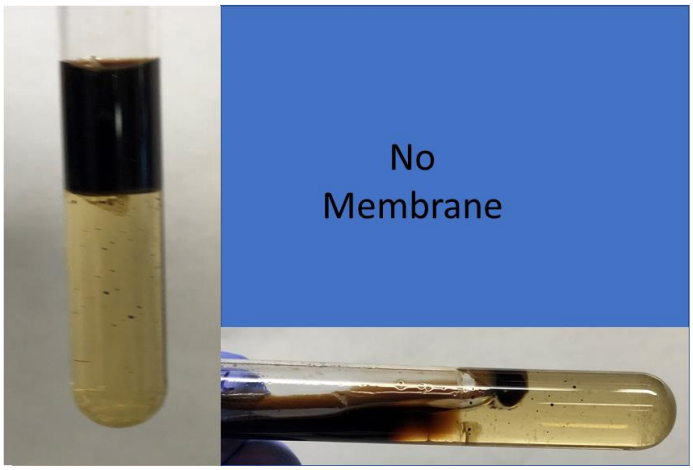

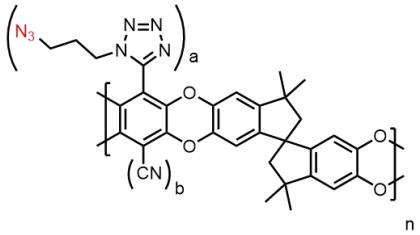

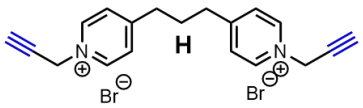

3 (a) 80% (b) 20%

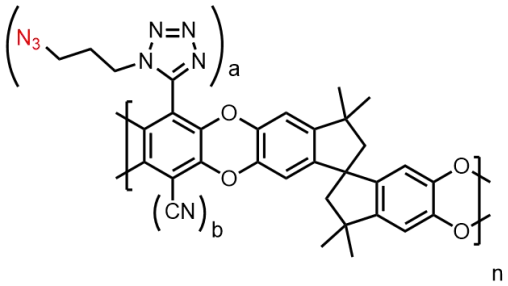

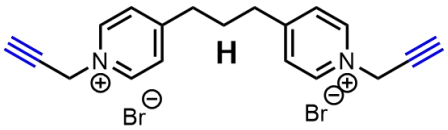

4 (a) 30% (b) 70%

3.4.6 BET Isotherms

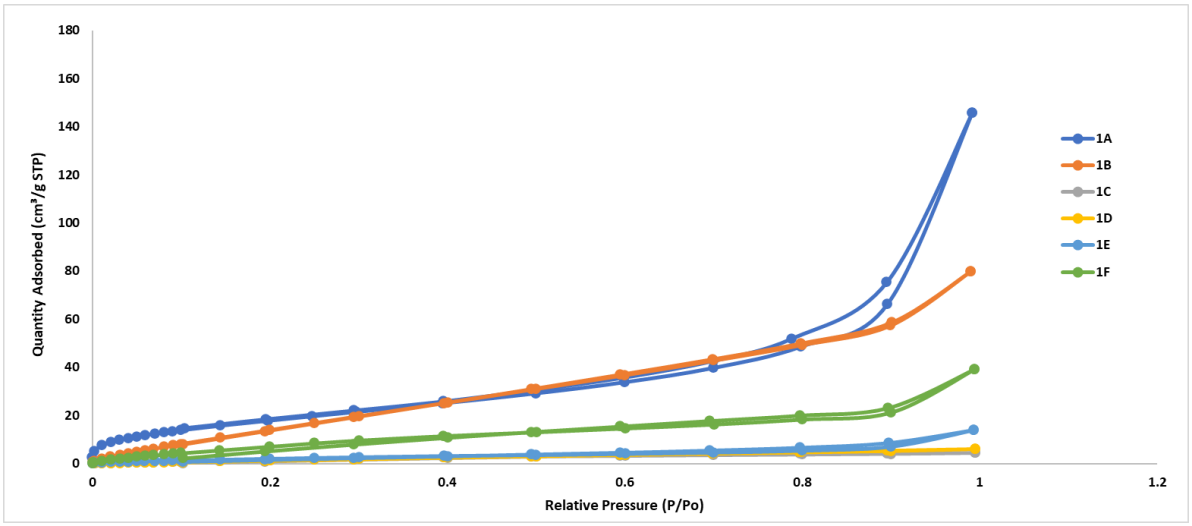

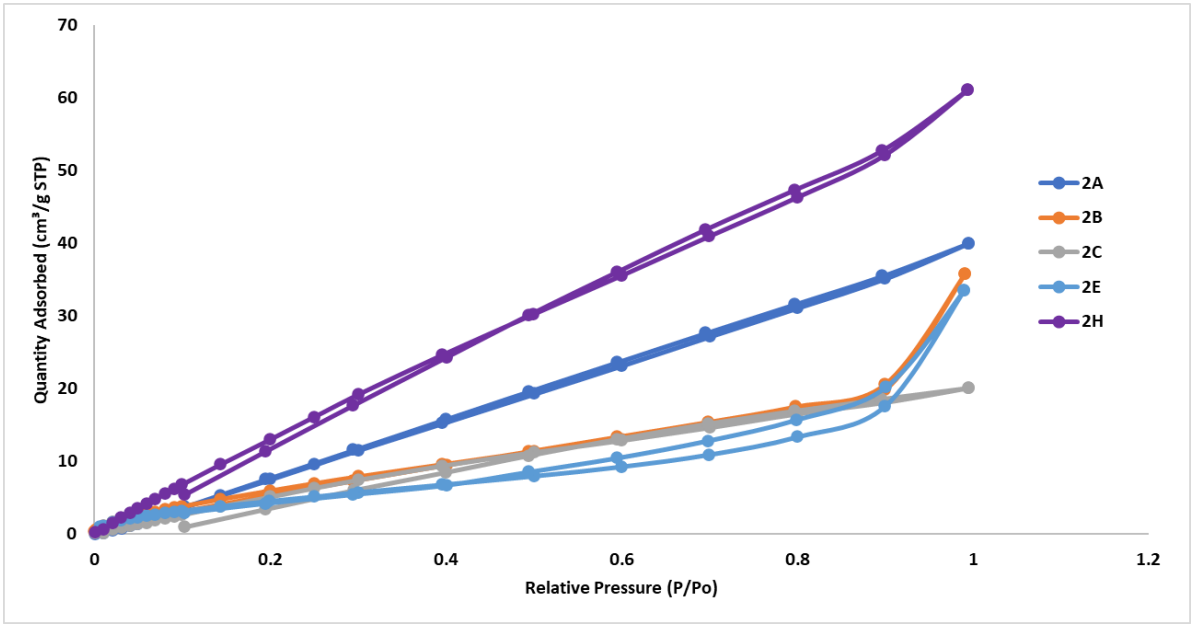

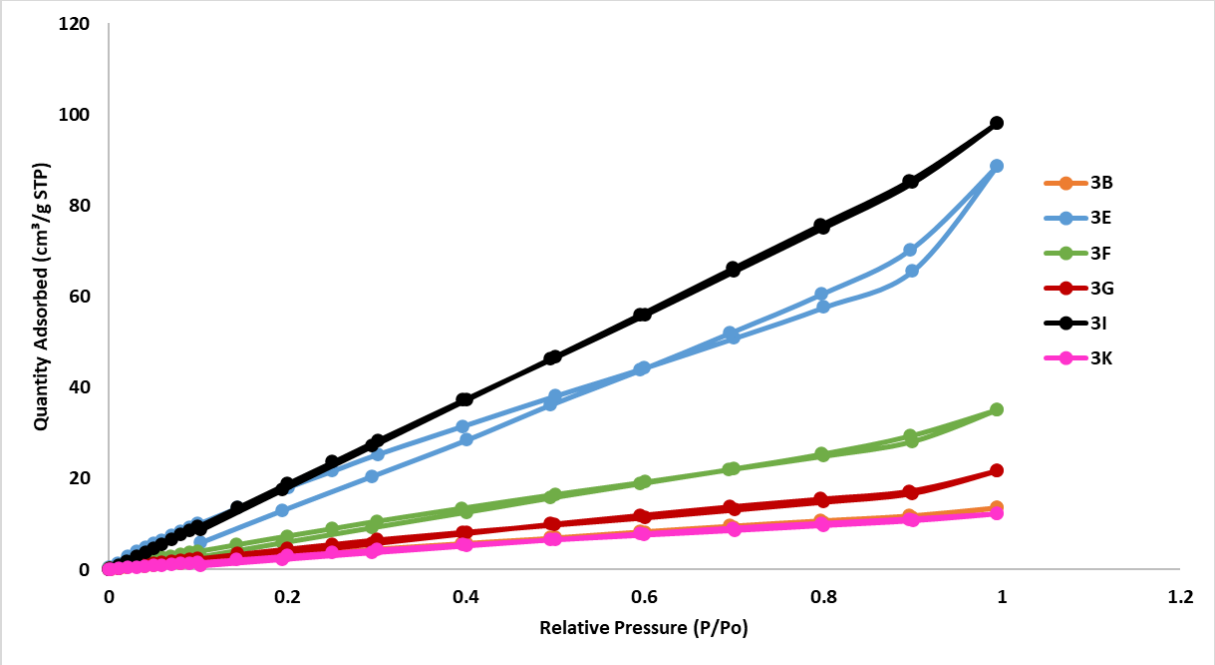
120
100
80
60
40
20
0
Quantity Adsorbed (cm³/g STP)
0
0.2
0.4
0.6
0.8
1
1.2
Relative Pressure (P/Po)
3B
3E
3F
3G
3I
3K

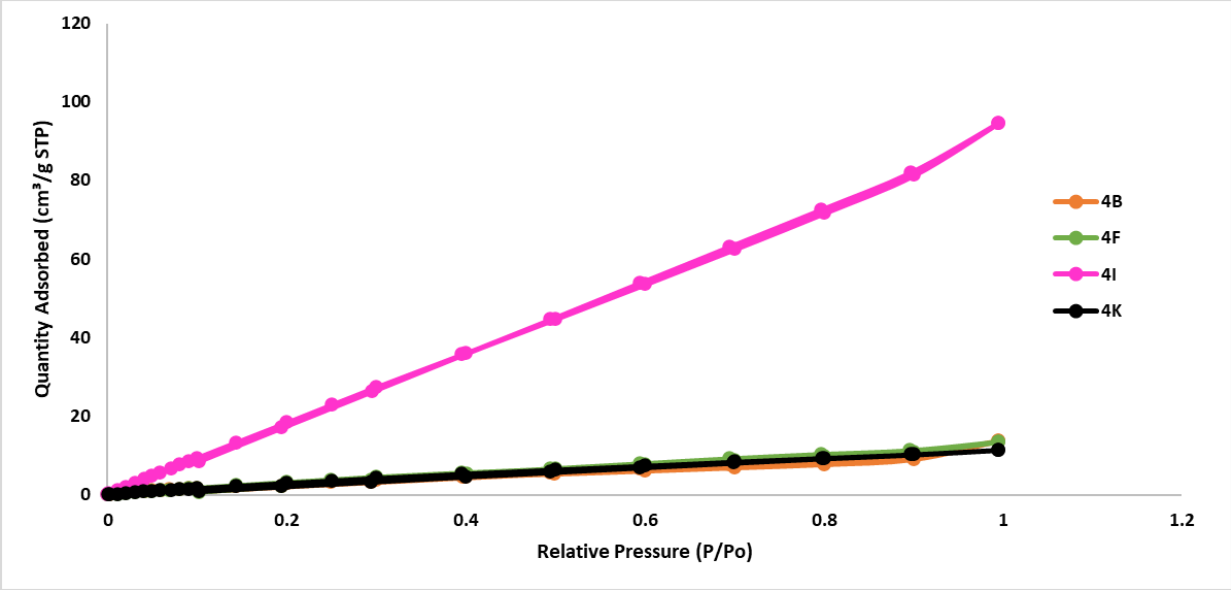
120
100
80
60
40
20
0
Quantity Adsorbed (cm³/g STP)
0
0.2
0.4
0.6
0.8
1
1.2
Relative Pressure (P/Po)
4B
4F
4I
4K

3.4.7 TGA

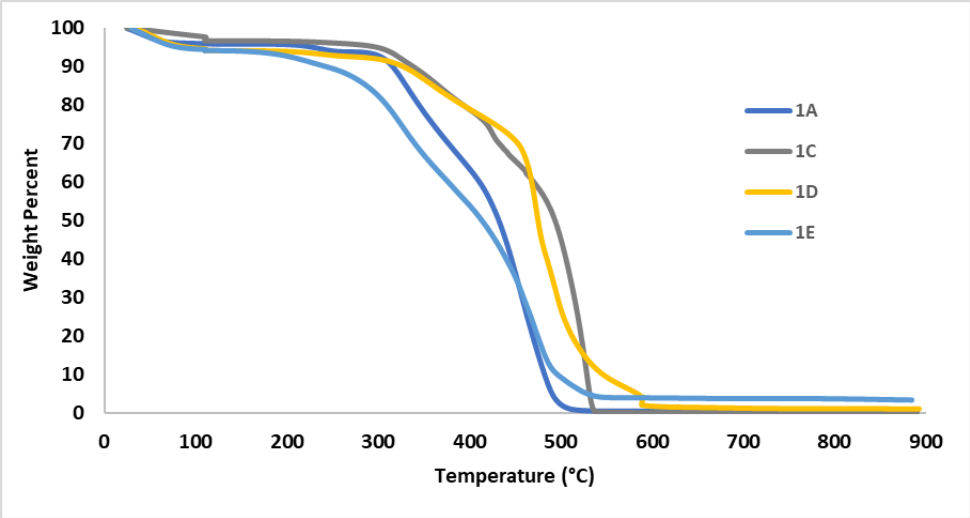
Weight Percent
Temperature (°C)
1A
1C
1D
1E

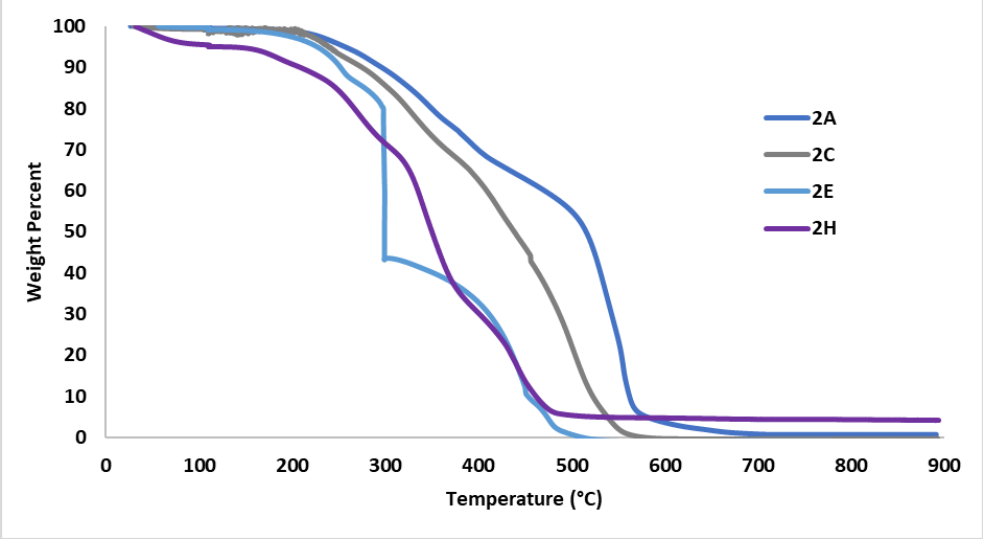
Weight Percent
Temperature (°C)
2A
2C
2E
2H

3.4.8 DSC

Example of DSC of Polytriazole with no T_g (3A). All polytriazole samples looked similar with none showing a T_g.

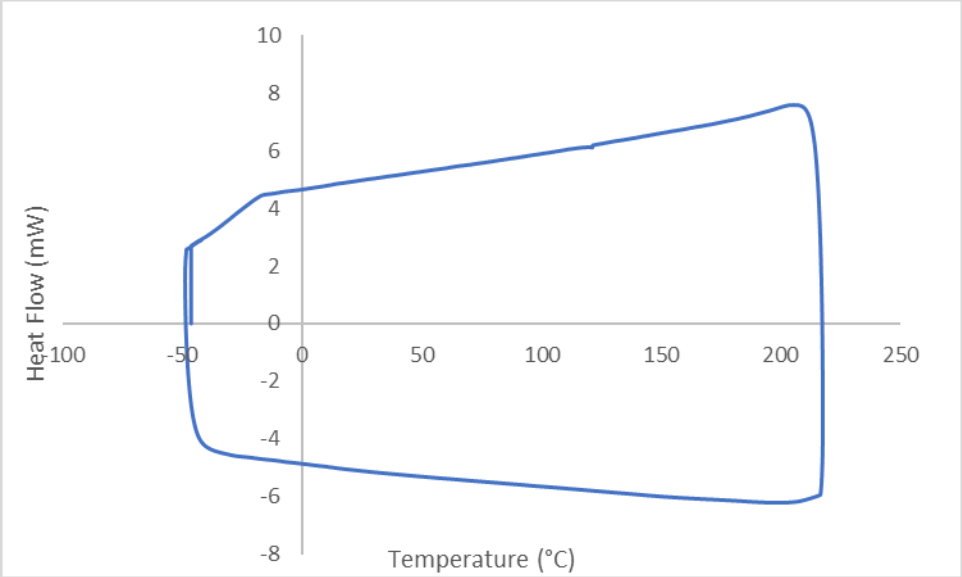

CHAPTER 4. CROSSLINKED POLYTRIAZOLE MEMBRANES SUPPORTED AND CATALYZED BY CU NANOPARTICLE COATED CUO HOLLOW FIBER MEMBRANES

(Currently this work is being drafted into a manuscript that will be submitted for peer review.)

The work presented in Chapter 4 could not have been possible without the collaboration from Dr. Ryan Lively's lab in the department of Chemical and Biomolecular Engineering at the Georgia Institute of Technology. Cu(II)O fibers and Cu(II)O fibers coated with Cu(0) nanoparticles were provided by. Dr. Yun-Ho Ahn in in Dr. Lively's lab. He also took all SEM images in Chapter 4. Additionally, Dr. Ahn conducted all functional membrane testing, including flux, permeance, and polystyrene rejections.

Interfacial polymerization of polytriazoles failed to create continuous, flat sheet membranes with the mechanical strength for functional testing, alternative polymerization and casting techniques were explored. The use of heterogenous, solid-phase Cu as both the copper source for the CuAAC polymerization and the microporous, solid support material for the membrane composite was studied. This is a unique and unexplored approach to membrane composite fabrication.

4.1 Hollow Fiber Membranes

Flat-sheet membranes produced via interfacial polymerization are normally developed into spiral wound modules for large-scale industrial use. Spiral wound modules

consist of multiple layers of flat sheet membranes separated by spacers that are rolled into a tube. By rolling the flat membranes into spiral wound modules the packing density and surface area of the membrane is increased. However, a hollow fiber membrane module design has an even higher packing density and surface area when compared to spiral wound modules. Hollow fiber membranes are cylindrical tubes that can separate molecules from inside-out or outside-in. Many hundreds of hollow fibers are bundled together to create a hollow fiber membrane module. [83]

4.2 Heterogenous Copper CuAAC

Multiple studies have shown that solid Cu(0) can be used as an alternative to the traditional Cu(I) catalysts for the CuAAC reaction.[41-42] Cu tubing, Cu sheets, and Cu nanoparticles have all successfully catalyzed this reaction. The is due to the oxidative dissolution of Cu(0) into Cu(I) in the presence of air. Alternatively, Cu(II)O species have also catalyzed the reaction. However, this is thought to be due to trace amounts of Cu(I) contamination. The combination of Cu(0) metals and Cu(II)O salts result in the indiscriminate transfer of electrons from Cu species to Cu species, resulting in a presence of the Cu(I) required for the CuAAC reaction.

4.3 Cu Nanoparticle Coated Cu(II)O Hollow Fiber Membranes

For this study Cu nanoparticles were embedded in hollow fiber membranes made of CuO. This would allow for Cu(I) ions to be present and the CuAAC reaction to occur at the surface of the hollow fiber. Once the surface is in contact with solutions of azides and alkynes, CuAAC reaction occurs, coating the fibers with a thin layer of polytriazoles. This

allows the CuO hollow fibers to act as both the catalyst for the CuAAC reaction and the macroporous support layer to add mechanical strength to the membranes.

4.4 Monomer Design

For the surface coating of Cu hollow fiber membranes, multi-functional azide and alkyne monomers were chosen based on their rigidity and membrane forming properties. Each azide and alkyne set included: (1) a rigid monomer, (2) a flexible monomer, (3) a highly functionalized PIM polymer, and (4) a low functionalized PIM polymer (Figure 4-1). These are the same monomer and polymer combinations that are described in Chapter 3. It was hypothesized that rigid monomers would increase porosity and separation properties of the membranes. However, rigid monomers also tend to precipitate before membrane formation occurs. Conversely, flexible monomers have poor separation properties due to the conformational changes that happen in the backbone but, can make continuous films. All of the monomer ad polymer combinations were explored and Chapter 3 and all were film-forming groupings.

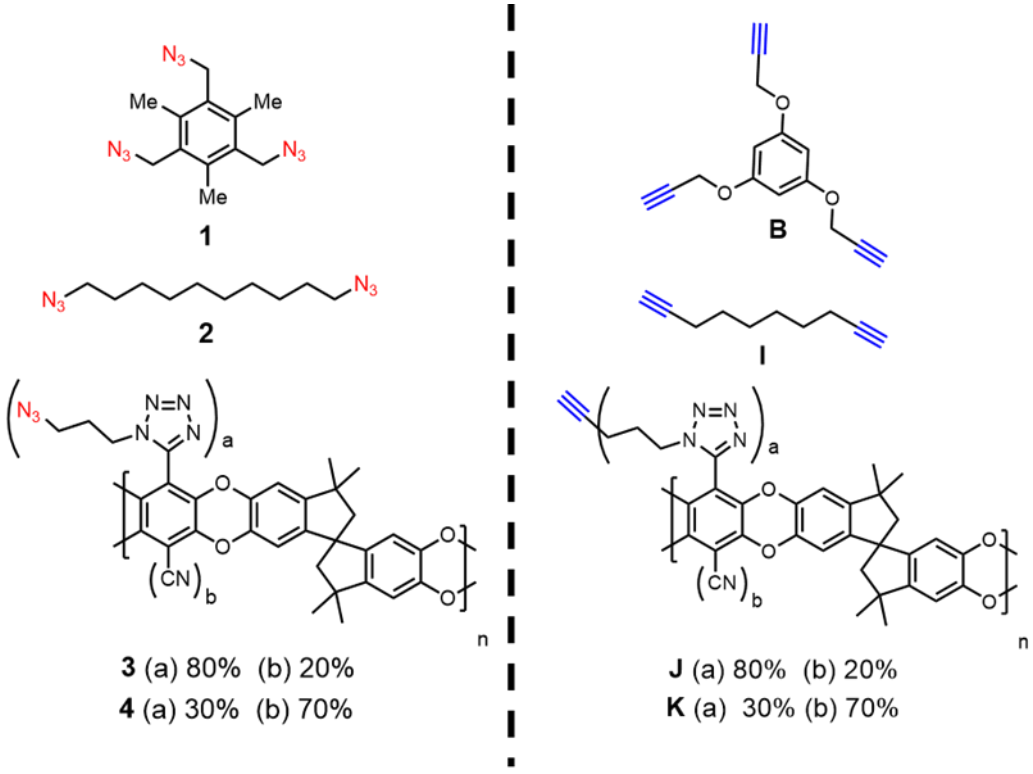

Figure 4-1: Azide and alkyne monomers for the surface CuAAC reactions CuO hollow fiber membranes.

4.5 Results and Discussion

4.5.1 CuO Hollow Fiber Membranes

The CuO hollow fiber membranes were produced through a hollow fiber spinning process with Cu(0) nanoparticles (90-250nm in diameter) and polyethersulfone (PES) as the polymer support matrix. Once phase-inversion of the fibers occurs, solvents are removed. The PES polymer matrix is removed and the Cu(0) is converted to Cu(II)O in air at high temperatures. Uncoated Cu(II)O fibers have surface pores that are too large to

facilitate membrane formation. (Figure 4-2A). This results in non-continuous membrane formation, similar to the use of macroporous stainless steel support in Chapter 3. The fibers are then coated with a solution of Cu nanoparticles in MeOH and the nanoparticles fill the pores of the CuO fibers, creating a smoother surface for membrane formation to occur (Figure 4-2B). This is done by dipping Cu(II)O fibers quickly into 1 wt% solution of Cu nanoparticle in MeOH and then dried in air. The fibers were also sealed at both end by epoxy to encourage polytriazole formation on the shell side of the fiber and avoid reaction on the bore side.

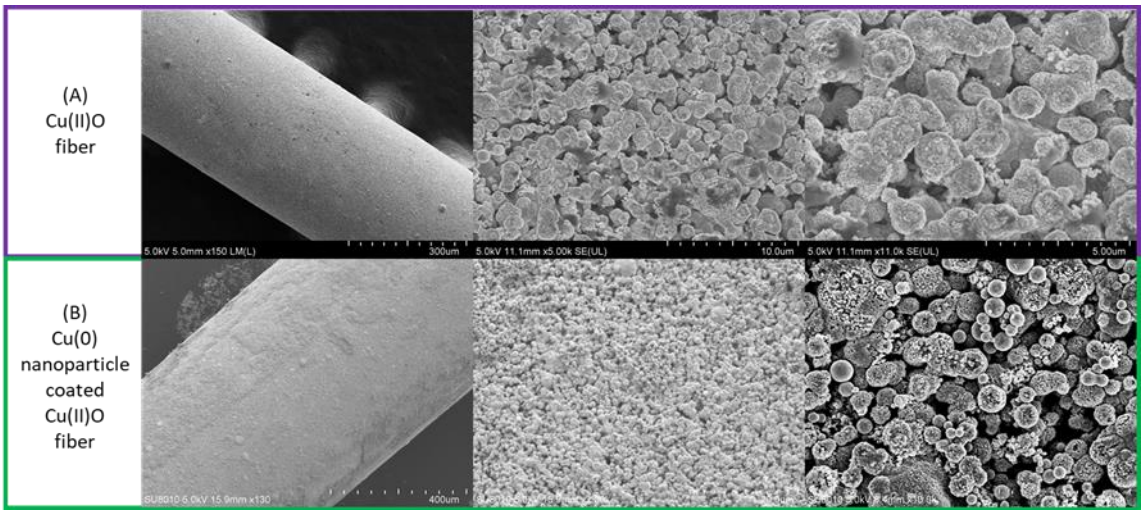

Figure 4-2: SEM imaging of Cu(II)O hollow fiber membranes (A) without and (B) with Cu(0) nanoparticle coating

4.5.2 Polytriazole Coating of Cu Nanoparticle Cu(II)O Hollow Fiber Membranes

To coat the CuO hollow fiber membranes with a polytriazole layer, the fibers were submerged in a solution of azide and alkyne monomers in chloroform for 72 hours. Induvial fibers were placed into NMR tubes with 2 mL of monomer solutions. This was done to reduce the amount of monomer solutions being used per reaction and separate the fibers

into separate reaction vessels to avoid the fibers touching during the reaction. The CuAAC reaction proceeded at room temperature while the reaction vessels were rotated. Once the reactions were completed, the fibers were removed from the reaction vessels by hand and places into hollow fiber modules.

SEM imaging of fibers before insertion into a module was conducted as an initial test of membrane formation. A summary of the monomer combinations that formed continuous polytriazole layers on the CuO fibers is shown in Table 4-1.

Table 4-1: Azide and alkyne combinations ability to form continuous membranes on CuO hollow fiber.

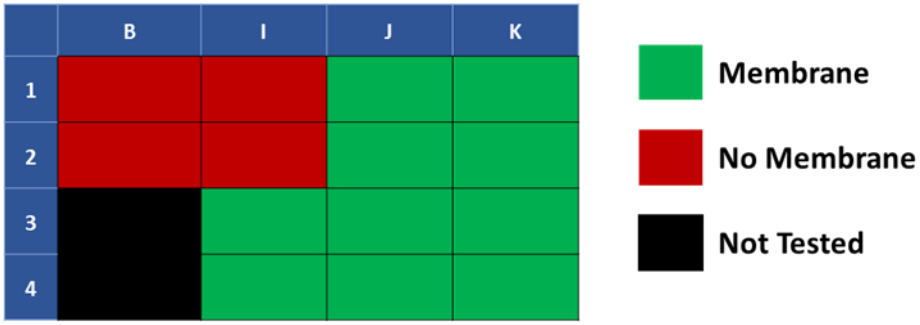

Small molecule combinations did not create continuous membranes on the CuO fibers, while groupings containing functionalized PIM molecules did. It is hypothesized that this is due to the small molecules needing more CuAAC reactions to occur to create a network, while large PIM molecules only need very few CuAAC crosslinks to create a network.

4.5.3 Continuous Membrane Analysis

Once the membranes were inserted into a stainless-steel module housing, flux of toluene as a function of pressure was used to determine if a continuous polymer layer was

formed. OSN membranes have a linear dependence and as pressure increases flux also increases. OSRO membranes are similar to OSN membranes until a transition point where the flux reaches an asymptotic value. This is a phenomenon for solution-diffusion membranes and it used in the OSRO classification.[84] Additionally, toluene permeance as a function of pressure was also tested. A linear correlation between permeance and pressure is indicative of an OSN membrane, while OSRO membranes show a decrease in permeance as pressure is increased. As shown in Figure 4-3, the sample 2-J fiber modules were prepared in triplicate and each was tested for continuous membrane formation and polystyrene rejection in toluene. SEM imaging did not show a continuous membrane formation for this batch of fibers. While all of the triplicate samples were made in the same reaction batch, it was hypothesized that the physical removal of the fibers from the reaction vessel and then into the modules, resulted in the polymer membrane layer to be destroyed in 2 out of the 3 modules created. It is possible that the SEM imaging only captured sections of the fiber where the membrane layer had been damaged. However, one module (Fiber-3) did show a linear increase in flux as pressure increase but, since pressure was not increased further, an OSRO vs OSN classification could not be made since an asymptotic value was not reached. However, there was a slight decrease in permeance as pressure increase indicating an OSRO membrane. Lastly, a polystyrene molecular weight rejection curve showed low polystyrene rejection in toluene for both the non-continuous and continuous membrane fibers. However, Fiber-3 did show a higher polystyrene rejection than the non-continuous polymer coated Fiber-1.

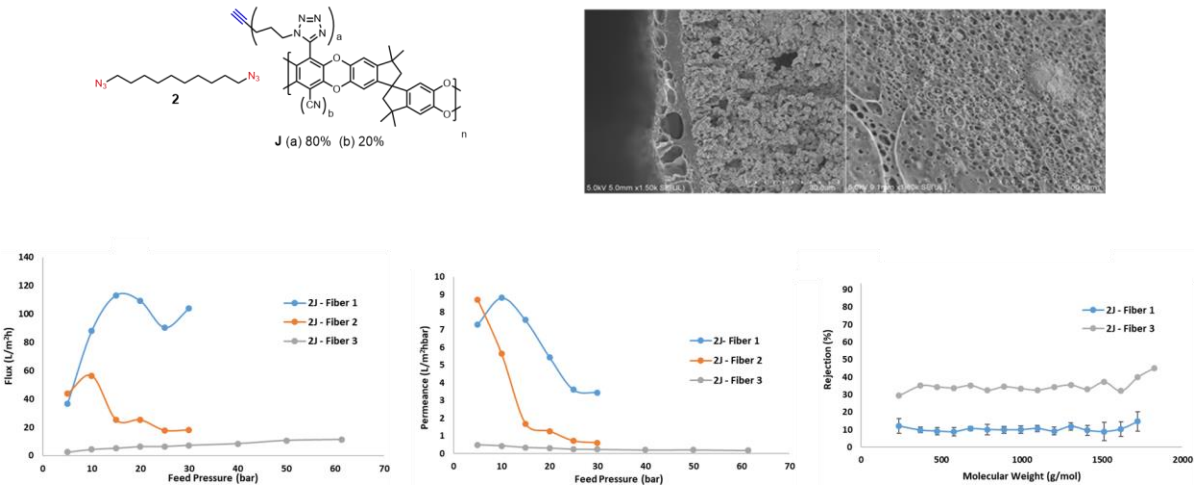

Figure 4-3: 2-J polymer coating on CuO hollow fiber membranes. SEM images show a non-continuous membrane on fiber surface. Fibers 1 and 2 show non-continuous membranes through toluene permeance testing, while Fiber 3 shows a continuous membrane layer. However, polystyrene rejections are low for all membranes.

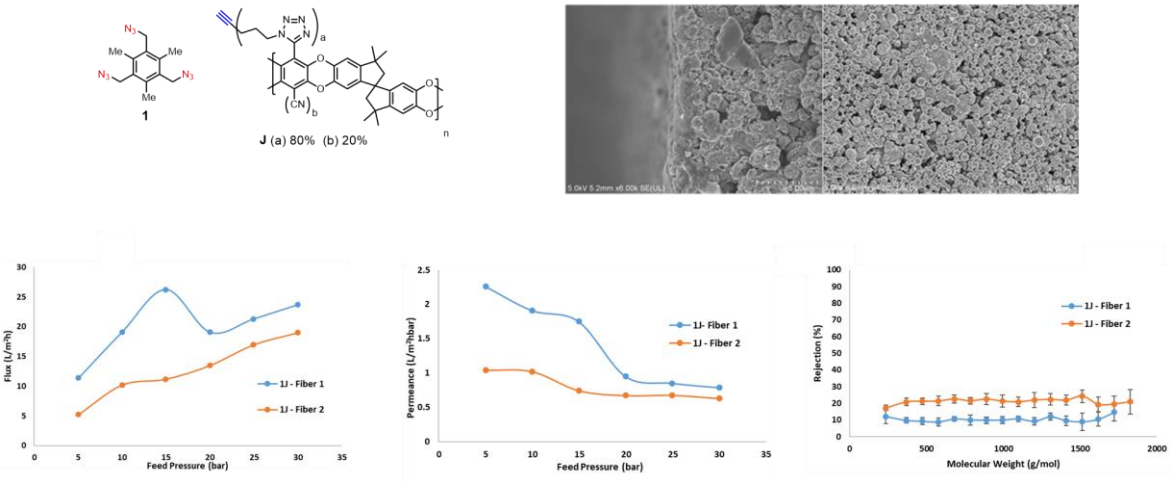

Figure 4-4: 1-J polymer coating on CuO hollow fiber membranes. SEM images show a non-continuous membrane on fiber surface. Fiber 1 show non-continuous membranes through toluene permeance testing, while Fiber 2 shows a continuous membrane layer. However, polystyrene rejections are low for both membranes.

Fibers coated with 1-J were also tested and showed similar results to that of 2-J coated fibers (Figure 4-4). SEM images showed a non-continuous membrane covering the CuO fibers. However, one fiber (Fiber-2) showed a continuous layer via toluene permeance experiments. However, all membranes showed low polystyrene rejection in toluene.

4.6 Conclusion

In this study, polytriazole linked membranes were formed on Cu(0) nanoparticle coated Cu(II)O hollow fiber membranes using a heterogenous CuAAC reaction. The crosslinking of functionalized polymers produced membranes on the hollow fibers, while small molecule polymerization reactions did not. In the two studies where modules were made from the polytriazole coated hollow fibers, reproducibility was difficult due to the physical handling of the fibers when removing from the reaction vessel and constructing modules. The intact membrane modules showed toluene permeance data consist with continuous film formation but, showed low polystyrene rejections in toluene. For use as a commercial hydrocarbon separation membrane or water desalination membrane, reproducibility as well as performance needs to be increased.

4.7 Analysis

4.7.1 General Analytical Methods

High-resolution imaging of the composite morphology was achieved using a Hitachi SU8230. Cold Field Emission Scanning Electron Microscope (CFE-SEM). The dry samples were attached to aluminium stubs using copper tape. The samples were then coated

with a 20 nm layer of gold/palladium using a Hummer 6 Gold/Palladium Sputterer. Imaging was taken at a working distance of 8 mm and a working voltage of 3 kV using a mix of upper and lower secondary electron detectors.

The membrane's performance in organic solvent nanofiltration separations was evaluated according to membrane permeabilities and molecular weight cut off (MWCO) curves. All nanofiltration experiments were carried out at using a crossflow filtration system. Customized module were made from 1/4" stainless steel tubing and Swagelok fittings with an effective length of the fiber close to 2 cm. Solvent-resistant J-B Weld 8272 epoxy was used to seal the void area of the end of the module and separate the bore and shell side from one another. Modules were left to cure overnight at ambient condition before testing.

4.7.2 SEM Imaging

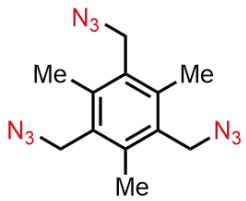

1

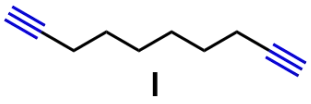

I

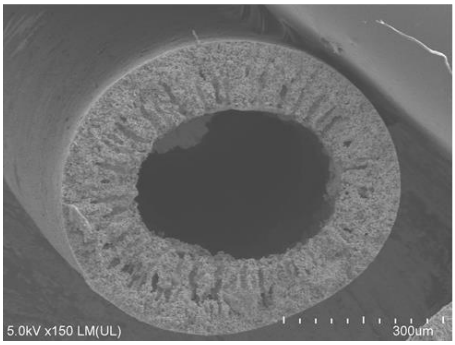

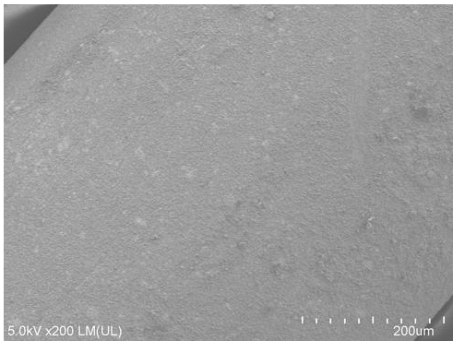

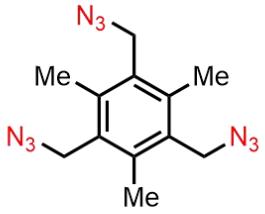

1

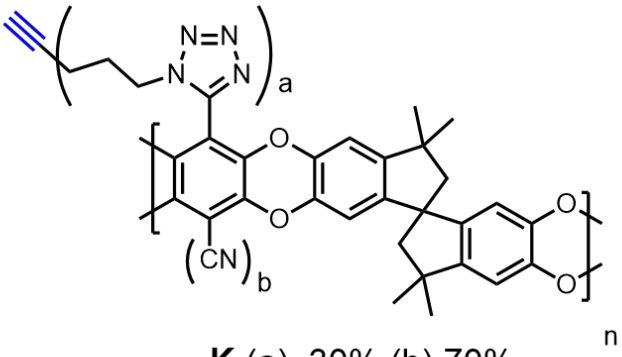

K (a) 30% (b) 70%

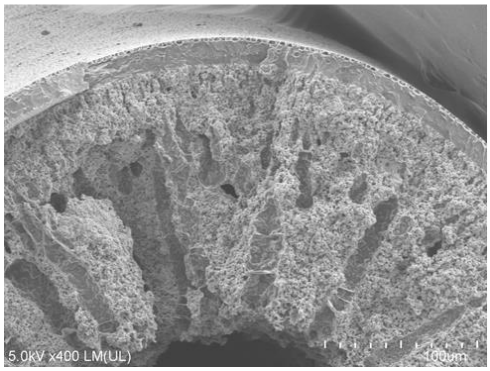

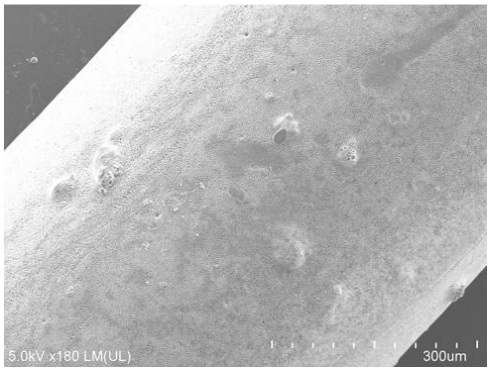

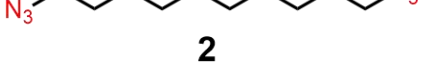

2

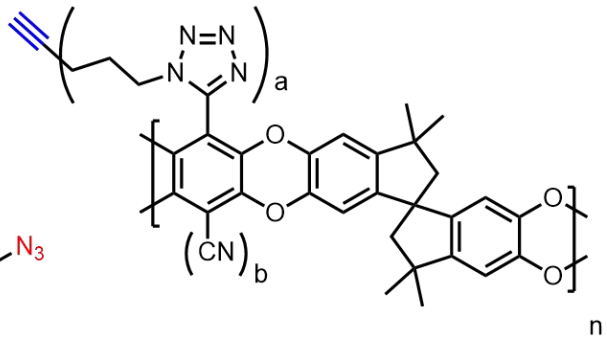

J (a) 80% (b) 20%

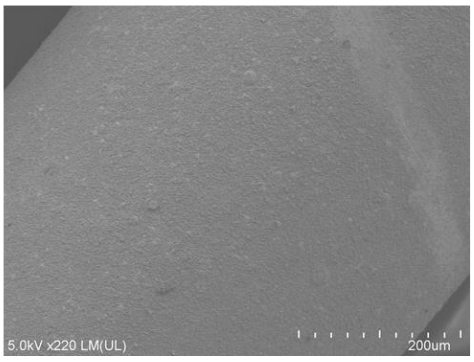

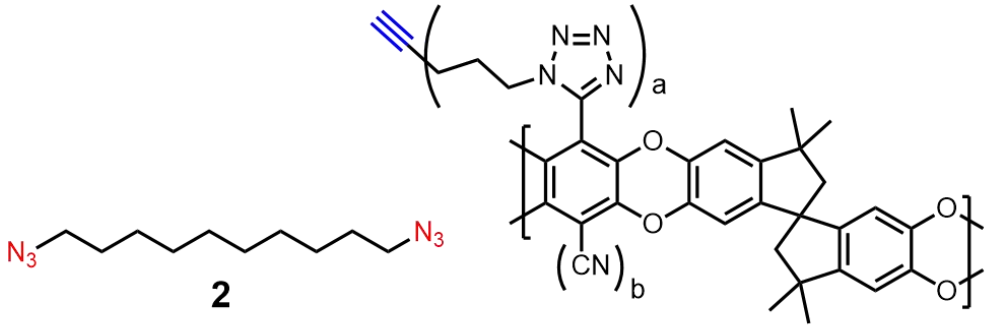

2

K (a) 30% (b) 70%

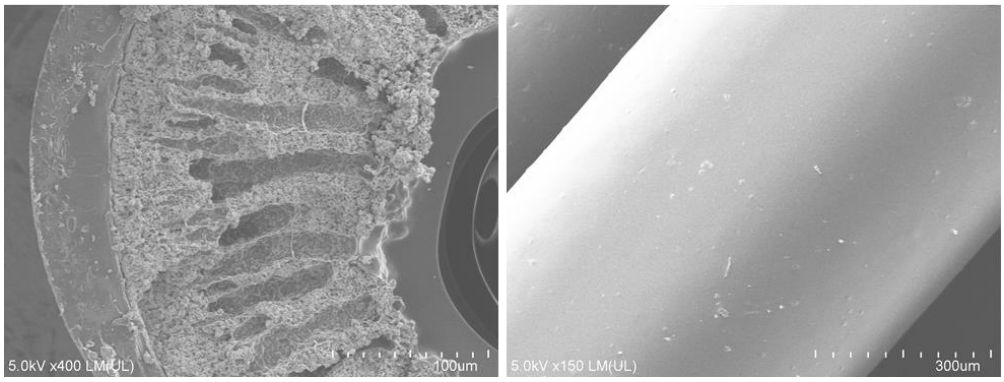

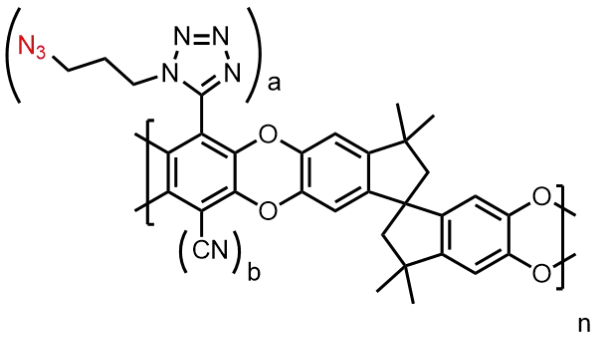

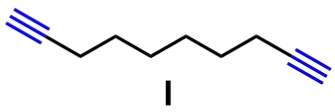

I

3 (a) 80% (b) 20%

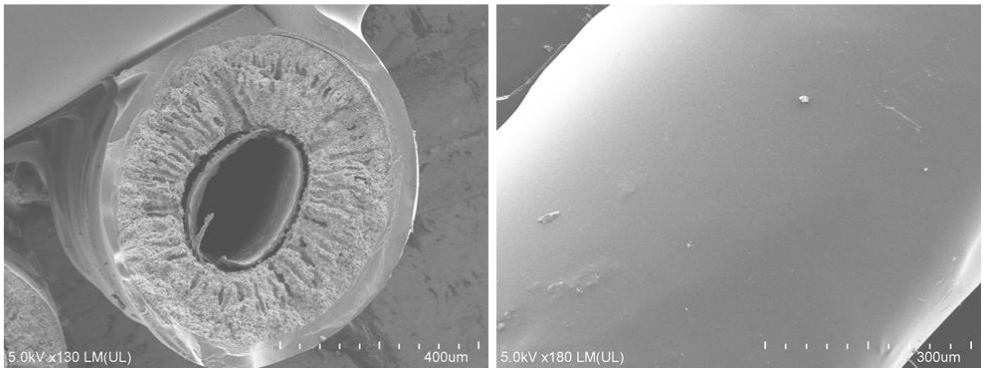

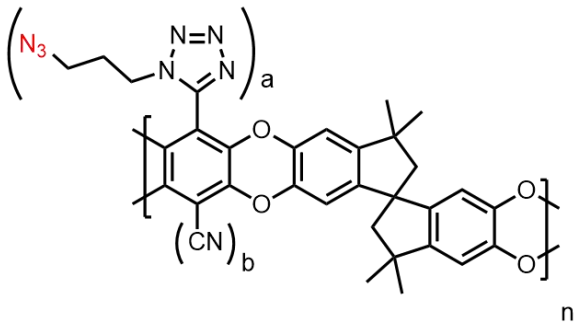

n

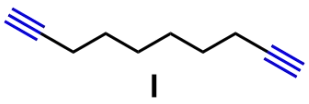

I

4 (a) 30% (b) 70%

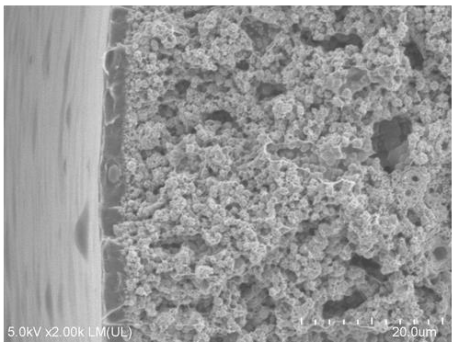

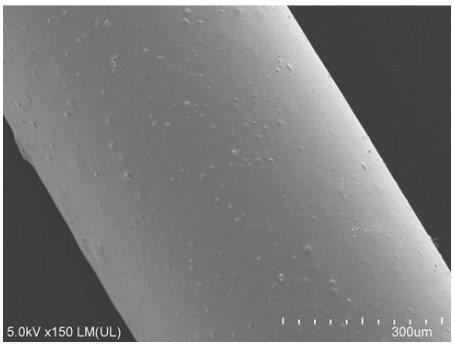

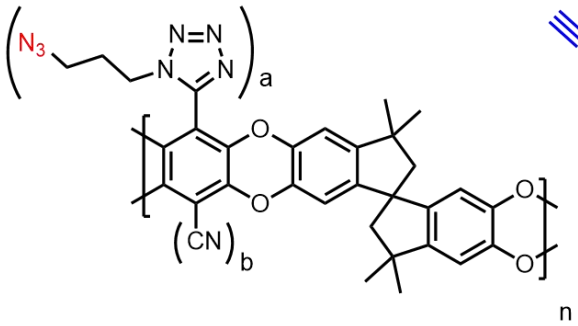

n

4 (a) 30% (b) 70%

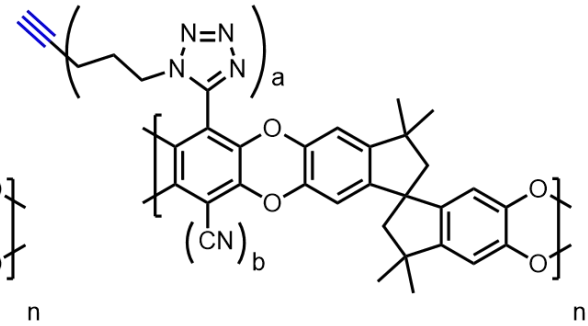

n

J (a) 80% (b) 20%

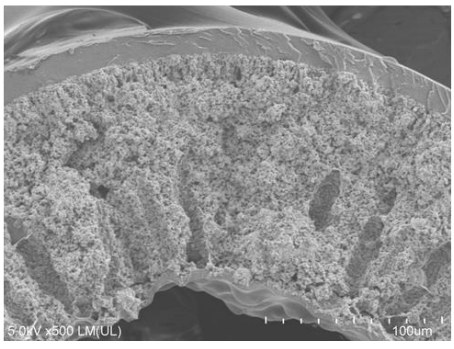

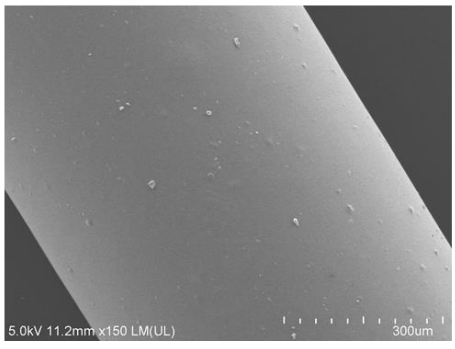

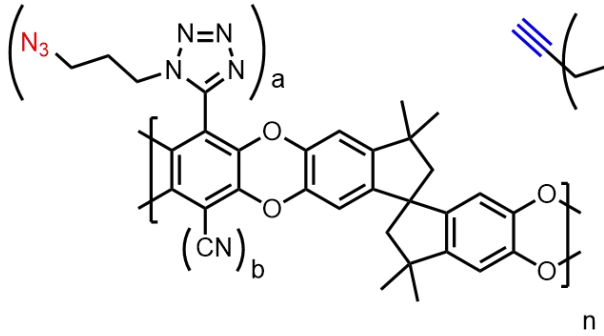

4 (a) 30% (b) 70%

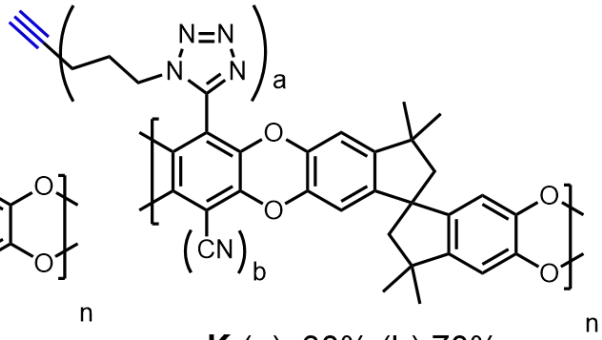

K (a) 30% (b) 70%

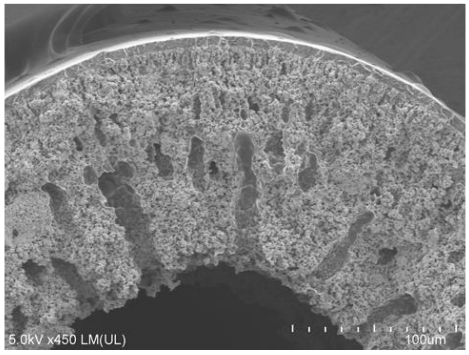

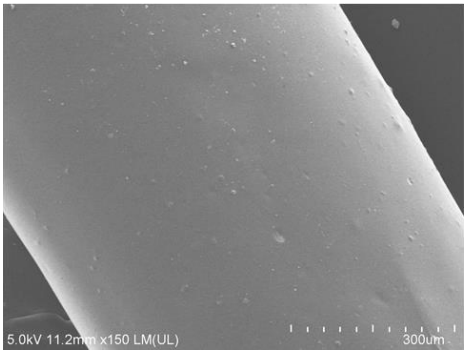

CHAPTER 5. CONCLUSION AND FUTURE DIRECTIONS

This thesis sets the foundation for the novel use of polytriazoles and the CuAAC reaction in membrane reaction design. The various synthetic advantages provided by CuAAC reaction, including ease of starting material synthesis, fast reaction kinetics, simple workup, no byproducts, and a chemically stable triazole product makes it a very attractive reaction for use in membrane synthesis and materials design.

For use in water desalination membranes, triazoles have shown to be more stable to harsh cleaning conditions, such as acids, bases, and oxidants when compared to the commercially used polyamide membranes. This stability increases the lifetime of the membrane and avoids any expensive, time-consuming, or high energy pretreatment steps that are needed to protect polyamide membranes from oxidative degradation.

This work explored the amalgamation of interfacial polymerization and the CuAAC reaction to create flat sheet polytriazole membranes. While continuous membranes could be formed interfacially, the mechanical strength of the resulting polytriazole was too low to make composites and functional testing was not completed. Interfacially polymerization polytriazole directly onto a macroporous support led to non-continuous and cracked membranes. However, other macroporous support layers besides stainless steel, should be explored further. By decreasing the support's surface pore diameter, continuous membrane formation is more favorable. Additionally, avoiding drying the membrane to dryness could also prevent cracking in the polytriazole layer. Many commercial membranes must be stored wet to avoid drying out and cracking the membranes.[85]

All interfacially polymerized polytriazoles showed low BET surface area compared to PIM-1 and a mesoporous structure compared to PIM-1's microporous structure. While a highly porous structure is advantageous to increase flux at lower pressures, nitrogen physisorption is not an ideal functional testing of a polymer's microstructure in organic solvents or water. Good separation properties in organic solvents and water can be obtained with non-porous polymers due to: (1) swelling of the polymer in liquids, which would be unlikely in the crosslinked polytriazoles and (2) sorption and diffusion of the solvents through the membrane. For true functional testing of interfacially polymerized polytriazoles in organic solvents and water, polytriazole composite membranes with high mechanical stability need to be created.

The use of CuO hollow fiber membranes as a support layer and Cu source in the formation of polytriazole was also investigated. This is a new and unexplored membrane casting technique. The use of a solid support as a reaction component or catalyst can open new areas of research, using various inorganic supports to catalyze a thin polymer layer on their surface. While a continuous polytriazole membrane is not currently reproducible, continuous membranes were formed on the surface of the copper fibers. In general, the ability to create a continuous and defect-free membrane coating by this new method is rare due to the numerous conditions that affect membrane formation: (1) coating and density of Cu nanoparticles within the CuO fiber, (2) variation in monomer concentration due to gelation of the monomer solutions, (3) physical manipulation of the fibers after polymerization had occurred, (4) monomer combinations and concentrations, (5) reaction time, and (6) the ability of the Cu ions to get pulled into and diffuse through the polymer matrix. It is unusual for continuous, defect-free membranes to be produced with relative

ease without optimization of all of the reaction conditions. Optimization of these conditions could lead to high reproducibility and high separation properties.

To increase reproducibility, the CuAAC reaction can occur *in situ*, once the fiber is already placed inside the module. Monomer solution will fill the module housing containing the fiber and reaction will occur on the bore side of the fiber. This would eliminate any physical contact with fibers after polymerization has occurred, which we hypothesize leads to the inconsistence in continuous membrane formation from fiber to fiber. Once reproducibility has been accomplished, understanding a true structure-to-functional relationship between monomer design and membrane function will be key to increasing selectivity.

Additionally, theoretically the crosslinked polytriazoles were not fully crosslinked in the interfacial polymerization reaction. This leaves both azide and alkyne functional handles present throughout the membrane. Post-polymerization functionalization can be used to further functionalize the membranes through the CuAAC reaction. Additional properties such as anti-fouling properties, addition of charged molecules, and further crosslinking can occur at the unreacted azides and alkynes.

Lastly, other macroporous support materials can be infused with Cu nanoparticles to test the effect of the support material on the functional separation properties of the membrane composite. While Cu(II)O fibers do provide a small amount of Cu(I) for the CuAAC reaction, the majority of the Cu(I) comes from the surface of the Cu(0) nanoparticles. This allows for other macroporous materials to be used as the support

material and various supports can be explored based on chemical and thermal stability needed for the separation process.

In general, the transition from high energy distillations to low energy membrane separations is a necessary and imminent change for large-scale, industrial separations. While water desalination pioneered the shift from distillation to membranes, commercial polyamide membranes could still be improved upon with regards to chemical stability. Polytriazole membranes could be a viable, chemically stability alternative to commonly used polyamides. The research and development of highly selective and low energy consuming membranes for hydrocarbon separation is still ongoing, however polytriazole-based polymers have shown chemical stability and the ability to polymerize into thin, flat-sheet membranes via liquid-liquid interfacial polymerization. The new and unprecedented casting method of polymerizing polytriazoles directly onto heterogenous Cu supports opens areas of solid-liquid interfacial polymerization in membrane design. Optimization of the reaction conditions could lead to a further understanding of a structure-to-property relationship and membranes with ideal separation properties can be established.

REFERENCES

1. Schmitt, F.; Do, K. U., Prediction of membrane fouling using artificial neural networks for wastewater treated by membrane bioreactor technologies: bottlenecks and possibilities. *Environ Sci Pollut Res Int* **2017,** *24* (29), 22885-22913.

2. Laboratory, O. R. N., Materials for Separation Technologies: Energy and Emission Reduction Opportunities. **2005**.

3. Sholl, D. S.; Lively, R. P., Seven chemical separations to change the world. *Nature* **2016,** *532* (7600), 435-7.

4. Smith, R.; Jobson, M., Distillations. *Encyclopedia of Separation Science* **2000**, 84-103.

5. Sahai, R., Membrane Separations-Filtration. *Encyclopedia of Separation Science* **2001**, 1717-1724.

6. Mulder, M., *Basic Principles of Membrane Technology*. 2 ed.; Kluwer Academic Publishers: Netherlands, 1996.

7. Chen, X. Y.; Vinh-Thang, H.; Ramirez, A. A.; Rodrigue, D.; Kaliaguine, S., Membrane gas separation technologies for biogas upgrading. *RSC Advances* **2015,** *5* (31), 24399-24448.

8. Laberty-Robert, C.; Valle, K.; Pereira, F.; Sanchez, C., Design and properties of functional hybrid organic-inorganic membranes for fuel cells. *Chem Soc Rev* **2011,** *40* (2), 961-1005.

9. A.F., I.; K.C., K.; T., M., Membrane Fabrication/Manufacturing Techniques. *Gas Separation Membranes* **2015**, 193-220.

10. Council, N. R., *Oil in the Sea*. The National Academies Press: Washington, DC, 1985.

11. Koros, W. J.; Zhang, C., Materials for next-generation molecularly selective synthetic membranes. *Nat Mater* **2017,** *16* (3), 289-297.

12. Lively, R. P.; Sholl, D. S., From water to organics in membrane separations. *Nature Materials* **2017,** *16*, 276.

13. Liang, B.; He, X.; Hou, J.; Li, L.; Tang, Z., Membrane Separation in Organic Liquid: Technologies, Achievements, and Opportunities. *Adv Mater* **2018**, e1806090.

14. Addams, L.; Boccaletti, G.; Kerlin, M.; Stuchtey, M. *Charting Our Water Future: Economic frameworks to inform decision-making*; 2009.

15. Amjad, Z., *Reverse osmosis : membrane technology, water chemistry & industrial applications*. Van Nostrand Reinhold: New York, 1993.

16. Pusch, W., Performance of RO membranes in correlation with membrane structure, transport mechanisms of matter and module design (fouling). State of the art. *Desalination* **1990,** *77*, 35-54.

17. Guo, W.; Ngo, H. H.; Li, J., A mini-review on membrane fouling. *Bioresour Technol* **2012,** *122*, 27-34.

18. Werber, J. R.; Osuji, C. O.; Elimelech, M., Materials for next-generation desalination and water purification membranes. *Nature Reviews Materials* **2016,** *1* (5), 16018.

19. Elimelech, M.; Phillip, W. A., The future of seawater desalination: energy, technology, and the environment. *Science* **2011,** *333* (6043), 712-7.

20. Mohammadi, T.; Madaeni, S. S.; Moghadam, M. K., Investigation of membrane fouling. *Desalination* **2003,** *153* (1-3), 155-160.

21. Zhang, R.; Yu, S.; Shi, W.; Tian, J.; Jin, L.; Zhang, B.; Li, L.; Zhang, Z., Optimization of a membrane cleaning strategy for advanced treatment of polymer flooding produced water by nanofiltration. *RSC Advances* **2016,** *6* (34), 28844-28853.

22. Glater, J.; Hong, S.-k.; Elimelech, M., The search for a chlorine-resistant reverse osmosis membrane. *Desalination* **1994,** *95* (3), 325-345.

23. Glater, J.; Zachariah, M. R.; McCray, S. B.; McCutchan, J. W., Reverse osmosis membrane sensitivity to ozone and halogen disinfectants. *Desalination* **1983,** *48* (1), 1-16.

24. Park, H. B.; Kamcev, J.; Robeson, L. M.; Elimelech, M.; Freeman, B. D., Maximizing the right stuff: The trade-off between membrane permeability and selectivity. *Science* **2017,** *356* (6343).

25. Koops, G. H.; Nolten, J. A. M.; Mulder, M. H. V.; Smolders, C. A., Selectivity as a Function of Membrane Thickness - Gas Separation and Pervaporation. *Journal of Applied Polymer Science* **1994,** *53* (12), 1639-1652.

26. Budd, P. M.; Elabas, E. S.; Ghanem, B. S.; Makhseed, S.; McKeown, N. B.; Msayib, K. J.; Tattershall, C. E.; Wang, D., Solution-Processed, Organophilic Membrane Derived from a Polymer of Intrinsic Microporosity. *Advanced Materials* **2004,** *16* (5), 456-459.

27. Jue, M. L.; McKay, C. S.; McCool, B. A.; Finn, M. G.; Lively, R. P., Effect of Nonsolvent Treatments on the Microstructure of PIM-1. *Macromolecules* **2015,** *48* (16), 5780-5790.

28. Kim, H. J.; Kim, D. G.; Lee, K.; Baek, Y.; Yoo, Y.; Kim, Y. S.; Kim, B. G.; Lee, J. C., A Carbonaceous Membrane based on a Polymer of Intrinsic Microporosity (PIM-1) for Water Treatment. *Sci Rep* **2016,** *6*, 36078.

29. Madrid, E.; Cottis, P.; Rong, Y.; Rogers, A. T.; Stone, J. M.; Malpass-Evans, R.; Carta, M.; McKeown, N. B.; Marken, F., Water desalination concept using an ionic rectifier based on a polymer of intrinsic microporosity (PIM). *Journal of Materials Chemistry A* **2015,** *3* (31), 15849-15853.

30. Kolb, H. C.; Finn, M. G.; Sharpless, K. B., Click Chemistry: Diverse Chemical Function from a Few Good Reactions. *Angewandte Chemie International Edition* **2001,** *40* (11), 2004-2021.

31. Hein, C. D.; Liu, X. M.; Wang, D., Click chemistry, a powerful tool for pharmaceutical sciences. *Pharm Res* **2008,** *25* (10), 2216-30.

32. Rostovtsev, V. V.; Green, L. G.; Fokin, V. V.; Sharpless, K. B., A Stepwise Huisgen Cycloaddition Process: Copper(I)-Catalyzed Regioselective "Ligation" of Azides and Terminal Alkynes. *Angewandte Chemie International Edition* **2002,** *41* (14), 2596-2599.

33. Tornoe, C. W.; Christensen, C.; Meldal, M., Peptidotriazoles on solid phase: [1,2,3]-triazoles by regiospecific copper(i)-catalyzed 1,3-dipolar cycloadditions of terminal alkynes to azides. *J Org Chem* **2002,** *67* (9), 3057-64.

34. Kolb, H. C.; Sharpless, K. B., The growing impact of click chemistry on drug discovery. *Drug Discovery Today* **2003,** *8* (24), 1128-1137.

35. Moses, J. E.; Moorhouse, A. D., The growing applications of click chemistry. *Chem Soc Rev* **2007,** *36* (8), 1249-62.

36. He, Y.; Hoi, H.; Montemagno, C. D.; Abraham, S., Functionalized polymeric membrane with aquaporin using click chemistry for water purification application. *Journal of Applied Polymer Science* **2018,** *135* (35).

37. Goud, V. D.; Dsouza, R.; Valiyaveettil, S., Solution processable polyamines via click chemistry for water purification. *RSC Advances* **2015,** *5* (59), 47647-47658.

38. Song, Y.; Fan, J.-B.; Wang, S., Recent progress in interfacial polymerization. *Materials Chemistry Frontiers* **2017,** *1* (6), 1028-1040.

39. Jimenez-Solomon, M. F.; Song, Q.; Jelfs, K. E.; Munoz-Ibanez, M.; Livingston, A. G., Polymer nanofilms with enhanced microporosity by interfacial polymerization. *Nature Materials* **2016,** *15*, 760.

40. Meldal, M.; Tornoe, C. W., Cu-catalyzed azide-alkyne cycloaddition. *Chem Rev* **2008,** *108* (8), 2952-3015.

41. Chassaing, S.; Bénéteau, V.; Pale, P., When CuAAC 'Click Chemistry' goes heterogeneous. *Catalysis Science & Technology* **2016,** *6* (4), 923-957.

42. Accurso, A. A.; Delaney, M.; O'Brien, J.; Kim, H.; Iovine, P. M.; Diaz Diaz, D.; Finn, M. G., Improved metal-adhesive polymers from copper(I)-catalyzed azide-alkyne cycloaddition. *Chemistry* **2014,** *20* (34), 10710-9.

43. Diaz, D. D., Click Chemistry in Materials Synthesis: The Beginning. *Macromol Symp* **2015,** *358* (1), 10-20.

44. Lin, S.; Sharma, A., Recent advances in the synthesis and synthetic applications of 1,2,3-triazoles (microreview). *Chemistry of Heterocyclic Compounds* **2018,** *54* (3), 314-316.

45. Huisgen, R. In *Centenary Lecture - 1,3-Dipolar Cycloadditions*, Proceedings of the Chemical Society of London: 357, 1961.

46. Hein, J. E.; Fokin, V. V., Copper-catalyzed azide-alkyne cycloaddition (CuAAC) and beyond: new reactivity of copper(I) acetylides. *Chem Soc Rev* **2010,** *39* (4), 1302-15.

47. McKeown, N. B.; Budd, P. M., Polymers of intrinsic microporosity (PIMs): organic materials for membrane separations, heterogeneous catalysis and hydrogen storage. *Chem Soc Rev* **2006,** *35* (8), 675-83.

48. McKeown, N. B.; Budd, P. M., Polymers of Intrinsic Microporosity *Encyclopedia of Polymer Science and Technology* **2009**.

49. Kwon, Y.-N.; Leckie, J. O., Hypochlorite degradation of crosslinked polyamide membranes. *Journal of Membrane Science* **2006,** *283* (1-2), 21-26.

50. Schulze, B.; Schubert, U. S., Beyond click chemistry - supramolecular interactions of 1,2,3-triazoles. *Chem Soc Rev* **2014,** *43* (8), 2522-71.

51. Kislukhin, A. A.; Hong, V. P.; Breitenkamp, K. E.; Finn, M. G., Relative performance of alkynes in copper-catalyzed azide-alkyne cycloaddition. *Bioconjug Chem* **2013,** *24* (4), 684-9.

52. Woo, C. M.; Felix, A.; Zhang, L.; Elias, J. E.; Bertozzi, C. R., Isotope-targeted glycoproteomics (IsoTaG) analysis of sialylated N- and O-glycopeptides on an Orbitrap Fusion Tribrid using azido and alkynyl sugars. *Analytical and Bioanalytical Chemistry* **2017,** *409* (2), 579-588.

53. Jurczak, J.; Chmurski, K.; Stepniak, P., Improved Synthesis of C2 and C6 Monoderivatives of α- and β-Cyclodextrin via the Click Chemistry Approach. *Synthesis* **2015,** *47* (13), 1838-1843.

54. He, W.; Yu, J.; Wang, D.; Ran, G.; Xia, X.-F., Synthesis of tri-substituted allyl alcohols via a copper/iron co-catalyzed cascade perfluoroalkylation/rearrangement of aryl propynyl ethers. *Organic Chemistry Frontiers* **2019,** *6* (20), 3575-3579.

55. Kumar, D.; Beena; Khare, G.; Kidwai, S.; Tyagi, A. K.; Singh, R.; Rawat, D. S., Synthesis of novel 1,2,3-triazole derivatives of isoniazid and their in vitro and in vivo antimycobacterial activity evaluation. *Eur J Med Chem* **2014,** *81*, 301-13.

56. Zhao, J. W.; Guo, J. W.; Huang, M. J.; You, Y. Z.; Wu, Z. H.; Liu, H. M.; Huang, L. H., Design, synthesis and biological evaluation of new steroidal beta-triazoly enones as potent antiproliferative agents. *Steroids* **2019,** *150*, 108431.

57. Arafa, W. A. A.; Nayl, A. E. A. A., Water as a solvent for Ru-catalyzed click reaction: Highly efficient recyclable catalytic system for triazolocoumarins synthesis. *Applied Organometallic Chemistry* **2019,** *33* (10).

58. Cilliers, P.; Seldon, R.; Smit, F. J.; Aucamp, J.; Jordaan, A.; Warner, D. F.; N'Da, D. D., Design, synthesis, and antimycobacterial activity of novel ciprofloxacin derivatives. *Chem Biol Drug Des* **2019,** *94* (2), 1518-1536.

59. Wen, J.; Wu, K.; Yang, D.; Tian, J.; Huang, Z.; Filatov, A. S.; Lei, A.; Lin, X. M., Low-Pressure Flow Chemistry of CuAAC Click Reaction Catalyzed by Nanoporous AuCu Membrane. *ACS Appl Mater Interfaces* **2018,** *10* (31), 25930-25935.

60. Zych, D.; Kurpanik, A.; Slodek, A.; Maron, A.; Pajak, M.; Szafraniec-Gorol, G.; Matussek, M.; Krompiec, S.; Schab-Balcerzak, E.; Kotowicz, S.; Siwy, M.; Smolarek, K.; Mackowski, S.; Danikiewicz, W., NCN-Coordinating Ligands based on Pyrene Structure with Potential Application in Organic Electronics. *Chemistry* **2017,** *23* (62), 15746-15758.

61. Mason, C. R.; Maynard-Atem, L.; Al-Harbi, N. M.; Budd, P. M.; Bernardo, P.; Bazzarelli, F.; Clarizia, G.; Jansen, J. C., Polymer of Intrinsic Microporosity Incorporating Thioamide Functionality: Preparation and Gas Transport Properties. *Macromolecules* **2011,** *44* (16), 6471-6479.

62. Gao, Y.; Mao, Y.; Zhang, B.; Zhan, Y.; Huo, Y., Regioselective nitration of anilines with Fe(NO3)3.9H2O as a promoter and a nitro source. *Org Biomol Chem* **2018,** *16* (21), 3881-3884.

63. Raaijmakers, M. J. T.; Benes, N. E., Current trends in interfacial polymerization chemistry. *Progress in Polymer Science* **2016,** *63*, 86-142.

64. Roux, R.; Sallet, L.; Alcouffe, P.; Chambert, S.; Sintes-Zydowicz, N.; Fleury, E.; Bernard, J., Facile and Rapid Access to Glyconanocapsules by CuAAC Interfacial Polyaddition in Miniemulsion Conditions. *ACS Macro Letters* **2012,** *1* (8), 1074-1078.

65. Poltorak, K.; Durand, A.; Léonard, M.; Six, J.-L.; Nouvel, C., Interfacial click chemistry for improving both dextran shell density and stability of biocompatible

nanocapsules. *Colloids and Surfaces A: Physicochemical and Engineering Aspects* **2015,** *483*, 8-17.

66. Matsumoto, M.; Valentino, L.; Stiehl, G. M.; Balch, H. B.; Corcos, A. R.; Wang, F.; Ralph, D. C.; Mariñas, B. J.; Dichtel, W. R., Lewis-Acid-Catalyzed Interfacial Polymerization of Covalent Organic Framework Films. *Chem* **2018,** *4* (2), 308-317.

67. Guiver, M. D.; Lee, Y. M., Materials science. Polymer rigidity improves microporous membranes. *Science* **2013,** *339* (6117), 284-5.

68. George, S. C.; knörgen, M.; Thomas, S., Effect of nature and extent of crosslinking on swelling and mechanical behavior of styrene–butadiene rubber membranes. *Journal of Membrane Science* **1999,** *163* (1), 1-17.

69. Glaser, C., Untersuchungen über einige Derivate der Zimmtsäure. *Annalen der Chemie und Pharmacie* **1870,** *154* (2), 137-171.

70. Worrell, B. T.; Malik, J. A.; Fokin, V. V., Direct evidence of a dinuclear copper intermediate in Cu(I)-catalyzed azide-alkyne cycloadditions. *Science* **2013,** *340* (6131), 457-60.

71. Safety, C. L. Stainless Steel Chemical Compatibility Chart. https://www.calpaclab.com/stainless-steel-chemical-compatibility-chart/#.

72. Sing, K. S. W., Physisorption of nitrogen by porous materials. *Journal of Porous Materials* **1995,** *2* (1), 5-8.

73. Zdravkov, B.; Čermák, J.; Šefara, M.; Janků, J., Pore classification in the characterization of porous materials: A perspective. *Open Chemistry* **2007,** *5* (2).

74. Bertier, P. S., Kevin & Stanjek, Helge & Ghanizadeh, Amin & Clarkson, Christopher & Busch, Andreas & Kampman, Niko & Prinz, D. & Amann, Alexandra & Krooss, Bernhard & Pipich, Vitaliy. , On the use and abuse of N2 physisorption for the characterisation of the pore structure of shales. In *The Clay Minerals Society Workshop Lectures Series*, 2006; Vol. 1.

75. Jue, M. PIM-1-derived carbon molecular sieve hollow fiber membranes for organic solvent reverse osmosis. Georgia Institute of Technology, 2017.

76. Nielsen, L. E., Cross-Linking–Effect on Physical Properties of Polymers. *Journal of Macromolecular Science, Part C* **2008,** *3* (1), 69-103.

77. Kaur, S.; Singh, A.; Mithu, V. S.; Singh, P., A rationally designed molecule for removal of cyanide from human blood serum and cytochrome c oxidase. *RSC Adv.* **2014,** *4* (106), 61884-61890.

78. Bera, R.; Ansari, M.; Mondal, S.; Das, N., Selective CO2 capture and versatile dye adsorption using a microporous polymer with triptycene and 1,2,3-triazole motifs. *European Polymer Journal* **2018,** *99*, 259-267.

79. Du, N.; Park, H. B.; Robertson, G. P.; Dal-Cin, M. M.; Visser, T.; Scoles, L.; Guiver, M. D., Polymer nanosieve membranes for CO2-capture applications. *Nat Mater* **2011,** *10* (5), 372-5.

80. Lee, K. M.; Kim, H. J.; Kang, C.-S.; Tojo, T.; Chae, J. A.; Oh, Y.; Cha, M. C.; Yang, K. S.; Kim, Y. A.; Kim, H., Preparation of carbon-containing, compressible, microporous, polymeric monoliths that regulate macroscopic conductivity. *Polymer Chemistry* **2019,** *10* (7), 852-859.

81. Khanam, S.; Rai, S. K.; Verma, D.; Khanna, R. S.; Tewari, A. K., An efficient and controlled synthesis of persulfonylated G1 dendrimers via click reaction. *RSC Advances* **2016,** *6* (62), 56952-56962.

82. Xie, Z.; Wei, Y.; Zhao, X.; Li, Y.; Ding, S.; Chen, L., Facile construction of butadiynylene based conjugated porous polymers by cost-effective Glaser coupling. *Materials Chemistry Frontiers* **2017,** *1* (5), 867-872.

83. Rackley, S. A., *Carbon Capture and Storage*. 2 ed.; 2017.

84. Jang, H. Y.; Johnson, J. R.; Ma, Y.; Mathias, R.; Bhandari, D. A.; Lively, R. P., Torlon® hollow fiber membranes for organic solvent reverse osmosis separation of complex aromatic hydrocarbon mixtures. *AIChE Journal* **2019**.

85. Nanotech, R. *Storage and preservation of spiral wound membrane elements* Russia, 2016.